

Wiadomości Lekarskie

Medical Advances

Official journal of the Polish Medical Association
Wiadomości Lekarskie has been published since 1928



Volume LXXVII, Issue 9, SEPTEMBER 2024

ISSN 0043-5147

E-ISSN 2719-342X

Wiadomości Lekarskie

Medical Advances

Official journal of the Polish Medical Association

Wiadomości Lekarskie has been published since 1928



Volume LXXVII, Issue 9, SEPTEMBER 2024



Memory of
dr Władysław
Biegański

Wiadomości Lekarskie Medical Advances is abstracted and indexed in:
PUBMED/MEDLINE, SCOPUS, EMBASE, INDEX COPERNICUS,
MINISTRY OF SCIENCE AND HIGHER EDUCATION, POLISH MEDICAL BIBLIOGRAPHY

Copyright: © ALUNA Publishing

Articles published on-line and available in open access are published under Creative Commons Attribution-Non Commercial-No Derivatives 4.0 International (CC BY-NC-ND 4.0) allowing to download articles and share them with others as long as they credit the authors and the publisher, but without permission to change them in any way or use them commercially.

Distribution and Subscriptions:

Bartosz Guterman prenumerata@wydawnictwo-aluna.pl

Graphic design / production:

Grzegorz Sztank

fajne.work

Publisher:

ALUNA Publishing
29 Przesmyckiego st.,
05-510 Konstancin – Jeziorna, Poland
www.wydawnictwo-aluna.pl
www.wiadomoscilekarskie.pl
www.wiadlek.pl

Wiadomości Lekarskie

Medical Advances

Official journal of the Polish Medical Association
Wiadomości Lekarskie has been published since 1928



Editorial Team

Editor in-Chief:

Prof. Paweł Kalinski – Buffalo, USA

Honorary Editor in-Chief:

Prof. Władysław Pierzchała – Katowice, Poland

Deputy Editor in-Chief:

Prof. Waldemar Kostewicz – Warsaw, Poland
President Polish Medical Association

Statistical Editor:

Dr Lesia Rudenko – Konstancin – Jeziorna, Poland

Managing Editor:

Agnieszka Rosa – amarosa@wp.pl

International Editorial Office:

Nina Radchenko (editor) – n.radchenko@wydawnictwo-aluna.pl

International Editorial Board – in-Chief:

Marek Rudnicki Chicago, USA










International Editorial Board – Members:

Stalbek M. Akhunbaev	Bishkek, Kyrgyzstan	Jerzy Robert Ładny	Białystok, Poland
Kris Bankiewicz	San Francisco, USA	Stella Nowicki	Memphis, USA
Christopher Bara	Hannover, Germany	Alfred Patyk	Gottingen, Germany
Krzysztof Bielecki	Warsaw, Poland	Palmira Petrova	Yakutsk, Russia
Zana Bumbuliene	Vilnius, Lithuania	Waldemar Priebe	Houston, USA
Stanislav Czudek	Ostrava, Czech Republic	Maria Siemionow	Chicago, USA
Mowafaq Muhammad Ghareeb	Baghdad, Iraq	Aleksander Sieroń	Katowice, Poland
Nataliya Gutorova	Kharkiv, Ukraine	Vladyslav Smiiianov	Sumy, Ukraine
Marek Hartleb	Katowice, Poland	Tomasz Szczepański	Katowice, Poland
Roman Jaeschke	Hamilton, Canada	Andrzej Witek	Katowice, Poland
Andrzej Jakubowiak	Chicago, USA	Jerzy Woy-Wojciechowski	Warsaw, Poland
Peter Konturek	Saalfeld, Germany	Zbigniew Wszolek	Jacksonville, USA
George Krol	New York, USA	Vyacheslav Zhdan	Poltava, Ukraine

CONTENTS

ORIGINAL ARTICLES

- Alina Tarasiuk, Vitalii Kondratiuk, Oleg A. Bychkov, Tetiana Ostashevskia
Features of the clinical course of arterial hypertension in patients with vitamin D deficiency 1647
- Aidyn G. Salmanov, Grygorii O. Kostromin, Yuliia V. Strakhovetska, Olha D. Leshchova, Roman V. Honza, Oleg V. Balaban, Ruslan S. Tsymbaliuk, Inna A. Nazarenko, Volodymyr M. Ivantsok
Epidemiology of surgical site infection after abdominal surgery in Ukraine: results a multicenter study (2021-2023) 1654
- Haneen Sajid Mahmoud, Hussein A. Saheb, Bassim Mohammad, Ahmed M. Sultan, Sinaa Abdul Amir Kadhim, Asma A. Swadi
Association between plasma angiotensinogen level and response to valsartan among sample of Iraqi hypertensive patients 1662
- Kostyantyn Barannyk, Valeriy Ishkov, Serhiy Barannyk, Ruslan Duka, Robert Molchanov
Features of the morphogenesis of oxalate and urate urinary stones in urolithiasis patients from heavily industrialized region 1672
- Ivan V. Kucher, Andrii P. Liabakh
Features of the macroscopic structure of the posterior inferior tibiofibular ligament based on anatomical study 1680
- Bayan Jabr Hussein, Ban A. Ghani
Evaluation of immunohistochemical expression of collagen type I in bone defect treated by local application of collagen and beta-tricalcium phosphate in rats 1686
- Valeria Tyshchenko, Tymur Ksenzov, Tetiana Odynets, Tetiana Bogoslav, Artur Ksenzov, Ivan Hlukhov, Kateryna Drobot
The research clinical and instrumental methods of examination of athletes related to the process of intervertebral disk degeneration and stenosis 1693
- Nataliia V. Zaviazkina, Tetiana Nefedova
Psychological well – being in breast cancer patients: the role of social support in managing anxiety and depression 1704

- Iryna Vasylieva, Oksana Nakonechna, Liudmyla Popova, Natalia Yarmysh, Anastasiia Bezrodna, Nataliia Pustova
Blood serum interleukins levels and their relationship with colon tissue prostanoids in experimental ulcerative colitis 1712 
- Oleksandra Pryshliak, Oleksandr Boichuk, Sergii Fedorov, Victoriya Kvasniuk, Nadiya Vaskul, Andrii Protsyk, Zoriana Tylishchak
Lyme borreliosis in Ivano-Frankivsk district, Ukraine: a epidemiological and clinical characteristics (2000-2022) 1718 
- Israa Mohammed Mahdy, Hussein A Saheb, Ahmed M Sultan, Bassim I Mohammad, Asma A Swadi, Sinaa Abdul Amir Kadhim
Genetic polymorphism of the CYP11B2 gene in an Iraqi patient with essential hypertension 1726 
- Sanaa Ghali Jabur
Molecular investigate of slim and adhesion genes of *Staphylococcus saprophyticus* isolated from pregnant women with asymptomatic bacteriuria in Thi-Qar governorates 1733 
- liudmyla A. Vygivska, Yevgenia B. Radzishavska, Olesia O. Pliekhova
Features of pregnancy and childbirth in mothers and girls suffering from abnormal uterine bleeding during puberty 1740 
- Siham Mahmood Al-Rehemi, Rasha Hatem Dosh, Maha Jamal Frayyeh, Rihab Hameed Al Mudhafar, Hussein Abdulkadhim
Histopathological, immunohistochemical and physiological study for the hepatoprotective effect of melatonin against inhrifampicin-induced hepatotoxicity in mice model 1745 
- Asma A Swadi, Hussein A Saheb, Ahmed M Sultan
The efficacy and safety of vitamin D supplementation in women with polycystic ovarian syndrome undergoing ovulation induction using letrozole 1753 
- Nataliia I. Preys, Ivan V. Savytskyi, Olga Yu. Denisiuk, Vasyl M. Sarakhan
The study of the hypoxia markers against the background of prolonged hyperglycemia in experimental animals 1759 
- REVIEW ARTICLES**
- Lyudmyla Kaskova, Nataliia Yanko, Iryna Vashchenko, Olena Khmil
Problems of diagnostic of the state of pulp and pulpal diagnoses in children 1763 

Bartłomiej Antoń, Piotr Kaszczewski, Sławomir Nazarewski, Jolanta Małyszko, Zbigniew Gałązka
Advancements in preventing post-contrast acute kidney injury in EVAR: clinical strategies and future directions 1769

Andrii Kovtun, Andrii Gurando, Vadym Telniy, Tetiana Kozarenko
Multimodal management of breast architectural distortion: an analytical literature review 1775

Andrii Yanchyshyn, Inha Samborska, Oleksandr Maievskiy, Iryna Dzevulska
Features of the proteo-peptidome composition and the influence of the scorpion venom toxins on the structure of the heart of mammals (review) 1782

Agnieszka Rolek, Piotr Pławewski
Advancements and applications of laser technology in modern dentistry 1789

Andrii S. Zaitsev, Oleksandr R. Pulyk, Rooslan S. Vastyanov, Oleksandr M. Stoyanov, Yaroslav V. Biesieda, Volodymyr P. Maidanyuk, Serhii V. Zaitsev
Pulmonotoxic xenobiotics and methods of their determination in ambient air of nuclear power plant equipment 1793

Klaudia Korycka, Agata Mormul, Michał Korab, Joanna Smalira
Choking in children: causes, prevention and intervention strategies 1802

SHORT COMMUNICATION

Wojciech Tański, Andrzej Teplicki, Anna Stapkiewicz, Adrianna Szalonka, Izabela Kulas, Beata Jankowska-Polańska
Challenges and opportunities in implementing telemedical solutions for COPD management in the Polish healthcare sector: a presenting own experience 1808

VARIA

Ignat Ignatov, Teodora P. Popova, Alexander I. Ignatov, Ivan Angushev
Graphical modeling of additive color mixing. Perception of objects with different color shades for different observers 1818

Features of the clinical course of arterial hypertension in patients with vitamin D deficiency

Alina Tarasiuk, Vitalii Kondratiuk, Oleg A. Bychkov, Tetiana Ostashevskva

BOGOMOLETS NATIONAL MEDICAL UNIVERSITY, KYIV, UKRAINE

ABSTRACT

Aim: To determine the peculiarities of the daily profile of blood pressure in patients with arterial hypertension (AH) and vitamin D deficiency and insufficiency, to evaluate the parameters of the lipid profile and quality of life in these patients.

Materials and Methods: A total number of 97 patients with uncomplicated AH stage 1 and 2 were divided into 3 groups depending on the level of vitamin D in the blood serum. All patients underwent office blood pressure (BP) measurement and daily ambulatory BP monitoring for 24 hours, biochemical blood test with the determination of indicators of lipid metabolism, questionnaires for quality of life indicators. Statistical processing of the study results was carried out using "IBM SPSS Statistics 22".

Results: "Non-dippers" are most often identified in groups 1 and 2. Their prevalence is 1.8 times higher than in group 3 ($p < 0.05$). The frequency of "night-peakers" in group 1 is 1.7 times higher than in group 2 and 2.6 times higher than in group 3 ($p < 0.05$). Patients with AH and vitamin D deficiency have severe lipid metabolism disorders ($p < 0.05$). The correlation analysis shows a direct relationship of average strength between them and average daily systolic and diastolic BP indicators ($p < 0.05$).

Conclusions: Patients with AH and vitamin D deficiency has an increase in cardiovascular risk, which is manifested by increase in pressure load indicators, frequency of detection of "night-peakers" and lipid metabolism disorders which is worsens of vascular accidents prognosis.

KEY WORDS: quality of life, vitamin D, arterial hypertension, blood pressure monitoring, lipid metabolism

Wiad Lek. 2024;77(9):1647-1653. doi: 10.36740/WLek/191876 DOI

INTRODUCTION

Arterial hypertension (AH) is one of the most important risk factors for global mortality and morbidity and is associated with non-communicable diseases such as atherosclerosis, cardiomyopathy and acute myocardial infarction [1]. In addition, hypertension increases the risk of stroke, heart attack, and chronic renal failure, which imposes a large economic burden on society [2]. The prevalence of hypertension varies in different parts of the world and may depend on demographic factors such as age, race, gender, and socioeconomic status [3].

This problem remains extremely important for Ukraine. Thus, according to STEPS 2019 data, a third part of the population of Ukraine (34.8%, among those surveyed) had high blood pressure (BP) or hypertension or were taking antihypertensive drugs, and the prevalence of the population with high BP increases with age.

Several modifiable and non-modifiable risk factors, such as age, gender, genetics, high sodium intake, low potassium intake, obesity, lack of physical activity, and unhealthy diet are actively involved in the increase of BP

and subsequent development of hypertension [4]. In recent years, another reason for a possible increase in blood pressure has been put forward: vitamin D deficiency [5].

Vitamin D deficiency or insufficiency is becoming a very common disease worldwide. Recent large-scale observational data indicate that about 40% of Europeans have vitamin D deficiency, and 13% – severe deficiency [6, 7]. Vitamin D is already considered not only as a vitamin itself, but also as a fat-soluble steroid hormone that is directly involved in maintaining the health of the musculoskeletal system and calcium-phosphorus metabolism. The two most important forms of vitamin D are ergocalciferol (vitamin D₂), which enters the body with food products, and cholecalciferol (vitamin D₃), which is also synthesized endogenously [8, 9]. The best marker for assessing vitamin D status is serum 25(OH) D, which reliably reflects free fractions of vitamin D metabolites, despite the fact that theoretically bioavailable fractions may be more clinically informative [10, 11].

A large number of studies, both in the field of basic science and clinical research, have highlighted the

strong connection of vitamin D deficiency with many chronic diseases, among which a significant percentage consider vitamin D deficiency as another cause of a possible increase in blood pressure [12-14]. These studies aim to reveal the potential positive effects of vitamin D use in patients with vitamin D deficiency and hypertension [15, 16]. The use of vitamin D supplements is being studied in the treatment of essential hypertension because they are safe and well tolerated by patients and can potentially reduce systolic and diastolic blood pressure [17, 18]. Antihypertensive benefits of vitamin D can be explained by renin-angiotensin-aldosterone system inhibition, prevention and reduction of proteinuria, direct effect on endothelial cells due to the expression of vitamin D receptors in endothelial cells, vascular smooth muscle cells, and cardiac cardiomyocytes [19, 20].

AIM

To determine the peculiarities of the daily profile of blood pressure in patients with arterial hypertension against the background of vitamin D deficiency and its insufficiency, to evaluate the parameters of the lipid profile and quality of life in these patients.

MATERIALS AND METHODS

The study was conducted on the basis of the therapeutic department of the University clinic, which is the clinical base of the department of propaedeutics of internal medicine No. 2 of Bogomolets National medical university. This work is a prospective study. To achieve the goal, we conducted instrumental and laboratory tests, as well as patient questionnaires.

Clinical trial was conducted in accordance with the provisions of the Helsinki Declaration and the study protocol had been agreed with the Bioethics Commission of Bogomolets National Medical University. All patients signed an informed consent before the study.

97 patients with uncomplicated arterial hypertension degree 1 and 2 were examined in total between December 2022 and September 2023. Among patients with hypertension, 3 groups were distinguished depending on the level of vitamin D in the blood serum of patients according to the Endocrine Practice Guidelines Committee [17]. The first group – 33 patients with hypertension and vitamin deficiency D (below 20 ng/ml or 50 nmol/l); the second group – 32 patients with hypertension and vitamin D insufficiency (from 21 to 29 ng/ml or from 50.1 to 74.9 nmol/l); and the third group – 32 patients with hypertension and a sufficient level of vitamin D (above 30 ng/ml or 75 nmol/l). All groups of patients

are comparable in age and sex, groups of patients with AH are comparable in the duration of AH.

Criteria for inclusion in the study: age from 45 to 74 years (middle and old age, according to WHO classification, 1968); the diagnosis of stage II hypertension of the 1st and 2nd degree is established (ESC/ESH Guidelines for the management of arterial hypertension, 2018, 2023); chronic kidney disease not higher than II stage (glomerular filtration rate 60-89 ml / min. / 1.73 m²); ejection fraction of the left ventricle is more than 40%; informed consent to participate in the study. All patients with uncomplicated hypertension received antihypertensive therapy: valsartan 80-160 mg in combination with a calcium channel antagonist (amlodipine 5-10 mg per day). In addition to existing combined antihypertensive therapy, patients received vitamin D3 in a dose of 4000 IU (in case of insufficiency) and 6000 IU (in case of deficiency) [21].

All patients with uncomplicated hypertension underwent office blood pressure (BP) measurement and 24-hour daily blood pressure monitoring (BPM). Office BP was measured according to ESH recommendations. Daily blood pressure monitoring was carried out using the ABPM-04 monitor of the Meditech company (Hungary). Blood pressure was recorded on the “non-working arm” of the patient, and when the asymmetry of the measurements on the right and left arm was more than 10 mm Hg. – on the arm with a higher blood pressure value. The cuff was fixed on the forearm 2 cm above the elbow bend. BP was measured periodically every 15 minutes from 6:00 to 23:00 and every 30 minutes from 23:00 to 6:00, which made it possible to comprehensively analyze its parameters both in the active and passive periods.

All patients underwent a biochemical blood test with the determination of indicators of lipid metabolism: total cholesterol and its fractions - high-density lipoproteins (HDL-C), low-density lipoproteins (LDL-C), very low-density lipoproteins (VLDL-C), triglycerides (TG).

Quality of life indicators were assessed using the SF-36 questionnaire. The 36-Item Short Form Health Survey questionnaire (SF-36) is a very popular instrument for evaluating Health-Related Quality of Life. The SF-36 measures eight scales: physical functioning (PF), role physical (RP), bodily pain (BP), general health (GH), vitality (VT), social functioning (SF), role emotional (RE), and mental health (MH). There are two distinct concepts measured by the SF-36: a physical dimension, represented by the Physical Component Summary (PCS), and a mental dimension, represented by the Mental Component Summary (MCS). All scales do contribute in different proportions to the scoring of both PCS and MCS measures [22].

Table 1. Main indicators of daily blood pressure monitoring in patients with arterial hypertension depending on the concentration of vitamin D

Parameter	Patients with arterial hypertension and vitamin D deficiency (group 1, n=33)	Patients with arterial hypertension and vitamin D insufficiency (group 2, n=32)	Patients with arterial hypertension and normal values of vitamin D (group 3, n=32)
24-hour average SBP, mmHg	146.4±3.98 *	143.7±3.54 *	133.2±2.35
24-hour average DBP, mmHg	86.5±2.36 *	84.8±2.08 *	77.6±1.87
Daytime SBP, mmHg	151.8±4.06 *	147.1±3.84 *	135.1±1.86
Daytime DBP, mmHg	89.8±2.83 *	86.7±2.18 *	80.9±1.33
Nighttime SBP, mmHg	143.6±3.72 *	138.2±3.27 *	122.6±2.25
Nighttime DBP, mmHg	83.7±2.94 *	81.1±2.19 *	70.6±1.62
Time index of the SBP, %	78.2±3.76 * #	69.4±3.18 *	43.8±3.44
Time index of the DBP, %	54.7±3.68 * #	48.6±2.98 *	39.2±2.85
Area index of the SBP, mmHg×h/24h	296.1±44.6 * #	272.8±49.5 *	159.8±29.6
Area index of the DBP, mmHg×h/24 h	120.8±27.9 * #	105.3±24.7 *	61.1±12.8

Note: * – p < 0.05 compared to group 3;

– p < 0.05 compared to group 2;

n – number of patients.

Table 2. The level of lipids in the blood of patients with arterial hypertension depending on the concentration of vitamin D

Parameter	Patients with arterial hypertension and vitamin D deficiency (group 1, n=33)	Patients with arterial hypertension and vitamin D insufficiency (group 2, n=32)	Patients with arterial hypertension and normal values of vitamin D (group 3, n=32)
Total cholesterol, mmol/l	7.24±0.31*#	6.96±0.13*	6.23±0.12
Triglycerides, mmol/l	2.81±0.14*#	1.88±0.13*	1.42±0.11
LDL, mmol/l	4.86±0.18*#	4.24±0.12*	4.08±0.10
HDL, mmol/l	0.96±0.07*#	1.09±0.06*	1.18±0.08
VLDL, mmol/l	0.98±0.06*#	0.85±0.09*	0.66±0.04
Atherogenicity index	4.89±0.11*#	4.39±0.21*	4.18±0.19

Note: * – p < 0.05 compared to group 3;

– p < 0.05 compared to group 2;

n – number of patients.

Statistical processing of the obtained results was carried out using the program "IBM SPSS Statistics. Version 22". Given the normal distribution of the investigated characteristics, parametric statistical methods were used in the samples: for descriptive statistics, the mean value of the indicator (M), standard deviation (SD), standard error (SE), a confidence interval for the mean of 95% (95% CI). Group comparisons were performed using qualitative paired data using Pearson's χ^2 test (with Yates correction), Fisher's exact test. Pearson's correlation coefficient was used to measure the association between variables (BP indicators and the lipidogram).

RESULTS

Daily monitoring of BP makes it possible to assess not only the average, maximum and minimum values of systolic

blood pressure (SBP) and diastolic blood pressure (DBP) at different times of the day, but also to detect the presence or absence of episodes of hypertension and hypotension, to analyze the severity of hypertension according to the time index (TI) and area index (AI), to evaluate the circadian dynamics of blood pressure, which is important for stratifying the risk of developing complications from the patient's target organs. We took these indicators as a basis for the analysis of BP indicators in our patients (Table 1).

As a result of the analysis of the obtained data, we found significantly increased (p<0.05) levels of average daily systolic, diastolic blood pressure in all groups of patients compared to the normal values. The same regularities were observed when analyzing day and night periods separately.

Indicators of pressure load - time index and area index of SBP and DBP - were also significantly higher in all groups of patients with hypertension (p<0.05).

Table 3. Indicators of life quality according to the SF-36 scale in patients with arterial hypertension and vitamin D deficiency and its insufficiency

SF-36 scales	Patients with arterial hypertension and vitamin D deficiency (group 1, n=33)	Patients with arterial hypertension and vitamin D insufficiency (group 2, n=32)	Patients with arterial hypertension and normal values of vitamin D (group 3, n=32)
Physical Functioning, PF	65.3±1.86 *#	71.4±2.59	74.43±2.68
Role Physical, RP	74.4±1.97 *#	79.8±2.35	85.1±2.47
Bodily Pain, BP	61.2±2.66	62.8±2.85	65.1±2.92
General Health, GH	68.7±2.14	70.4±2.36	73.7±2.28
Vitality, V	71.8±1.84 *#	76.7±2.44	80.6±2.62
Social Functioning, SF	67.3±2.08 *#	73.6±2.34	80.1±2.85
Role Emotional, RE	72.3±2.06 *#	82.3±2.26	88.3±2.43
Mental Health, MH	71.3±2.31	73.8±2.62	76.1±2.58

Note: * – $p < 0.05$ compared to group 3;

– $p < 0.05$ compared to group 2;

n – number of patients.

Table 4. Assessment of the «currently» state of health in patients with arterial hypertension and vitamin D deficiency and its insufficiency

«Currently» state of health	Patients with arterial hypertension and vitamin D deficiency (n=33)	Patients with arterial hypertension and vitamin D insufficiency (n=32)	Patients with arterial hypertension and normal values of vitamin D (n=32)
Distinctive	0	0	0
Very beautiful	0	2 (6.3%)	5 (15.6%)
Good	5 (15.2%)	12 (37.5%)	15 (46.9%)
Mediocre	21 (63.6%)	15 (46.9%)	11 (34.3%)
Bad	7 (21.2%)	3 (9.3%)	1 (3.2%)

Note: n – number of patients.

To assess the effect of vitamin D concentration on blood pressure, we compared indicators between three groups of patients.

Thus, the average value of SBP per day in patients with deficiency and insufficiency of vitamin D significantly exceeded the values of SBP in patients with arterial hypertension with a normal concentration of vitamin D by 9.91% and 7.89%, respectively ($p < 0.05$). Similar results were observed for DBP indicators per day, which exceeded the indicators of the third group of patients by 11.46% and 9.28%, respectively ($p < 0.05$). In the patients of the first and second groups, significantly increased levels of average values of blood pressure were also found when analyzing the active and passive periods of the day separately ($p < 0.05$). It should be noted that the average daily BP values in patients with vitamin D deficiency were higher than in patients with insufficiency, but the difference between them was not statistically significant ($p > 0.1$).

In the group of patients with vitamin D deficiency, a significant increase in the in the load of systolic and diastolic pressure per day was found for SBP and DBP.

These indicators statistically significantly exceeded the corresponding values in patients with vitamin D insufficiency by 12.8% for SBP and 12.6% for DBP ($p < 0.05$), as well as the indicators in the group patients with its normal concentration 78.5% for SBP and 39.5% for DBP ($p < 0.05$).

We also studied the level of total cholesterol and its fractions in patients with arterial hypertension depending on their concentration of vitamin D (Table 2).

When analyzing the obtained data, we established a high frequency of increased levels of total cholesterol, LDL-C, TG, VLDL-C and a decrease in HDL-C content, which occurred both in patients with hypertension with a normal concentration of vitamin D and in the presence of its insufficiency and deficiency.

Thus, compared to patients with a normal concentration of vitamin D, hypertensive patients with vitamin D insufficiency had a significantly higher content of total cholesterol by 11.71% ($p < 0.05$), TG – by 32.39% ($p < 0.001$), VLDL-C - by 28.79% ($p < 0.001$). The level of LDL cholesterol was higher than the data of the comparison group by 5.08% ($p < 0.05$). It should be noted

that the level of HDL cholesterol was lower by 7.63% ($p < 0.05$). At the same time, atherogenic index was higher by 6.02% ($p < 0.05$).

Hypertensive patients with vitamin D deficiency had more severe lipid metabolism disorders. The level of cholesterol exceeded the value of the group 3 by 16.21% ($p < 0.001$); the content of LDL cholesterol exceeded the data by 19.12% ($p < 0.001$); the level of VLDL cholesterol also exceeded by 48.49% ($p < 0.001$); the TG level was higher by 97.89% ($p < 0.001$). The level of HDL cholesterol was significantly reduced by 18.64% ($p < 0.001$) from the level of the comparing group. As a result of the above-mentioned violations of the main fractions atherogenic index in these patients was higher by 16.98% compared to the group 3. It should be noted that the above-identified changes statically reliably differed from the corresponding indicators in the group of patients with vitamin D insufficiency ($p < 0.05$).

Based on the results of patient questionnaires using the SF-36 questionnaire, quality of life scores were obtained in the range from 0 to 100, according to which, the more limitations the patients experienced in everyday life, the lower the indicators demonstrated by this questionnaire. In patients with hypertension, depending on the concentration of vitamin D, the following distribution of indicators on the scales was recorded (Table 3).

A decrease in quality of life indicators was observed in patients on most scales.

To the greatest extent, the patients had reduced indicators of physical activity and pain syndrome was observed due to the presence of patients' complaints about headaches, which, according to the patients, "prevent them from working." These changes caused problems at work and in the performance of daily duties. Obviously, it is precisely with these circumstances, as well as with a decrease in vitality and indicators of general and psychological health that a sharp decrease in social functioning (SF) of patients is associated ($p < 0.05$).

Thus, in patients of group 1, a decrease in the physical component of health is observed significantly more often than in groups 2 and 3 (respectively, $\chi^2 = 5.1$ and $\chi^2 = 4.9$, $p < 0.05$), and a decrease in the mental component of health in 2.8 times more often than in group 3 ($\chi^2 = 8.4$, $p < 0.05$). The structure of the quality of life is dominated by a decrease in physical, role, emotional, social functioning and vitality. PF in patients with vitamin D deficiency was 8.6% lower than in patients with vitamin D insufficiency and 12.3% lower than in patients with normal concentration ($p < 0.05$); RP – respectively lower by 6.8% and 12.6% ($p < 0.05$); RE – respectively lower by 12.2% and 18.1% ($p < 0.05$); SF – respectively

lower by 8.5% and 15.9% ($p < 0.05$); V – respectively lower by 6.4% and 10.9% ($p < 0.05$).

One of the points of the SF-36 questionnaire, the so-called "transition point of health", which is not used in the processing of points on any of the scales, allowed to determine the state of health (in the opinion of the patient) at this moment in time (Table 4).

The most indicative data were precisely in the case of a combination of hypertension and vitamin D deficiency. The majority of patients - 21 (63.6%) at the time of the survey noted their state of health as "mediocre"; 7 patients (21.2%) indicated "poor" and only 5 patients (15.2%) indicated "good" health. All patients with a daily BP profile of "Night-peackers" rated their condition as mediocre or poor.

DISCUSSION

Having conducted a comprehensive assessment of the obtained results, we noted certain features of the clinical course of the combined pathology in our patients. During the analysis of the circadian profile of blood pressure, we established that "non-dippers" are most often identified in groups 1 and 2. Their prevalence does not differ among both groups ($p > 0.1$), but is 1.8 times higher than in patients of group 3 ($\chi^2 = 4.2$, $p < 0.05$). Among patients of group 1, the highest frequency of the most unfavorable circadian profile was found "night-peackers", which is 1.7 times higher than in group 2 ($\chi^2 = 3.9$, $p < 0.05$) and 2.6 times higher than in group 3 ($\chi^2 = 4.3$, $p < 0.05$). The high frequency of "non-dippers" found in patients with deficiency and insufficiency of vitamin D may indicate an increase in cardiovascular risk in these patients [19, 23].

We also established a high frequency of lipid metabolism disorders in patients with hypertension, as well as when it is combined with deficiency and insufficiency of vitamin D, in which the content of TG, LDL-C, VLDL-C and atherogenic index was significantly higher than in patients of the comparison group. This statement is due to a higher frequency of metabolic disorders in such patients and a higher percentage of people with excess body weight and obesity of the I-II degree [13, 22].

Correlation analysis to assess the relationship between blood pressure indicators and the lipidogram showed a direct relationship of average strength between average daily SBP indicators and the level of total cholesterol ($r = 0.58$, $p < 0.05$), LDL-C ($r = 0.61$, $p < 0.05$) and TG ($r = 0.54$, $p < 0.05$), as well as a negative relationship between average strength and HDL-C level ($r = -0.38$, $p < 0.05$) in the group of patients with hypertension with a deficiency of vitamin D. Similar changes were observed for indicators of average DBP. With its increase,

the levels of total cholesterol ($r=0.56$, $p<0.05$), LDL-C ($r=0.57$, $p<0.05$), and TG ($r=0.53$, $p<0.05$) increased, and the HDL-C level decreased ($r=-0.36$, $p<0.05$).

The study of indicators of life quality in patients with combined pathology is important for assessing the total impact of diseases on the physical, psychological and social state of a person through an integral assessment of the patient's subjective feelings. Based on the test data, we assume that vitamin D deficiency makes a significant contribution to the decrease in quality of life indicators of the studied patients. In patients of group 1, a decrease in the physical component of health is observed significantly more often than in groups 2 and 3 (respectively, $\chi^2=5.1$ and $\chi^2=4.9$, $p<0.05$), and a decrease in the mental component of health in 2.8 times more often than in group 3 ($\chi^2=8.4$, $p<0.05$). The structure of the life quality is dominated by a decrease in physical, role, emotional functioning and vitality ($p<0.05$). This can be explained by the fact that, in addition to the complaints inherent in hypertension, such as headache, dizziness, heart pain, patients experience unusual fatigue, bone and joint pain, muscle pain, and urination disorders. The combination of these characteristic complaints leads to a violation of the performance of even ordinary daily work. Since both hypertension and vitamin D deficiency are chronic diseases that lead to long-term physical deterioration, they also cause secondary problems of a psychological and social nature.

CONCLUSIONS

Patients with hypertension in combination with vitamin D deficiency have more significant changes in the daily blood pressure profile, which are manifested by an increase in

pressure load time index (statistically significantly exceeded the corresponding values in patients with vitamin D insufficiency by 12.8% for SBP and 12.6% for DBP ($p<0.05$), as well as the indicators in the group patients with its normal concentration 78.5% for SBP and 39.5% for DBP ($p<0.05$)) and also an increase in the frequency of detection of "night-peackers" by 1.7 and 2.6 times respectively ($p<0.05$), which may indicate an increase in cardiovascular risk in patients.

A high frequency of lipid metabolism disorders are established in patients with hypertension combined with a deficiency of vitamin D. The patients have a significantly higher level of cholesterol, TG, LDL-C and atherogenic index compared to patients with vitamin D insufficiency and with its normal concentration ($p<0.05$). The indicators of the daily profile of blood pressure, such as average daily SBP and average daily DBP have a direct relationship correlation with the level of cholesterol ($r=0.58$, $r=0.56$, respectively, $p<0.05$), LDL-C ($r=0.61$, $r=0.57$, respectively, $p<0.05$) and TG ($r=0.54$, $r=0.53$, respectively, $p<0.05$), as well as a negative relationship with the level of HDL-C ($r=-0.38$, $r=-0.36$, respectively, $p<0.05$).

The identified changes are also confirmed in the patients' subjective assessment of the indicators of the quality of life, which is manifested by a decrease in physical, role, emotional functioning and vitality ($p<0.05$), and is observed to the greatest extent in patients with hypertension with vitamin D deficiency – a decrease in the physical component of health is observed significantly more often than in groups 2 and 3 (respectively, $\chi^2=5.1$ and $\chi^2=4.9$, $p<0.05$), and a decrease in the mental component of health in 2.8 times more often than in group 3 ($\chi^2=8.4$, $p<0.05$).

REFERENCES

1. Virani SS, Alonso A, Benjamin EJ et al. American Heart Association Council on Epidemiology and Prevention Statistics Committee and Stroke Statistics Subcommittee. Heart Disease and Stroke Statistics–2020 Update: A Report From the American Heart Association. *Circulation*. 2020;141(9):e139–e596. doi: 10.1161/CIR.0000000000000757. DOI
2. Unger T, Borghi C, Charchar F, Khan NA. 2020 International Society of Hypertension Global Hypertension Practice Guidelines. *Hypertension*. 2020;75(6):1334–1357. doi: 10.1161/HYPERTENSIONAHA.120.15026. DOI
3. Oori MJ, Mohammadi F, Norouzi K et al. Conceptual Model of Medication Adherence in Older Adults with High Blood Pressure–An Integrative Review of the Literature. *Curr Hypertens Rev*. 2019;15(2):85–92. doi: 10.2174/1573402114666181022152313. DOI
4. Mills KT, Stefanescu A, He J. The global epidemiology of hypertension. *Nat Rev Nephrol*. 2020;16(4):223–237. doi: 10.1038/s41581-019-0244-2. DOI
5. Mehta V, Agarwal S. Does Vitamin D Deficiency Lead to Hypertension? *Cureus*. 2017;9(2):e1038. doi: 10.7759/cureus.1038. DOI
6. Cashman KD, Dowling KG, Škrabáková Z et al. Vitamin D deficiency in Europe: pandemic? *Am J Clin Nutr*. 2016;103(4):1033–44. doi: 10.3945/ajcn.115.120873. DOI
7. Cashman KD. Vitamin D Deficiency: Defining, Prevalence, Causes, and Strategies of Addressing. *Calcif Tissue Int*. 2020;106(1):14–29. doi: 10.1007/s00223-019-00559-4. DOI
8. Ross AC, Taylor CL, Yaktine AL et al. Committee to Review Dietary Reference Intakes for Vitamin D and Calcium. Dietary Reference Intakes for Calcium and Vitamin D. Institute of Medicine (US). Washington (DC): National Academies Press (US). 2011.
9. Martucci G, Tuzzolino F, Arcadipane A et al. The effect of high-dose cholecalciferol on bioavailable vitamin D levels in critically ill patients: a post hoc analysis of the VITdAL-ICU trial. *Intensive Care Med*. 2017;43(11):1732–1734. doi: 10.1007/s00134-017-4846-5. DOI

10. Bikle DD. Vitamin D: Newer Concepts of Its Metabolism and Function at the Basic and Clinical Level. *J Endocr Soc.* 2020;4(2):bvz038. doi: 10.1210/jendso/bvz038. [DOI](#)
11. Bouillon R, Carmeliet G, Lieben L et al. Vitamin D and energy homeostasis: of mice and men. *Nat Rev Endocrinol.* 2014;10(2):79-87. doi: 10.1038/nrendo.2013.226. [DOI](#)
12. Mokhtari E, Hajhashemy Z, Saneei P. Serum Vitamin D Levels in Relation to Hypertension and Pre-hypertension in Adults: A Systematic Review and Dose-Response Meta-Analysis of Epidemiologic Studies. *Front Nutr.* 2022;9:829307. doi: 10.3389/fnut.2022.829307. [DOI](#)
13. Gholami F, Moradi G, Zareei B et al. The association between circulating 25-hydroxyvitamin D and cardiovascular diseases: a meta-analysis of prospective cohort studies. *BMC Cardiovasc Disord.* 2019;19(1):248. doi: 10.1186/s12872-019-1236-7. [DOI](#)
14. Kunutsor SK, Apekey TA, Steur M. Vitamin D and risk of future hypertension: meta-analysis of 283,537 participants. *Eur J Epidemiol.* 2013;28(3):205-21. doi: 10.1007/s10654-013-9790-2. [DOI](#)
15. He S, Hao X. The effect of vitamin D3 on blood pressure in people with vitamin D deficiency: A system review and meta-analysis. *Medicine (Baltimore).* 2019;98(19):e15284. doi: 10.1097/MD.00000000000015284. [DOI](#)
16. Legarth C, Grimm D, Wehland M et al. The Impact of Vitamin D in the Treatment of Essential Hypertension. *Int J Mol Sci.* 2018;19(2):455. doi: 10.3390/ijms19020455. [DOI](#)
17. Sheikh V, Mozaianimonfared A, Gharakhani M et al. Effect of vitamin D supplementation versus placebo on essential hypertension in patients with vitamin D deficiency: a double-blind randomized clinical trial. *J Clin Hypertens (Greenwich).* 2020;22(10):1867-1873. doi: 10.1111/jch.13926. [DOI](#)
18. Wu L, Sun D. Effects of calcium plus vitamin D supplementation on blood pressure: a systematic review and meta-analysis of randomized controlled trials. *J Hum Hypertens.* 2017;31(9):547-554. doi: 10.1038/jhh.2017.12. [DOI](#)
19. Zhang D, Cheng C, Wang Y et al. Effect of Vitamin D on Blood Pressure and Hypertension in the General Population: An Update Meta-Analysis of Cohort Studies and Randomized Controlled Trials. *Prev Chronic Dis.* 2020;17:E03. doi: 10.5888/pcd17.190307. [DOI](#)
20. Qi D, Nie X, Cai J. The effect of vitamin D supplementation on hypertension in non-CKD populations: A systemic review and meta-analysis. *Int J Cardiol.* 2017;227:177-186. doi: 10.1016/j.ijcard.2016.11.040. [DOI](#)
21. Grygorieva N, Tronko M, Kovalenko V et al. Ukrainian Consensus on Diagnosis and Management of Vitamin D Deficiency in Adults. *Nutrients.* 2024;16(2):270. doi: 10.3390/nu16020270. [DOI](#)
22. Lins L, Carvalho FM. SF-36 total score as a single measure of health-related quality of life: Scoping review. *SAGE Open Med.* 2016;4:2050312116671725. doi: 10.1177/2050312116671725. [DOI](#)
23. Chen C, Chen Y, Weng P et al. Association of 25-hydroxyvitamin D with cardiometabolic risk factors and metabolic syndrome: a mendelian randomization study. *Nutr J.* 2019;18(1):61. doi: 10.1186/s12937-019-0494-7. [DOI](#)

CONFLICT OF INTEREST

The Authors declare no conflict of interest

CORRESPONDING AUTHOR

Oleg A. Bychkov

Bogomolets National Medical University
13T. Shevchenko boulevard, 01601 Kyiv, Ukraine
e-mail: oleg_bichkov@yahoo.com

ORCID AND CONTRIBUTIONSHIP

Alina Tarasiuk: 0000-0003-0079-232X [A](#) [B](#) [C](#) [D](#)
Vitalii Kondratiuk: 0000-0002-4891-2338 [A](#) [E](#) [F](#)
Oleg A. Bychkov: 0000-0002-6820-1736 [A](#) [D](#) [E](#)
Tetiana Ostashevskaya: 0000-0001-9878-7304 [D](#) [E](#)

[A](#) – Work concept and design, [B](#) – Data collection and analysis, [C](#) – Responsibility for statistical analysis, [D](#) – Writing the article, [E](#) – Critical review, [F](#) – Final approval of the article

RECEIVED: 11.03.2024

ACCEPTED: 01.08.2024



Epidemiology of surgical site infection after abdominal surgery in Ukraine: results a multicenter study (2021-2023)

Aidyn G. Salmanov¹, Grygorii O. Kostromin², Yuliia V. Strakhovetska³, Olha D. Leshchova⁴, Roman V. Honza², Oleg V. Balaban², Ruslan S. Tsymbaliuk², Inna A. Nazarenko², Volodymyr M. Ivantsok²

¹SHUPYK NATIONAL HEALTHCARE UNIVERSITY OF UKRAINE, KYIV, UKRAINE

²BOGOMOLETS NATIONAL MEDICAL UNIVERSITY, KYIV, UKRAINE

³MEDICAL CENTRE "ASHERA", KHARKIV, UKRAINE

⁴PRIVATE ESTABLISHMENT OF HIGHER EDUCATION "DNIPRO INSTITUTE OF MEDICINE AND PUBLIC HEALTH", DNIPRO, UKRAINE

ABSTRACT

Aim: To estimate the incidence, and to describe of antimicrobial resistance in responsible pathogens, and risk factors for surgical site infection (SSI) after abdominal surgery in Ukraine.

Materials and Methods: This were a multicenter, prospective cohort study performed in ten tertiary care hospitals from different regions of Ukraine. Definitions of SSIs after abdominal surgery were adapted from the European Centre for Disease Prevention and Control Surveillance of SSI. The incidence of SSI and predisposing risk factors were noted.

Results: Among 6,740 patients, 1,110 (16.5%) SSIs after abdominal surgery were observed. Of these cases, 45.8% superficial SSIs, 37.3% deep SSIs, and 16.9% was as organ/space SSIs. Of all SSI cases, 29.9% were detected after hospital discharge. The independent predictors of SSI were open surgical approach, emergency operation, and longed operation duration. The main pathogens of SSI were *Escherichia coli* (52%), followed by *Staphylococcus aureus* (9.1%), *Enterococcus* spp. (7.3%), *Pseudomonas aeruginosa* (7.1%), *Acinetobacter baumannii* (6.3%), *Stenotrophomonas maltophilia* (5.7%), *Serratia marcescens* (5.3%), and *Klebsiella pneumoniae* (5.1%). Meticillin resistance *S. aureus* (MRSA) and vancomycin resistance *Enterococcus* spp. (VRE) was found in 21.3% and 14.8% isolates, respectively.

Conclusions: This study found a high prevalence of SSI after abdominal surgery caused by multidrug-resistant organisms, varying widely depending on the bacterial species, and antimicrobial group in Ukraine. To minimise the risk of complications after abdominal surgery, it is essential to take several preventive measures before, during, and after the surgery.

KEY WORDS: abdominal surgery, open surgery, laparoscopic surgery, surgical site infection, risk factors, antimicrobial resistance, Ukraine

Wiad Lek. 2024;77(9):1654-1661. doi: 10.36740/WLek/193762 DOI

INTRODUCTION

Surgical site infection (SSI) is a type of healthcare-associated infection (HAI) in which a wound infection occurs after an surgical procedure. SSIs are one of the most frequent complications in abdominal surgery and is associated with substantial morbidity and cost. SSIs have been shown to compose up to 20% of all healthcare-associated infections. At least 5% of patients undergoing a surgical procedure develop a surgical site infection [1]. The human and financial costs of treating SSIs are increasing [2]. According to the literature, SSIs command the highest economic toll, tallying an annual average cost of USD 3.3 billion [3].

To enhance patients' quality of life and reduce their total medical expenditures, it is vital to reduce the frequency of their SSI claims. This enduring issue is further compounded by the mounting challenge of

antibiotic resistance, a surge in surgical interventions, and the presence of comorbidities among patients. Thus, a comprehensive exploration of all discernible risk factors, as well as proactive preventive and prophylactic strategies, becomes imperative [4].

Most SSIs are preventable. Measures can be taken in the pre-, intra- and postoperative phases of care to reduce the risk of infection [1]. However, the prevalence of multidrug-resistant microorganisms has reached alarming proportions [5, 6]. Many pathogens of SSIs may be implicated in these infections, especially multi-drug-resistant organisms (MDROs), which have the ability to spread from patient to patient and to easily acquire antibiotic resistance [7-9]. Therefore, the identification of bacterial pathogens and their antibiotic susceptibility pattern is required for the successful treatment of SSI and curb antimicrobial resistance. Consequently,

there is an acute need to investigate and scrutinize all potential therapeutic interventions to counter this burgeoning threat.

According to the literature, SSIs are more common in elderly patients, patients undergoing emergency surgeries, those with a longer preoperative hospital stay and longer surgical duration, and patients with a high American Society of Anesthesiologists (ASA) Index [10]. According to the literature, the ASA index has been recognized as a risk factor of SSI in many studies [11-13]. Consequently, there is an acute need to investigate and scrutinize all potential therapeutic interventions to counter these infections.

In Ukraine few studies have evaluated the relative importance of surgical site infection risk factors in terms of consistency in abdominal surgery. Currently, antimicrobial resistance in responsible pathogens, and risk factors for SSIs after abdominal surgery in Ukraine for developing the condition remain largely unknown. Therefore, should be conducted to study the risk factors, pathogens, complications, and outcomes of surgical site infections in depth.

AIM

The aim this study to estimate the prevalence and incidence, and to describe of antimicrobial resistance in responsible pathogens, and risk factors for SSIs after abdominal surgery in Ukraine.

MATERIALS AND METHODS

DESIGN, SETTING AND PATIENTS

This were a multicenter, prospective cohort study performed in ten tertiary care hospitals from different regions (Kyiv, Zhytomyr, Vinnytsia, Lviv, Dnipro, Kharkiv, Odesa) of Ukraine. This study was performed partly as a cross-sectional study to estimate occurrence of SSI, partly as a case-control study to look for factors associated with SSIs. This study was conducted over a period of 36 months, from January 2021 to December 2023. The study included adult patients (male and female) aged ≥ 18 years who underwent abdominal surgery who stayed for more than 48 h in hospitals. In this study all patients were local residents. This study including patients undergoing abdominal surgery (vascular, gastrointestinal, colorectal, appendectomy, gynecological, urological or plastic indications). Liver resection, pancreatectomy, organ transplantation, pregnant women, and patients with urinary tract infection, and gastrointestinal infections were excluded from this

study. Patients who left the operating theatre with an open packed wound or with a vacuum-assisted dressing were also excluded.

DEFINITIONS

The surgical procedure records included in the study were of patients and performed in accordance with the National Healthcare Safety Network (NHSN). An NHSN procedure is defined as that performed in an operating room where the surgeon makes at least one incision that is closed before leaving the operating room [14]. An SSI associated with abdominal surgery was defined as an infection arising >48 h after operative procedure and not present or incubating on admission, unless the patient had been discharged from hospital within a defined period. An incident of SSI after abdominal surgery was defined by microbiologically confirmed European Centre for Disease Prevention and Control (ECDC) surveillance of surgical site infections and prevention indicators [15]. The surgical wound classification is categorized by the degree of gross contamination (clean, clean-contaminated, contaminated, and dirty) [16]. Physical status classification developed by the American Society of Anesthesiologists (ASA) [17].

DATA COLLECTION

We collected data from medical records, including demographic, clinical, microbiological data, and radiographic investigations, and invasive procedures, smoking status, body mass index, and comorbid. Operative variables included operation performed, duration of surgery, use of prophylactic antibiotics, wound contamination class, surgical approach (open v. laparoscopic), urgency of surgery and drain use. In this study, data were collected for two types of surgical approaches used for abdominal surgery: (1) open surgery and (2) laparoscopic or endoscopic surgery. SSI was classified as superficial (involving the skin and subcutaneous tissue only), deep (involving deeper soft tissues such as fascia and muscle layers) or organ space (involving any part of the anatomy that was opened or manipulated during surgery) [15]. We used the American Society of Anesthesiologists (ASA) classification for categorization of a patient's physiological status that can help predict operative risk [16].

MICROBIOLOGICAL ANALYSIS

In this study pathogens identification was performed with standard microbial methods. Antibiotic suscepti-

Table 1. Distribution of surgical site infection by wound class after open and laparoscopic surgery in Ukraine, 2021-2023

Wound class	All surgical procedures (n=6,740)	Type of surgical approaches				Total SSI (n=1,110)	
		Open (n=2,760)		Laparoscopic (n=3,980)		n	%
		Number of procedure	SSI n (%)	Number of procedure	SSI n (%)		
Clean	4112	1628	237(5.8)	2484	73(1.8)	310	7.5
Clean-contaminated	1689	662	346(20.5)	1027	97(5.7)	443	24.1
Contaminated	712	299	197(27.7)	413	79(11.1)	276	35.8
Dirty or infected wounds	227	171	69(30.4)	56	12(5.3)	81	32.6
Total	6740	2760	849(12.6)	3980	261(3.8)	1,110	16.5

Table 2. Demographic and preoperative characteristics of patients, who underwent abdominal surgeries in Ukraine (2021-2023)

Variable	SSI		p value
	No (n=5,640)	Yes (n=1,110)	
	n (%)	n (%)	
Age, yr, median	40 (31–52)	54 (43–61)	< 0.001
Gender			
Male	2,080 (36.9)	800 (73.0)	
Female	3,560 (63.1)	300 (27.0)	
Body mass index (median)	29 (25–36)	27 (25–31)	0.02
ASA score			< 0.001
1	2,860 (50.7)	320 (29.0)	
2	2,140 (37.9)	260 (24.0)	
3	620 (11.0)	360 (33.0)	
4	20 (0.4)	120 (11.0)	
5	0 (0.0)	40 (4.0)	
Diabetic	1,040 (18.4)	360 (33.0)	0.02
Smoking status			0.004
Current smoker	720 (12.8)	100 (9.0)	
Former smoker	160 (2.8)	100 (9.0)	
Nonsmoker	4,320 (76.6)	680 (62.0)	
Unknown	440 (7.8)	220 (20.0)	
Steroid use	220 (3.9)	80 (7.0)	0.3
Chemotherapy	120 (2.1)	80 (7.0)	0.04
Preoperative hemoglobin level, g/L, median	13 (12–14)	12 (11–14)	0.1
Preoperative albumin level, g/L, median	36 (33–38)	31 (26–35)	< 0.001
Benign disease	5,340 (94.7)	660 (60.0)	< 0.001

ASA, American Society of Anesthesiologists; SSI, surgical site infection

bility testing of isolates was determined according to the protocol of the European Committee on Antimicrobial Susceptibility Testing (EUCAST) (<http://euca.st.org>). In this study an isolate is considered resistant to an antimicrobial agent when tested and interpreted as R in accordance with the EUCAST. When combining results for antimicrobial agents representing an antimicrobial group, the outcome is based on the most resistant result.

ETHICS

Approval for this study was obtained from the Institutional ethics committee, Shupyk National Healthcare University of Ukraine.

STATISTICAL ANALYSIS

In this study all clinical and microbiological data were recorded in the Microsoft excel sheets. Statisti-

Table 3. Operative and postoperative characteristics of patients, who underwent abdominal surgeries in Ukraine (2021-2023)

Variable	SSI		p value
	No	Yes	
	n (%)	n (%)	
Type of operative procedure			<0.001
Laparoscopic gynecologic surgery	2120 (37.6)	100 (9.0)	
Hernia repair	1220 (21.6)	120 (11.0)	
Gastric sleeve/bypass	1120 (19.8)	0 (0)	
Appendectomy	280 (5.0)	80 (7.0)	
Laparotomy	220 (3.9)	480 (44.0)	
Colectomy/abdominoperineal resection	120 (2.1)	100 (9.0)	
Cholecystectomy	80 (1.4)	160 (14.0)	
Other	480 (8.5)	60 (5.0)	
Wound class			<0.001
Clean	1,060 (18.8)	60 (5.0)	
Clean-contaminated	4,380 (77.6)	760 (69.0)	
Contaminated/dirty	200 (3.5)	280 (25.0)	
Urgency			<0.001
Emergent	1000 (17.7)	600 (54.0)	
Elective	4,640 (82.3)	500 (45.0)	
Approach			<0.001
Laparoscopic	3,840 (68.1)	140 (13.0)	
Laparoscopic converted to open	60 (1.1)	60 (5.0)	
Open midline	700 (12.4)	700 (64.0)	
Open nonmidline	1,040 (18.4)	200 (18.0)	
Length of operation, min, median	83 (110–155)	184 (113–292)	<0.001
Drains	1,560 (27.6)	540 (49.0)	0.007
Blood transfusion	280 (5.0)	440 (40.0)	<0.001
Postoperative stay, d, median	2 (1–3)	14 (6–25)	<0.001
Intensive care unit admission	440 (7.8)	560 (51.0)	<0.001
Death within 30 d	40 (0.7)	40 (4.0)	0.07

SSI, surgical site infection.

cal analysis was carried out using a computer based statistical analysis program Microsoft Excel 2019 and statistical packages, SPSS version16 (IBM Corp, Armonk, NY, USA). Frequencies and percentages were calculated for categorical variables. Mean and standard deviation (SD) were calculated for continuous variables. The overall incidence of SSI was calculated and correlated with predisposing risk factors. We used the Pearson and Wilcoxon univariable tests to guide the multivariable models for discrete and continuous variables, respectively. We used multivariable logistic regression models to identify preoperative and operative variables independently associated with SSI. The results are presented using tables. P-value ≤ 0.05 was taken as significant.

RESULTS

INCIDENCE OF SSI

A total of 6,740 patients, who underwent abdominal surgeries from January 2021 to December 2023 in Ukrainian tertiary care hospitals, were included in this cohort study. Among these patients, 1,110 (16.5%, 95% CI: 16.2-16.6) after surgery procedures were found to have SSIs. Of these cases, 45.8% superficial SSIs, 37.3% deep SSIs, and 16.9% was as organ/space SSIs. Of the total SSI, 29.9% were detected after hospital discharge. SSIs after abdominal surgery were the most common in contaminated wounds (35.8%) followed by dirty (32.6%), clean-contaminated (24.1%), and clean wounds (7.5%) (Table 1). However, the results were not

Table 4. Multivariate logistic regression analysis of factors associated with surgical site infection after abdominal surgery in Ukraine, 2021–2023

Risk factor	OR (95% CI)
Male sex	2.6 (1.02–6.6)
Length of operation (86 min v. 181 min [25th v. 75th percentile])	2.1 (1.23–3.6)
Urgency (emergent v. elective)	4.7 (1.58–14.4)
Approach (open vs. laparoscopic)	6.5 (2.16–19.6)
Age	1.09 (0.57–2.1)
Body mass index	1.20 (0.68–2.1)
Smoking	0.55 (0.15–2.1)
Diabetic	1.52 (0.52–4.5)
ASA score	1.27 (0.75–2.2)
Blood transfusion	0.93 (0.28–3.2)
Preoperative albumin level	0.91 (0.63–1.3)
Malignant disease	2.35 (0.65–8.5)
Preoperative antibiotic	2.32 (0.71–7.6)
Wound type (contaminated/dirty vs. clean-contaminated)	1.59 (0.48–5.3)

ASA, American Society of Anesthesiologists; CI, confidence interval; OR, odds ratio.

statistically significant. Open and laparoscopic types of surgical approaches for abdominal surgery were, 40.9% (2,760/6,740) and 59.1% (3980/6740), respectively. The incidence of SSI depended on the microbial contamination of wounds and was discrepant between open and laparoscopic types of surgical approaches surgeries. Incidence rate of SSIs were, 12.6% (open surgery) and 3.8% (laparoscopic surgery), respectively. The distribution of SSI by wound classes after open and laparoscopic surgeries is presented in Table 1.

Of the 6,740 abdominal surgical procedures, 2,880 (42.7%) were performed on males and 3,860 (57.3%) on females. The mean age of the study patients was 43.7 ± 5.9 years. In this study SSI was more common in male gender than in female (14.5% vs. 4.5%). The mean body mass index was 31 ± 5.7 . In this study 20.8% patients, who underwent abdominal surgeries were diabetic, and 12.2% were current smokers, and 82.8% had an ASA score less than 3. Demographic and preoperative characteristics of patients, who underwent abdominal surgeries are presented in Table 2.

The mean operative time in surgical procedures was 145.2 minutes. Of all surgical procedures, 59.1% were performed laparoscopically. Most patients (76.3%) underwent elective abdominal surgery. In this study, the most frequent type of abdominal surgery was laparoscopic gynecologic procedure (32.9%), followed by hernia repair (19.9%) and gastrointestinal surgery (16.6%). Operative and postoperative characteristics of patients, who underwent abdominal surgeries are presented in Table 3.

The highest SSI rate among patients, who underwent abdominal surgeries was detected in laparotomy proce-

dures: In our study, postoperative SSI developed in 69% of the 700 patients in this group. The incidence rate of SSI after abdominal surgery was 12.6% following open operations, compared to 3.8% following laparoscopic procedures ($p < 0.001$). Postoperative SSI developed in 61% of the 720 patients with malignant disease, compared to 11.0% of the 6,000 patients with benign disease ($p < 0.001$). In this study, the 30-day mortality rate was 0.7% among non-infected patients and 3.6% among infected patients.

RISK FACTORS

In present study, patients with postoperative SSI were older than noninfected patients (73% vs. 36.9%, respectively, $p < 0.001$). Almost half (47.2%) of all patients with SSI had an ASA physical status classification score >2 . The most patients (54.1%) of patients with postoperative SSI underwent emergency surgery, and most (87%) had an open surgical approach. Use of steroids, preoperative hemoglobin level, prophylactic antibiotic therapy and death within 30 days were not associated with SSI on univariable analysis. In this study, SSI after abdominal surgery was more likely to develop in patients who underwent emergent operations than those who underwent elective procedures. Surgical procedure duration (operation time) also are predictors of SSI, with odds ratios (OR) of 2.1 (95% CI 1.23–3.6). We found that length of hospital stay was predicted to increase with open versus laparoscopic procedures, long operative times. Multivariate logistic regression analysis of factors associated with SSI after abdominal surgery is presented in Table 4.

RESPONSIBLE PATHOGENS AND ANTIMICROBIAL RESISTANCE

In this study microbiological cultures were available for all patients with SSI. In total, 1,487 pathogens (Gram-negative and -positive bacteria) were isolated from 1,110 patients with postoperative SSI. The most commonly implicated pathogens were *Escherichia coli* (52%), followed *Staphylococcus aureus* (9.1%), *Enterococcus* spp. (7.3%), *Pseudomonas aeruginosa* (7.1%), *Acinetobacter baumannii* (6.3%), *Stenotrophomonas maltophilia* (5.7%), *Serratia marcescens* (5.3%), and *Klebsiella pneumoniae* (5.1%). Among responsible pathogens, methicillin resistance *S. aureus* (MRSA) and vancomycin resistance *Enterococcus* spp. (VRE) was found in 21.3% and 14.8% isolates, respectively. Resistance to third-generation cephalosporins was detected in *K. pneumoniae* (61.2%) and *E. coli* (36.1%). Carbapenem resistance was found in 22.1% of all Enterobacteriales. In present study, all of our patients were given the antibiotic prophylaxis according to our standard hospital protocols. However, only 24.5% of responsible pathogens of SSIs were sensitive to the prophylactic antibiotic given preoperatively.

DISCUSSION

The results presented in this study are based on multicentre, prospective surveillance data. The primary objectives of this study were to describe the incidence and risk factors associated with SSI in patients undergoing abdominal surgery. The secondary objectives were to study the microbiological pattern of SSI in our population and their antibiotic resistance in responsible pathogens in Ukrainian tertiary care hospitals. We found a high incidence of SSI cases caused by MDROs. These pathogens varying depending on the bacterial species, and antimicrobial group in Ukraine. This study expands upon the previous reports and is the first study to publish frequent pathogens and/or characterization of the antimicrobial resistance of responsible pathogens of SSI after abdominal surgery in Ukraine [5, 6].

According to the literature, the incidence of SSI after abdominal surgery ranges from 1.2 to 7.5% [18-20]. However, our rate of SSI is slightly higher than those reported in these studies. In our study, SSI developed in 16.5% undergoing abdominal surgery, compatible with reported in the literature [21, 22]. A higher incidence rate (21.8% and 24.2%) of SSI after abdominal surgery was found in two studies [23, 24].

In present study, multivariable analysis identified open surgical approach, emergency operation, length of the operation and male sex as independent predictors of SSI after abdominal surgery. According to

the literature, open surgical approach and emergency surgery were documented as risk factors for SSI in previous reports [19-21, 25]. We found that patients who had open surgery were 6.5 times more likely to get SSI than those who had laparoscopic surgery. Emergency surgery increased the risk of SSI fivefold compared to elective surgery. The duration of surgery procedure was an independent predictor for SSI. A patient who had an operation lasting longer than the 75th percentile (> 3 h in our cohort) had double the risk of SSI in contrast to an operation lasting less than the 25th percentile (86 min). This finding is in keeping with previous study [22].

According to the literature, longer operative time reflects the complexity of the surgery. It would also increase the wound susceptibility to infection by increasing the exposure to potential contamination and decreasing the tissue concentration of antibiotic [26].

The ASA score and wound class were not significant predictors of SSI after abdominal surgery in the multivariable model in our study. Certain other known risk factors for SSI such as body mass index, diabetes and smoking were also not found to be statistically significant.

In this study, the commonest organisms isolated from patients with SSI after abdominal surgery were gram-negative bacteria. The most commonly implicated responsible pathogens of SSIs were *E. coli*, followed *S. aureus*, *Enterococcus* spp., *P. aeruginosa*, *A. baumannii*, *S. maltophilia*, *S. marcescens*, and *K. pneumoniae*. The most authors reported findings similar to ours, with more common gram-negative bacteria isolated from the infected abdominal wounds [4-6]. We also found that most of the pathogens were multidrug-resistant organisms to the commonly prescribed prophylactic antibiotics. This might explain why we found a high rate of deep SSI after abdominal surgery. Therefore, further consideration regarding the selection of appropriate prophylactic antibiotics will be needed, especially in patients at high risk.

Knowing the risk factors can help us in earlier risk stratification, prevention as well as diagnosis of the SSI after abdominal surgery. The relative importance of these causes of SSI after abdominal surgery may differ from country to country. Understanding the magnitude of SSI after abdominal surgery is critical for interventions, for monitoring access to quality medical care, and for mitigating risk factors for and consequences of SSI in worldwide.

STRENGTH AND LIMITATIONS

This work may be considered the first of more-detailed epidemiological studies of SSI after abdominal

surgery in Ukraine. The primary objective of this study is to meticulously assess the origins and risk elements intertwined with surgical site infections across a diverse spectrum of surgical procedures. As the medical landscape continues to evolve, this critical analysis seeks to provide a nuanced understanding of the multi-faceted factors contributing to surgical site infections, with the overarching aim of facilitating more effective management and mitigation strategies. By exploring these dimensions comprehensively, we endeavor to enhance patient safety and the quality of surgical care in this era of evolving healthcare challenges. No other reports in the literature based on nationwide data collection describe the proportion of SSI after abdominal surgery. This study was some limitations. Limitations include conducting the study only in 29.2% regions

(7 out of 24) of Ukraine. Therefore, the results may not be representative of other regions of Ukraine.

CONCLUSIONS

This study found a high incidence rate of SSI after abdominal surgery caused by MDROs, varying widely depending on the bacterial species, and antimicrobial group in Ukraine. To minimise the risk of complications after abdominal surgery, it is essential to take several preventive measures before, during, and after the surgery. Preoperative skin preparation should be conducted and, whenever possible, laparoscope or robot-assisted surgery. Duration of surgery should be as short as possible while maintaining surgery quality and improving patient care. These steps can help ensure a safe and successful procedure, as well as a smooth recovery process.

REFERENCES

1. Surgical site infections: prevention and treatment. London: National Institute for Health and Care Excellence (NICE); 2020 Aug 19. (NICE Guideline, No. 125.). <https://www.ncbi.nlm.nih.gov/books/NBK542473/> [Accessed 04 December 2023]
2. Berríos-Torres SI, Umscheid CA, Bratzler DW et al. Healthcare Infection Control Practices Advisory Committee. Centers for Disease Control and Prevention Guideline for the Prevention of Surgical Site Infection, 2017. *JAMA Surg.* 2017;152(8):784-791. doi: 10.1001/jamasurg.2017.0904. [DOI](#)
3. European Centre for Disease Prevention and Control Surveillance of Surgical Site Infections and Prevention Indicators in European Hospitals—HAISSI Protocol. <https://www.ecdc.europa.eu/en/publications-data/surveillance-surgical-site-infections-and-prevention-indicators-european> [Accessed 04 December 2023]
4. Bucataru A, Balasoiu M, Ghenea AE et al. Factors Contributing to Surgical Site Infections: A Comprehensive Systematic Review of Etiology and Risk Factors. *Clin Pract.* 2023;14(1):52-68. doi: 10.3390/clinpract14010006. [DOI](#)
5. Salmanov A, Shcheglov D, Svyrydiuk O et al. Epidemiology of healthcare-associated infections and mechanisms of antimicrobial resistance of responsible pathogens in Ukraine: Results of a multicentre study (2019-2021). *J Hosp Infect.* 2023;131:129-138. doi: 10.1016/j.jhin.2022.10.007. [DOI](#)
6. Salmanov AG, Kostikov VV, Lytvak O et al. Postoperative Infections after Gynecological Surgeries in Ukraine. *Pol Merkur Lekarski.* 2023;51(4):299-305. doi: 10.36740/Merkur202304101. [DOI](#)
7. Magiorakos AP, Srinivasan A, Carey RB et al. Multidrug-resistant, extensively drug-resistant and pandrug-resistant bacteria: an international expert proposal for interim standard definitions for acquired resistance. *Clin Microbiol Infect.* 2012;18(3):268-81. doi: 10.1111/j.1469-0691.2011.03570.x. [DOI](#)
8. Mirande C, Bizine I, Giannetti A et al. Epidemiological aspects of healthcare-associated infections and microbial genomics. *Eur J Clin Microbiol Infect Dis.* 2018;37(5):823-831. doi: 10.1007/s10096-017-3170-x. [DOI](#)
9. Salmanov A, Shcheglov D, Artyomenko V et al. Nosocomial transmission of multi-drug-resistant organisms in Ukrainian hospitals: results of a multi-centre study (2019-2021). *J Hosp Infect.* 2023;132:104-115. doi: 10.1016/j.jhin.2022.12.008. [DOI](#)
10. Ansari S, Hassan M, Barry HD et al. Risk Factors Associated with Surgical Site Infections: A Retrospective Report from a Developing Country. *Cureus.* 2019;11(6):e4801. doi: 10.7759/cureus.4801. [DOI](#)
11. Saunders L, Perennec-Olivier M, Jarno P et al. Improving prediction of surgical site infection risk with multilevel modeling. *PLoS One.* 2014;9(5):e95295. doi: 10.1371/journal.pone.0095295. [DOI](#)
12. Marchi M, Pan A, Gagliotti C et al. The Italian national surgical site infection surveillance programme and its positive impact, 2009 to 2011. *Euro Surveill.* 2014;19(21):20815. doi: 10.2807/1560-7917.es2014.19.21.20815. [DOI](#)
13. Carvalho RLR, Campos CC, Franco LMC et al. Incidence and risk factors for surgical site infection in general surgeries. *Rev Lat Am Enfermagem.* 2017;25:e2848. doi: 10.1590/1518-8345.1502.2848. [DOI](#)
14. NHSN. Surgical site infection (SSI) event. Center for Disease Control. 2019. <https://www.cdc.gov/nhsn/pdfs/pscmanual/9pscscscurrent.pdf> 20197. [Accessed 04 December 2023]
15. European Centre for Disease Prevention and Control. Surveillance of surgical site infections and prevention indicators in European hospitals - HAI-Net SSI protocol, version 2.2. Stockholm: ECDC. 2017.

16. Surgical Site Infection (SSI) Event: Center for Disease Control. 2010. <http://www.cdc.gov/nhsn/PDFs/pscManual/9pscSSlcurrent.pdf?agree=yes&next=Accept>. [Accessed 04 December 2023]
17. American Society of Anesthesiologists. ASA physical status classification system. 2014. <https://www.asahq.org/standards-and-practice-parameters/statement-on-asa-physical-status-classification-system> [Accessed 04 December 2023]
18. Allegranzi B, Bagheri Nejad S, Combescure C et al. Burden of endemic health-care-associated infection in developing countries: systematic review and meta-analysis. *Lancet*. 2011;377(9761):228-241. doi:10.1016/S0140-6736(10)61458-4. [DOI](#)
19. Wang Z, Chen J, Wang P et al. Surgical Site Infection After Gastrointestinal Surgery in China: A Multicenter Prospective Study. *J Surg Res*. 2019;240:206-218. doi:10.1016/j.jss.2019.03.017. [DOI](#)
20. Li Z, Li H, Lv P et al. Prospective multicenter study on the incidence of surgical site infection after emergency abdominal surgery in China. *Sci Rep*. 2021;11(1):7794. doi: 10.1038/s41598-021-87392-8. [DOI](#)
21. Mihaljevic AL, Müller TC, Kehl V et al. Wound edge protectors in open abdominal surgery to reduce surgical site infections: a systematic review and meta-analysis. *PLoS One*. 2015;10(3):e0121187. doi: 10.1371/journal.pone.0121187. [DOI](#)
22. Alkaaki A, Al-Radi OO, Khoja A et al. Surgical site infection following abdominal surgery: a prospective cohort study. *Can J Surg*. 2019;62(2):111-117. doi: 10.1503/cjs.004818. [DOI](#)
23. Pinkney TD, Calvert M, Bartlett DC et al. Impact of wound edge protection devices on surgical site infection after laparotomy: multicentre randomised controlled trial (ROSSINI Trial). *BMJ*. 2013;347:f4305. doi:10.1136/bmj.f4305. [DOI](#)
24. Magill SS, Edwards JR, Bamberg W et al. Multistate point-prevalence survey of health care-associated infections. *N Engl J Med*. 2014;370(13):1198-208. doi: 10.1056/NEJMoa1306801. [DOI](#)
25. Segal CG, Waller DK, Tilley B et al. An evaluation of differences in risk factors for individual types of surgical site infections after colon surgery. *Surgery*. 2014;156(5):1253-60. doi: 10.1016/j.surg.2014.05.010. [DOI](#)
26. Leong G, Wilson J, Charlett A. Duration of operation as a risk factor for surgical site infection: comparison of English and US data. *J Hosp Infect*. 2006;63(3):255-262. doi:10.1016/j.jhin.2006.02.007. [DOI](#)

We thank the all the study participants and participating hospitals, and the infection control community who provided us with the information required for conducting this study.

CONFLICT OF INTEREST

The Authors declare no conflict of interest

CORRESPONDING AUTHOR

Aidyn G. Salmanov

Shupyk National Healthcare University of Ukraine,
9 Dorohozhytska St., 04112, Kyiv, Ukraine
e-mail: mozsago@gmail.com

ORCID AND CONTRIBUTIONSHIP

Aidyn G. Salmanov: 0000-0002-4673-1154 [A](#) [C](#) [D](#) [E](#) [F](#)
 Grygorii O. Kostromin: 0000-0001-5907-1880 [B](#) [C](#) [D](#) [F](#)
 Yuliia V. Strakhovetska: 0009-0008-7996-924X [B](#) [C](#) [D](#) [F](#)
 Olha D. Leshchova: 0000-0001-6496-7307 [B](#) [C](#) [D](#) [F](#)
 Roman V. Honza: 0009-0007-9357-3260 [B](#) [D](#) [F](#)
 Oleg V. Balaban: 0009-0004-5024-6081 [B](#) [D](#) [F](#)
 Ruslan S. Tsybaliuk: 0000-0002-2024-6425 [B](#) [D](#) [F](#)
 Inna A. Nazarenko: 0009-0005-9514-8220 [B](#) [D](#) [F](#)
 Volodymyr M. Ivantsok: 0000-0002-3933-3043 [B](#) [D](#) [F](#)

[A](#) – Work concept and design, [B](#) – Data collection and analysis, [C](#) – Responsibility for statistical analysis, [D](#) – Writing the article, [E](#) – Critical review, [F](#) – Final approval of the article

RECEIVED: 17.04.2024

ACCEPTED: 22.08.2024



Association between plasma angiotensinogen level and response to valsartan among sample of Iraqi hypertensive patients

Haneen Sajid Mahmoud, Hussein A. Saheb, Bassim Mohammad, Ahmed M. Sultan, Sinaa Abdul Amir Kadhim, Asma A. Swadi

DEPARTMENT OF PHARMACOLOGY AND THERAPEUTICS, COLLEGE OF MEDICINE, UNIVERSITY OF AL-QADISIYAH, AL-QADISIYAH, IRAQ

ABSTRACT

Aim: The main aim of the present paper is to investigate allele frequencies of rs1799983 polymorphism eNOS genes and to determine association between rs1799983 polymorphism of eNOS gene and essential hypertension in Iraqi hypertensive patients.

Materials and Methods: Data obtained at the Al-Diwaniyah teaching hospital in Iraq by researchers from the Department of Pharmacology and Therapeutics in the College of Medicine at University of Al-Qadisiyah from July 2022 to July 2023. All participants (aged 20 to 70) had been taking valsartan 160 mg once day for essential hypertension for at least two weeks before to the study. There were a total of 90 participants, 37 males and 53 women. Initial investigations of hypertension have indicated that the angiotensinogen gene has a substantial impact in susceptibility to essential hypertension through observational cross sectional descriptive single center study.

Results: Indicate, in patients with essential hypertension, that the "AGT gene A>G (rs699) and C>T(rs5051)" have high angiotensinogen level, and there is no significant association between these two (rs699, rs5051) and responsiveness to valsartan ($P > 0.05$).

Conclusions: Result showed the most common allele for rs699 was G allele (67%) while the most frequent genotype was AG (49%) and regarding rs5051 the most frequent allele was C (54%) while the most frequent genotype was CT (46%). In this study we demonstrate the lack of significant association between two these polymorphisms and clinical response to valsartan ($P > 0.05$).

KEY WORDS: AGT Gen, polymorphism, essential hypertension, valsartan, Iraq

Wiad Lek. 2024;77(9):1662-1671. doi: 10.36740/WLek/191331 DOI

INTRODUCTION

Essential hypertension is a complex illness influenced by both genetics and the environment. It has been postulated that the renin-angiotensin system (RAS) controls blood pressure. Through its interaction with renin, the protein angiotensinogen (AGT) generates angiotensin I, the prohormone of angiotensin II, which is then used to form angiotensin II, the primary effector molecule of the renin-angiotensin-aldosterone system (RAAS). Angiotensin II (Ang II)'s inactive precursor is called angiotensinogen (AGT). Valsartan is typically used as a first-line treatment in patients with hypertension, despite the fact that therapeutic efficacy demonstrates inter individual variation in this patient population. High blood pressure, often known as hypertension, occurs when arterial blood pressure is consistently elevated to 140/90 mm Hg or greater. It's common, but if left untreated, it can be quite dangerous. Hypertension affects almost two-thirds of the world's 1.28 billion adults 30-79, all of whom live in

low- and middle-income countries. Roughly 50% of people with hypertension are unaware that they have the condition. Less than half of adults 42% have been diagnosed with hypertension. Twenty percent or so of those who suffer from hypertension manage to keep it under control. Hypertension is a prominent cause of death among individuals around the world. One of the global targets for non-communicable illnesses is a 33 percent decrease in hypertension prevalence between 2010 and 2030. There may be no outward signs of hypertension in some patients [1].

Risk factors for hypertension include age, family history, body mass index (BMI), inactivity, food heavy in salt, and alcohol consumption. Changes in nutrition, smoking cessation, and increased physical activity have all been linked to reduced blood pressure. Some individuals might still benefit from taking medication. Blood pressure is measured using two numbers. Systolic pressure, or the pressure in the arteries during a complete cardiac contraction, is represented by the first value. The arterial pressure measured while

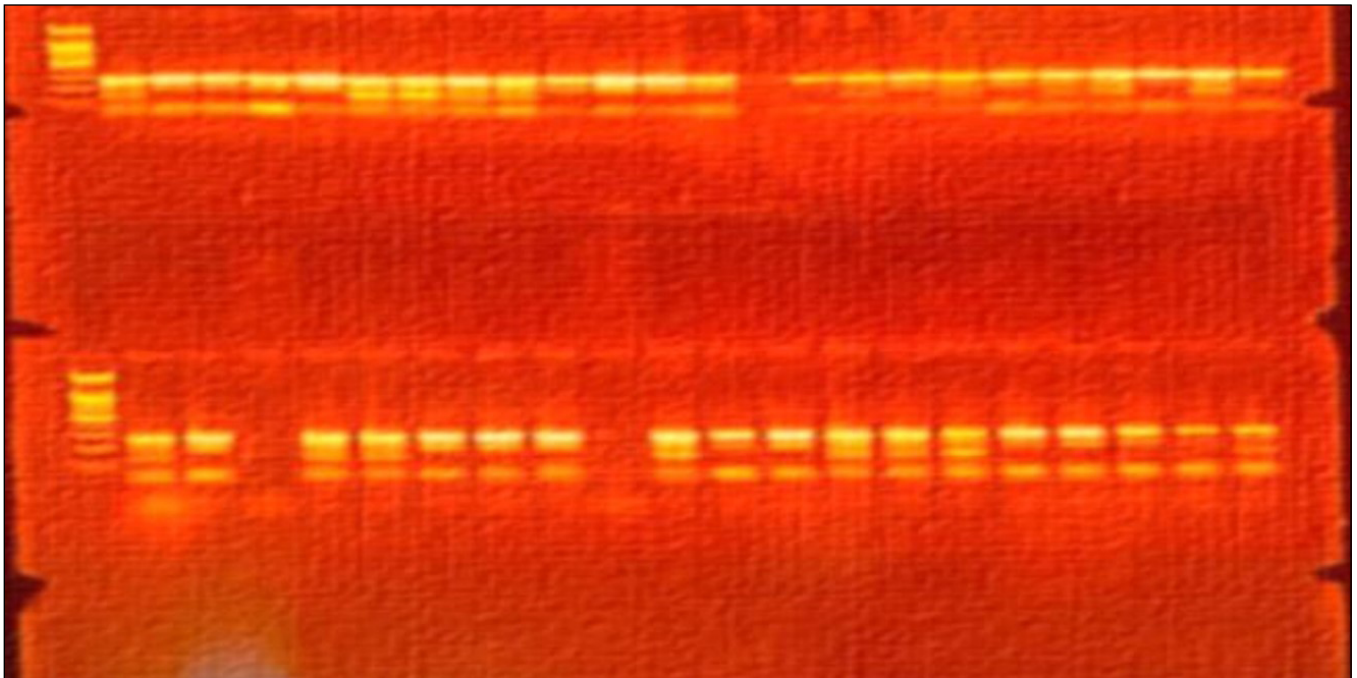


Fig. 1. The PCR product analysis of the AGT (rs5051) gene in a patient's blood, visualized on an agarose gel electrophoresis.

the heart is at rest (during diastole) is called diastolic blood pressure. Two separate measurements of blood pressure that show a systolic pressure of more than or equal to 140 mm Hg and/or a diastolic pressure of more than or equal to 90 mm Hg indicate the presence of hypertension (HTN), a condition that raises the risk of cardiovascular disease, kidney disease, neurological disease, and death. Early detection and intervention may mitigate the severity of this health issue.

According to the World Health Organization, hypertension affects up to 40 percent of Iraqis less than 25 years old, with a higher prevalence among females [2]. Prevalence estimates for HTN among patients aged 60 and over vary widely across Iraq, from 88.8% in Erbil (2019) [3] to 77.8% in Nasiriya (2014) [4] to 63.5% in Bagdad (2019) [4]. Over the past decade, Iraq was one of the Eastern Mediterranean countries caught up in a whirlwind of unrest, war, and other armed conflicts that has had a significant negative influence on the country's mental and physical health. Destruction of the health care system, absence of medical care, and health services contributed to and exacerbated many social and health problems during and after the conflicts and unstable situations. These variables may be contributing to the rising rate of hypertension in Iraq. There is evidence to suggest that being overweight is one of the leading causes of high blood pressure. It's possible that HTN and obesity are connected in Iraq because of the country's eating habits [5]. Since AGT was initially linked to the condition, it is possible that it is still "the most scrutinized" gene in this connection. Liver, adipose tissue, heart, vessel wall, brain, and kidney are only some of the

tissues that express it, and their expression varies from cell to cell. AGT is expressed by astrocytes and certain neurons in the brain, hepatocytes in the liver, adipocytes in the adipose tissue, and epithelial cells in the proximal tubule of the kidney. The human AGT gene is a small 12 kb in size (starting at nucleotide 22715602) and is situated on chromosome 1 (1q42-q43) [6]. Drugs like valsartan, telmisartan, candesartan, losartan, olmesartan, and irbesartan all fall under the category of angiotensin II receptor blockers (ARBs). Hypertensive effects, including as vasoconstriction, promotion of aldosterone and ADH synthesis, cardiac stimulation, and renal reabsorption of sodium, are blocked by ARBs via binding preferentially to angiotensin receptor 1 (AT1). Reduced blood pressure, decreased aldosterone levels, decreased cardiac activity, and enhanced sodium excretion are all results of valsartan's physiologic effects [7].

AIM

The aim of this research is to ascertain if AGT polymorphism [rs699 (T235M), rs5051 (A-6G)] affects the success of valsartan treatment for essential hypertension in Iraqi patients.

MATERIALS AND METHODS

STUDY DESIGN, PATIENTS' RECRUITMENT, SETTING AND TIMING

Patients with hypertension diagnosed in accordance with ESH 2023 are the focus of this observational cross-sectional

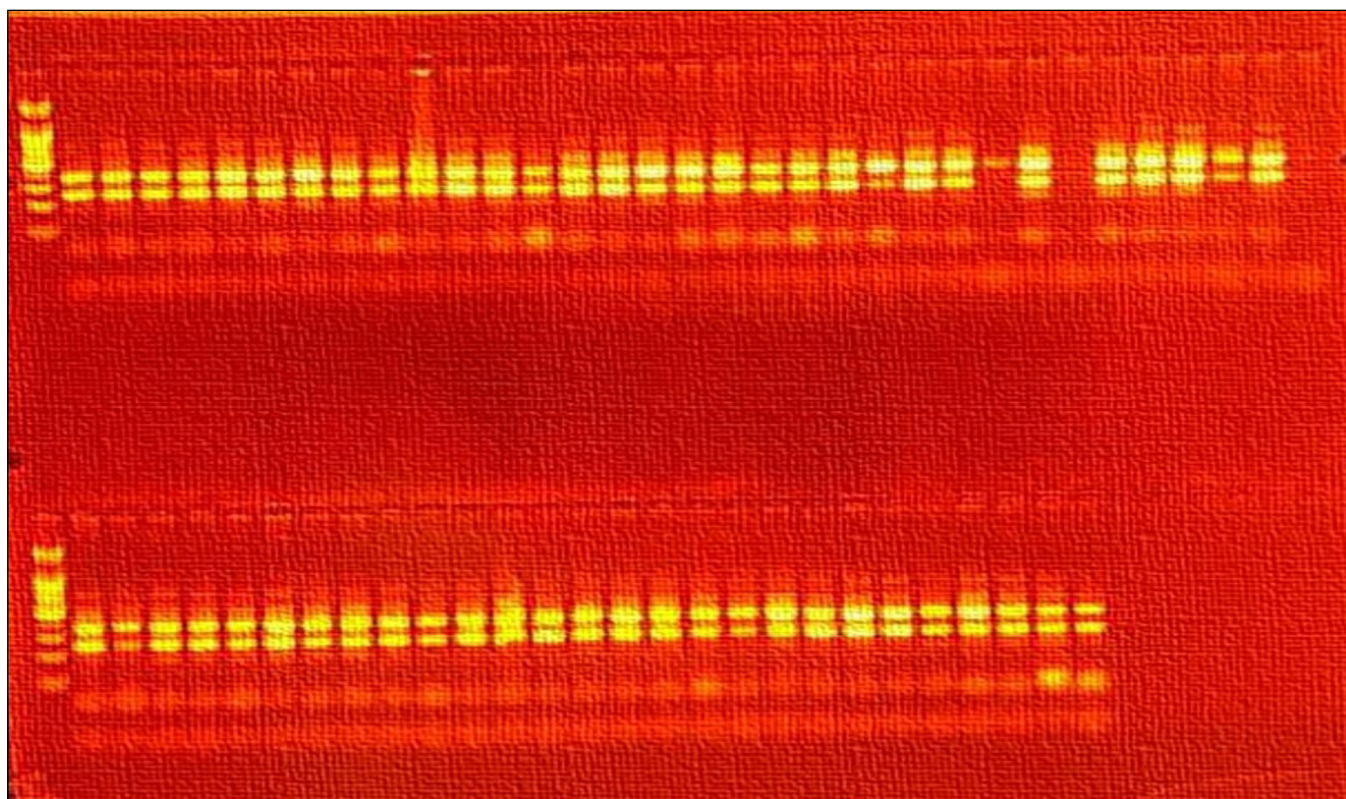


Fig. 2. The PCR product analysis of the AGT (rs699) gene in a patient's blood, visualized on an agarose gel electrophoresis.

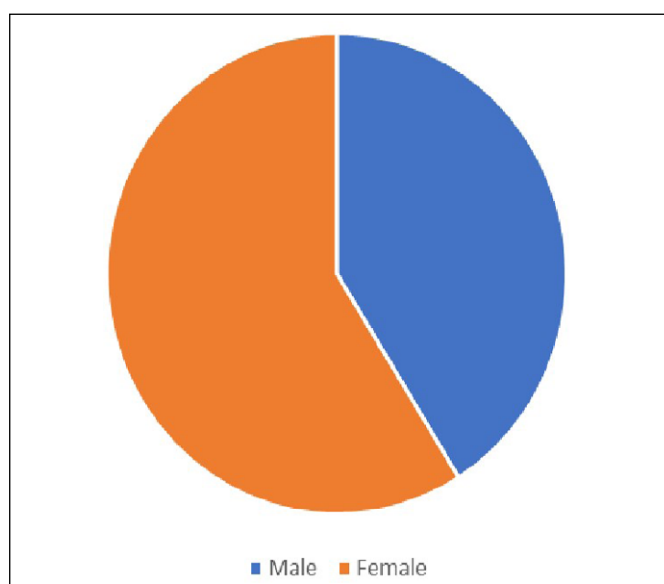


Fig. 3. Gender distribution of hypertensive patients participating in the study (n=90).

descriptive single-center study. All eligible patients were identified and recruited by a cardiologist or other cardiology professional. The study was conducted at the University of Al-Qadisiyah's College of Medicine and the Al-Diwaniyah Teaching Hospital in Iraq between July 2022 and July 2023. The experiments were carried out in the Department of Pharmacology and Therapeutics in the College of Medicine at

Al-Qadisiyah University in Diwaniyah province. After receiving thorough and accurate information about the research design and purpose, all participants will be asked for their written informed consent prior to registration. Participants ranged in age from 20 to 70, with all having been diagnosed with essential hypertension. There were 90 participants in total.

QUESTIONNAIRE FORMULA

Information was taken from the patients: name, age, sex, race, weight, length, BMI, SBP, DBP, comorbidities (smoker, DM, IHD). and biochemical parameters were being measured for all patients with valsartan which were: urea, creatinine, uric acid, glucose serum lipid (LDL, HDL, total cholesterol, triglyceride, atherogenic index), aldosterone level, renin level, aldosterone/renin ratio and angiotensinogen level.

ETHICAL CONSIDERATIONS

The trial was approved by the Ethics Committee of the College of Medicine at Al-Qadisiyah University, and prior to patient enrolment, all methods were explained in detail, and informed permission was obtained.

PRIMERS USED IN THE CURRENT STUDY

Polymerase chain reaction (PCR) primers for *AGT (rs699)* and *AGT (rs5051)* gene were built using the Integrated

Table 1. The PCR primers with their sequence, amplicon size and annealing temp

Primer	Sequence	Amplicon	Annealing
AGT Rs5051 x	Inner forward CAGAACAACGGCAGCTTCTCCACC	C-allele 173 bp.	66 °C
	Inner reverse TAAATAGGGCATCGTGACCCGGACA		
	Outer forward TCCTCCTGTAAGACCCAGGTGGG	Two outer primers 376 bp.	
	Outer reverse CGTGAGTGTGCTTCTGGCATCTGT		
AGT Rs699	Inner forward GCTGTCCACACTGGCTCACG	G- allele 169 bp.	63 °C
	Inner reverse ATGGAAGACTGGCTGCTCCCTTAT	A-allele 122 bp.	
	Outer forward GATACTAAGTCTAGGGCCAGAGCCA	Two outer primers 247 bp.	
	Outer reverse CTGAAGCAGCCGTTTGTGCA		

Table 2. Chemicals, manufacturers, and countries of origin used in this investigation

No.	Chemical materials	Company and Origin
1	TBE buffer	Intron (Korea)
2	Agarose	MarLiJu (Korea)
3	Ethidium bromide	BioBasic (Canada)
4	Ladder	Bioneer (Korea)
5	Primers	Macrogen (Korea)

DNA Technologies (IDT) website and National Center for Biotechnology Information data (NCBI). The primers were designed especially for this study using information for SNP sequence available online SNP data and online tool for tetra arms primer design and for sequence SNP primer design. In addition, the BLAST gene bank tool was utilized to check that the provided primers were complementary to the target gene and not the non-targeted gene. The lyophilized primers were dissolved in deionized distilled water (DDH₂O) in the master tube to achieve 100 pmol/μl, and then 10 pmol/l was created as a working solution by transferring 10 l from the master tube to another tube and completing the volume to 100 l by adding DDH₂O. Table 1 displays the primers provided by Bioneer Company, Korea.

CHEMICALS USED IN THE CURRENT STUDY

The chemical materials that were used in this study have been demonstrated with the corresponding country of origin and manufacturing company (Table 2).

BLOOD SAMPLING

Four milliliters of blood were taken from the patient's antecubital veins; one milliliter was placed in a tube con-

taining EDTA for DNA extraction; and the tube was kept at -20 degrees Celsius until the time of DNA extraction. The serum was separated from the remaining 3 ml of blood by centrifuging it at 5,000 RPM for 5 minutes. This was done so that it could be used in biochemical tests.

BLOOD PRESSURE MEASUREMENT

A mercury sphygmomanometer was used to assess the subjects' blood pressure (BP). The respondent was asked to sit quietly for 5 minutes with his legs crossed and his right arm exposed to allow accurate measurements to be taken. Then the right hand was placed on the table with the palm facing up. The right size cuff was chosen. While readings were taken, the cuff was maintained at the same height as the patient's heart. The ESH classification is used to categorize patients (Table 3).

Score for BP control or response [8]

- Good Responders: were defined as patients that achieved a target BP in which (SBP < 140 mm Hg or DBP < 90 mm Hg).

- Moderate responders: were defined as patient that BP 150/100 mm Hg.

- Poor responders: were defined as patients that BP > 150/100 mm Hg.

GENOTYPING

Genomic DNA was extracted using gene aid DNA extraction kit (USA).

PCR – TETRA ARM TECHNIQUE

The PCR-TETRA ARM technique was performed for genotyping and detecting AGT (rs699) and AGT (rs5051)

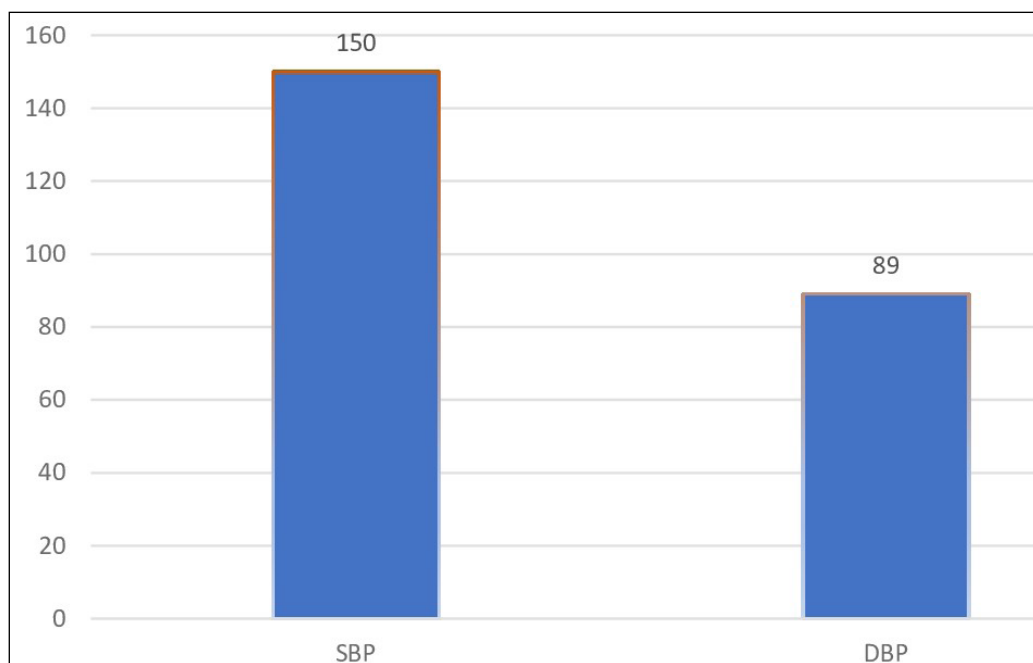


Fig. 4. Mean systolic and diastolic blood pressure of recruited hypertensive patients (n=90) who were took valsartan 160 mg/day. SBP – systolic blood pressure, DBP – diastolic blood pressure.

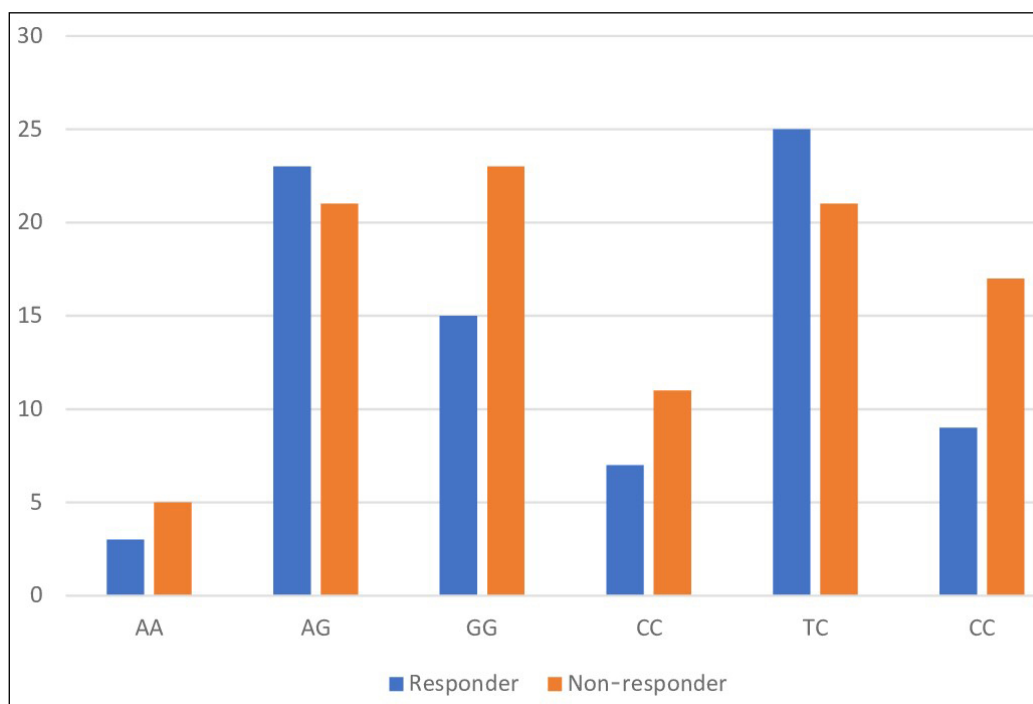


Fig. 5. Shows responder (< 140/90 mmHg) and non-responder (>140/90 mmHg) of Iraqi hypertensive patients with AGT rs699 (T235M) and rs45051 (A-6G) polymorphisms taken valsartan 160 mg/day.

gene polymorphism in blood samples of human. PCR reactions were performed by using Accupower kit (Bioneer, Korea) (Fig. 1, 2).

GENOTYPE

Table 4 show characteristics and consequences of the AGT SNPs in pathway of Angiotensin synthesis and their drug response data from pharm GKB.

STATISTICAL ANALYSIS

A mean and standard deviation (SD) were used to represent the data. Statistical analysis was performed using SPSS version 26. Analysis of variances (one-way ANOVA) was used to compare more than two means. The Fissure exact test and the Chi-square were used to see if there was a significant difference in demographic data between the two sets of categorical data. The allele frequencies of hypertensive patients and An-

Table 3. 2023 ESH classification of hypertension

Blood Pressure Category	Systolic Blood Pressure(mmHg)	Diastolic Blood Pressure(mmHg)
Optimal	<120	and <80
Normal	120-129	and 80-84
High normal	130-139	and /or 85-89
Stage 1 hypertension	140 – 159	and /or 90-99
Stage 2 hypertension	160-179	and /or 100-109
Stage 3 hypertension	≥180	and /or ≥110
Isolated systolic hypertension	≥140	and <90
Isolated diastolic hypertension	<140	and ≥90

Table 4. Characteristics and consequences of the AGT SNPs in pathway of angiotensin synthesis

Gene	Genomic position	Variation type	SNP ID	alleles	Effect	Pathway
AGT	Chrom 1 (intron)	SNP	Rs5051	C>T	T was associated with elevated plasma angiotensinogen levels and increased risk of elevated blood pressure	enzyme
		SNP	Rs699	A>G	G was associated with elevated plasma angiotensinogen levels and increased risk of elevated blood pressure	

Table 5. Illustrating values of blood urea, serum creatinine and metabolic profiles characteristics of recruited hypertensive patients (n = 90) taken valsartan 160 mg/day

	Minimum	Maximum	Mean	Standard Deviation
Blood urea	16.8	60	36.9	9.3
Creatinine	0.45	1.4	0.9	0.2
Cholesterol	105.0	357.0	195.9	44.8
Triglyceride	91.0	722.0	223.7	105.7
Atherogenic Index	0.3	2.7	0.7	0.3
Uric acid	2.9	12.5	5.2	1.5

Table 6. Effect of AGT rs699 (T235M) polymorphism on systolic and diastolic blood pressure in Iraqi hypertensive patients taken valsartan 160 mg/day

Genotype rs699	Systolic BP (mm/Hg)		P value	Diastolic BP (mm/Hg)		P value
	mean	SE		mean	SE	
AA	154	3.4	0.7 ^{NS}	90	1.4	0.08 ^{NS}
AG	148	2,2		88	1.05	
GG	151	2.9		89	1.4	

^{NS} – non significant

Table 7. Effect of AGT rs5051 (A-6G) polymorphism on systolic and diastolic blood pressure in Iraqi hypertensive patients taken valsartan 160 mg/day

Genotype rs5051	Systolic BP (mm/Hg)		P value	Diastolic BP (mm/Hg)		P value
	mean	SE		mean	SE	
CC	144	4.7	0.3 ^{NS}	88	1.4	0.6 ^{NS}
CT	152	1.9		89	0.9	
TT	149	2.8		90	1.2	

^{NS} – non significant

giotensinogen level were compared using odds ratios (ORs) and 95% confidence intervals (CIs). There was a statistically significant probability value (P value) in all statistical analyzes in this study at the p≤0.05 level. A

Hardy – Weinberg law this law state that the allele and genotype frequencies in a population will remain constant from generation to generation in the absence of evolutionary influences.

Table 8. Association between AGT rs699 (T235M) and rs5051 (A-6G) polymorphism with responsiveness to valsartan 160 mg/day in Iraqi hypertensive patients [responder (<140 mmHg), non-responder (≥ 140 mmHg)]

	Rs699			P value	Rs5051			P value
	AA	AG	GG		CC	CT	TT	
Responder	23	23	15	0.4 ^{NS}	9	25	7	0.2 ^{NS}
Nonresponder	5	21	23		17	21	17	

^{NS} – non significant

RESULT

DEMOGRAPHIC DATA

This study included 90 Iraqi hypertensive patients, 58.9% (n=53) females and 41.1% (n=37) males, with a mean ± SD of age (years) 53.2 ± 13.8 years old, and mean ± SD of BMI 29 ± 5.32 kg/m² (Fig.3).

METABOLIC PROFILE

Among study patients, the mean ± SD of total serum cholesterol, triglyceride, atherogenic index and uric acid was 195.8 ± 44.8 mg/dL, 223.7 ± 105.7 mg/dL, 0.7 ± 0.3, 5.2 ± 1.5 mg/dL respectively (Table 5).

BLOOD PRESSURE

All patients participated in this study were hypertensive on valsartan 160mg/day, so the mean ± SD of systolic blood pressure was 150±14.9 mmHg while the mean ± SD of diastolic blood pressure was 89.3±6.9 mmHg. From these 90 hypertensive patients (45.6%) n=41 meet the target level of blood pressure (responders<140/90 mmHg) while (54.4%) n=49 remain doesn't meet the target of treatment (≥ 140 mmHg non-responders) (Fig.4).

EFFECT OF AGT POLYMORPHISM RS699 (T235M) ON BLOOD PRESSURE

Table 6 displays that there was no significant difference between the systolic blood pressures of patients who were homozygous for allele A (AA), heterozygous for allele G (AG), or homozygous for allele G (GG), with a P value of 0.7. However, the average diastolic BP of AA homozygotes, AG heterozygotes, and GG homozygotes was 90±1.4/88±1.05/89±1.4 mm/Hg, with a P-value of 0.08. AGT rs699 did not influence blood pressure on either the systolic or diastolic side.

EFFECT OF AGT POLYMORPHISM RS5051 (A-6G) ON BLOOD PRESSURE

Table 7 displays the mean±SE of systolic blood pressure of patients who were carriers of the CC allele, the

CT allele, and the TT allele. The significance level was 0.3. However, the average diastolic BP of CC homozygotes, CT heterozygotes, and TT homozygotes was 88±1.4/89±0.9/90±1.2 mm/Hg (P=0.6) respectively. Systolic and diastolic blood pressure was not affected by AGT rs5051 in a statistically meaningful way.

EFFECT OF AGT POLYMORPHISM RS699 (T235M) AND RS 5051 (A-6G) ON VALSARTAN RESPONSIVENESS

The allelic and genotypic frequency of AGT polymorphism rs699 and rs5051 doesn't showed significant association between polymorphism and responsiveness to valsartan (Table 8, Fig.5).

DISCUSSION

GENOTYPE/PHENOTYPE RELATIONSHIP AND IMPACT OF AGT GENE RS699 AND RS5051 ON VALSARTAN EFFECT

Angiotensinogen concentration was shown to be significantly (P=0.001) related to rs699 genotype frequency. The AA genotype was found to have angiotensinogen levels that were lower than the GG genotype 2.9 ng/dl. There is no correlation between the rs699 AGT polymorphism and valsartan sensitivity, as measured by allelic and genotypic frequency. There was no significant difference between the GG genotype (15 responses, 23 non-responses) and the AA genotype (23 responses, 5 non-responses), P=0.4. There is no correlation between the rs5051 AGT polymorphism and valsartan sensitivity, as measured by allelic and genotypic frequency. We obtained a P value of 0.2 between the CC genotype (9 responses, 11 non-responses) and the TT genotype (7 responses, 17 non-responses). In this study, we discovered that polymorphism (rs5051 C>T and rs699 A>G) was significantly associated with angiotensinogen level in Iraqi patients with essential hypertension, but snps (rs5051 C>T and rs699 A>G) were not. There is not enough information to say whether or not the AGT gene (-20 A/C, -6 A/G) affects the effectiveness of antihypertensive drug treatment at this time. Here, we analyzed

the relationship between telmisartan's antihypertensive efficacy and the -6 A/G and -20 A/C polymorphisms in the AGT gene promoter region in Han patients with mild and severe hypertension for eight weeks [9, 10]. No association between telmisartan's antihypertensive impact and the AGT-6 A/G or -20 A/C genotypes was found. The available evidence does not support the AGT (M235T) variant's association with ARBs' blood pressure-lowering effects. Another study of the same AGT variant in Swedish patients with hypertension found that homozygous carriers of the AA alleles responded best to treatment with atenolol (17 mmHg compared to 3 mmHg for homozygous carriers of the GG variant), while there was no difference in response by genotype after treatment with the ARB irbesartan 80 mg [11, 12]. In addition to rs698, which results in the replacement of Thr235 for Met in AGT, rs699 has been widely researched in relation to therapy response in hypertension. We found no indication of a substantial difference in BP responses to multiple antihypertensive medications based on the AGT Met235Thr polymorphism genotype, which is consistent with the majority of previous studies [13]. Increased responsiveness to angiotensin II has been seen in individuals with the C allele of the AGTR1 polymorphism, which has also been linked to hypertension [14]. African-American women with the A/A genotype of AGTR1 have been demonstrated to have better blood pressure responses to HCT, however for losartan, it has been hypothesized that the C allele supports higher BP response. The study's limited sample size calls for additional prospective research to confirm the findings [15].

GENOTYPE/PHENOTYPE RELATIONSHIP AND IMPACT OF AGT GENE RS699 AND RS5051 ON BLOOD PRESSURE

Systolic blood pressure in this study was found to be similar across persons who were homozygous for allele A (AA), heterozygous for allele G (AG), and homozygous for allele G (GG), with a matching P value of 0.7. The average diastolic blood pressure of AA homozygotes, AG heterozygotes, and GG homozygotes was 90 ± 1.4 , 88 ± 1.05 , 89 ± 1.4 mmHg, respectively ($P=0.08$). AGT rs699 did not influence blood pressure on either the systolic or diastolic side. Patients who were either homozygous for the CC allele or heterozygous for the CT allele had systolic blood pressure readings of 144 ± 4.7 mmHg, 152 ± 1.9 mmHg, and 149 ± 2.9 mmHg, respectively ($P=0.3$), however, the average diastolic BP of CC homozygotes, TT heterozygotes, and TT homozygotes was $88 \pm 1.4/90 \pm 1.2$ mmHg. The probability coefficient was 0.60. AGT rs5051 did not have a detectable impact. In this study of Iraqi patients with essential hypertension,

we found no evidence of a link between polymorphism (rs5051 C>T and rs699 A>G) and systolic or diastolic blood pressure. Importantly, recent research has found that systolic blood pressure is significantly associated with rs5051 C>T and/or rs699 A>G in Black people in the UK Biobank, with a 4-fold bigger impact size than that identified in White participants [16,17]. Notably, rs699 A>G and rs5051 C>T allele frequencies are around twice as common in people of African ancestry as they are in people of European heritage. Minor allele frequencies aren't the only thing that vary between Whites and Blacks; it's also been established that the linkage disequilibrium blocks of AGT are different [18]. It is possible that rs5051 C>T or rs699 A>G mediate blood pressure changes more significantly in Black patients due to variations in AGT expression or abundance, given that salt-sensitive hypertensive phenotypes are more common in people of African ancestry [19]. Patients of African descent respond better to calcium channel blockers and diuretics than beta-blockers or RAS acting antihypertensive [20, 21] because of their reduced plasma renin activity and retained aldosterone levels. In line with this idea, the Eighth Joint National Committee (JNC 8) recommends distinct courses of first antihypertensive treatment for Caucasian and Black patients. The JNC only recommends angiotensin converting enzyme inhibitors as first-line therapy in Caucasian patients with normal kidney function [22]. Here, we present evidence that the genetic variants rs5051 C>T and rs699 A>G may be linked in the recognized discrepancies in antihypertensive medication efficacy between people of European and African ancestry. Despite this, there is substantial mixing among populations. This type of research will allow doctors to stop using racial identity as a stand-in for genotype [23] once whole genome sequencing becomes more widely available in clinical care. The AGTR1 1166 A/C and ACE I/D polymorphisms were not associated with BP responses. Studies on the AGT Met235Thr polymorphisms have shown that patients with the AGT 235Thr allele have a better response to beta-blockers and angiotensin-converting enzyme (ACE) inhibitors [24, 25], while other studies have found no gene-drug interaction between AGT Met235Thr genotypes and BP response to beta-blockers, ACE inhibitors, calcium channel antagonists, or angiotensin receptor blockers. We found no statistically significant association between the AGT Met235Thr genotype and blood pressure (BP) response to multiple antihypertensive medicines, which is in line with previous studies [26].

CONCLUSIONS






Our result showed the most common allele for rs699 was G allele (67%) while the most frequent genotype

was AG (49%), frequency of another genotype GG and AA were 38% and 8% respectively. Regarding rs5051 the most frequent allele was C (54%) while the most frequent genotype was CT (46%), frequency of other

genotypes TT and CC were 2% and 29% respectively. In this study we demonstrate the lack of significant association between two these polymorphisms and clinical response to valsartan.

REFERENCES

1. World Health Organization. Noncommunicable diseases country profiles 2018. 2018. <https://www.who.int/publications/i/item/ncd-country-profiles-2018>. [Accessed 05 March 2024]
2. Saka M, Shabu S, Shabila N. Prevalence of hypertension and associated risk factors in older adults in Kurdistan, Iraq. *East Mediterr Health J*. 2020;26(3):268-275. doi: 10.26719/emhj.19.029. [DOI](#)
3. World Health Organization. Urbanization and health. *Bull World Health Organ*. 2010;88:245–246. doi:10.2471/BLT.10.010410. [DOI](#)
4. Wang H, Naghavi M, Allen C et al. Global, regional, and national life expectancy, all-cause mortality, and cause-specific mortality for 249 causes of death, 1980–2015: a systematic analysis for the Global Burden of Disease. *Lancet*. 2016;388(10053):1459-1544. doi: 10.1016/S0140-6736(16)31012-1. [DOI](#)
5. Gardemann A, Stricker J, Humme J et al. Angiotensinogen T174M and M235T gene polymorphisms are associated with the extent of coronary atherosclerosis. *Atherosclerosis*. 1999;145(2):309-314. doi:10.1016/s0021-9150(99)00082-9. [DOI](#)
6. Yang G, Gray TS, Sigmund CD et al. The angiotensinogen gene is expressed in both astrocytes and neurons in murine central nervous system. *Brain Res*. 1999;817(1-2):123-131. doi:10.1016/s0006-8993(98)01236-0. [DOI](#)
7. Black HR, Bailey J, Zappe D et al. Valsartan: more than a decade of experience. *Drugs*. 2009;69(17):2393-2414. doi: 10.2165/11319460-000000000-00000. [DOI](#)
8. Unniachan S, Wu D, Rajagopalan S et al. Evaluation of blood pressure reduction response and responder characteristics to fixed-dose combination treatment of amlodipine and losartan: a post hoc analysis of pooled clinical trials. *J Clin Hypertens (Greenwich)*. 2014;16(9):671-677. doi:10.1111/jch.12390. [DOI](#)
9. Mulerova T, Uchasova E, Ogarkov M et al. Genetic forms and pathophysiology of essential arterial hypertension in minor indigenous people of Russia. *BMC Cardiovasc Disord*. 2020;20(1):169. doi:10.1186/s12872-020-01464-7. [DOI](#)
10. Wang Y, Peng L, Lu H et al. Genetic polymorphisms of very important pharmacogene variants in the blang population from Yunnan province in China. *Pharmgenomics Pers Med*. 2021;14:1647-1660. doi:10.2147/PGPM.S327313. [DOI](#)
11. Kunz R, Kreutz R, Beige J et al. Association between the angiotensinogen 235T-variant and essential hypertension in whites: a systematic review and methodological appraisal. *Hypertension*. 1997;30(6):1331-1337. doi:10.1161/01.hyp.30.6.1331. [DOI](#)
12. Frossard PM, Hill SH, Elshahat YI et al. Associations of angiotensinogen gene mutations with hypertension and myocardial infarction in a gulf population. *Clin Genet*. 1998;54(4):285-293. doi:10.1034/j.1399-0004.1998.5440405.x. [DOI](#)
13. Plotnikov D, Huang Y, Khawaja AP et al. High blood pressure and intraocular pressure: A Mendelian randomization study. *Invest Ophthalmol Vis Sci*. 2022;63(6):29. doi:10.1167/iovs.63.6.29. [DOI](#)
14. Giri A, Hellwege JN, Keaton JM et al. Trans-ethnic association study of blood pressure determinants in over 750,000 individuals. *Nat Genet*. 2019;51(1):51-62. doi:10.1038/s41588-018-0303-9. [DOI](#)
15. Van Der Harst P, Verweij NJC. Identification of 64 novel genetic loci provides an expanded view on the genetic architecture of coronary artery disease. *Circ Res*. 2018;122(3):433-443. doi:10.1161/CIRCRESAHA.117.312086. [DOI](#)
16. Liu C, Kraja AT, Smith JA et al. Meta-analysis identifies common and rare variants influencing blood pressure and overlapping with metabolic trait loci. *Nat Genet*. 2016;48(10):1162-1170. doi:10.1038/ng.3660. [DOI](#)
17. Bis JC, Smith NL, Psaty BM et al. Angiotensinogen Met235Thr polymorphism, angiotensin-converting enzyme inhibitor therapy, and the risk of nonfatal stroke or myocardial infarction in hypertensive patients. *Am J Hypertens*. 2003;16(12):1011-1017. doi:10.1016/j.amjhyper.2003.07.018. [DOI](#)
18. Do AN, Lynch AI, Claas SA et al. The effects of genes implicated in cardiovascular disease on blood pressure response to treatment among treatment-naïve hypertensive African Americans in the GenHAT study. *J Hum Hypertens*. 2016;30(9):549-554. doi:10.1038/jhh.2015.121. [DOI](#)
19. Liljedahl U, Kahan T, Malmqvist K et al. Single nucleotide polymorphisms predict the change in left ventricular mass in response to antihypertensive treatment. *J Hypertens*. 2004;22(12):2321-2328. doi:10.1097/00004872-200412000-00014. [DOI](#)
20. Kurland L, Melhus H, Karlsson J et al. Polymorphisms in the angiotensinogen and angiotensin II type 1 receptor gene are related to change in left ventricular mass during antihypertensive treatment: results from the Swedish Irbesartan Left Ventricular Hypertrophy Investigation versus Atenolol (SILVHIA) trial. *J Hypertens*. 2002;20(4):657-663. doi:10.1097/00004872-200204000-00023. [DOI](#)
21. Kurland L, Liljedahl U, Karlsson J et al. Angiotensinogen gene polymorphisms: relationship to blood pressure response to antihypertensive treatment: results from the Swedish Irbesartan Left Ventricular Hypertrophy Investigation vs Atenolol (SILVHIA) trial. *Am J Hypertens*. 2004;17(1):8-13. doi:10.1016/j.amjhyper.2003.09.009. [DOI](#)

22. Sarhan NM, Shahin MH, El Rouby NM et al. Effect of genetic and nongenetic factors on the clinical response to mineralocorticoid receptor antagonist therapy in Egyptians with heart failure. *Clin Transl Sci.* 2020;13(1):195-203. doi:10.1111/cts.12702. DOI 
23. Inoue I, Nakajima T, Williams CS et al. A nucleotide substitution in the promoter of human angiotensinogen is associated with essential hypertension and affects basal transcription in vitro. *J Clin Invest.* 1997;99(7):1786-1797. doi:10.1172/JCI119343. DOI 
24. Mopidevi B, Kaw MK, Sivankutty I et al. A polymorphism in intron I of the human angiotensinogen gene (hAGT) affects binding by HNF3 and hAGT expression and increases blood pressure in mice. *J Biol Chem.* 2019;294(31):11829-11839. doi:10.1074/jbc.RA119.007715. DOI 
25. Bonnardeaux A, Davies E, Jeunemaitre X et al. Angiotensin II type 1 receptor gene polymorphisms in human essential hypertension. *Hypertension.* 1994;24(1):63-69. doi:10.1161/01.hyp.24.1.63. DOI 
26. O'Donnell CJ, Lindpaintner K, Larson MG et al. Evidence for association and genetic linkage of the angiotensin-converting enzyme locus with hypertension and blood pressure in men but not women in the Framingham Heart Study. *Circulation.* 1998;97(18):1766-1772. doi:10.1161/01.cir.97.18.1766. DOI 

CONFLICT OF INTEREST

The Authors declare no conflict of interest

CORRESPONDING AUTHOR



Haneen Sajid Mahmoud



University of Al-Qadisiyah



University District, Al Diwaniyah, Al-Qadisiyah Governorate, Iraq



e-mail: sgahmed1331962@outlook.com



ORCID AND CONTRIBUTIONSHIP



Haneen Sajid Mahmoud: 0009-0006-4466-6690  

Hussein A Saheb: 0000-0002-0137-8932  

Bassim Mohammad:0000-0001-6732-5940  

Ahmed M Sultan: 0000-0001-6819-0208  

Sinaa Abdul Amir Kadhim:0000-0001-9375-5581  

Asma A Swadi: 0000-0002-7679-1596  

 – Work concept and design,  – Data collection and analysis,  – Responsibility for statistical analysis,  – Writing the article,  – Critical review,  – Final approval of the article

RECEIVED: 07.08.2023

ACCEPTED: 17.07.2024



Features of the morphogenesis of oxalate and urate urinary stones in urolithiasis patients from heavily industrialized region

Kostyantyn Barannyk¹, Valeriy Ishkov², Serhiy Barannyk¹, Ruslan Duka¹, Robert Molchanov¹

¹ DNIPRO STATE MEDICAL UNIVERSITY, DNIPRO, UKRAINE

² NATIONAL TECHNICAL UNIVERSITY "DNIPRO POLYTECHNIC", DNIPRO, UKRAINE

ABSTRACT

Aim: Determining the characteristics of urinary stone composition in inhabitants of an industrially advanced region afflicted with oxalate and urate urolithiasis.

Materials and Methods: A comparative analysis of the morphology of 246 kidney stones from residents of one of heavily industrialized region of Ukraine, was conducted. Petrographic examination of the calculi was performed through microscopic analysis. The qualitative composition of the calculi was investigated using X-ray structural analysis of fragments and dust remnants of the stones, which were formed during the preparation of thin sections.

Results: A distinctive characteristic of all mineral components is their varying microblock structure and the presence of organic material inclusions. The inclusion of an organic component reduces the strength of the crystalline layers. Urolith resembles a brittle-hollow environment, which in certain cases allows for the selection of the most effective methods of their destruction (lithotripsy).

Conclusions: A common feature among all mineral components is their diverse microblock structure and the presence of organic inclusions, which diversify the strength characteristics of uroliths. The prior determination of these characteristics allows for the selection of the most effective method for destructive treatment (lithotripsy). The combination of data on the ontogenesis of uroliths, their mineral composition, and the state of the electrolyte balance in the body of a patient with urolithiasis will allow choosing an individually effective method of metaphylaxis of the disease.

KEY WORDS: structure, composition, pollutions, industrial region, Keywords: urolithiasis, urolith ontogenesis

Wiad Lek. 2024;77(9):1672-1679. doi: 10.36740/WLek/191325 DOI

INTRODUCTION

Minerals of biogenic origin are integral elements of many living organisms. Alongside genetically physiogenic minerals, pathogenic biominerals are also prevalent. Among them are urinary stones, or uroliths, which form as a result of urolithiasis development. Urolithiasis is rightfully referred to as the "disease of civilization" [1-3]. According to the World Health Organization, the incidence of this disease has increased by 1.5 times over the past 12 years. Globally, one person out of a hundred suffers from it. The prevalence of urolithiasis among the adult population in an intensive industrial region exceeds the overall defined indicators by 3.4 times, correlating with indicators of environmental pollution by heavy metals, particularly lead and cadmium, which can accumulate in the renal parenchyma and cause toxic nephropathy, secondary crystalluria, and urolithiasis [2]. Throughout many centuries, information on disease symptoms and treatment methods has been accumulated, but many questions in mineralogy, including uro-

lith ontogeny, remain insufficiently explored. Currently, the ontogeny of minerals is a well-developed branch of genetic mineralogy. It allowed for the initial exploration of the composition and microstructure of kidney calculi in residents of an industrial region in Ukraine [3-6]. Subsequent investigations have demonstrated that the acquired information can assist in reconstructing the conditions of their nucleation and growth by examining the external form and internal structural characteristics of minerals and mineral aggregates. The rich experience in the study of inorganic compounds can and should be effectively applied in biology and medicine to elucidate possible mechanisms of biomineral formation in pathogenic processes based on their geological analogs [7-8].

AIM

Determining the characteristics of urinary stone composition in inhabitants of an industrially advanced region afflicted with oxalate and urate urolithiasis.

MATERIALS AND METHODS

A comparative analysis of the morphology of over 246 renal uroliths from the Dnipropetrovsk region, one of the highly industrialized regions of Ukraine, was performed. Petrographic examination of the uroliths was conducted using a stereoscopic binocular microscope MBS-9 and optical polarization microscope MIN-8. The qualitative composition of urinary calculi was investigated using X-ray structural analysis of fragments and dust remnants of the stones, which were formed during the preparation of thin sections.

RESULTS

During the investigation of kidney stones from residents of the Dnipropetrovsk region using optical petrography methods, we identified the following compounds: oxalates such as weddellite and whewellite; urates including uricite, pseudomalachite, ammonium urate, monohydrate sodium urate; phosphates like struvite, hydroxyapatite, brushite, whitlockite; as well as xanthine, cystine, quartz, gypsum, and goethite. Monomineral formations were exceedingly rare (<1%). Among them, uric acid (urate) stones constituted 14.5%, struvite - 11.3%, calcium phosphates - 11.3%, calcium phosphates + oxalates - 29%, and calcium oxalates - 33.9% (Fig. 1).

Based on morphological characteristics, five types of urinary calculi have been identified. The first type of calculi exhibits a dendritic surface composed of numerous small crystals. In thin sections, there is an evident growth direction of crystals from the center of the calculus to its periphery. The second type of calculi is characterized by a "budding" surface. Individual "nephron" sizes can vary from a few micrometers to several millimeters in diameter. The third type of calculi combines features of the morphology of the first two types, and this surface morphology is referred to as "combined." The surface of the fourth type of calculi is intensely grooved, resembling "bay-like" structures. The fifth type of calculi has irregular shapes. Their forms cannot be categorized into specific types of geometric solids; often, they are cylindrical aggregates with deviations from the long axis, exhibiting numerous branching formations.

In the case of oxalate uroliths, a wide spectrum of colors was observed, spanning from light gray to dark brown. These uroliths exhibited a cluster-like shape with small crystals dispersed irregularly across their surface formations. Notably, the surfaces of these stones displayed a distinct rough and nodular texture, which manifested at varying scales (Fig. 2A). Another configuration of oxalate uroliths showcased a different

color palette, ranging from pure white to dark brown and black. These uroliths assumed an irregular, kidney-shaped form, with occasional nodular structures appearing on the surface, contributing to their unique appearance (Fig. 2B). Furthermore, oxalate uroliths displayed a variation in texture, with a color range from light gray to dark brown and black. Their irregular shape was accentuated by a surface texture characterized by roughness, spikiness, cavernous formations, and nodular protrusions, which could be observed at multiple scales (Fig. 2C).

In contrast, urate uroliths presented a distinct color profile, transitioning from yellowish-white to various shades of orange (Fig. 2D). Their surfaces were primarily uneven, featuring prominent bumps, cavernous features, and occasional fine nodular structures. Notably, a matte shine was observed on the majority of urate uroliths, with occasional instances of a subtle glassy sheen. The macrostructure of these uroliths was primarily fine-grained, with sporadic occurrences of thin-grained patterns.

The microstructure of the majority of uroliths was cryptocrystalline. They consisted of a cryptocrystalline aggregate, primarily composed of individual cryptocrystalline grains of weddellite and whewellite, with minor admixture of uric acid dihydrate (predominantly enriched in the 5th generation, located in the peripheral part of the urolith). The organic material was generally distributed unevenly. The main portion of organic matter accumulated in the 5th generation of stone formation as separate flake-like inclusions and layers. In other generations of stone formation, the organic material was mainly localized as inclusions within the hollow spaces between mineral substance aggregates, high-dispersion film inclusions between individual grains and their microblocks ("organic shell"). Additionally, a slightly smaller amount of organic material was localized within micropores and the "organic core."

Microscopically, the structure of uric acid uroliths was predominantly fine-crystalline and hypidiomorphic. The uric acid stone consisted of an aggregate of small crystals, primarily composed of individual small grains of uric acid monohydrate. On the surface, a thin sprinkling of well-developed crystals of uric acid dihydrate was often observed. In the central part of the uric acid uroliths, calcium oxalate crystals (wedellite) were present, mainly as inclusions ("mineral hostages") within relatively large crystals of uric acid monohydrate, along with occasional accumulations of collophane. The organic material was distributed unevenly. The main portion of organic matter was concentrated as high-dispersion inclusions between individual micro-

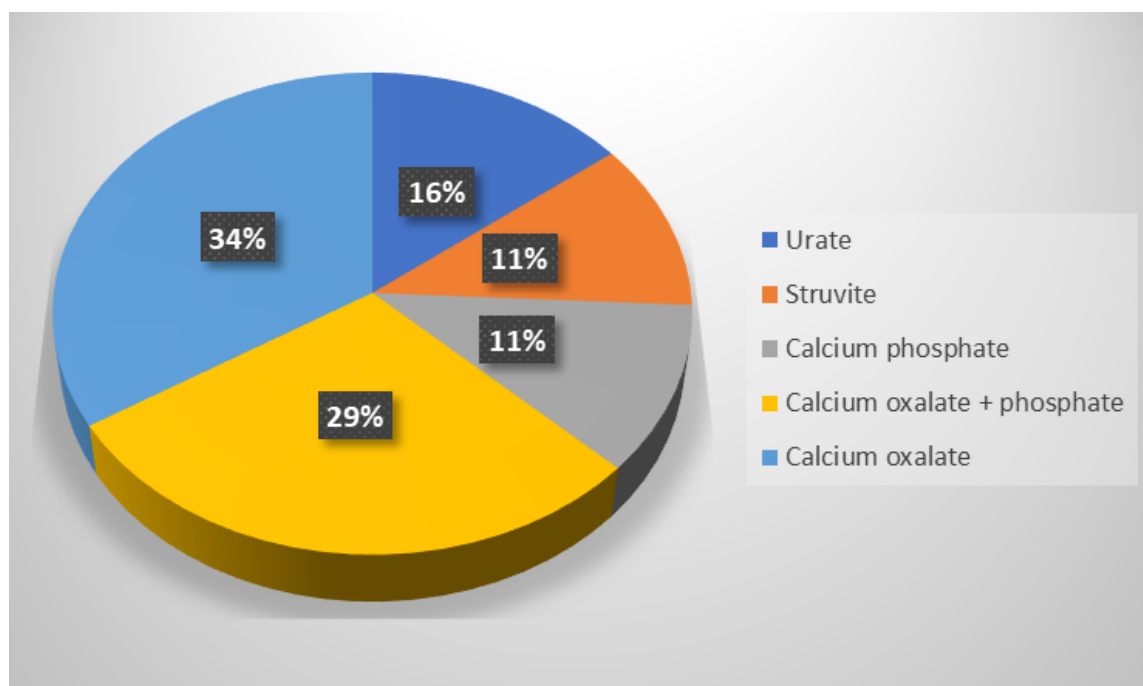


Fig. 1. Results of the study of stones in the kidneys of residents of the Dnipropetrovsk region.

blocks of mineral grains, within fractures and micropores. Simultaneously, some amount of organic material was localized as an irregularly shaped “organic core” resulting from multiple phases of a single generation. The analysis of mineral phase interactions indicated a sequential mineral replacement process: collophane (phosphate) → weddellite (oxalate) → uric acid monohydrate (urate).

Special attention was drawn to various options for the construction of the urate stones themselves. Moreover, the main portion of the examined section was composed of mineral material consisting of polydisperse crystals of uric acid monohydrate (Fig. 3.A). However, inclusions of whewellite (calcium oxalate monohydrate) were observed within the large crystals of uric acid monohydrate. Sometimes, in addition to these inclusions, a second inclusion of phosphate - collophane within the “shell” of vaterite was observed. Furthermore, fragments of the “organic core” with a thin rim of collophane were repeatedly observed. The analysis of these observations also confirms the sequential replacement of mineral phases. The organic matter (matrix) was mainly concentrated in the form of extremely thin films (“organic shell”) along the surfaces of crystals and their microblocks, as well as numerous fine-dispersed inclusions within the microblocks of individual crystals. Occasionally, during the observation, clusters with polygonal microblock crystals of uric acid monohydrate and clusters of collophane accumulation were found.

Characteristics of the structure of the peripheral part of urate (Fig. 3B). The field of view reveals the struc-

ture of a concentric-zonal spherulite predominantly composed of uric acid. At this scale, the presence of 5 zones corresponding to sequential stages of mineral formation is clearly observed. The zones are separated by layered accumulations of organic matter inclusions. A characteristic feature of the structure of the first zone (the central or “core” of the spherulite) is the presence of polygonal crystals of uric acid monohydrate and a relatively large, singular cluster of collophane. The second zone is composed of radially elongated tabular crystals of uric acid monohydrate. The third zone is formed by the largest tabular crystals of uric acid monohydrate, also arranged radially. Analysis of the elongation of crystals in the second and third zones (based on 34 measurements) shows their equality within the margin of error. In contrast to the other zones, the fourth zone is discontinuous and manifested as several thin lenses of collophane grains. The fifth zone is composed of a combination of polygonal and radially elongated tabular grains of uric acid monohydrate. It should be noted that the composition of the third and fifth zones includes individual small crystals of whewellite and uric acid dihydrate.

The peculiarities of the structure of the central part of oxalate uroliths consisted mainly of various fragments tracing the gradual generation of stone formation. This was particularly evident in the conditions of urolith formation with relatively stable saturation of urine with mineral components, without sharp fluctuations in their concentration. The field of view captured distinct areas of stone generation. The first

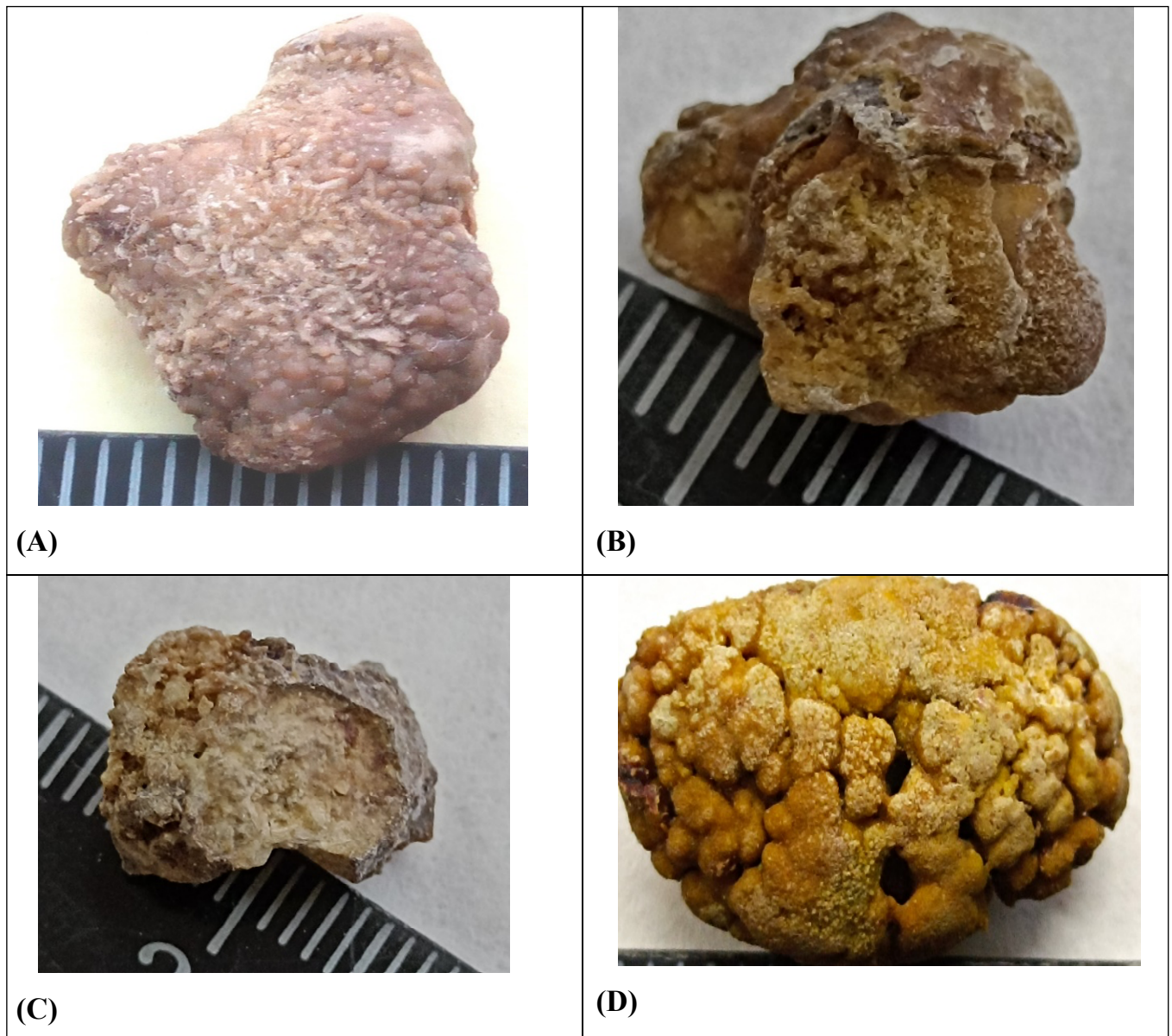


Fig. 2. Macroscopic appearance of uroliths: (A,B,C) Oxalate urolith; (D) Urate urolith.

generation was represented by a concentric-zonal aggregate of whewellite in a bud-like form, formed around the fragment of the “organic core” (Fig. 4A). The mineral substance of the second generation of stone formation, in the form of bud-like aggregates of vaterite with concentric-zonal structure, radially encompassed the aggregate of the first generation. As for the structure of the third generation of stone formation, it often exhibited combinations of spherical aggregates with layered and bud-like alternations, which were immersed in organic matter (Fig. 4C). In terms of mineral composition, there was a slight predominance of vaterite over whewellite.

Features of the construction of the peripheral part of oxalate uroliths consisted of clear variations in the mineral composition, differences in color and forms of

organic matter concentration in the fourth generation (Fig. 4B). The fifth generation of stone formation was characterized by a significant increase in the content of organic matter (up to 62%), the presence of crystals of calcium oxalate dihydrate, a predominance of calcium oxalate dihydrate (weddellite) in the oxalate composition, a finer-grained mineral component, and smaller aggregates.

Additionally, in the microphotographs of the peripheral part of oxalate uroliths, the main component of the mineral composition consisted of various-sized crystals of oxalates (weddellite and whewellite), with a minor presence of urates - dispersed crystals of calcium oxalate dihydrate in the form of small sharp-edged crystals and their aggregates, concentrated around the external surface of the stone and often spatially close to areas

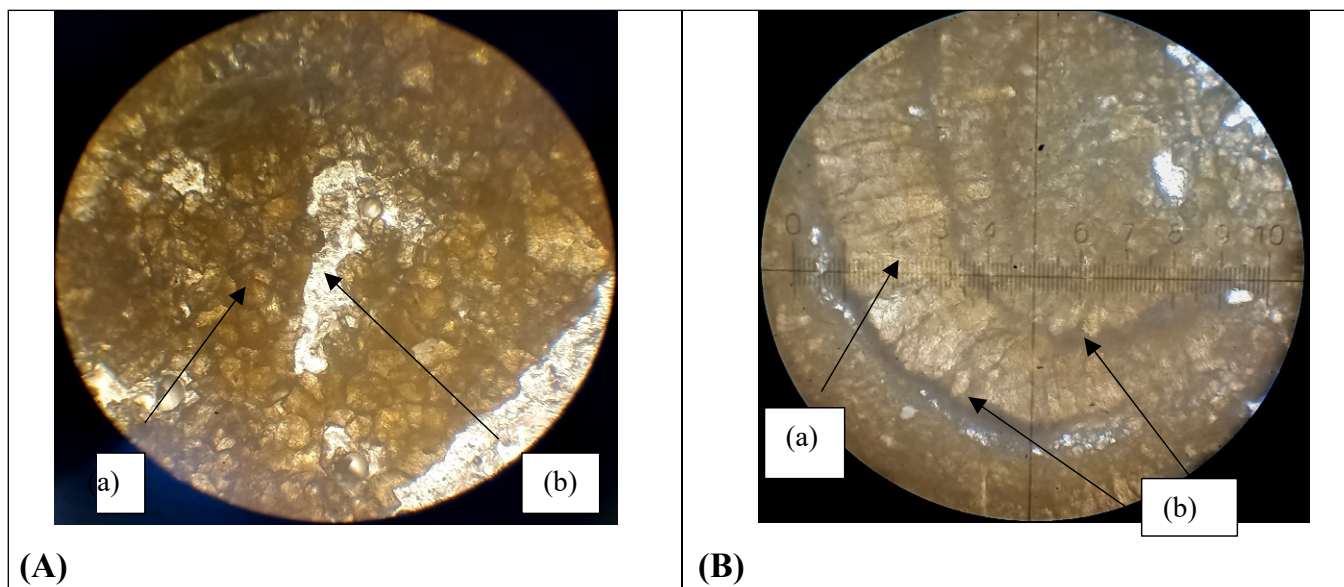


Fig. 3. Microscopic appearance of urates: (A) Central part of the urate structure. Area with polygonal microblock crystals of uric acid monohydrate (a). Formation of colophane (b). Simple transmitted light. Magnification: (x115). (B) Peripheral part of the urate structure. (a)- structure of a concentric-zonal spherulite predominantly composed of urate. (b)- organic matter inclusions. Simple transmitted light. Magnification: (x110).

enriched with organic matter (Fig. 4D). The organic matter was primarily concentrated in separate layers along the perimeter of the stone, less frequently in the form of thin films ("organic shell") on the surface of crystals and their microblocks, as well as in numerous fine-dispersed inclusions within the microblocks of individual crystals.

DISCUSSION

The analysis of stones is an important part of the clinical characterization of urolithiasis. In our study of the qualitative and microstructural composition of kidney stones in residents of heavily industrialized region in Ukraine, we utilized petrographic analysis using a microscopic method and X-ray structural analysis of fragments and dust residues from stones that formed during the manufacturing of thin sections. These methods are widely used worldwide and are continuously being improved and modified.

Indeed, the widespread use of physical methods, such as X-ray diffraction and Fourier-transform infrared spectroscopy (FTIR), has significantly improved the analysis of urinary stones, allowing for precise determination of the chemical nature, crystalline phases, and relative proportions of stone components. However, for common calcium nephrolithiasis, which represents the majority of urinary stones worldwide, simple identification of calcium oxalate (CaOx) and/or calcium phosphate (CaP) as constituents provides incomplete etiological information since stones with the same elemental composition can result from different lithogenic processes [14]. Summarizing the data from microscopic analysis of urolith structure, it can be asserted that their structure

is heterogeneous. This is evident in the fact that urinary stones primarily have a layered structure with varying strength coefficients. The inclusion of an organic component reduces the strength of the crystalline layers. Urolith resembles a brittle-hollow environment, which in certain cases allows for the selection of the most effective methods of their destruction (lithotripsy). However, these data on urolith strength are necessary at the stage of disease diagnosis and determination of strength characteristics before selecting an appropriate method of destruction.

The authors proposed in that Micro-CT has proven to be a powerful modern tool for visualizing urinary stones. The X-ray attenuation values of common stone minerals allow for easy visualization of the stone's structure and identification of minerals, especially when a standard attenuation profile is added to the sample. However, Micro-CT alone cannot identify many rare types of stones, which still require spectroscopic analysis. The 3D visualization capabilities of Micro-CT enable the understanding of the structure of newly formed stones, making this method highly valuable for studying the pathophysiological mechanisms of urolithiasis [8].

The accumulated worldwide experience in studying the treatment and prevention of recurrent urinary stone disease not only highlights its prevalence and continuous increase in many countries but also reveals certain peculiarities in the ontogenesis of stone formation depending on local and general factors in specific regions.

Based on the information from cited literature sources [9-12], a comparative analysis of the composition of

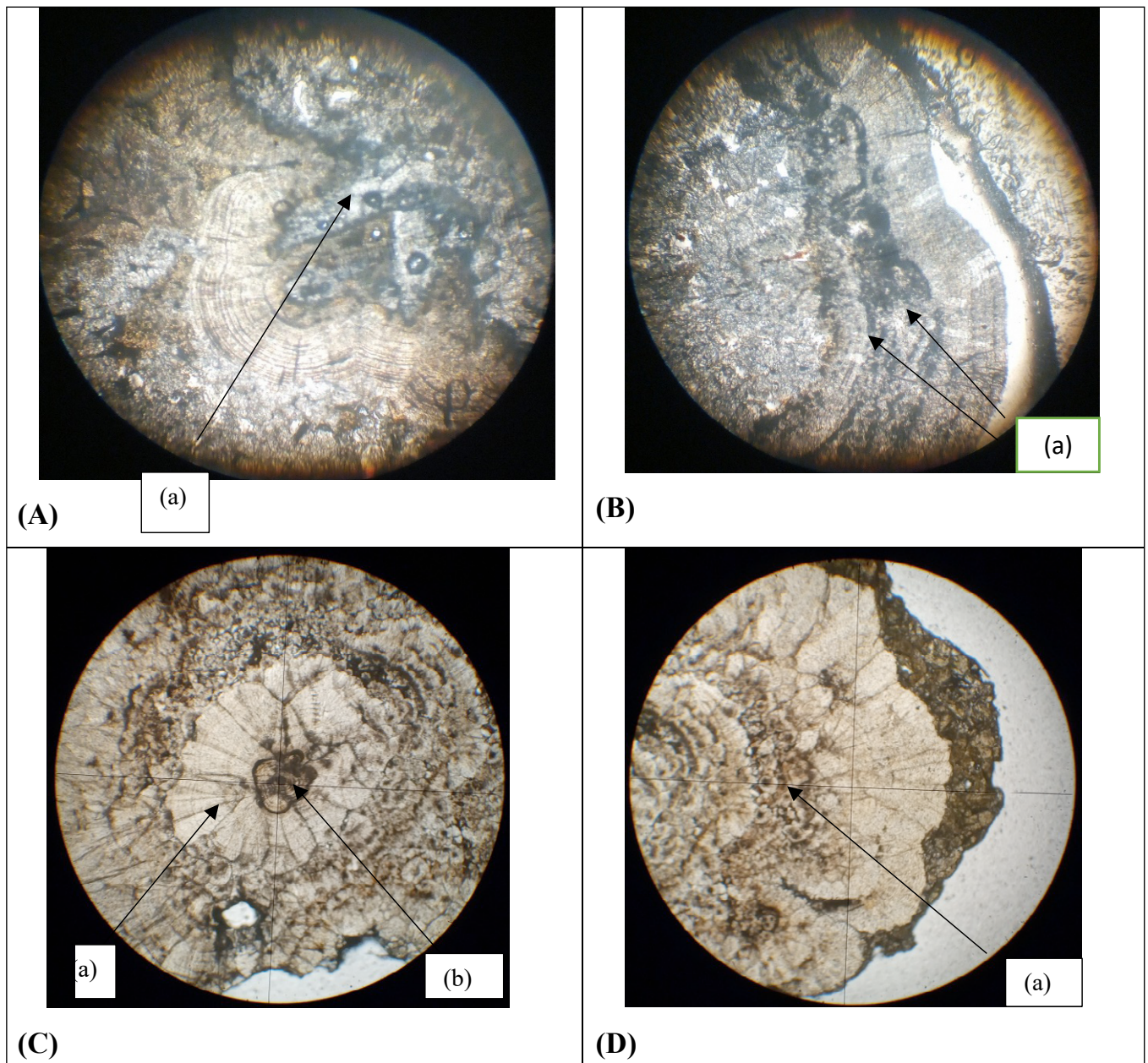


Fig. 4. Microscopic appearance of oxalate: (A) Central part of the oxalate structure. At the crossroads of the threads, there is a vertex of a large weddellite crystal (a). Simple transmitted light. Magnification (x80). (B) Peripheral part of the specimen. Organic matter and the presence of its vein-like form of deposition (a). Simple transmitted light. Magnification (x90). (C) Central part of the oxalate structure. The first generation is represented by a concentric zonal aggregate of bud-like weddellite (a) formed around the "organic core" fragment (b). Simple transmitted light. Magnification (x110). (D) Peripheral part of the oxalate. Boundaries between the 5th, 4th, and 3rd generations of stone formation(a). Simple transmitted light. Magnification (x110).

kidney stones in residents of countries with specific endemic regions afflicted by urinary stone disease has been conducted.

Based on the analysis of the characteristics of urinary stone disease, countries with endemic urinary stone disease have been identified, particularly those located in arid regions with high-temperature climates [13]. In these environments, among various epidemiological factors contributing to stone formation, the factor of high ambient temperature has the most significant impact on the functional status of the kidneys. In the com-

position of kidney stones of residents in these regions, a relatively high level of monocrystalline components is often observed. Moreover, there are significant differences in the frequency of infectious stones depending on the continent and region, ranging from 2.7% in Asia to 13% in South America and 42.9% in sub-Saharan Africa. These differences reflect the infectious risk factors specific to certain population groups, such as dietary habits and the availability of modern medications and antibiotics in each specific locality. Under such conditions, the persistent reduction in renal blood flow leads

to a high concentration of primary urine and constant slowing down of reabsorption processes in the renal tubules. This is evidenced by the relatively high percentage of monomineralic stones and struvite stones.

In industrially developed regions, kidney stones in patients with urinary stone disease predominantly have a mixed composition. However, variations in their composition are minimal and show little difference from one another. In industrially developed countries, there has been a decrease in the number of infectious stones over the course of several decades, but there has also been a continuous increase in the proportion of stones associated with infection [13]. Such significant growth can be attributed to various factors, including the evolution of antibiotic-resistant bacteria and changes in the renal status, the development of secondary nephropathies under the influence of harmful regional factors [2, 3]. Furthermore, the differences in the structure of urinary stones are influenced by various local factors, which may be related to the nature of industrial production, environmental conditions, climatic elements, and more.

The research conducted on kidney stones in residents of our industrial region who suffer from urinary stone disease has shown that they also predominantly have a mixed composition, which depends on various local causative factors. Monocrystalline components of the urinary stones make up less than 1%. However, the presence of a common set of components does not significantly distinguish their composition from the stones in residents of other industrial regions [6].

The multifactorial nature of the influence is reflected in the character of urolithiasis. In the formation of urinary stones, not only thermodynamic but also kinetic factors play an important role [9]. This significantly complicates the physico-chemical analysis of potential crystallization phenomena and necessitates a comprehensive consideration of factors such as the degree of solution saturation, the presence of inhibitors that hinder the formation of microcrystals and their aggregation, the nature of the organic matrix, epitaxial phenomena, as well as the conditions under which nucleation and growth of the urolith occurred [6].

In the studied kidney uroliths, we also examined distinct zones of formation and growth, ranging from 3 to 5 zones, separated by layers of organic matter.

These zones not only differed in their microstructure but also in their chemical composition within the layers. Studying the zonal generation of urinary stones allows us not only to make assumptions that they result from fluctuations in the acid-base balance in the human body but also, through further investigation, to determine the causative factors in urolithic ontogenesis.

Therefore, the obtained information can potentially help in reconstructing the conditions of their nucleation and growth based on their external form and internal structure of minerals and mineral aggregates. Understanding the unique characteristics of the composition of urinary stones in residents of industrially developed regions who suffer from urinary stone disease may contribute to uncovering the underlying causes of their ontogenesis.

CONCLUSIONS

The composition of kidney stones, as determined by optical petrography methods, reveals the presence of 15 mineral species, with oxalate and urate compounds being predominant. A common feature among all mineral components is their diverse microblock structure and the presence of organic inclusions, which diversify the strength characteristics of uroliths. The prior determination of these characteristics allows for the selection of the most effective method for destructive treatment (lithotripsy).

Based on morphological characteristics, five types of uroliths have been identified. The study of the morphological construction of uroliths allows the identification of five zones corresponding to gradually changing stages according to the conditions of mineral formation. These zones are separated by layered accumulation of organic inclusions.

Combining morphological analysis of samples with petrographic research confidently establishes the fundamental patterns of their ontogenesis. This approach also helps determine appropriate and definitive decisions regarding the choice of methods and strategies for preventing this disorder and for the prophylaxis of stone recurrence. The combination of data on the ontogenesis of uroliths, their mineral composition, and the electrolyte balance in the body of a patient suffering from urolithiasis will allow for the selection of an individually effective method of disease prophylaxis.

REFERENCES

1. Tefekli A, Cezayirli F. The History of Urinary Stones: In Parallel with Civilization. *The Scientific World Journal*. 2013. doi:10.1155/2013/423964. DOI
2. Chen Yu-H, Wei Ch-F, Cheng Y-Yu et al. Cadmium Exposure and Urolithiasis: A Systematic Review and Meta-Analysis. 2023. doi:10.2139/ssrn.4534147. DOI
3. Saydakova NO, Shulyak OV, Shylo VM et al. Urolithiasis: state and problematic issues of providing specialized care to the population of Kyiv city. *Urology*. 2018;22(1):33-40. doi: 10.26641/2307-5279.22.1.2018.128123. DOI

4. Dmytrishyn SP. Urolithiasis: epidemiological features in a regional aspect. *Urology*. 2015;19(75):21-29.
5. Lesovoy VN, Kolupaev SM, Andonyeva NM, Emets DA. Structural types of kidney stones and features of their fragmentation by shock waves. *Urology, Andrology, Nephrology - Achievements, Problems, Solutions: materials of online sci.-pract. conf., Kharkiv, September 9-10, 2021. Kharkiv. 2021, pp. 156-157.*
6. Kozar MA, Ishkov VV, Kozly ES. Mineralniy sklad urolitiv meshkantsiv Pridniprov'ya. *Geologichna nauka v nezalezhnii Ukraini. [Mineral warehouse urolitiv meshkantsiv Pridniprov'ya. Geologichna science v nezalezhnii Ukraine]. Zbirnik tez naukovoii konferentsii Institutu geochimii, mineralogii ta rudoutvorennia Im. M.P. Semenena NAN Ukraini, 2021, pp. 52-55. (Ukrainian)*
7. Rodriguez-Plata IT, Medina-Escobedo M, Basulto-Martinez M et al. Implementation of a technique based on Hounsfield units and Hounsfield density to determine the composition of kidney stones. *Tomography* 2021;7(4):606-613. doi: 10.3390/tomography7040051. [DOI](#)
8. Williams JC, Lingeman JE, Daudon M, Bazin D. Using micro computed tomographic imaging for analyzing kidney stones. *Comptes Rendus. Chimie*. 2022;25(1):61-72. doi: 10.5802/crchim.89. [DOI](#)
9. Wang Zh, Zhang Yi, Zhang J et al. Recent advances on the mechanisms of kidney stone formation (Review). *International journal of molecular medicine*. 2021;48(2):149-2-10. doi: 10.3892/ijmm.2021.4982. [DOI](#)
10. Hossain RZ, Ogawa Y, Hokama S et al. Urolithiasis in Okinawa, Japan: A relatively high prevalence of uric acid stones. *International journal of Urology*. 2003;10(8):411-415.
11. Wróbel A, Rokita E, Tatoń G, Thor P. Chemical composition and morphology of renal stones. *Folia Medica Cracoviensia*. 2013;5(53):5–15.
12. Yang X, Zhang Ch, Qi Sh et al. Multivariant Analyses of urinary calculi composition: A 13-year Single Center Study. *Journal of Clinical laboratory analysis*. 2016;30(6):873-879.
13. Daudon M, Petey M, Vimont S et al. Urinary tract infection causing stones: some clinical and chemical findings. *Comptes Rendus. Chimie*. 2022;25(1):315-334.
14. Daudon M, Desombs A, Frocheau V et al. Comprehensive morpho-constitutional analysis of urinary stones improves the etiological diagnosis and treatment strategy of nephrolithiasis. *Comptes Rendus. Chimie*. 2016;19(11-12):1470-1491.

CONFLICT OF INTEREST

The Authors declare no conflict of interest

CORRESPONDING AUTHOR

Kostyantyn Barannyk

Dnipro State Medical University

3 Volodymyr Vernadskyi st, 49044 Dnipro, Ukraine

e-mail: k.barannik1984@gmail.com

ORCID AND CONTRIBUTIONSHIP

Kostyantyn Barannyk: 0000-0002-1009-4990 [A](#) [B](#) [C](#) [D](#)

Valeriy Ishkov: 0000-0002-3987-208X [B](#) [C](#)

Serhiy Barannyk: 0000-0002-4089-6126 [A](#) [C](#) [E](#)

Ruslan Duka: 0000-0003-3962-8746 [A](#) [B](#) [C](#) [E](#) [F](#)

Robert Molchanov: 0000-0002-9589-8364 [A](#) [C](#) [E](#) [F](#)

[A](#) – Work concept and design, [B](#) – Data collection and analysis, [C](#) – Responsibility for statistical analysis, [D](#) – Writing the article, [E](#) – Critical review, [F](#) – Final approval of the article

RECEIVED: 14.11.2023

ACCEPTED: 17.07.2024



Features of the macroscopic structure of the posterior inferior tibiofibular ligament based on anatomical study

Ivan V. Kucher, Andrii P. Liabakh

STATE INSTITUTION "INSTITUTE OF TRAUMATOLOGY AND ORTOPEDICS OF THE NATIONAL ACADEMY OF MEDICAL SCIENCES OF UKRAINE", KYIV, UKRAINE

ABSTRACT

Aim: To study the anatomy of the posterior inferior tibiofibular ligament (PITFL) and specify the features of its morphology and linear parameters.

Materials and Methods: The peculiarities of morphology and linear parameters of PITFL on 10 fresh amputated lower limbs were studied. The average age of the patients was 64.7 ± 9.3 (7 males, 3 females). Macroscopic characteristics, insertion, orientation in relation to the corresponding bony and ligamentous anatomical structures were studied, and linear parameters of PITFL were measured using a caliper. Average values were calculated.

Results: PITFL was detected in all the studied samples. It represented a strong, compact anatomical structure of a trapezoidal or triangular shape. The proximal width of the PITFL averaged 20 ± 3.65 mm, while the distal width was 36.6 ± 4.62 mm. The attachment length of PITFL to the posterior part of the tibia was 28.6 ± 5.13 mm and to the fibula was 17.4 ± 3.2 mm. The ligament is closely connected to the posterior intermalleolar ligament, the inferior transverse ligament, and the tendinous sheaths of the posterior tibial and fibular muscles.

Conclusions: The obtained results of the study of linear and morphological parameters of PITFL should contribute to a better understanding of the anatomy of the posterior part of the ankle joint and improve surgical approaches to the treatment of posterior malleolus fractures and related PITFL injuries.

KEY WORDS: ankle joint, posterior malleolus fracture, distal tibiofibular syndesmosis, posterior inferior tibiofibular ligament, anatomical study

Wiad Lek. 2024;77(9):1680-1685. doi: 10.36740/WLek/191326 DOI

INTRODUCTION

Ankle fractures are one of the most common injuries of the ankle joint, with 40% of the cases being associated with posterior malleolus fractures (PMF) and 20% with injuries of the distal tibiofibular syndesmosis (DTFS) [1]. The anatomical features of the structure of the DTFS ligament complex are closely related to the biomechanics of ankle injuries, which significantly explains the patterns of occurrence of PMF and forms the basis for proper approach to the treatment of these injuries. Despite the fact that the structure of the DTFS has been sufficiently covered in a number of scientific publications in recent years [2–5], there are still disagreements in the terminology, naming, and morphology of certain anatomical formations, in particular, the posterior inferior tibiofibular ligament (PITFL). The current interest in the study of the anatomy of DTFS can be explained by its influence on the stability of the ankle joint, which, even with the precise restoration of the position of ankle fractures, often requires additional surgical treatment. A detailed study of the anatomical features of the PITFL may clarify the pathogenesis of PMF and may help to resolve a number of debatable practical issues regarding the treatment of these injuries.

AIM

The aim of the work was to analyze the anatomy of the posterior inferior tibiofibular ligament and clarify the features of its morphology and linear parameters.

MATERIALS AND METHODS

The material for the study consisted of 10 fresh amputated lower limbs, on which the anatomy of the posterior inferior tibiofibular ligament was examined. The average age of the patients was 64.7 ± 9.3 (range 50–78 years). There were 7 male, 3 female patients. The nosological forms that led to the amputation of the lower limb were obliterating angiopathy of the arteries of lower limbs and consequences of injuries. Inclusion criteria for amputated lower limbs in the study: absence of anatomical defects and tissue damage in the area of the tibiotalar joint, absence of contractures of the ankle and foot joints, and pronounced necrotic changes in the soft tissues of the ankle and foot. All anatomical specimens had no external signs of previous surgical intervention, congenital or acquired deformities, or signs of rheumatic diseases. The use

Table 1. The results of measurements of angular and linear parameters of the posterior inferior tibiofibular ligament according to the results of the study

Parameters	Measurement results in mm ($M \pm \sigma$; min-max)
Proximal width of PITFL	20 ± 3.65 ; (15-26)
Distal width of PITFL	36.6 ± 4.62 ; (30-44)
The length of PITFL on the tibia	28.6 ± 5.13 ; (20-36)
The length of PITFL on the fibula	17.4 ± 3.2 ; (12-22)
Angle°	$30^\circ \pm 4.35^\circ$

Notes. $M \pm \sigma$ – mean and standard error; min-max — minimum and maximum values.

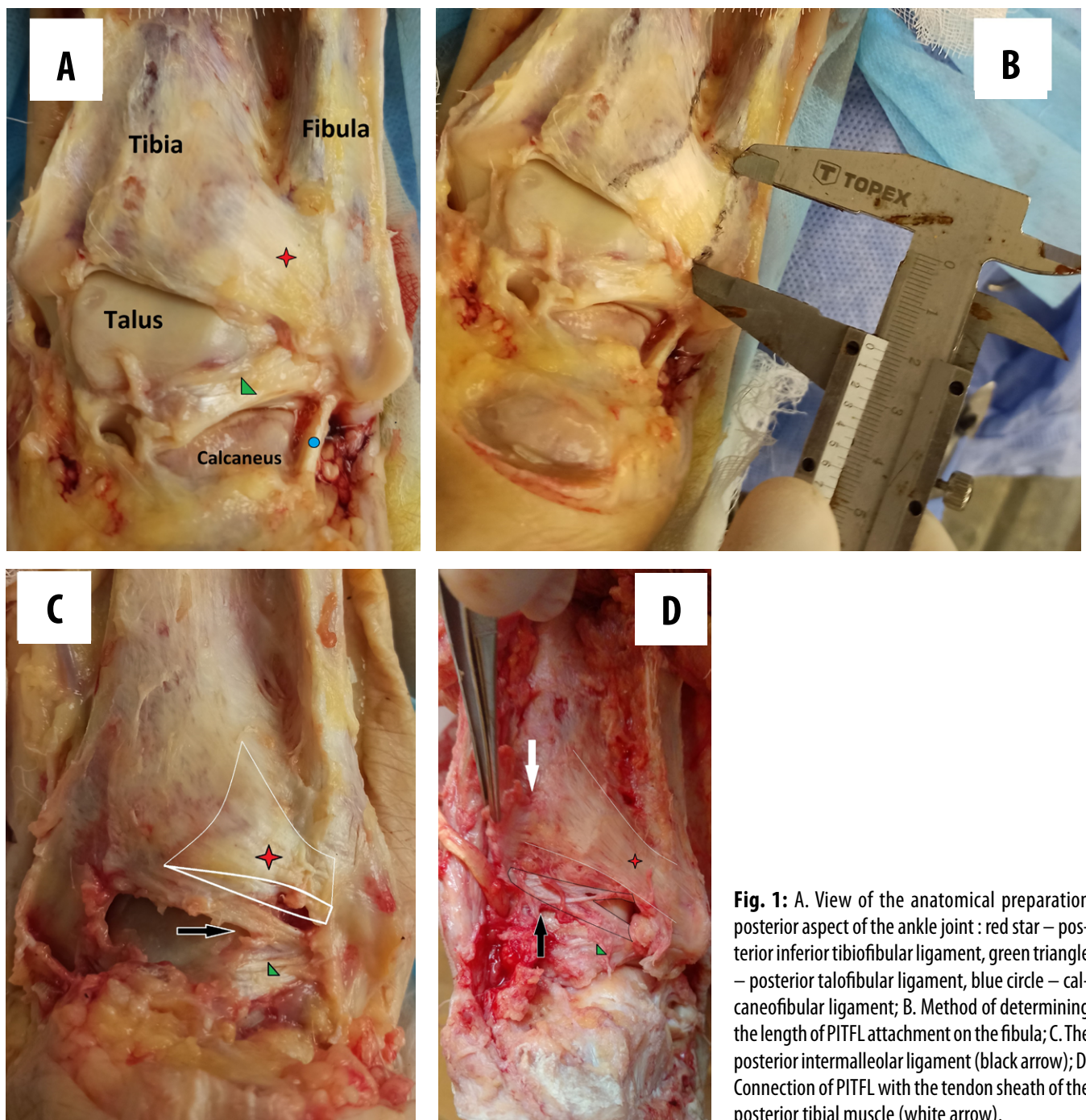


Fig. 1: A. View of the anatomical preparation posterior aspect of the ankle joint : red star – posterior inferior tibiofibular ligament, green triangle – posterior talofibular ligament, blue circle – calcaneofibular ligament; B. Method of determining the length of PITFL attachment on the fibula; C. The posterior intermalleolar ligament (black arrow); D. Connection of PITFL with the tendon sheath of the posterior tibial muscle (white arrow).

of patient medical history data was carried out in accordance with the requirements of the Bioethics Committee of the State Institution “The Institute of

Traumatology and Orthopedics of NAMS”, and all procedures performed with the patients met the ethical standards of the institutional and/or national research

committee, as well as the Helsinki Declaration of 1964 and its later amendments.

Preparation (dissection) was carried out in order to identify the morphology of the posterior inferior tibiofibular ligament (Fig. 1A). The amputated segment of the lower limb was fixed to the table with the ventral surface of the ankle, while the ankle joint was in a neutral position outside the dissection table. Among the 10 ankle and foot joints studied, 6 were left and 4 were right. The results of the preparation were recorded in digital format for comparing the morphological characteristics of the studied samples. All anatomical specimens were prepared in the same sequence. In the first stage, the skin was removed from the posterior surface of the tibia along with the subcutaneous adipose tissue. The Achilles tendon was cut off from its attachment point on the calcaneus in a proximal direction along with the gastrosoleus complex and the Kager's fat pad. Deep fasciae of the ankle, muscles and tendons such as *m. flexor hallucis longus*, *m. peronei*, *m. flexor digitorum longus* and *m. tibialis posterior*, along with the vascular and nerve bundles, were carefully removed in all samples. The tendon sheath was cut in the midline and the tendons were removed, leaving the base of the sheath. A caliper (calibrated to 0.1 mm) was used to conduct direct measurements of the linear parameters of PITFL (Fig. 1B). The results of the dissection of all anatomical specimens were assessed by both authors. Macroscopic characteristics, insertion, orientation in relation to the corresponding bony and ligamentous anatomical structures, as well as linear measurements of PITFL, and were performed in an identical sequence. Each measurement was repeated three times, and the average values were calculated. The calculated data were entered into an electronic spreadsheet and descriptive statistics were calculated.

RESULTS

In our study, PITFL was detected in all anatomical samples. Visually, the ligament consisted of well-defined fibers throughout its length and presented a multifascicular, strong, compact anatomical structure of a trapezoidal or triangular shape. The PITFL originated on the posterior surface of the lateral malleolus and extended in the upper medial direction, attaching along the posterior border of the tibia (Volkman's triangle) with a gradual transition to the posterior surface of the distal epimetaphysis of the tibia, integrating into the periosteum in the periphery. In the proximal direction, the PITFL had a strong connection with the posterior fibers of the interosseous ligament. The average proximal width of the PITFL was 20 ± 3.65 mm, the distal

width was 36.6 ± 4.62 mm. The attachment length of the PITFL on the posterior part of the tibia was 28.6 ± 5.13 mm, and on the lateral malleolus was 17.4 ± 3.2 mm. The data from our anatomical study is consistent with the data of Jayatilaka et al. [6], indicating that the PITFL has a dense connection with the tendon sheath of the posterior tibial muscle medially and with the tendon sheath canal of the peroneal muscles laterally (Fig. 1D). The mentioned study by Jayatilaka categorizes the surface of PITFL into oblique and transverse portions, which, in our opinion, is challenging to differentiate in anatomical preparations due to the lack of clear defined anatomical landmarks of the transition of the surface of the PITFL to the specified segments and the gradual integration of the ligament into the periosteum. However, it should be noted that the lateral part of the PITFL had a thicker structure, which thinned as it spread medially to the distal epimetaphysis of the tibia. The angle between the vertical axis of the lateral bone and PITFL was $30^\circ \pm 4.35^\circ$. The data on the results of the linear parameters of PITFL are presented in Table 1.

DISCUSSION

The measurements of the linear parameters of PITFL in our study correlate well with the study by Martins et al. [7], however, the authors provide slightly smaller values of the linear parameters, which may be due to anthropometric features and different measurement methodologies. Ebraheim et al. [8] described the shape of PITFL as triangular, narrowing at the point of transition to the lateral malleolus, while Williams et al. [3] indicate a trapezoidal shape, which is consistent with the results of our study.

There is a discussion in the scientific literature regarding the anatomical definition of the inferior transverse ligament (ITL). A number of anatomical, radiological and clinical studies describe the inferior transverse ligament as a component of PITFL, while others indicate the inferior transverse ligament as a separate anatomical structure [9]. For example, Lilyquist et al. [10] showed that the ITL is found in 70% of anatomical preparations and is a well-defined anatomical structure. Ebraheim et al. also describes the ITL as a separate anatomical structure, and indicates that there is an additional fibrous and adipose connective tissue between the PITFL and ITL [8]. Lee et al. [11] demonstrated that MRI arthrography allows distinguishing between the superficial and deep components of the posterior tibial ligament. Similar findings are reported by Muhle et al. [12], who, using high-resolution MRI, clearly distinguish between PIT-

FL and ITL in all examined samples during dorsal or plantar flexion of the foot. In contrast to these studies, Bartoníček et al. [13] distinguish the superficial and deep fibers of PITFL, without describing the ITL as a separate ligament. Martins et al. [7], agree with this view, pointing to the morphological and functional homogeneity of these structures. The controversial nature of these data, in our opinion, may be due to the different methodologies of the conducted studies and the corresponding criteria for assessment these structures. In our study, the inferior transverse ligament was found in all cases and was closely adjacent to the PITFL. The ligament is originated below the attachment of PITFL in the area of the lateral malleolar fossa with further attachment in the medial parts of the distal epimetaphysis of the tibia. ITL was placed more horizontally and visually characterized by denser fibers.

Some anatomical studies show that PITFL and ITL form a distinct joint lip or “meniscus-like addition” to the ankle joint, which allows to increase the articular surface and improve the congruence of the tibial plateau [13–15]. It remains interesting that the posterior intermalleolar ligament, which is characterized by a significant anatomical variability [7], has a place of adjacent attachment to the posteromedial edge of the tibial plateau. The anatomical study of Edama M. et al. [16] shows that in 70.3% of cases these anatomical structures have additional connections. According to some authors, the given morphological features can be important factors influencing the pathophysiological mechanism of the occurrence of the posteromedial fragment of the PMF in ankle fractures [17,18]. In our study, the posterior interosseous ligament had a variable morphology from a thick “rope-like” structure to separate thin bundles, and represented a distinct anatomical structure that, together with ITL, was attached to the posteromedial part of the posterior margin of the tibia (Fig. 1C, D).

Obtained in our study results of the linear measurements of the PITFL demonstrate a significant area of ligament attachment to the distal tibia and its close relationship with the dynamic (ligamentous) stabilising complex of the ankle joint. Taking into account these data, it’s logical to assume, that different morphological types of PMF may be accompanied by concomitant injuries of the PITFL and anatomically related structures of the posterior aspect of the ankle joint, which vary significantly in each case and, accordingly, affect the stability of the DTFS. Fujimoto et al. [19] demonstrated the need to assess the size of the PMF in the mediolateral dimension, which allows to analyse the possibility

of additional damage to the PITFL and, accordingly, increase syndesmotic instability. Beumer et al. [20] showed that, along with the highest biomechanical strength and stiffness of the PITFL among the ligaments of DTFS, the predominant type of damage to this ligament, along with avulsion, is substance ruptures. Warner et al. [21] showed that in rotationally unstable ankle fractures, even in the absence of a PMF, in 97% of cases, the PITFL was delaminated from the posterior malleolus, which necessitates additional surgical treatment. Another study by Warner SJ et al. [22] showed that PER IV ankle fracture-dislocations have worse functional outcomes and a higher risk of malreduction, which may be associated with substantial articular damage.

The majority of studies have demonstrated the advantages of using a buttress plate in the treatment of PMF compared to screws [23–25]. In our opinion, the studied morphological features of the PITFL, confirm the advantages of osteosynthesis of even small fragments of the PMF with the buttress plate, which provides not only stable fixation of PMF, but also, due to the larger contact area, improves the stability of the DTFS, due to additional stabilisation of the damaged PITFL and its related components («articular lip of the ankle joint»).

Our study had several limitations. Firstly, a relatively small number of specimens of anatomic preparations were studied, the studied ankle joints were obtained from patients of a similar age and racial origin. Further studies evaluating a larger sample of preparations in different age groups and races are needed. Secondly, PITFL was studied by means of a macroscopic examination, which may create an additional probability of error in the assessment by researchers. Thirdly, the insertion sites of PITFL during macroscopic examination may differ from histological ones, which requires further histological examination.

CONCLUSIONS

PITFL is a strong, compact anatomical structure of a trapezoidal or triangular shape, which has a wide attachment in the posterior malleolus area. The ligament has a tight fusion with the interosseous ligament, inferior transverse ligament, as well as with the tendon sheaths of the posterior tibial and fibular muscles. The anatomical features of the PITFL indicate that osteosynthesis of PMF with plate and screws indirectly creates additional stabilisation of the PITFL and associated ligamentous structures, which can improve the syndesmotic stability of the ankle joint.

REFERENCES

1. Mason LW, Marlow WJ, Widnall J, Molloy AP. Pathoanatomy and Associated Injuries of Posterior Malleolus Fracture of the Ankle. *Foot Ankle Int* 2017;38:1229–35. doi:10.1177/1071100717719533. [DOI](#)
2. Lilyquist M, Shaw A, Latz K et al. Cadaveric Analysis of the Distal Tibiofibular Syndesmosis. *Foot Ankle Int* 2016;37:882–90. doi:10.1177/1071100716643083. [DOI](#)
3. Williams BT, Ahrberg AB, Goldsmith MT et al. Ankle Syndesmosis. *Am J Sports Med* 2015;43:88–97. doi:10.1177/0363546514554911. [DOI](#)
4. Hermans JJ, Beumer A, De Jong TAW, Kleinrensink G-J. Anatomy of the distal tibiofibular syndesmosis in adults: a pictorial essay with a multimodality approach. *J Anat.* 2010;217:633–45. doi:10.1111/j.1469-7580.2010.01302.x. [DOI](#)
5. Kikuchi S, Tajima G, Sugawara A et al. Characteristic features of the insertions of the distal tibiofibular ligaments on three-dimensional computed tomography- cadaveric study -. *J Exp Orthop.* 2020;7:3. doi:10.1186/s40634-020-0220-6. [DOI](#)
6. Jayatilaka MLT, Philpott MDG, Fisher A et al. Anatomy of the Insertion of the Posterior Inferior Tibiofibular Ligament and the Posterior Malleolar Fracture. *Foot Ankle Int.* 2019;40:1319–24. doi:10.1177/1071100719865896. [DOI](#)
7. Martins CF, Miranda M, Cortegana IM et al. Posteroinferior tibiofibular ligament – A cadaveric study. *Foot and Ankle Surgery.* 2021;27:296–300. doi:10.1016/j.fas.2020.06.005. [DOI](#)
8. Ebraheim NA, Taser F, Shafiq Q, Yeasting RA. Anatomical evaluation and clinical importance of the tibiofibular syndesmosis ligaments. *Surgical and Radiologic Anatomy* 2006;28:142–9. doi:10.1007/s00276-006-0077-0. [DOI](#)
9. Hermans JJ, Beumer A, De Jong TAW, Kleinrensink G-J. Anatomy of the distal tibiofibular syndesmosis in adults: a pictorial essay with a multimodality approach. *J Anat.* 2010;217:633–45. doi:10.1111/j.1469-7580.2010.01302.x. [DOI](#)
10. Lilyquist M, Shaw A, Latz K et al. Cadaveric Analysis of the Distal Tibiofibular Syndesmosis. *Foot Ankle Int.* 2016;37:882–90. doi:10.1177/1071100716643083. [DOI](#)
11. Lee SH, Jacobson J, Trudell D, Resnick D. Ligaments of the Ankle: Normal Anatomy with MR Arthrography. *J Comput Assist Tomogr* 1998;22:807–13. doi:10.1097/00004728-199809000-00027. [DOI](#)
12. Muhle C, Frank LR, Rand T et al. Tibiofibular Syndesmosis. *J Comput Assist Tomogr.* 1998;22:938–44. doi:10.1097/00004728-199811000-00019. [DOI](#)
13. Bartonicek J. Anatomy of the tibiofibular syndesmosis and its clinical relevance. *Surgical and Radiologic Anatomy.* 2003;25:379–86. doi:10.1007/s00276-003-0156-4. [DOI](#)
14. Golanò P, Mariani PP, Rodríguez-Niedenfuhr M et al. Arthroscopic anatomy of the posterior ankle ligaments. *Arthroscopy: The Journal of Arthroscopic & Related Surgery.* 2002;18:353–8. doi:10.1053/jars.2002.32318. [DOI](#)
15. Ferkel RD, Kwong C, Farac R et al. Arthroscopic Posterior Ankle Ligament Anatomy. *Foot Ankle Orthop.* 2021;6:247301142110006. doi:10.1177/24730114211000624. [DOI](#)
16. Edama M, Takabayashi T, Inai T et al. Morphological features of the deep component of the posterior inferior tibiofibular ligament. *Surgical and Radiologic Anatomy.* 2020;42:691–3. doi:10.1007/s00276-019-02417-2. [DOI](#)
17. Jayatilaka MLT, Philpott MDG, Fisher A et al. Anatomy of the Insertion of the Posterior Inferior Tibiofibular Ligament and the Posterior Malleolar Fracture. *Foot Ankle Int.* 2019;40:1319–24. doi:10.1177/1071100719865896. [DOI](#)
18. Vosoughi AR, Jayatilaka MLT, Fischer B et al. CT Analysis of the Posteromedial Fragment of the Posterior Malleolar Fracture. *Foot Ankle Int.* 2019;40:648–55. doi:10.1177/1071100719830999. [DOI](#)
19. Fujimoto S, Teramoto A, Anzai K et al. Tibial Plafond Attachment of the Posterior-Inferior Tibiofibular Ligament: A Cadaveric Study. *Foot Ankle Orthop.* 2020;5:247301142094568. doi:10.1177/2473011420945689. [DOI](#)
20. Beumer A, van Hemert WLW, Swierstra BA et al. A Biomechanical Evaluation of the Tibiofibular and Tibiotalar Ligaments of the Ankle. *Foot Ankle Int.* 2003;24:426–9. doi:10.1177/107110070302400509. [DOI](#)
21. Warner SJ, Garner MR, Schottel PC et al. Analysis of PITFL Injuries in Rotationally Unstable Ankle Fractures. *Foot Ankle Int.* 2015;36:377–82. doi:10.1177/1071100714558845. [DOI](#)
22. Warner SJ, Schottel PC, Hinds RM et al. Fracture-Dislocations Demonstrate Poorer Postoperative Functional Outcomes Among Pronation External Rotation IV Ankle Fractures. *Foot Ankle Int.* 2015;36:641–7. doi:10.1177/1071100715572222. [DOI](#)
23. Baumbach SF, Herterich V, Dambelmont A et al. Open reduction and internal fixation of the posterior malleolus fragment frequently restores syndesmotomic stability. *Injury.* 2019;50:564–70. doi:10.1016/j.injury.2018.12.025. [DOI](#)
24. O'Connor TJ, Mueller B, Ly TV et al. "A to P" Screw Versus Posterolateral Plate for Posterior Malleolus Fixation in Trimalleolar Ankle Fractures. *J Orthop Trauma.* 2015;29:e151–6. doi:10.1097/BOT.0000000000000230. [DOI](#)
25. Bennett C, Behn A, Daoud A et al. Buttress Plating Versus Anterior-to-Posterior Lag Screws for Fixation of the Posterior Malleolus: A Biomechanical Study. *J Orthop Trauma.* 2016;30:664–9. doi:10.1097/BOT.0000000000000699. [DOI](#)

CONFLICT OF INTEREST

The Authors declare no conflict of interest

CORRESPONDING AUTHOR

Ivan V. Kucher

Institute of traumatology and ortopedics
of the National Academy of Medical Sciences of Ukraine
27 Bulvarno-Kudriavska, 01601, Kyiv, Ukraine
e-mail: ivkucher906@ukr.net

ORCID AND CONTRIBUTIONSHIP

Ivan V. Kucher: 0000-0001-6006-1241 **A** **B** **C** **D**

Andrii P. Liabakh: 0000-0001-5734-2392 **A** **D** **E** **F**

A – Work concept and design, **B** – Data collection and analysis, **C** – Responsibility for statistical analysis, **D** – Writing the article, **E** – Critical review, **F** – Final approval of the article

RECEIVED: 18.11.2023

ACCEPTED: 17.07.2024



Evaluation of immunohistochemical expression of collagen type I in bone defect treated by local application of collagen and beta-tricalcium phosphate in rats

Bayan Jabr Hussein, Ban A.Ghani

DEPARTMENT OF ORAL DIAGNOSTIC SCIENCES, COLLEGE OF DENTISTRY, UNIVERSITY OF BAGHDAD, BAGHDAD, IRAQ

ABSTRACT

Aims: This study aimed to estimate outcome of combined application of collagen/ β -tricalcium phosphate (Coll / β -TCP) on bone defect healing by immunohistochemical localization of collagen type I.

Materials and Methods: A total of 20 adult male rats (albino rats) were used in this study. Four intra bony defects were created in both femurs of each rat, three defects were treated with Coll, β -TCP and combination of Coll / β -TCP while forth defect left to heal spontaneously as control. Scarification of animals was done after 2- and 4-weeks healing periods (10 rats for each). Immunohistochemical localization of collagen type I (COL1) monoclonal antibody was done for all bone specimens.

Results: Immunohistochemical results showed positive expression of (COL1) by bone cells osteoblast (OB), osteocyte (OC), osteoclast (OCL) and bone marrow stromal cells (BMSCs) at 2- and 4-week duration for all examined groups with variable rates of intensity. Mean values of immunoreactive score (IRS) decreased with time for bone cells and for BMSCs except for OC where values increased with time as the highest values were recorded in combination group at 4 weeks.

Conclusions: Combined application of (Coll / β -TCP) was effective in accelerating bone healing process through elevating the IRS of (COL1) noticed by osteoblast, osteocyte and bone marrow stromal cells.

KEY WORDS: bone defect, collagen, β -TCP, collagen type I

Wiad Lek. 2024;77(9):1686-1692. doi: 10.36740/WLek/192861 DOI

INTRODUCTION

Bones are hard structures that are a component of the endoskeleton of vertebrates. In addition to producing red and white blood cells and storing minerals, they support and shield the body's numerous organs [1]. Bone, being a structural tissue, has the ability to repair itself via a process called "bone remodeling," where in new bone tissue (formation) replaces aged bone tissue (resorption) [2]. Bone deformities and fractures were traditionally treated with autologous or artificial bone grafting techniques. However, these operations are not always advised because of the risks connected to bone replacement surgery, including infection and morbidity. The use of artificial scaffolds, which stimulate osteoblasts to differentiate and generate new bone tissue to replace the damaged areas, is an additional method for bone repair and regeneration [3]. Beta-tricalcium phosphate, denoted as β -TCP, represents a calcium phosphate compound derived from phosphoric acid, characterized by the chemical formula $\text{Ca}_3(\text{PO}_4)_2$ [4]. β -TCP is a material that is frequently used in clinical

orthopedics because it is highly osteoconductive and osteoinductive with lack of histotoxicity [5]. These characteristics, along with its cell-mediated resorption enable the regeneration of entire bone defects [6], also has the ability to modulate osteogenic events that contribute to bone repair and healing including the differentiation of mesenchymal stem cells towards bone-forming cells, the generation of blood vessels, the secretion of growth factors that promote angiogenesis, and the initiation of blood clot formation [7]. The most prevalent macromolecule in the body is collagen (Coll) which is found in different tissues as extracellular matrix. Collagen's intricate structure plays a significant function in the body's various biological processes during the processes of development and regeneration. The process of calcification in bone tissue is one instance [8]. Products containing collagen have been shown to have a significant positive impact on human health, particularly in older adults, clinical trials on the effects of collagen treatment on a variety of conditions, such as rheumatoid arthritis, osteoarthritis, sarcopenia,

dental therapy, wound healing, and skin regeneration [9]. β -TCP/Coll, a biocompatible and bioresorbable composite material, mimics the characteristics of the inorganic component of bone, leading to the generation of newly formed bone tissue [10]. Collagen type I marker (COL1) is referred to as a triple-helical domain because of its composition in the formula of G-X-Y. Here, X and Y can be any amino acid, but glycine (G) is a persistent amino acid. Typically, proline and hydroxyproline use X and Y [11]. Each of these three units will show up more than once as repeated units. Glycine comes in third position is important for confirming the helical structure construction. Later on, this will be contained in a different dimension of the hexagon and quasi-hexagonal formulae to form fibrillar COL1. Therefore, COL1 is normally discovered as a long fibril [12]. Collagen type I constitutes the primary organic element within the mineralized structure of bone matrix and its expression in the bone matrix was found through the use of immunohistochemical staining. The extracellular matrix made up of type I collagen and several noncollagenous proteins must be deposited in order for osteoblastic cells to form bone, which afterward mineralizes by hydroxyapatite crystals formation [13].

AIM

This study aimed to estimate outcome of combined application of collagen/ β -tricalcium phosphate (Coll/ β -TCP) on bone defect healing by immunohistochemical localization of collagen type I.

MATERIALS AND METHODS

Twenty adult male albino rats weighing approximately 250–350 g and aged 3–4 months were used in this study. They received injectable ketamine hydrochloride 50 mg intramuscularly (1 ml/kg body weight) plus 2% xylazine (0.2 ml/kg body weight). Surgery was achieved under sterile conditions by making an incision on the skin and underlying fascia. Then, reflection was performed to expose the rat femurs. Intrabony defects approximately 3 mm in depth and 2 mm in width were induced in both femurs of each animal (Fig. 1), with intermittent drilling and constant cooling with normal saline using a micro engine that was set at a rotational speed of 2500 rpm. The operation sites were cleaned with normal saline to eliminate debris. Then subdivided into group A (20 defects) as the control group, were left untreated for spontaneous healing. Groups B (20 defects) filled with collagen, group C (20 defects) filled with β -TCP and finally group D (20 defects) were filled with combination of Coll and β -TCP materials in a ratio

of 1:1. Animals were sacrificed after 2- and 4-weeks healing periods (10 rats for each) by administering an excessive amount of anesthesia.

IMMUNOHISTOCHEMICAL PREPARATION

Collected bone specimens were fixed for 24 hours using 10% freshly made formalin. Then the process of decalcification was carried out using 10% formic acid for 2-3 days afterward they were embedded in paraffin wax. A microtome was used for section of the blocks for serial slices of 4 μ m, which were positioned on charged slide. Following immunohistochemical staining, the analysis of COL1 localization by bone cells and bone marrow stromal cells (BMSCs) was done for all bone specimens in 2- and 4-weeks durations.

STATISTICAL ANALYSIS

Descriptive analysis of mean, standard deviation (SD), minimum (Min), and maximum (Max) values of the IRS of COL1 by bone cells (OB, OC, and OCL) and bone marrow stromal cells (BMSCs) at 2- and 4-week duration was done for all investigated groups. For immunohistochemical evaluation of COL1, a x40 objective lens was used as follows: positively stained cells were counted in five representative fields (x40). The approximation of the percentage of positively stained cells was obtained by dividing the total number of stained cells by the total number of cells present, then multiplying this result by 100. The scores were: 0 (no stain), 1 (<25%), 2 (25-50%), 3 (>51-80%) and 4 (>80%) stained cells in two sections and scoring the intensity of stain as: 0 (no clear stain), 1 (mild stain), 2 (moderate stain), 3 (intense stain) and accomplishing the immunoreactive score (IRS), which is the result of multiplying the staining intensity score by the percentage of positive cells (0–4), has a range of 0–12 [14].

ETHICAL APPROVAL

The study was approved by the College of Dentistry/ University of Baghdad's local ethics commission (Ref. number:429. Date 27/12/2021).

RESULTS

IMMUNOHISTOCHEMICAL RESULT FOR EXPRESSION OF COLLAGEN TYPE I AFTER 2- AND 4-WEEKS DURATIONS

TWO WEEKS DURATION

Immunohistochemical localization of COL1 in control groups shows positive expression of COL1 in bone

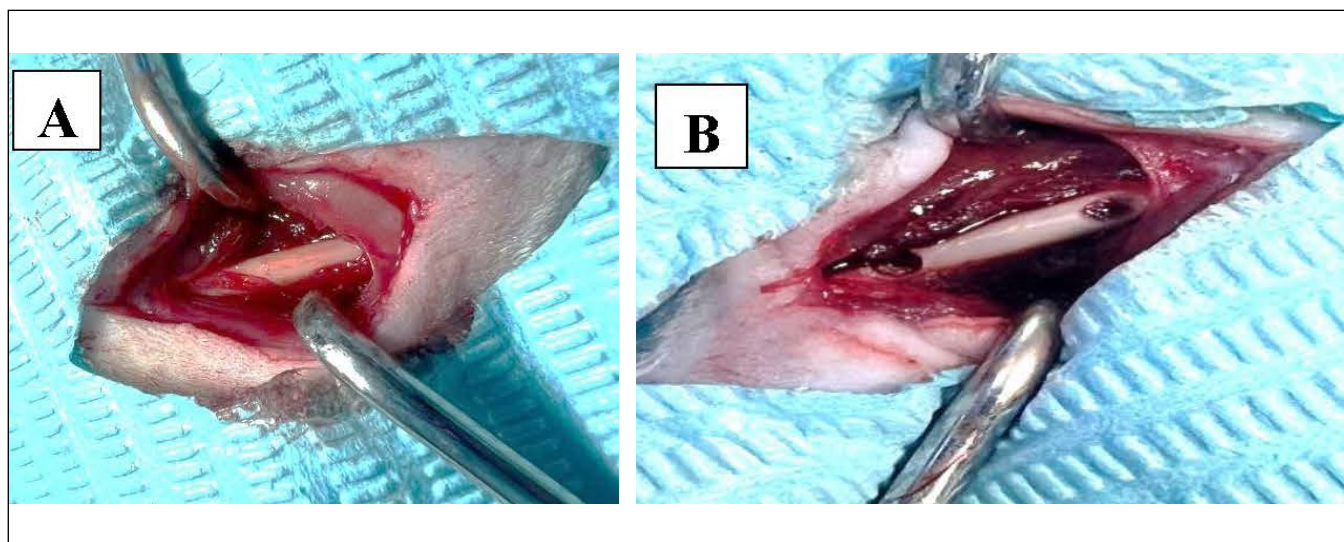


Fig. 1. Intra-bony defects in femurs of animal: A) exposure of rat femur; B) intra-bony defects prepared.

marrow stromal cell, osteoblasts, osteocytes and osteoclasts, bone trabeculae are negatively stained (Fig. 2). Microphotograph view of defect area of collagen group shows positive expression of COL1 monoclonal antibody by bone marrow stromal cells, osteoblasts, osteocytes, osteoclasts (Fig. 3). In β -tricalcium phosphate group immunohistochemical localization of COL1 monoclonal antibody noticed by osteoblasts, osteocytes, and BMSCs, whereas bone trabeculae are negatively stained (Fig. 4). Immunohistochemical positive localization of COL1 in bone section of combination group shown in osteocytes, osteoblasts, osteoclasts and bone marrow stromal cells (Fig. 5).

FOUR WEEKS DURATION

Immunohistochemical expression of COL1 in bone section of control group at 4 weeks duration shows positive expression in osteoblasts, osteocytes and bone marrow stromal cells, negative expression noticed in bone trabeculae (Fig. 6). For collagen group immunohistochemical localization of COL1 at 4 weeks duration shows positive expression in osteocytes, while bone is negatively stained (Fig. 7). Immunohistochemical expression of COL1 in bone section of β -TCP group after 4 weeks duration seen in osteoblasts, osteocytes and bone marrow stromal cells. Mature bone shows negative expression (Fig. 8). Immunohistochemical localization of COL1 at 4 weeks duration of combination group (β -TCP +Collagen) showed positive expression in osteocytes, osteoblasts and bone marrow stromal cells (Fig. 9).

STATISTICAL ANALYSIS OF IMMUNOHISTOCHEMICAL RESULTS

DESCRIPTIVE DATA ANALYSIS FOR PERCENTAGES OF POSITIVELY STAINED CELLS FOR COL1 IN STUDIED GROUPS AND DURATIONS

The descriptive data of mean, SD, Min., and Max. values of the immunoreactive score (IRS) expression of COL1 by bone cells (osteoblasts, osteocytes, osteoclast) and bone marrow stromal cells at 2- and 4-week durations for all studied groups are illustrated in table 1 and figures 10A-D. Mean values of IRS decreased with time for bone cells and BMSCs except for OC where mean values of IRS increased with time as the highest values were recorded in combination group at 4 weeks. The highest mean values of IRS noticed in combination groups for OB and BMSCs and for OC at 2 and 4 weeks respectively.

GROUP COMPARISON FOR BONE CELLS AND BMSCS IN HEALING DURATIONS (2 AND 4 WEEKS)

The group comparison of IRS and COL1 for bone cells (OB, OC, and OCL) and BMSCs are illustrated in table 2. An ANOVA test was conducted, and the results showed that all groups had a highly significant difference ($P < 0.01$) for osteoblasts, osteocytes, osteoclasts and BMSCs after 2 and 4 weeks.

DISCUSSION

The process of bone healing is intricate and dynamic, involving a carefully planned sequence of biological

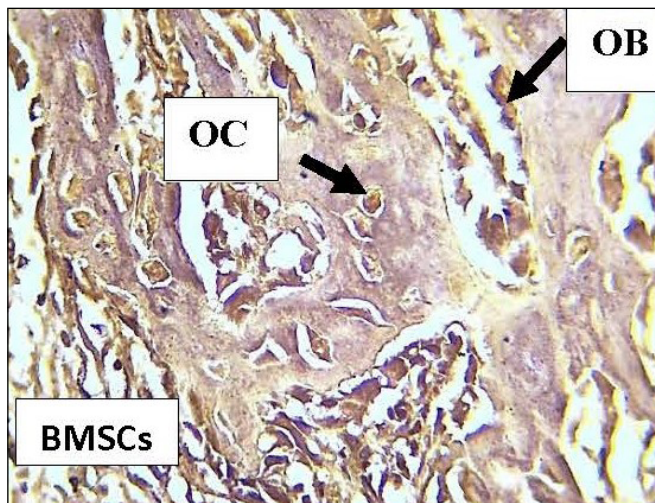


Fig. 2. View of control group after 2 weeks shows positive localization of COL1 in bone marrow stromal cells (BMSCs), osteoblasts (OB), osteocytes (OC). DAB stain with hematoxylin counter stain (x40).

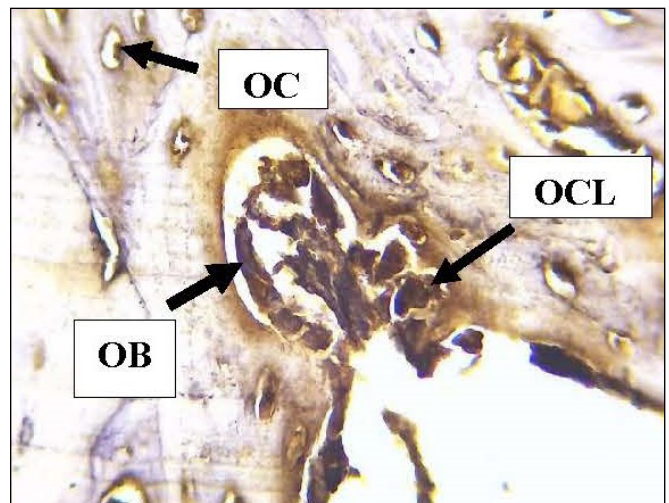


Fig. 4. Microphotograph view of β -TCP group at 2 weeks duration shows positive expression of COL1 in osteocytes (OC), osteoblast (OB) and osteoclasts (OCL). DAB stain with hematoxylin counter stain (x40).

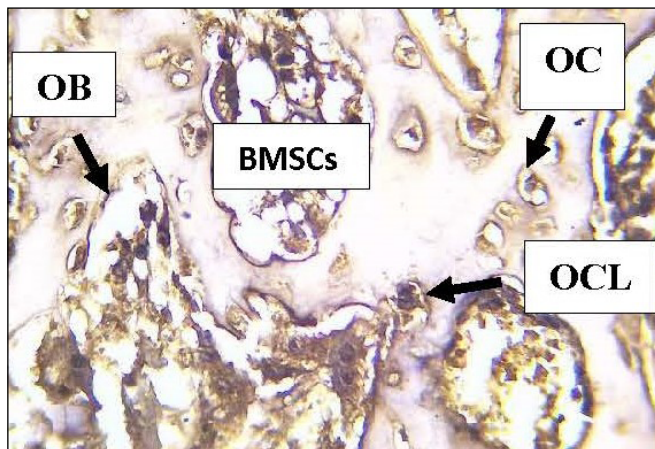


Fig. 3. Defect area of collagen group after 2 weeks shows positive staining of COL1 in bone marrow stromal cells (BMSC) osteocytes (OC), osteoblasts (OB) and osteoclasts (OCL). DAB stain with hematoxylin counter stain (x40).

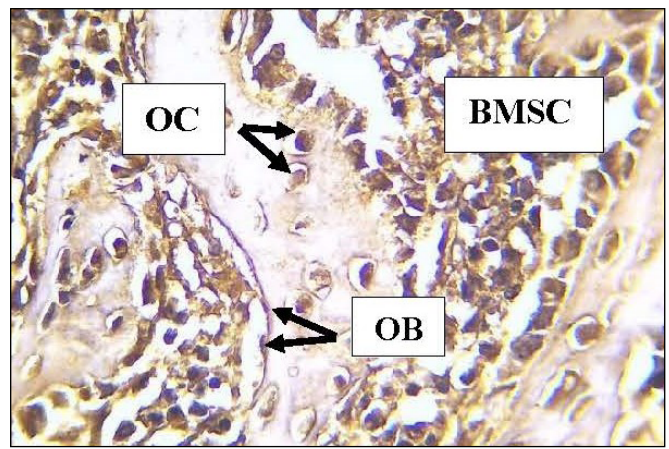


Fig. 5. View of combination group at 2 weeks duration shows positive expression of COL1 in osteocytes (OC), osteoblasts (OB) and bone marrow stromal cells. DAB stain with hematoxylin counter stain (x40).

events such as cellular recruitment, proliferation, and differentiation [15]. In most cases, bone tissue heals on its own unless there are complex circumstances such as large bone defects. There are three stages to bone healing: inflammatory, reparative and remodeling [16]. Osteoblasts produce type 1 collagen during the reparative stage of bone healing [17]. It has been demonstrated that this collagen subtype, which predominates in the extracellular matrix of bone, is essential to osseous repair and is connected to osteoblast maturation [18]. Findings of this study showed that after two weeks that the expression of COL1 was higher in experimental groups than in control groups specifically with the combination group exhibiting the highest expression which might suggest that collagen and β -TCP have a role in regulating healing response, promoting the formation of new bone, besides differ-

entiation and proliferation of bone cells, supported by a previous study conducted by Tsuruoka N et al. [19], who found the expression of COL1 was high in the early stages of bone healing with oral administration of collagen tripeptide at fracture model rats, expression decreased with time, this indicates that all groups accomplished a satisfactory healing process at varying rates. The current study showed that high mean values of IRS for COL1 expression by BMSCs detected in the combination group after 2 weeks may be attributed to biocompatibility and bioresorbable properties of applied materials with properties similar to the inorganic phase of bone. Osteoblasts, which are essential for mineralization of bone matrix, were considered to originate mainly from stromal cells in the bone marrow [20]. In this study the recorded mean values of IRS for COL1 expression by osteocyte increased with time

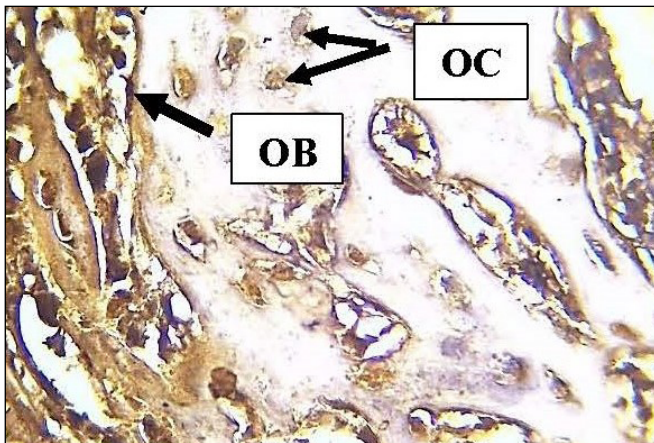


Fig. 6. View of control group at 4 weeks shows positive expression of COL1 in osteoblasts (OB), osteocytes (OC). DAB stain with hematoxylin counter stain (x40).

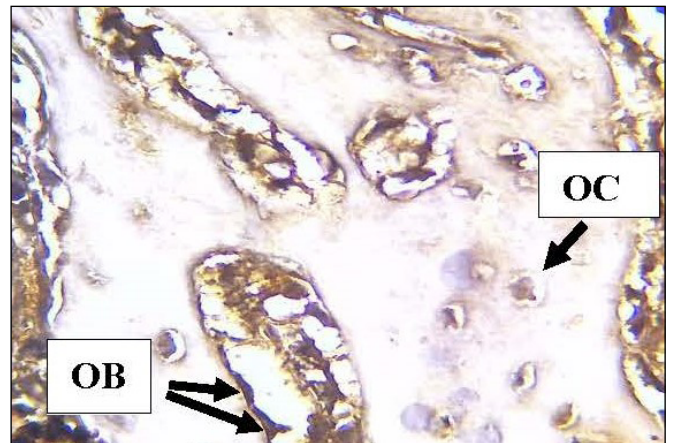


Fig. 8. View of β -TCP group at 4 weeks duration show positive expression of COL1 in osteoblasts (OB), osteocytes (OC). DAB stain with hematoxylin counter stain (x40).

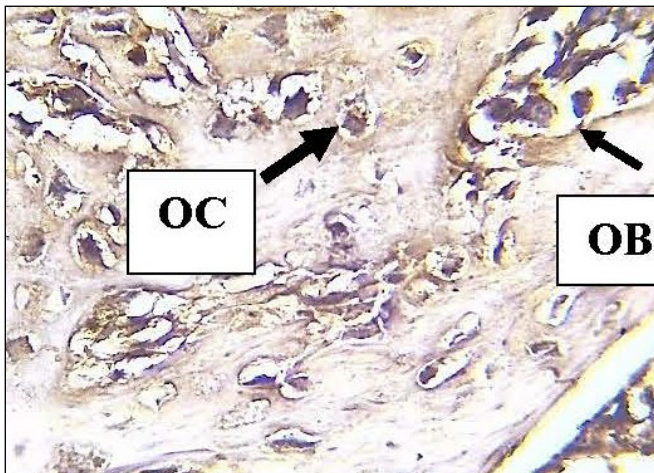


Fig. 7. View of collagen group at 4 weeks duration shows positive expression of COL1 in osteocytes (OC), osteoblast (OB). DAB stain with hematoxylin counter stain (x40).

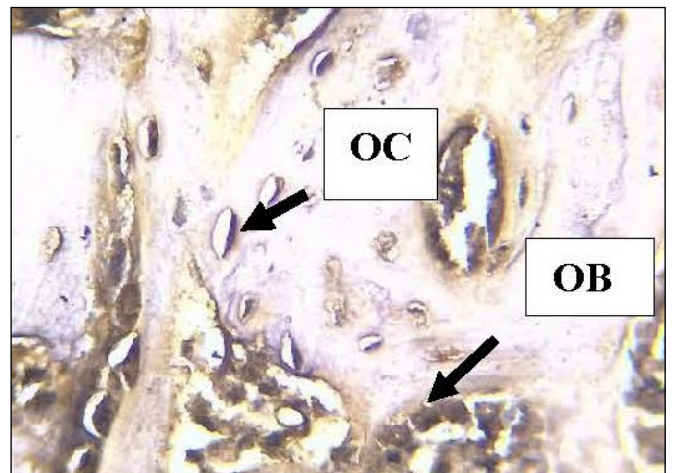


Fig. 9. View of combination group after 4 weeks duration shows positive localization of COL1 in osteoblast (OB) and osteocyte (OC). DAB stain with hematoxylin counter stain (x40).

and highest values recorded in combination group at 4 weeks and this agree with Kusumawati I et al. [22], who evaluated the effect of amelogenin as implant coating material in rabbit tibia on osteointegration through immunohistochemical localization of COL1 and reported that expression of COL1 was noticed during the first stages of extracellular matrix biosynthesis and proliferation. Following differentiation, osteoblasts generate a variety of proteins, including alkaline phosphates, osteocalcin and type I collagen, which, after producing newly formed bone, differentiate under an osteocyte phenotype, consequently, the bone marker COL1, which is linked to osteocyte differentiation. However, statistical analysis showed that the mean value of IRS for positive COL1 expression was highest in osteoblast in all groups examined for 2 and 4 weeks, this agreed with Kresnoadi U et al. [23], who demonstrated that COL1 expression appears strongly by osteoblast sited at bone trabeculae at 7

and 14 days in alveolar bone of rabbits during open flap debridement treated by 10% propolis carbonated hydroxyapatite. Highly significant difference ($P < 0.01$) among all groups at 2- and 4-weeks durations was recorded for osteoblasts, osteocytes, osteoclasts and BMSC in this study in line with findings of Kresnoadi U et al. [23] where significant differences in expression of COL1 between control and experimental groups treated with mangosteen peel extract combined with demineralized freeze-dried bovine bone xenograft as a mean of tooth extraction socket preservation at 7 and 30 days.

CONCLUSIONS

Combined application of Coll/ β -TCP was effective in accelerating bone healing process through elevating the IRS of COL1 noticed by osteoblast, osteocyte and bone marrow stromal cells.

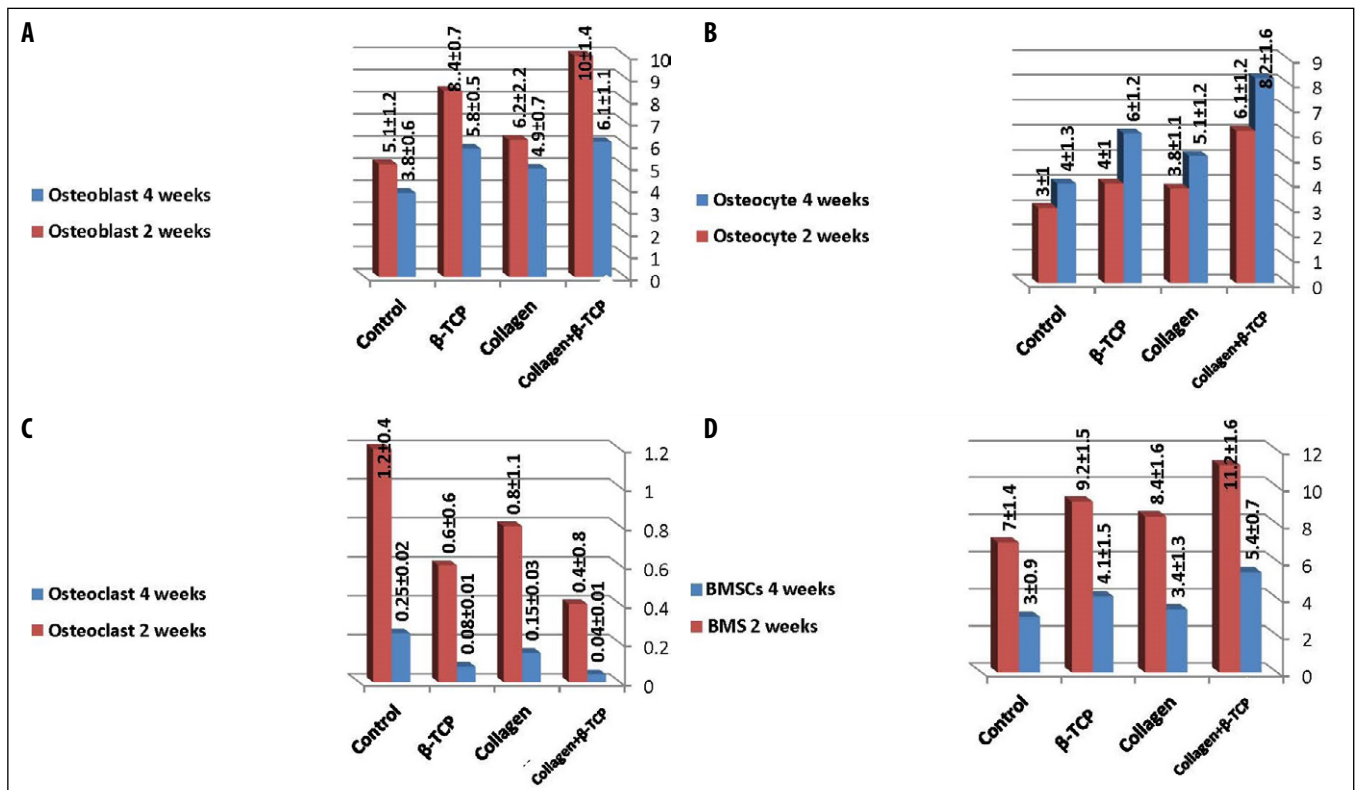


Fig. 10. A. Mean values of IRS for COL1 in OB after 2- and 4-weeks healing durations.

B. Mean value of IRS for COL1 in OC after 2- and 4-weeks healing durations.

C. Mean value of IRS for COL1 in OCL after 2- and 4-weeks healing durations.

D. Mean values of IRS for COL1 in BMSCs after 2- and 4-weeks healing intervals.

REFERENCES

- Kadhim EF. Histological evaluation of vitronectin protein/angiopoietin-like 4 protein on bone healing in rats. *Iran J War Publ Health*. 2022;14(2):231-342. URL: <http://ijwph.ir/article-1-1149-en.html>.
- Al-Ghani B, Al-Hijazi A, AL-Zubaydi T. In vivo immunohistochemical investigation of bone deposition at collagen-coated Ti implant surface. *J Bagh Coll Dent*. 2011;23:10-5. doi:10.4103/2348-2915.146490 [DOI](#)
- Alsaeed MA, Al-Ghaban NM. Chitosan nanoparticle/simvastatin for experimental maxillary bony defect healing: a histological and histomorphometric study. *Biomimetics*. 2023;8(4):363. doi:10.3390/biomimetics8040363 [DOI](#)
- Kang HJ, Makkar P, Padalhin AR et al. Comparative study on biodegradation and biocompatibility of multichannel calcium phosphate based bone substitutes. *Mater Sci Eng C Mater Biol Appl*. 2020;110:110694. doi:10.1016/j.msec.2020.110694 [DOI](#)
- Razouki NA, Ghani BA. Histological evaluation of effect of beta-tricalcium phosphate on bone healing in alloxan-induced diabetes. *J Bagh Coll Dent*. 2016;325(3765):1-7. doi:10.12816/0031112 [DOI](#)
- Böhner M, Santoni BLG, Döbelin N. β -tricalcium phosphate for bone substitution: Synthesis and properties. *Acta Biomater*. 2020;113:23-41. doi:10.1016/j.actbio.2020.06.022 [DOI](#)
- Lu H, Zhou Y, Ma Y et al. Current application of beta-tricalcium phosphate in bone repair and its mechanism to regulate osteogenesis. *Front Mater*. 2021;8:698915. doi:10.3389/fmats.2021.698915. [DOI](#)
- Ueda H, Hong L, Yamamoto M et al. Use of collagen sponge incorporating transforming growth factor- β 1 to promote bone repair in skull defects in rabbits. *Biomaterials*. 2002;23(4):1003-1010. doi:10.1016/s0142-9612(01)00211-3 [DOI](#)
- Wang H. A review of the effects of collagen treatment in clinical studies. *Polymers*. 2021;13(22):3868. doi:10.3390/polym13223868 [DOI](#)
- Mizar MA, Hassan KS, Mohammed AK et al. Platelet rich fibrin versus collagen membrane combined with beta tri calcium phosphate/collagen for treatment of dehiscence around immediately placed implants clinical and radiographic comparative study. *Al-Azhar Assiut Dent J*. 2021;4(2):189-196. doi:10.21608/aadj.2021.208221 [DOI](#)
- Bou-Gharios G, Abraham D, Crombrugge B. Type I collagen structure, synthesis, and regulation. In: Bilezikian JP et al. (eds). *Principles of Bone Biology*; Elsevier: Alpharetta, GA, USA, 2020:295-337. doi:10.1016/B978-0-12-814841-9.00013-0 [DOI](#)
- Naomi R, Bahari H, Ridzuan PM et al. Natural-based biomaterial for skin wound healing (Gelatin vs. collagen): Expert review. *Polymers*. 2021;13(14):2319 doi:10.3390/polym13142319 [DOI](#)

13. Sun P, Wang J, Zheng Y et al. BMP2/7 heterodimer is a stronger inducer of bone regeneration in peri-implant bone defects model than BMP2 or BMP7 homodimer. *Dental Materials J.* 2011;31(2):239-248. doi:10.4012/dmj.2011-191 [DOI](#)
14. Fedchenko N, Reifenrath J. Different approaches for interpretation and reporting of immunohistochemistry analysis results in the bone tissue - a review. *Diagn Pathol.* 2014;9:221. doi:10.1186/s13000-014-0221-9 [DOI](#)
15. Mohamed IF, Ghani BA, Fatalla AA. Histological evaluation of the effect of local application of punica granatum seed oil on bone healing. *Int J Biomater.* 2022;2022:4266589. doi:10.1155/2022/4266589 [DOI](#)
16. Jassim HO, Al-Ghaban NM. Effect of eucommia ulmoides on healing of bone defect using histological and histomorphometric analysis in rat: in vivo study. *Archives of Razi Institute.* 2023;78(2):691-697. doi:10.22092/ARI.2022.359483.2434 [DOI](#)
17. Kruger TE, Miller AH, Wang J. Collagen scaffolds in bone sialoprotein-mediated bone regeneration. *Sci World J.* 2013;2013:812718. doi:10.1155/2013/812718. [DOI](#)
18. Steinbrech DS, Mehrara BJ, Rowe NM et al. Gene expression of TGF- β , TGF- β receptor, and extracellular matrix proteins during membranous bone healing in rats. *Plastic and reconstructive surgery.* 2000;105(6):2028-2038. doi:10.1097/00006534-200005000-00018 [DOI](#)
19. Tsuruoka N, Yamato R, Sakai Y et al. Promotion by collagen tripeptide of type I collagen gene expression in human osteoblastic cells and fracture healing of rat femur. *Biosci Biotechnol Biochem.* 2007;71(11):2680-2687. doi:10.1271/bbb.70287. [DOI](#)
20. Al-Nawas B, Kämmerer PW, Morbach T et al. Ten-year retrospective follow-up study of the TiOblast dental implant. *Clin Implant Dent Relat Res.* 2012;14(1):127-134. doi:10.1111/j.1708-8208.2009.00237.x [DOI](#)
21. Al-Molla BH, Al-Ghaban NM, Taher A. In vivo immunohistochemical investigation of bone deposition at amelogenin coated ti implant surface. *Smile Dent J.* 2014;9(1):12-17. doi:10.12816/0008316. [DOI](#)
22. Kusumawati I, Suryono, Syaify A. The enhancement of type 1 collagen expression after 10% propolis-carbonated hydroxyapatite application in periodontitis-induced rabbits. *Dent J (Maj Kedokt Gigi).* 2021; 54(1):16-20. doi:10.20473/j.djmk.v54.i1.p16-20 [DOI](#)
23. Kresnoadi U, Raharjo T, Rostiny R. Effects of mangosteen peel extract combined with demineralized freeze-dried bovine bone xenograft on osteocalcin, collagen 1, and osteoblast as alveolar bone regeneration in socket preservation. *J Ind Prosthodont Soc.* 2018;18(2):117. doi:10.4103/jips.jips_326_17. [DOI](#)

ORCID AND CONTRIBUTIONSHIP

Ban A. Ghani: 0009-0000-7542-3858 [A](#) [F](#)

Bayan Jabr Hussein: 0009-0007-5944-3868 [B](#) [C](#) [D](#) [E](#)

CONFLICT OF INTEREST

The Authors declare no conflict of interest

CORRESPONDING AUTHOR

Ban A. Ghani

Department of Oral Diagnostic Sciences

University of Baghdad,

Baghdad, Iraq

e-mail: drban871961@gmail.com

[A](#) – Work concept and design, [B](#) – Data collection and analysis, [C](#) – Responsibility for statistical analysis, [D](#) – Writing the article, [E](#) – Critical review, [F](#) – Final approval of the article

RECEIVED: 01.07.2024

ACCEPTED: 02.09.2024



The research clinical and instrumental methods of examination of athletes related to the process of intervertebral disk degeneration and stenosis

Valeria Tyshchenko¹, Tymur Ksenzov², Tetiana Odynets³, Tetiana Bogoslav⁴, Artur Ksenzov⁵, Ivan Hlukhov⁶, Kateryna Drobot⁶

¹ZAPORIZHZHIA NATIONAL UNIVERSITY, ZAPORIZHZHIA, UKRAINE

²HOUSE OF MEDICINE ODREX, ODESA, UKRAINE

³KHORTYTSIA NATIONAL ACADEMY, ZAPORIZHZHIA, UKRAINE

⁴ZAPORIZHZHIA STATE MEDICAL AND PHARMACEUTICAL UNIVERSITY, ZAPORIZHZHIA, UKRAINE

⁵ZAPORIZHZHIA REGIONAL CLINICAL HOSPITAL, ZAPORIZHZHIA, UKRAINE

⁶KHERSON STATE UNIVERSITY, KHERSON, UKRAINE

ABSTRACT

Aim: To determine the level structure of the graph model of the system of clinical and instrumental indicators of athletes with herniated intervertebral discs complicated by spinal stenosis, and to determine the regression model for these indicators.

Materials and Methods: This observational study involved 64 athletes (14 – rugby players, 16 – handball players, 15 – basketball players, 19 – football players) with intervertebral disc herniation, complicated by stenosis of spinal canal. Research methods: visual method to evaluate the likelihood of a data set's normal distribution; correlation and regression analysis; method for determining the ordinal function of a graph through the application of an adjacency matrix, specifically utilizing Demucron's algorithm. This process is accompanied using a topological sorting of the graph.

Results: The results showed the lack of correlation between age and VAS, muscle strength and VAS, as well as VAS and the channel space; little feedback between age and the channel space; weak positive relationship between size of herniated intervertebral disc had a with the length of the illness. The data showed, strong feedback was observed for hernia size and the channel space, hernia size and muscle strength, the channel space, and length of the illness.

Conclusions: The evaluation on the complexity and depth of the interconnections between clinical and instrumental metrics in athletes was conducted. The hierarchical organization within the graphical representation was ascertained. A predictive regression model delineating the correlations between clinical and instrumental variables in patients suffering from herniated intervertebral discs, with the complication of spinal canal stenosis was established.

KEY WORDS: athletes, stenosis of spinal canal, regression model, demucron's algorithm

INTRODUCTION

The intensive training and competitive activities in team sports significantly elevate the risk of accelerated degenerative disc disease in athletes, underscoring the importance of specialized training and preventive measures [1-3]. For example, in handball, basketball, rugby, football where agility, speed, strength, and frequent bending and twisting are essential, athletes face unique spinal challenges, making tailored training and injury prevention strategies crucial for their long-term health and performance. Given the high biomechanical stress on the lumbar spine in team sports focused training programs that balance strength and flexibility are vital to minimize the risk of spinal injuries. The specific demands of team sports on athletes' spines highlight

the need for dedicated research and development of targeted training routines to enhance performance while reducing injury risks [4-6]. In team sports, where quick movements and intense physical exertion are common, developing training protocols that address the high incidence of spinal issues is critical for athlete longevity and success.

Low back pain indicates the presence of a serious health problem in only 1-2% of cases, and indicates the corresponding symptoms, a kind of "red flags". Example of such symptoms is impaired sensitivity of the extremities, muscle weakness, dysfunction of the pelvic organs, the appearance of pain at night, fever and unmotivated weight loss, cancer and ets. [7, 8]. Various etiological factors can be manifested a similar clinical picture.

The problem of vertebrogenic pathology in sport was considered quite widely. At the same time, a number of specific methodological issues remain poorly developed. Athletes spend a significant part of their lives in training and competitive activities, developing agility, speed, strength, power, bending and twisting in their sport. The high intensity and repetition of these exercises predisposes athletes to accelerated degenerative disc disease (DDD), which is theoretically higher than among the general population [9, 10]. This may be due to the fact the lumbar spine is the recipient of the heaviest biomechanical stress.

An important role in the intervertebral connection and the movement of the spine in general is played by the intervertebral disc (IVD), the degeneration of which is a common and chronic process. And as a result, it leads to serious symptoms of the spine, which causes corresponding pain in the lower back of athletes. It is generally known that low back pain and other neurological symptoms caused by intervertebral disc herniation can develop as a secondary condition, and is usually accompanied by a narrowing of the intervertebral disc, the formation of osteophytes and, as a result, stenosis of the spinal canal. This may be of great importance in the choice of tactics and operative treatment of mid-spinal discs, accelerated by stenosis of the spinal canal, which can lead to the "Failed Back Surgery Syndrome" (FBSS) [11]. Surgery does not stop the degenerative process and symptoms may reappear within several years. So, a number of scientists in Japan conducted a cross-sectional, Internet-based survey to assess the prevalence and characteristics of FBSS, which showed – 20.6% of patients with FBSS at 94% – low back pain, 71.1% – dull ache and 69.8% – cold sensations [12], in the UK achieved a response rate of 52% [13]. In general, a recent published study suggested avoiding the use of the term FBSS with regard to its partially stigmatizing connotation and its inherent hindering to provide individualized medicine, due to the fact that he rather unspecific and a variety of conditions may underlie this label [14].

The large number of cases are missed with information from the public domain and introduces bias into the internet-based study. No studies of lumbar disc herniation utilized team medical record data [15]. Therefore, an important step is to create a network (an international panel of spine surgeons, neurosurgeons, and pain specialists with a particular interest in FBSS established the chronic back and leg pain (CBLP) network with the aim of addressing the challenges and barriers in the clinical management of FBSS patients by building a common transdisciplinary vision) [16].

Clinical manifestations of spinal canal stenosis (SCS) sometimes lead to disability (this is likely related to the excessive mechanical stress and physical injury sustained by athletes), so solving the problem of timely diagnosis and, accordingly, proper treatment is important.

AIM

Aim of the study to determine the level structure of the graph model of the system of clinical and instrumental indicators of athletes with herniated intervertebral discs complicated by spinal stenosis, and to determine the regression model for these indicators.

MATERIALS AND METHODS

PARTICIPANTS

To achieve this goal on the basis of the neurosurgical department of "Zaporizhzhia Regional Clinical Hospital" (Zaporizhzhia, Ukraine) and Department of Orthopedics and Traumatology, "House of Medicine Odrex", (Odesa, Ukraine) during the period from 2017 to 2022 y.o. we performed a prospective, cohort, comparative study involving 64 athletes (14 – rugby players, 16 – handball players, 15 – basketball players, 19 – football players) with an established diagnosis (according to a comprehensive clinical and neuroimaging study within 24 hours of the onset of the disease): intervertebral disc herniation, complicated by stenosis of spinal canal. Clinical neurological manifestations and MRI criteria of the spinal canal were analyzed of all patients by age, size and location of intervertebral disc herniation, level and type of spinal canal stenosis, disease duration, in accordance with muscle strength scale of the British Research Committee and Visual Analogue Scale (VAS).

All patients volunteered to participate in the research. Prior to the testing, the procedures were explained to all of them, including possible risks involvement, and, after the explanation, an informed consent form was signed. The participants entered the study after providing their written informed consent. The study has been approved by the Institutional Ethics Committee, complied with all relevant national regulations and institutional policies, followed the tenets of the declaration of Helsinki, and has been approved by the authors' ethical review committee of Zaporizhzhia National University (number 2022/21–01). Exclusion criteria were a history of injury or disease that would prevent participants from safely performing the study protocol.

A systematic science review was applied in accordance with the Preferred Reporting Items for system-

Table 1. Average values of clinical and instrumental indicators

Indicators	Intervertebral disc herniation size, mm	Spinal canal area, mm ²	Duration of the disease, months	Muscle strength, score	VAS
Arithmetic mean	7,57	58,77	9,84	3,75	7,53
Mo	7,5	66,00	10	4	7
Me	8	65,00	10	5	8
Standard deviation	1,91	21,01	12,35	1,30	1,47
Arithmetic mean error	0,21	2,35	1,38	0,15	0,16
As (Askp=1.25)	-0,04	-0,48	1,39	-0,70	-0,01
Ex (Ex _{kp} =3.5)	-0,42	-0,63	0,39	-0,54	-0,79

atic reviews and meta-analyses. Electronic databases: Scopus, Web of Science, PubMed – were searched for relevant publications. The publications included met the following criteria and principles: included handball players; contained relevant data concerning in handball; were written in English, Poland, Ukraine.

RESEARCH METHODS

- a graphical technique for assessing whether or not a data set is approximately normally distributed (Normal Probability Plot);
- methods for determination of the correspondence of the distribution to the normal law according to the indicators of the distribution form;
- method of average values;
- correlation analysis;
- regression analysis.

Also, method for finding the ordinal function of a graph, based on the use of an adjacency matrix (Demucron's algorithm) [17] is used in the study, and topological sorting of the graph is carried out.

To check the correspondence of the series to the normal distribution law, we used a graphical method for determining the correspondence of the sample values to the normal distribution (Normal Probability Plot), indicators of the central tendency and indicators of the distribution form.

A symmetrical distribution is called normal, in which the maximum values of the studied feature are concentrated around the average value. The curve of normal distribution is symmetric under the y-axis and asymptotically approaches to the abscissa. As a rule, the empirical (actual) distribution differs to some extent from the normal one [17]. The central tendency is the property of the values of the studied feature to be grouped around the center of frequency distribution, the statistical characteristic of which is the average value.

The condition for normal distribution (as symmetric) is the following ratio of the indicators of the distribution center:

- equality of the average (sample mean) value, mode (the most common value of a feature in units of a given population) and median (the value of a feature falling in the middle of a ranked (ordered) population);

- in symmetric distribution series, the value of the mode and the median coincide with the average value ($X_{av} = Me = Mo$) [Gorkavy & Yarova, 2004], and in moderately asymmetric series they are related in this way:

$$3(X_{av} - Me) \approx X_{av} - Mo$$

To assess the deviation of the empirical distribution from the normal, we have used the following indicators of the form of distribution:

⇒ *moment coefficient of asymmetry (As)*, as the most accurate and widespread indicator of asymmetry (a negative sign indicates the presence of left-sided asymmetry, a positive sign indicates right-sided asymmetry):

$$As = M_3 / \sigma^3,$$

where M_3 – is the central moment of the third order; σ – is the standard deviation, and M_3 is calculated by the formula:

$$M_3 = \frac{\sum (X_i - X_{cp})^3 f_i}{\sum f_i}$$

The assessment of the significance of the asymmetry indicator is given using the mean square error of the asymmetry coefficient:

$$s_{As} = \sqrt{\frac{6(n-2)}{(n+1)(n+3)}}$$

If the ratio $|As|/S_{As} < 3$, is satisfied, then the asymmetry is insignificant, its presence is explained by the influence of various random circumstances. If the ratio $|As|/S_{As} > 3$ takes place, then the asymmetry is significant and the distribution of the feature in the general population is not symmetrical [18].

⇒ *an indicator of kurtosis (peakedness)*, which is the fall of the top of the empirical distribution up or down from the top of the normal distribution curve. Most often, kurtosis is estimated using the indicator:

$$Ex = M_4 / \sigma^4 - 3,$$

where M_4 – is the central moment of the fourth order,

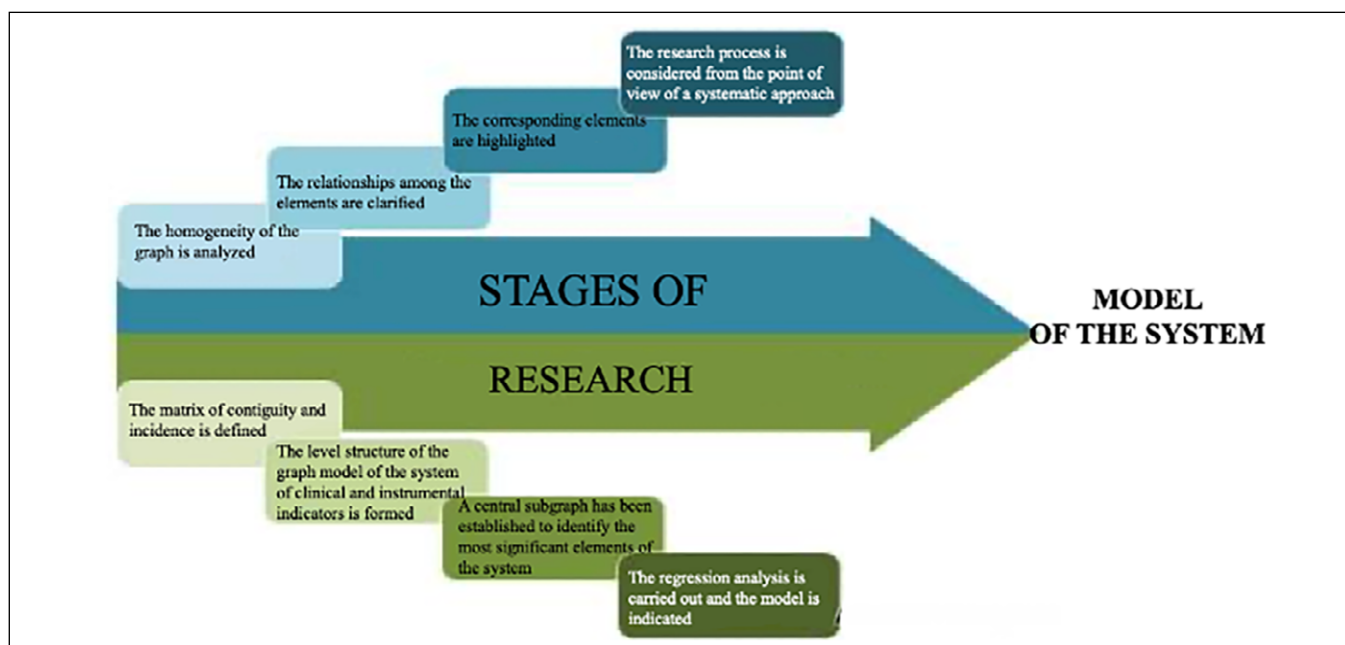


Fig. 1. Stages of research.

σ – is the standard deviation.

For distributions that are more peaked (elongated) than normal, the kurtosis index is positive ($Ex > 0$), for more flat-topped (oblate) – negative ($Ex < 0$), because for normal distribution:

$$M_4/\sigma^4 = 3,$$

to assess the significance of the kurtosis, the Ex/S_{Ex} statistics is calculated, where S_{Ex} is the mean square error of the kurtosis coefficient:

$$s_{Ex} = \sqrt{\frac{24n(n-2)(n-3)}{(n+1)^2(n+3)(n+5)}}$$

If the ratio $Ex/s_{Ex} > 3$, then the deviation from the normal distribution is considered significant.

Compliance with the normal distribution law (according to the indicators of the distribution form) was determined by the method: instantaneous asymmetry factor (As) (estimation of the significance of the asymmetry index was determined using the root mean square error of the asymmetry coefficient) and the kurtosis index Ex (the significance of the kurtosis was determined using the root mean square error of the kurtosis coefficient). We have used regression analysis to model the relationship between the selected variables as well as the predicted values based on the model. Regression analysis uses the chosen estimation method, the dependent variable, and one or more explanatory variables to create an equation that estimates the values of the dependent variable.

STAGES OF RESEARCH

Stage one. The research process is considered from the

point of view of a systematic approach.

Stage two. The corresponding elements are highlighted.

Stage three. The relationships among the elements are clarified (how the change in one element affects the state and parameters of the other elements).

Stage four. The homogeneity of the graph is analyzed.

Stage five. The matrix of contiguity and incidence is defined. The use of its adjacency matrix and incidence matrix instead of a graph makes it possible to involve the entire “arsenal” of matrix theory in the study of the graph.

Stage six. The level structure of the graph model of the system of clinical and instrumental indicators is formed.

Stage seven. A central subgraph has been established to identify the most significant elements of the system.

Stage eight. The regression analysis is carried out and the model is indicated.

RESULTS

Analysis of the experimental data results has revealed their compliance with the normal distribution law for each of the clinical and instrumental parameters (Table 1).

Pearson’s linear correlation coefficients and regression equations were calculated for all the above data.

The value of a special indicator, the correlation coefficient (r_{xy}), was used to estimate the relationship density in the correlation analysis.

$$r_{xy} = \frac{\sum_{i=1}^n (X_i - \bar{X})(Y_i - \bar{Y})}{\sqrt{\sum_{i=1}^n (X_i - \bar{X})^2 \sum_{i=1}^n (Y_i - \bar{Y})^2}}$$

where X_i and Y_i – variants of 2 samples; \bar{X} i \bar{Y} – the

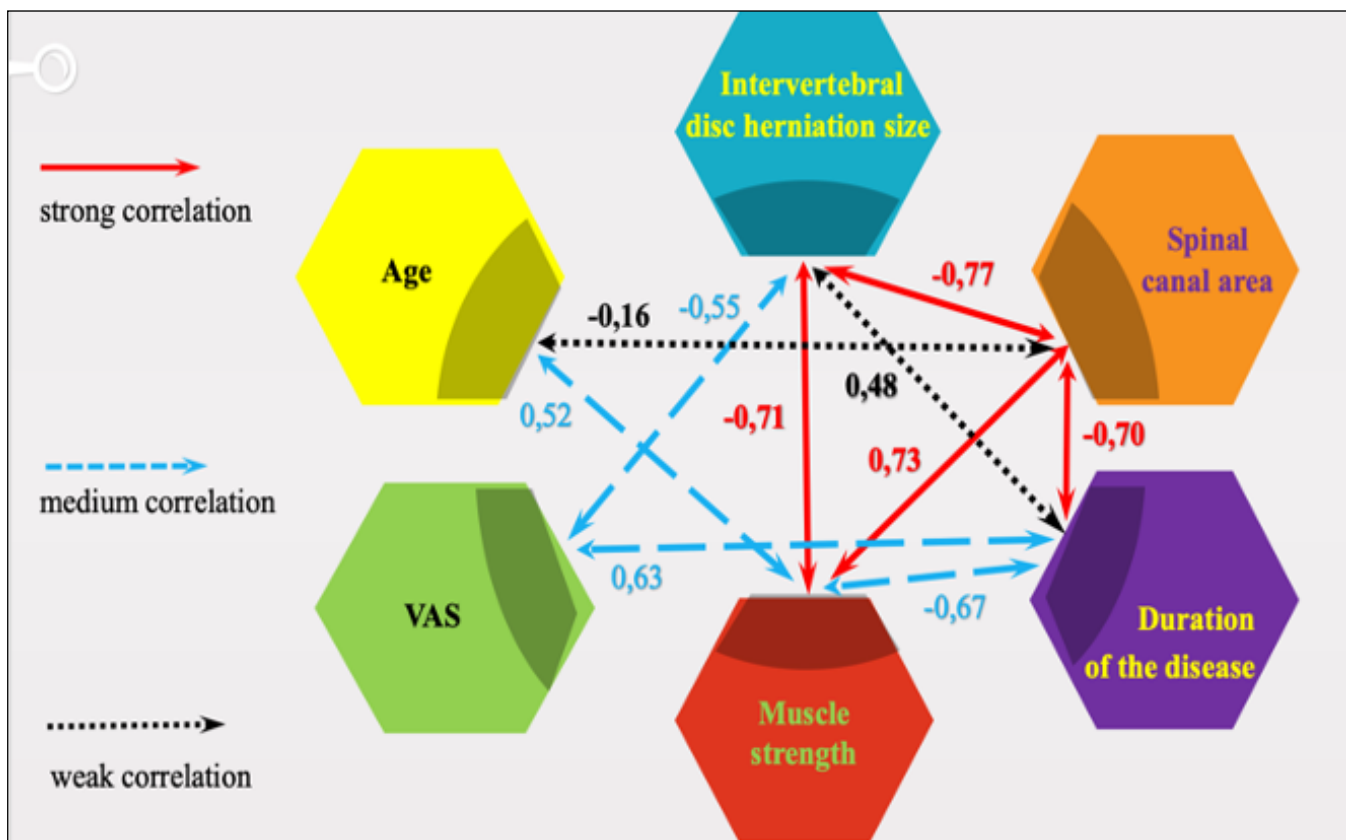


Fig. 2. Diagram of the relationship between clinical and instrumental parameters of patients with intervertebral disc herniation complicated by spinal canal stenosis.

arithmetic mean of the indicators X_i and Y_i .

The absolute value of the correlation coefficient is in the range from 0 to 1 – direct positive correlation statistical dependence and from (-1) to 0 – inverse negative correlation statistical dependence:

$$-1 \leq r_{xy} \leq 1$$

We explain the value of this factor in this way:

a) $r_{xy} = 1$ the relationship between the signs is very dense (functional relationship);

b) $r_{xy} = 0$ there is no connection between the signs of X_i and Y_i ;

c) the closer the value of r_{xy} to zero, the weaker the relationship, the closer the value of r_{xy} to one – the denser.

It is assumed that $r_{xy} = 0,2 \dots 0,49$ – weak connection; $r_{xy} = 0,5 \dots 0,69$ – average connection; $r_{xy} = 0,7 \dots 0,99$ – close (strong) connection.

According to the obtained data, we can state the lack of correlation between such indicators as: age and VAS, muscle strength and VAS, as well as VAS and the Spinal canal area (Fig. 1). It should be noted that there is little feedback between age and the Spinal canal area. Instead, indicators of intervertebral disc herniation size had a weak positive relationship with the duration of the disease. The average positive relationship was observed between age and muscle strength, between

the duration of the disease and VAS. However, average feedback was observed between intervertebral disc herniation size and VAS, duration of the disease, and muscle strength.

Our observations and special studies in this context have shown that in the end the close connection is obtained by the spinal canal area and the strength of the muscles. However, strong feedback was observed for intervertebral disc herniation size and the Spinal canal area, intervertebral disc herniation size and muscle strength, the Spinal canal area, and duration of the disease.

We also have analyzed the existing model of the relationship between clinical and instrumental indicators of patients with intervertebral disc herniation complicated by spinal canal stenosis by analyzing the graph $G = (V, E)$, which consists of many vertices (v_1, v_2, \dots, v_n), to which belong the indicators, and the set of edges $E = (e_1, e_2, \dots, e_n)$ – the presence of a relationship among them. So, v_1 – spinal canal area; v_2 – duration of the disease; v_3 – muscle strength; v_4 – VAS; v_5 – age of patients; v_6 – intervertebral disc herniation size.

To determine the homogeneity of the graph, the cardinality of the neighborhood of each of the vertices of the graph is recognized, which was calculated by establishing the set of vertices adjacent to the given $adj(v_i)$. The number of such vertices is called the degree

		v1	v2	v3	v4	v5	v6	deg(v _i)
A=	v1	0	1	1	0	0	1	3
	v2	1	0	1	1	0	1	4
	v3	1	1	0	0	1	1	4
	v4	0	1	0	0	0	1	2
	v5	0	0	1	0	0	0	1
	v6	1	1	1	1	0	0	4

Fig. 3. Adjacency matrix of graph G.

of the vertex deg(v_i), from which we can conclude that:

adj(v₁) = {v2, v3, v6}; deg(v₁)=3

adj(v₂) = {v1, v3, v4, v6}; deg(v₂)=4

adj(v₃) = {v1, v2, v5, v6}; deg(v₃)=4

adj(v₄) = {v2, v6}; deg(v₄)=2

adj(v₅) = {v3}; deg(v₅)=1

adj(v₆) = {v1, v3, v4, v6}; deg(v₆)=4

The graph is heterogeneous, since the degrees of the vertices are not the same.

For further analysis of the graph, the adjacency matrix and the incidence matrix of graph G were identified. Thus, we have considered the adjacency matrix as a symmetric square matrix A=[a_{ij}] of order n, in which the element a_{ij}=1 if the graph contains an edge {v_i v_j} (that is, the vertices are adjacent), and a_{ij}=0 if there is no such edge (Fig. 2).

The incidence matrix of the graph G is revealed as a square matrix B=[b_{ij}] of order n, in which the element b_{ij}=1, if the vertex v_i is incident to the edge e_i and b_{ij}=0 in the opposite case (Fig. 3).

To determine the central and peripheral vertices of the graph, its eccentricity (ecc(v_i)) is determined, showing the greatest distance between this and any other vertex of the graph – the distance to the farthest vertex

of the graph from v_i:

ecc(v₁) = ecc(v₂) = ecc(v₃)=ecc(v₆)=2

ecc(v₄)=ecc(v₅)=3

The radius r of the graph – the minimum eccentricity among all the vertices of the graph – was calculated by the formula: r(G)=min ecc(v_i) = 2

The diameter d of the graph – is the maximum eccentricity among all the vertices of the graph, that is, d – is the greatest distance between all pairs of the vertices of the graph.

d(G)=max ecc(v_i)=3

To find the diameter of the graph, first we have found the shortest paths among all pairs of vertices. The greatest length of the shortest path – is the diameter of the graph. The central vertex of the graph of radius r – is the vertex whose eccentricity is equal to r, that is, the vertex at which the radius is reached. Thus, we have defined the set of all central vertices of the graph: {v₁ (spinal canal area), v₂ (duration of the disease), v₃ (muscle strength), v₆ (intervertebral disc herniation size)}.

The peripheral vertex of the graph with diameter d – is the vertex whose eccentricity is d, therefore, the peripheral vertices were {v₄ (age of patients), v₅ (VAS)}.

Consequently, the level structure of the graph model

	e_1	e_2	e_3	e_4	e_5	e_6	e_7	e_8	e_9	B_i
v_1	1	0	1	0	0	0	0	0	1	3
v_2	1	1	0	0	1	0	0	1	0	4
v_3	0	1	1	1	0	0	1	0	0	4
v_4	0	0	0	0	0	1	0	1	0	2
v_5	0	0	0	0	0	0	1	0	0	1
v_6	0	0	0	1	1	1	0	0	1	4

Fig. 4. Incidence matrix of graph G.

of the system of clinical and instrumental indicators of athletes with herniated intervertebral discs complicated by stenosis of the spinal canal has been established (Fig. 4, Fig. 5). So, the center of the graph is the subgraph G_1 – a cycle (a chain in which the first and last vertices coincide). The subgraph G_1 is connected – all vertices are reachable from each, and is a maximally connected subgraph of the graph G. In order to carry out further research of the obtained data, a regression analysis has been made to calculate the assumed relationship between the dependent variable and one or more independent variables.

The following regression equation is made for muscle strength:

$$S_{\text{muscle}} = 3,12 + 0,04 \times A_{\text{spinal canal}} - 0,03 \times D_{\text{disease}} \quad (p < 0,001).$$

DISCUSSION

According to statistics, narrowing of the spinal canal is most common among senior and elderly people, whose structural elements of the spine have undergone age-related changes [18], such as fully fused epiphyses and degenerative wear on her vertebrae. However, other scientists, on the other hand, argue that this problem is more common among athletes than in the general population, due to constant pressure on the spine and simultaneous microtrauma that

is unable to heal [19]. Our results are consistent with previous studies that showed a higher incidence of these degenerative changes in the lumbar spine in athletes [20]. Thus, the issues of lumbar spine anomalies were considered in both adolescents [21] and adult athletes [22, 23]: in golf [24], in football [25], in baseball [26] and other kinds of sport. A 17-year study of injuries by the National Basketball Association (NBA) has found that 10.2% of all injuries were to the lumbar spine, where disc degeneration and lumbar contusion accounted for 7.9% and 0.9% of the total [27], which is comparable to our study. Researchers also found out that 95% of hockey players complained on low back pain in the last year of the game [28], and 75% of gymnasts had disc degeneration [29]. Among baseball players, 35.1% and 22.8% of [30] athletes showed signs of L5/S1 or L4/L5 disc degeneration. Researchers stresses the lifetime prevalence low back pain is as high as 77.5% in tennis players [31]. This is likely related to the excessive mechanical stress and physical injury sustained by athletes. Scientists insist on microdiscectomy of the lumbar, confirming the data on the return of 75% to 100% of elite athletes to training for 6 months [32]. Of course, given the popularity of sports and lumbar pathology that players face during and after their careers, we need future researches in order to understand better the

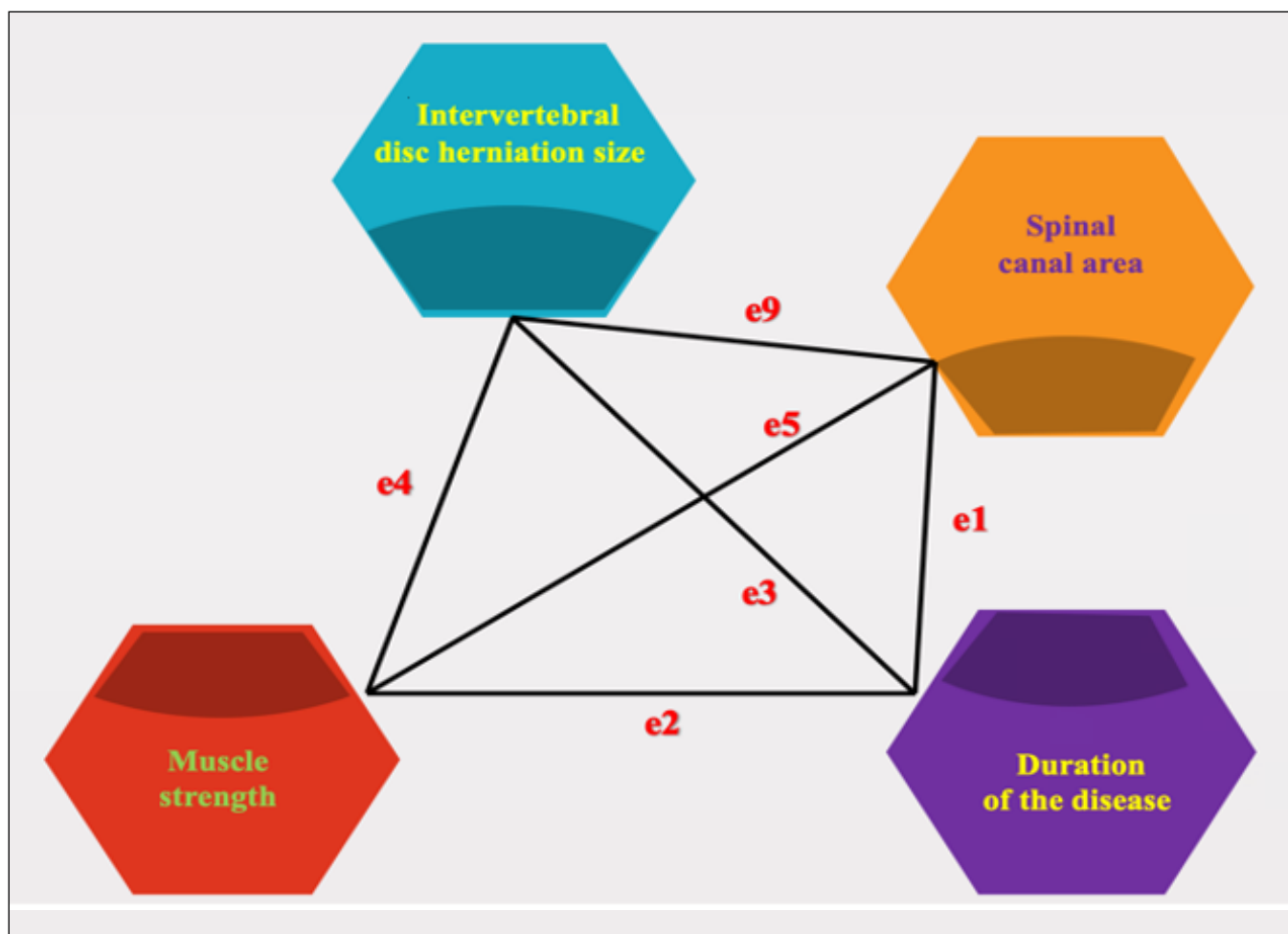


Fig. 5. Subgraph G1 of the graph model of the system of clinical and instrumental indicators of athletes with herniated intervertebral discs complicated by spinal canal stenosis.

mechanisms of injury.

Scientific publications on spontaneous resorption of intervertebral disc herniations (about 70%) have appeared regularly since 1984, and are confirmed by CT and MRI studies. In most cases, the resorption period lasts from 3 to 12 months. As a rule, the symptoms disappear much earlier [33]. Furthermore, our study has shown that this is due to the body's natural reactions, such as, an inflammatory reaction to fragments of the pulpal nucleus of the disc, from which the hernia consists of (phagocytosis, enzymes), immunological reactions or due to dehydration (dewatering) of the dropdown fragment (80% of the inner nucleus consists of water).

Progression of stenosis with intervertebral disc herniation at the cervical and thoracic levels can lead to irreversible damage, but at the lumbar level, due to anatomical features, due to the absence of the spinal cord below L1, can lead to severe spondylosis, and as a consequence to severe neurological disorders. Thus, the correct assessment of changes on MRI with the conducted clinical correlation is a key component

which should be considered in the course of a choice of surgical intervention at pathology of lumbar spine [34]. There are cases when MRI picture of stenosis of the spinal canal, 20% is asymptomatic or accompanied by minimal low back pain without the development of intermittent claudication [35]. According to MRI studies, disc herniation is often found without symptoms, i.e. without back and leg pain [36]. If you still have back pain, then an MRI hernia may not be the source of the pain.

The data obtained make it possible to optimize the indications for differential surgery or treatment tactics. May also be useful for identifying patients with risk of stress fracture. Earlier recognition of these conditions, a personalized approach, detailing the preoperative neuroimaging situation, features of the clinical picture of the disease, or rational differentiated use of various techniques based on the level structure of the graph model of the system of clinical and instrumental indicators can help not only in the development of methods for preventing early degenerative changes in the spine, but will also improve the

efficiency of rehabilitation means.

CONCLUSIONS

1. The assessment of the density of the relationship between clinical and instrumental parameters of athletes with herniated intervertebral discs complicated by spinal stenosis was carried out.
2. The level structure of the graph model of the system of clinical and instrumental indicators of patients with herniated intervertebral discs complicated by spinal stenosis was determined.
3. The most informative clinical and instrumental indicators of athletes with herniated intervertebral discs complicated by spinal canal stenosis were revealed.
4. A regression model of the relationship between clinical and instrumental parameters of patients with herniated intervertebral discs complicated by spinal canal stenosis was determined.

Prospects for further research will be aimed at analyzing of the frequency of occurrence and location of herniated intervertebral discs complicated by spinal stenosis, the

age of patients, specialization in sports, and gender characteristics.

REFERENCES

1. Lisenchuk G, Zhigadlo G, Tyshchenko V et al. Assess psychomotor, sensory-perceptual functions in sport games. *Journal of Physical Education and Sport*. 2019b;19(2):1205-1212. doi:10.7752/jpes.2019.02175. [DOI](#)
2. Malikov M, Tyshchenko V, Bogdanovska N et al. Functional fitness assessment of elite athletes. *Journal of Physical Education and Sport*. 2021;21(1): 374-380. doi:10.7752/jpes.2021.01036. [DOI](#)
3. Malikov M, Tyshchenko V, Hlukhov I et al. Enhancing the Sports Training of Elite Female Athletes in Academic Rowing. *Journal of Physical Education and Sport*, 2024;24(3):761–771. doi:10.7752/jpes.2024.03090. [DOI](#)
4. Valeria T, Olexander P. Control of general and special physical preparedness by qualified handballers. *Journal of Physical Education and Sport*. 2015;15(2):287-290. doi: 10.7752/jpes.2015.02043. [DOI](#)
5. Evhen P, Valeria T. Peculiar properties and dynamics of physiological indicators in handball team. *Journal of Physical Education and Sport*. 2017;17(1):335-341. doi: 10.7752/jpes.2017.01049. [DOI](#)
6. Tyshchenko V, Hnatchuk Y, Pasichnyk V et al. Factor analysis of indicators of physical and functional preparation for basketball players. *Journal of Physical Education and Sport*. 2018;18(4):1839-1844. doi:10.7752/jpes.2018.s4269.
7. Verhagen AP, Downie A, Popal N et al. Red flags presented in current low back pain guidelines: a review. *European Spine Journal*. 2016;25(9):2788-2802. doi: 10.1007/s00586-016-4684-0. [DOI](#)
8. Tyshchenko V, Tyshchenko D, Andronov V et al. Comprehensive evaluation of efficiency to identify deficiencies in muscle activity in different modes in team sports. *Wiadomości Lekarskie Medical Advances*. 2024;67(2):194-200. doi: 10.36740/WLek202402102. [DOI](#)
9. Abdalkader M, Guermazi A, Engebretsen L et al. MRI-detected spinal disc degenerative changes in athletes participating in the Rio de Janeiro 2016 Summer Olympics games. *BMC Musculoskeletal Disorders*. 2020;21(1):1-8. doi: 10.1186/s12891-020-3057-3. [DOI](#)
10. Wasserman MS, Guermazi A, Jarraya M et al. Evaluation of spine MRIs in athletes participating in the Rio de Janeiro 2016 Summer Olympic Games. *BMJ Open Sport & Exercise Medicine*. 2018;4:e000335. doi: 10.1136/bmjsem-2017-000335. [DOI](#)
11. Shum G, Cinnamon S, Hutton M et al. Decreased tibial nerve movement in patients with failed back surgery syndrome and persistent leg pain. *Eur Spine J*. 2019;28(9):2122-2128. doi: 10.1007/s00586-019-06056-4. [DOI](#)
12. Inoue S, Kamiya M, Nishihara M et al. Prevalence, characteristics, and burden of failed back surgery syndrome: the influence of various residual symptoms on patient satisfaction and quality of life as assessed by a nationwide Internet survey in Japan. *J Pain Res*. 2017;10:811-823. doi: 10.2147/JPR.S129295. [DOI](#)
13. Tharmanathan P, Adamson J, Ashby R, Eldabe S. Diagnosis and treatment of failed back surgery syndrome in the UK: mapping of practice using a cross-sectional survey. *British Journal of Pain*. 2012;6(4):142-152. doi: 10.1177/2049463712466321. [DOI](#)
14. Weigel R, Capelle HH, Al-Afif S, Krauss JK. The dimensions of "failed back surgery syndrome": what is behind a label? *Acta Neurochirurgica*. 2021;163(1):245-250. doi: 10.1007/s00701-020-04548-7. [DOI](#)
15. Weistroffer JK, Hsu WK. Return-to-play rates in National Football League linemen after treatment for lumbar disk herniation. *Am J Sports Med*. 2011;39(3):632-636. doi: 10.1177/0363546510388901. [DOI](#)
16. Rigoard P, Gatzinsky K, Deneuille JP et al. Optimizing the Management and Outcomes of Failed Back Surgery Syndrome: A Consensus Statement on Definition and Outlines for Patient Assessment. *Pain Research and Management*. 2019;1-12. doi: 10.1155/2019/8184592. [DOI](#)
17. Omelyanenko GA. Formuvannya naukovoho ta dozhyttyevoho myslennya bakalavriv fizychnoho vykhovannya i sportu zasobamy informatsiyno-komunikatsiynykh tekhnolohiy. [Formation of scientific and pre-life minds among bachelors from physical education and sports by means of information and communication technologies]. Thesis. Zhytomyr. 2012. (Ukrainian)

18. Ksenzov TA, Khyzhniak MV, Ksenzov AY, Tyshchenko VO. Criteria for selection of patients with lumbar intervertebral disc herniation complicated by spinal canal stenosis. *Zaporozhye Medical Journal*. 2021;23(6):828-833. doi: 10.14739/2310-1210.2021.6.234528. [DOI](#)
19. Ball JR, Harris CB, Lee J, Vives MJ. Lumbar spine injuries in sports: review of the literature and current treatment recommendations. *Sports Medicine-Open*. 2019;5(1):1-10. doi: 10.1186/s40798-019-0199-7. [DOI](#)
20. Fett D, Trompeter K, Platen P. Back pain in elite sports: a cross-sectional study on 1114 athletes. *PLoS One*. 2017;12(6):e0180130. doi: 10.1371/journal.pone.0180130. [DOI](#)
21. Connolly M, Rotstein AH, Roebert J et al. Lumbar spine abnormalities and facet joint angles in asymptomatic elite junior tennis players. *Sports Medicine-Open*. 2020;6(1):1-10. doi: 10.1186/s40798-020-00285-4. [DOI](#)
22. Gadia A, Shah K, Nene A. Outcomes of various treatment modalities for lumbar spinal ailments in elite athletes: a literature review. *Asian Spine Journal*. 2018;12(4):754-764. doi: 10.31616/asj.2018.12.4.754. [DOI](#)
23. Yamaguchi JT, Hsu WK. Intervertebral disc herniation in elite athletes. *International Orthopaedics*. 2019;43(4):833-840. doi: 10.1007/s00264-018-4261-8. [DOI](#)
24. Shifflett GD, Hellman MD, Louie PK et al. Return to golf after lumbar fusion. *Sports Health*. 2017;9:280-284. doi: 10.1177/1941738116680200. [DOI](#)
25. Plais N, Salzmann SN, Shue J et al. Spine injuries in soccer. *Current Sports Medicine Reports*. 2019;18(10):367-373. doi: 10.1249/JSR.0000000000000638. [DOI](#)
26. Earhart JS, Roberts D, Roc G et al. Effects of lumbar disk herniation on the careers of professional baseball players. *Orthopedics*. 2012;35:43-49. doi: 10.3928/01477447-20111122-40. [DOI](#)
27. Baker H, Rizzi A, Athiviraham A. Injury in the Women's National Basketball Association (WNBA) from 2015 to 2019. *Arthroscopy, sports medicine, and rehabilitation*. 2020;2(3):e213-e217. doi: 10.1016/j.asmr.2020.02.003. [DOI](#)
28. Jonasson P, Halldin K, Karlsson J et al. Prevalence of joint-related pain in the extremities and spine in five groups of top athletes. *Knee Surg Sports Traumatol Arthrosc*. 2011;19(9):1540-1546. doi: 10.1007/s00167-011-1539-4. [DOI](#)
29. Makovitch S, Eng C. Spine injuries in gymnasts. *Gymnastics Medicine: Evaluation, Management and Rehabilitation*. 2020. doi:10.1007/978-3-030-26288-4_8. [DOI](#)
30. Hangai M, Kaneoka K, Hinotsu S et al. Lumbar intervertebral disk degeneration in athletes. *Am J Sports Med*. 2009;37(1):149-255. doi: 10.1177/0363546508323252. [DOI](#)
31. Johansson F, Gabbett T, Svedmark P, Skillgate E. External training load and the association with back pain in competitive adolescent tennis players: results from the SMASH cohort study. *Sports Health*. 2022;14(1):111-118. doi:10.1177/1941738121105163. [DOI](#)
32. Cook RW, Hsu WK. Return to play after lumbar spine surgery. *Clinics in Sports Medicine*. 2016;35(4):609-619. doi: 10.1016/j.csm.2016.05.006. [DOI](#)
33. Zhong M, Liu JT, Jiang H et al. Incidence of Spontaneous Resorption of Lumbar Disc Herniation: A Meta-Analysis. *Pain Physician*. 2017;20(1):E45-E52.
34. Mysliwiec LW, Cholewicki J, Winkelpack MD, Eis GP. MSU Classification for herniated lumbar discs on MRI: toward developing objective criteria for surgical selection. *Eur. Spine J*. Jun 2010;19(7):1087-1093. doi: 10.1007/s00586-009-1274-4. [DOI](#)
35. Hartman J, Granville M, Jacobson RE. Radiologic Evaluation Of Lumbar Spinal Stenosis: The Integration Of Sagittal And Axial Views In Decision Making For Minimally Invasive Surgical Procedures. *Cureus Mar*. 2019;11(3):e4268. doi: 10.7759/cureus.4268. [DOI](#)
36. Ketola JH, Inkinen SI, Karppinen J et al. T2-weighted magnetic resonance imaging texture as predictor of low back pain: A texture analysis-based classification pipeline to symptomatic and asymptomatic cases. *J Orthop Res*. 2021;1-11. doi: 10.1002/jor.24973. [DOI](#)

This study was supported by Department of Neurosurgery, Zaporizhzhia Regional Clinical Hospital (Zaporizhzhia, Ukraine) and Department of Orthopedics and Traumatology, "House of Medicine Odrex", (Odesa, Ukraine). The authors wish to acknowledge the involvement sportsmen involved in this study.

CONFLICT OF INTEREST

The Authors declare no conflict of interest

CORRESPONDING AUTHOR

Valeria Tyshchenko

Zaporizhzhia National University

66 Zhukovskoho st, 69600 Zaporizhzhia, Ukraine
e-mail: valeri-znu@ukr.net

ORCID AND CONTRIBUTIONSHIP

Valeria Tyshchenko: 0000-0002-9540-9612 **A**

Tymur Ksenzov: 0000-0001-8305-8563 **D**

Tetiana Odynets: 0000-0001-8613-8470 **B**

Tetiana Bogoslav: 0000-0003-1932-8893 **A**

Artur Ksenzov: 0000-0002-4019-8184 **E**

Ivan Hlukhov: 0000-0003-4226-5253 **A**

Kateryna Drobot: 0000-0002-1421-2464 **B**

A – Work concept and design, **B** – Data collection and analysis, **C** – Responsibility for statistical analysis, **D** – Writing the article, **E** – Critical review, **F** – Final approval of the article

RECEIVED: 24.12.2023

ACCEPTED: 17.07.2024



Psychological well-being in breast cancer patients: the role of social support in managing anxiety and depression

Nataliia V. Zaviazkina, Tetiana Nefedova

KYIV INSTITUTE OF MODERN PSYCHOLOGY AND PSYCHOTHERAPY, KYIV, UKRAINE

ABSTRACT

Aim: To investigate the role of social support in the relationship between psychological well-being, anxiety, and depression among breast cancer patients.

Materials and Methods: A cross-sectional study included 98 women with breast cancer. Measures used were the Psychological General Well-being Index (PGWBI), the Hospital Anxiety and Depression Scale (HADS), the Multidimensional Scale of Perceived Social Support (MSPSS), and a sociodemographic questionnaire. Descriptive statistics, Cronbach's alpha, and regression analyses with moderation and mediation were conducted. T-tests estimated statistical significance in regression. Mediation effects were assessed using the quasi-Bayesian Monte Carlo method with bootstrapping.

Results: The initial linear regression analysis showed a strong negative relationship between anxiety/depression (HADS) and psychological well-being (PGWBI), with higher HADS scores were linked to lower psychological well-being. The regression analysis for social support (MSPSS) indicated a positive but small effect on psychological well-being. The moderation analysis showed no significant interaction between social support and anxiety/depression on psychological well-being. However, the mediation analysis demonstrated that social support significantly improves psychological well-being by reducing anxiety and depression, with a substantial proportion of the effect mediated.

Conclusions: The study found that while social support does not moderate the relationship between anxiety, depression and psychological well-being, it significantly enhances psychological well-being by reducing anxiety and depression.

KEY WORDS: breast cancer, psychological well-being, anxiety, depression, social support, psychodiagnostics

Wiad Lek. 2024;77(9):1704-1711. doi: 10.36740/WLek/192138 DOI

INTRODUCTION

Breast cancer diagnosis can have significant negative impact on mental health, causing problems like psychological distress, anxiety, post-traumatic stress, and depression [1]. At the same time, it remains one of the most common types of cancer in women worldwide. The diagnosis and treatment process may provoke substantial challenges that can persist even after remission [2].

Research indicates that anxiety and depression are among the most common psychological symptoms experienced by women at all stages of breast cancer [3]. These symptoms can severely undermine psychological well-being, affecting the quality of life and, in many cases, treatment outcomes [4,5].

Social support, in its turn, plays a crucial role in the experience of breast cancer patients. Research has shown that higher levels of emotional support are associated with lower levels of fatigue, pain interference, depressive symptoms and anxiety [6,7]. Moreover, social support has been studied as a mediator in the

relationship between resilience and quality of life [8], between optimism and distress in early-stage breast cancer survivors [9], and between body image and depressive symptoms and post-traumatic growth (PTG) in breast cancer patients [10]. However, the role of social support as a mediator between anxiety, depression and well-being in breast cancer patients has not been sufficiently explored.

AIM

Thus, the aims of the study are:

1. Examine whether social support moderates the relationship between psychological well-being (PGWBI) and anxiety/depression (HADS) in breast cancer patients.
2. Determine whether social support enhances psychological well-being (PGWBI) by reducing anxiety and depression (HADS), thereby serving as a mediator in this relationship.

MATERIALS AND METHODS

SAMPLE

The study involved 98 female breast cancer patients from Ukraine, recruited through specialized thematic groups for cancer patients on the social network Facebook, including the groups “Athena. Women against cancer” and “Inspiration family. All about cancer”, as well as among women undergoing psychotherapy using transactional analysis. Inclusion criteria were: (1) diagnosis of breast cancer within the last five years (including those currently in remission), (2) age between 18 and 70 years, and (3) willingness to participate in the study and provide informed consent. Exclusion criteria included: (1) diagnosis of any major psychiatric disorder, (2) inability to complete the questionnaires due to cognitive impairment or language barriers.

The inclusion of participants who had been diagnosed with breast cancer within the last five years, including those currently in remission, was intentional to capture a comprehensive range of psychological experiences and states. Breast cancer diagnosis and treatment significantly impact psychological well-being,

and these effects can persist long after treatment has concluded [11].

The final sample consisted of 98 participants (Table 1) with a mean age of $M = 43.19$ ($SD = 8.05$).

Demographic data collected included:

- Age;
- Marital status;
- Presence of children;
- Financial status;
- Stage of cancer;
- Presence of breast reconstruction;
- Presence of somatic diseases.

MEASURES

Psychological well-being, anxiety, depression, and perceived social support were assessed using several validated scales:

PSYCHOLOGICAL WELL-BEING

Psychological well-being was assessed using the Psychological General Well-being Index (PGWBI) [12]. This

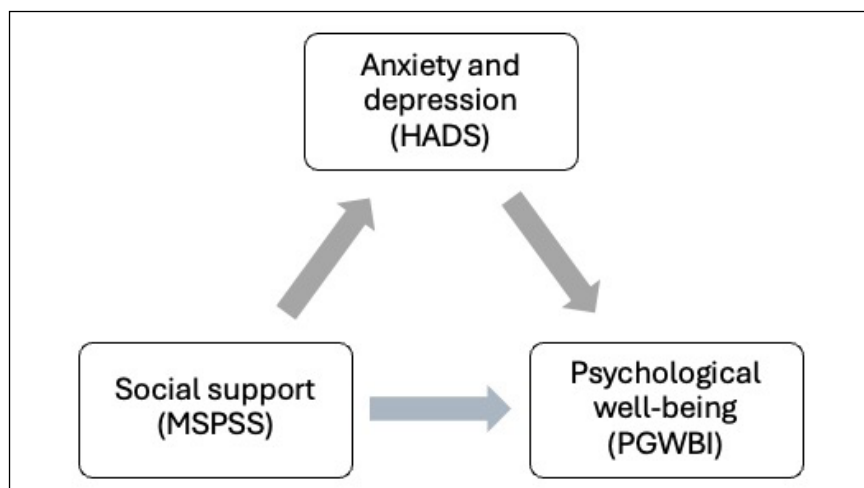


Fig. 1. Model illustrating the moderating role of social support (MSPSS) on the relationship between anxiety/depression (HADS) and psychological well-being (PGWBI) in breast cancer patients.

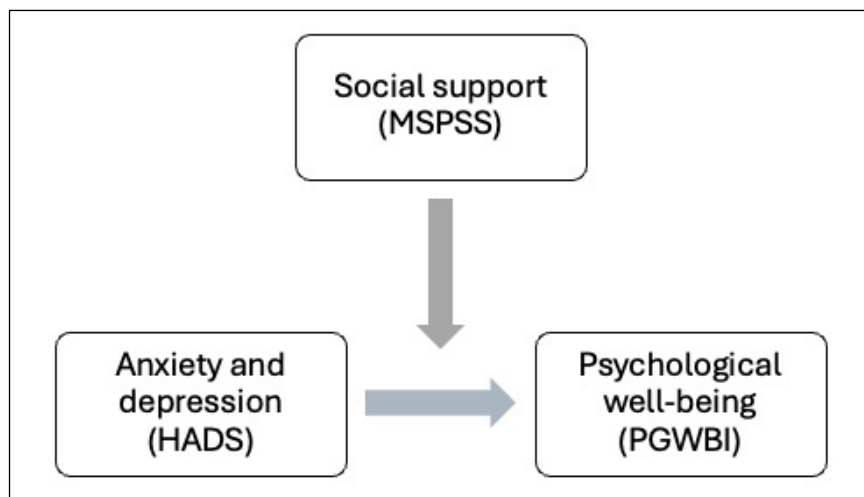


Fig. 2. Model illustrating the mediating role of anxiety and depression (HADS) in the relationship between social support (MSPSS) and psychological well-being (PGWBI) in breast cancer patients.

Table 1. Sample characteristics

Age	M = 43.19, SD = 8.05
Marital Status	
Single	16,33%
Married	62,24%
Living together/civil union	7,14%
Divorced	9,18%
Widowed	5,10%
Children	
None	28,57%
One	40,82%
Two	22,45%
Three or more	8,16%
Financial status	
1 (the poorest)	8,16%
2	35,71%
3	33,67%
4 (the richest)	22,45%
The stage of the disease	
Stage 0	13,27%
Stage IA / IB	9,18%
Stage IIA / IIB	17,35%
Stage IIIA / IIIB / IIIC	11,22%
Stage IV	15,31%
Recurrence	10,20%
Remission	33,67%
Breast reconstruction	
Yes	33,67%
No	66,33%
Somatic diseases	
Yes	32,65%
No	67,35%

scale includes questions covering six domains: general state of health, anxiety, depressive symptoms, positive well-being, self-control, and viability. Respondents were asked to rate the extent to which each statement applies to them on a scale from 0 (always) to 5 (never). When summed, the possible range of scores can range from 0 to 110, with higher values indicating higher psychological well-being.

ANXIETY AND DEPRESSION

The Hospital Anxiety and Depression Scale (HADS) was used to assess anxiety (HADS-A) and depression (HADS-D) levels [13]. The scale contains 14 items, of which 7 are designed to assess anxiety and the other 7 are depression. Responses are provided on a 4-point

scale, with scores ranging from 0 to 21 for each subscale, with higher values indicating higher levels of anxiety or depression.

SOCIAL SUPPORT

The perception of social support was assessed using the Multidimensional Scale of Perceived Social Support (MSPSS) [14]. The scale contains 12 items divided into three subscales: support from family, friends, and a significant other. Respondents answered the questions on a 7-point scale from 1 (very weak) to 7 (very strong), where higher values indicate a higher level of perceived support.

The reliability of the scales used was assessed using Cronbach’s α internal consistency index (Table 2).

Table 2. Reliability of the psychodiagnostic measures used

Scale/subscales	Cronbach's alpha (α)
PGWBI	0,95
Positive well-being	0,86
Anxiety	0,89
Depression	0,86
Self-control	0,67
General state of health	0,72
Viability	0,86
HADS	0,84
Depression	0,75
Anxiety	0,78
MSPSS	0,92
Significant Other	0,91
Family	0,91
Friends	0,92

Table 3. Linear regression analysis results for the effect of anxiety/depression on psychological well-being

Measure	Estimate	Std. Error	t-value	p-value	Significance
Intercept	96.91	2.53	38.35	<2e-16	***
HADS	-2.43	0.14	-17.01	<2e-16	***

Multiple R² = 0.7509
Adjusted R² = 0.7483

Notes: p ≤ 0^{'****'}, p ≤ 0.001^{'***'}, p ≤ 0.01^{'**'}, p ≤ 0.05^{'.'}, p ≤ 0.1, ^{'-'}1.

Table 4. Linear regression analysis results for the effect of social support on psychological well-being

Measure	Estimate	Std. Error	t-value	p-value	Significance
Intercept	33.72	7.55	4.47	2.15e-05	***
MSPSS	0.39	0.12	3.24	0.00162	**

Multiple R² = 0.09878
Adjusted R² = 0.0894

Notes: p ≤ 0^{'****'}, p ≤ 0.001^{'***'}, p ≤ 0.01^{'**'}, p ≤ 0.05^{'.'}, p ≤ 0.1, ^{'-'}1.

PROCEDURE

Data collection conducted in August 2022 via Survey-Monkey. Participants were informed about the study's purpose and procedures, and informed consent was obtained from all participants prior to data collection. The questionnaires were administered online, and all data were anonymized to ensure confidentiality.

HYPOTHESES

1. Social support (MSPSS) moderates the relationship between psychological well-being (PGWBI) and anxiety/depression (HADS) in breast cancer patients (Fig. 1).
2. Social support (MSPSS) enhances psychological well-being (PGWBI) by reducing anxiety and depression (HADS), thereby serving as a mediator in this relationship (Fig. 2).

MODERATION ANALYSIS

As illustrated in Fig. 1., to examine whether social support moderates the relationship between psychological well-being (PGWBI) and anxiety/depression (HADS), moderation analyses were conducted using the 'interaction' term between social support and psychological well-being. In these analyses, PGWBI served as the dependent variable (DV), HADS (anxiety and depression) as the independent variable (IV), and MSPSS as the moderator (M). Regression analyses were used to test these relationships, and t-tests were employed to estimate the statistical significance of the regression coefficients.

The model was specified as follows:

$$PGWBI = \beta_0 + \beta_1 HADS + \beta_2 MSPSS + \beta_3 (HADS \times MSPSS) + \epsilon$$

Table 5. Moderation analysis results for the effect of anxiety/depression on psychological well-being with social support as a moderator

Measure	Estimate	Std. Error	t- value	p-value	Significance
Intercept	96.99	9.79	9.91	2.88e-16	***
HADS	-2.56	0.47	-5.42	4.60e-07	***
MSPSS	-0.01	0.15	-0.07	0.95	-
Interaction: HADS*MSPSS	0.002	0.008	0.37	0.71	-
Multiple R ² = 0.7522					
Adjusted R ² = 0.7443					

Notes: p ≤ 0^{'***'}, p ≤ 0.001^{'**'}, p ≤ 0.01^{'*'}, p ≤ 0.05['], p ≤ 0.1, ^{'-'}1.

Table 6. Mediation analysis results for the effect of social support on psychological well-being through anxiety/depression as a mediator

Measure	Estimate	95% CI Lower	95% CI Upper	p-value	Significance
ACME	0.35	0.15	0.56	<2e-16	***
ADE	0.04	-0.09	0.16	0.57	-
Total effect	0.38	0.15	0.62	<2e-16	***
Proportion Mediated	0.90	0.59	1.39	<2e-16	***
Sample Size Used				98	
Simulations				1000	

Notes: p ≤ 0^{'***'}, p ≤ 0.001^{'**'}, p ≤ 0.01^{'*'}, p ≤ 0.05['], p ≤ 0.1, ^{'-'}1.

MEDIATION ANALYSIS

To investigate whether social support mediates the relationship between psychological well-being and anxiety/depression (Fig. 2), mediation analyses were performed. In these analyses, PGWBI was the independent variable (IV), HADS (anxiety and depression) were the dependent variables (DV), and MSPSS was the mediator (M). The mediation effect was assessed using the quasi-Bayesian Monte Carlo method with bootstrapping (5,000 resamples). The indirect effect was considered significant if the 95% confidence interval did not include zero.

The mediation model was specified with three steps:

1. The effect of MSPSS on the mediator (HADS):

$$HADS = \beta_0 + \beta_1 MSPSS + \epsilon$$

2. The effect of the mediator (HADS) on the dependent variable (PGWBI), including the independent variable (MSPSS):

$$PGWBI = \beta_0 + \beta_1 HADS + \beta_2 MSPSS + \epsilon$$

3. The total effect of MSPSS on PGWBI (without including HADS in the model):

$$PGWBI = \beta_0 MSPSS + \epsilon.$$

DATA CLEANING AND PREPARATION

Data cleaning and preparation were performed using Microsoft Excel (version 16.70). This included handling missing data, checking for outliers, and ensuring the accuracy of data entry. Descriptive statistics and reliability analyses (Cronbach's alpha) were conducted to evaluate the internal consistency of the measures.

STATISTICAL ANALYSIS

All statistical analyses were conducted using RStudio (version 2022.07.1). including descriptive statistics (means, standard deviations, frequencies), reliability analysis (Cronbach's alpha), simple linear regression (using 'lm' function with t-tests for significance), moderation analysis (interaction terms and regression analysis using 'lm' function with t-tests for significance), mediation analysis (quasi-Bayesian Monte Carlo method with bootstrapping using the 'mediation' package with significance testing), and significance testing (two-tailed tests with p-value < 0.05).

RESULTS

Initially, simple linear regression analyses were performed to evaluate the individual contributions of anxiety/depression and social support to psychological well-being. These models aimed to understand the direct impact of each predictor on the dependent variable. The regression analysis results for the effect of anxiety/depression on psychological well-being are summarized in Table 3 below.

The model demonstrates that higher scores on the Hospital Anxiety and Depression Scale (HADS) are associated with lower levels of psychological well-being (PGWBI), as indicated by the regression coefficient for HADS (-2.43, p < 2e-16). Specifically, each one-unit increase in the HADS score corresponds to a 2.43-unit decrease in psychological well-being. The intercept (96.91, p < 2e-16) suggests that in the absence of

anxiety and depression symptoms, individuals have high psychological well-being. The model explains approximately 75.09% of the variance in psychological well-being (Multiple $R^2 = 0.7509$, Adjusted $R^2 = 0.7483$), indicating a strong fit and robustness of the findings. These results underscore the substantial impact of anxiety and depression on psychological well-being, emphasizing the necessity for effective interventions to address these mental health issues.

As a next step, a simple linear regression analysis was conducted to evaluate the impact of social support on psychological well-being (Table 4).

This analysis revealed a positive relationship between these variables. The results indicate that higher levels of social support, as measured by the Multidimensional Scale of Perceived Social Support (MSPSS), are significantly associated with increased psychological well-being (PGWBI). Specifically, the regression coefficient for MSPSS is 0.39 ($p = 0.00162$), suggesting that for each one-unit increase in social support, psychological well-being improves by 0.39 units. The intercept of the model is 33.72 ($p = 2.15e-05$), indicating the baseline level of psychological well-being when social support is absent. Although the relationship between social support and psychological well-being is statistically significant, the model explains a relatively modest portion of the variance in psychological well-being, with Multiple $R^2 = 0.09878$ and Adjusted $R^2 = 0.0894$.

As a further step, a moderation analysis was conducted to evaluate the effect of anxiety/depression on psychological well-being with social support as a potential moderator. This analysis sought to understand whether social support influences the strength or direction of the relationship between anxiety/depression and psychological well-being (Hypothesis I). The results are presented in Table 5 below.

The regression analysis revealed that anxiety/depression, as measured by the Hospital Anxiety and Depression Scale (HADS), continues to have a significant negative impact on psychological well-being (Estimate = -2.56, $p = 4.60e-07$). The intercept (96.99, $p = 2.88e-16$) indicates the baseline level of psychological well-being in the absence of anxiety/depression and social support influences. Social support (MSPSS) alone did not show a significant main effect on psychological well-being (Estimate = -0.01, $p = 0.95$). Importantly, the interaction term between HADS and MSPSS (Estimate = 0.002, $p = 0.71$) was also not significant, suggesting that social support does not moderate the relationship between anxiety/depression and psychological well-being.

The model explains a substantial portion of the variance in psychological well-being, with Multiple $R^2 = 0.7522$ and Adjusted $R^2 = 0.7443$, indicating that

approximately 75.22% of the variance is accounted for by the predictors and their interaction. These findings suggest that while anxiety/depression significantly affects psychological well-being, the level of social support does not alter this relationship.

To further explore the relationship between social support and psychological well-being, a mediation analysis was performed to determine whether the effect of social support on psychological well-being is mediated by anxiety/depression (Table 6).

The Average Causal Mediation Effect (ACME) was found to be significant (Estimate = 0.35, 95% CI [0.15, 0.56], $p < 2e-16$), indicating that anxiety/depression mediates the relationship between social support and psychological well-being. This suggests that a portion of the effect of social support on psychological well-being operates through its impact on anxiety/depression. Specifically, as social support increases, it reduces anxiety/depression, which in turn enhances psychological well-being.

The Average Direct Effect (ADE) of social support on psychological well-being, excluding the mediation effect, was not significant (Estimate = 0.04, 95% CI [-0.09, 0.16], $p = 0.57$), indicating that social support does not directly affect psychological well-being when controlling for anxiety/depression.

The total effect of social support on psychological well-being was significant (Estimate = 0.38, 95% CI [0.15, 0.62], $p < 2e-16$), confirming that social support positively impacts psychological well-being, and this effect is largely mediated by anxiety/depression.

The proportion of the effect mediated was very high (Proportion Mediated = 0.90, 95% CI [0.59, 1.39], $p < 2e-16$), indicating that approximately 90% of the total effect of social support on psychological well-being is mediated through its effect on anxiety/depression.

In summary, while social support does not moderate the impact of anxiety/depression on psychological well-being, it significantly enhances psychological well-being by acting as a mediator, reducing anxiety and depression among breast cancer patients.

DISCUSSION

The results of this study add to the growing amount of research examining the relationships between social support, anxiety, depression, and psychological well-being in breast cancer patients. The initial hypothesis posited that social support (as measured by the MSPSS) would moderate the relationship between psychological well-being (PGWBI) and anxiety/depression (HADS). However, the results from the moderation analysis did not support this hypothesis. In particular,

social support did not show a significant impact on the strength or direction of the relationship between anxiety/depression and psychological well-being. This finding contrasts with some existing studies that suggest a buffering role of social support in mitigating the adverse effects of psychological distress [15].

At the same time, the mediation analysis strongly supported the second hypothesis, showing a significant indirect pathway through which social support improves psychological well-being by reducing anxiety and depression. The significant Average Causal Mediation Effect (ACME) indicates that social support positively impacts psychological well-being by lowering symptoms of anxiety and depression. This finding aligns with previous research that indicates the role of social support in enhancing quality of life [7,8]. The high proportion of the effect mediated (90%) emphasizes that social support mostly reduces anxiety and depression, rather than having direct effects, leading to improved psychological well-being.

These findings emphasize the critical role of social support in the mental health framework of breast cancer patients. Specifically, interventions aimed at enhancing

social support should focus not only on providing emotional and practical assistance but also on strategies that specifically target anxiety and depression.


CONCLUSIONS

This study explored the role of social support in moderating and mediating the relationship between anxiety, depression and psychological well-being in breast cancer patients. The findings did not support the hypothesis that social support moderates this relationship between anxiety, depression and psychological well-being. However, the mediation analysis revealed that social support significantly enhances psychological well-being by reducing anxiety and depression, with a substantial portion of its effect operating through this indirect pathway.

These results underscore the importance of addressing mental health symptoms in interventions designed to enhance social support for breast cancer patients. While social support may not buffer the direct impact of anxiety and depression, it significantly improves psychological well-being by alleviating these symptoms.

REFERENCES

- Fortin J, Leblanc M, Elgbeili G et al. The mental health impacts of receiving a breast cancer diagnosis: A meta-analysis. *British Journal of Cancer*. 2021;125(11):1582-1592. doi:10.1038/s41416-021-01542-3. [DOI](#)
- Muzzatti B, Bomben F, Flaiban C et al. Quality of life and psychological distress during cancer: a prospective observational study involving young breast cancer female patients. *BMC cancer*. 2020;20:1-8. doi:10.1186/s12885-020-07272-8. [DOI](#)
- Hajj A, Hachem R, Khoury R et al. Clinical and genetic factors associated with anxiety and depression in breast cancer patients: a cross-sectional study. *BMC cancer*. 2021;21:1-11. doi:10.1186/s12885-021-08615-9. [DOI](#)
- Fann JR, Thomas-Rich AM, Katon W et al. Major depression after breast cancer: a review of epidemiology and treatment. *General hospital psychiatry*, 2008;30(2):112-126. doi:10.1016/j.genhosppsych.2007.10.008. [DOI](#)
- Pedersen AE, Sawatzky JA, Hack TF. The sequelae of anxiety in breast cancer: a human response to illness model. In *Oncology Nursing Forum*. 2010;37(4):469-75. doi:10.1188/10.ONF.469-475. [DOI](#)
- Fisher HM, Winger JG, Miller SN et al. Relationship between social support, physical symptoms, and depression in women with breast cancer and pain. *Supportive Care in Cancer*. 2021;29:5513-5521. doi:10.1007/s00520-021-06110-2. [DOI](#)
- Ng CG, Mohamed S, See MH et al. Anxiety, depression, perceived social support and quality of life in Malaysian breast cancer patients: a 1-year prospective study. *Health and Quality of Life Outcomes*. 2015;13:1-9. doi:10.1186/s12955-015-0401-7. [DOI](#)
- Zhang H, Zhao Q, Cao P et al. Resilience and quality of life: exploring the mediator role of social support in patients with breast cancer. *Medical Science Monitor*. 2017;23:5969. doi:10.12659/MSM.907730. [DOI](#)
- Trunzo JJ, Pinto BM. Social support as a mediator of optimism and distress in breast cancer survivors. *Journal of Consulting and Clinical Psychology*. 2003;71(4):805. doi:10.1037/0022-006X.71.4.805. [DOI](#)
- Li M. Associations of body image with depressive symptoms and PTG among breast cancer patients: The mediating role of social support. *Frontiers in Psychology*. 2022;13:953306. doi:10.3389/fpsyg.2022.953306. [DOI](#)
- Stovall E, Greenfield S, Hewitt M. *From cancer patient to cancer survivor: lost in transition*. National Academies Press. 2005. doi:10.17226/11468. [DOI](#)
- Grossi E, Compare A. Psychological General Well-Being Index (PGWB). In: Michalos, A.C. (eds) *Encyclopedia of Quality of Life and Well-Being Research*. Springer, Dordrecht. 2014. doi: 10.1007/978-94-007-0753-5_2309. [DOI](#)
- Zigmond AS, Snaith RP. The hospital anxiety and depression scale. *Acta psychiatrica scandinavica*. 1983;67(6):361-370. doi: 10.1111/j.1600-0447.1983.tb09716.x. [DOI](#)
- Zimet G, Dahlem N, Zimet S et al. The Multidimensional Scale of Perceived Social Support. *Journal of Personality Assessment*. 1988;52:30-41. doi: 10.1207/s15327752jpa5201_2. [DOI](#)

15. Kinsinger SW, McGregor BA, Bowen DJ. Perceived breast cancer risk, social support, and distress among a community-based sample of women. *Journal of Psychosocial Oncology*. 2009;27(2):230-247. doi:10.1080/07347330902776002. 

CONFLICT OF INTEREST

The Authors declare no conflict of interest

CORRESPONDING AUTHOR







Nataliia V. Zaviazkina





Kyiv Institute of Modern Psychology and Psychotherapy

34 Lesi Ukrainki boulevard, 01133 Kyiv, Ukraine

e-mail: nmuz@ukr.net

ORCID AND CONTRIBUTIONSHIP

Nataliia V. Zaviazkina: 0000-0001-5565-8959      

Tetiana Nefedova: 0000-0003-2714-9975    

 – Work concept and design,  – Data collection and analysis,  – Responsibility for statistical analysis,  – Writing the article,  – Critical review,  – Final approval of the article

RECEIVED: 22.05.2024

ACCEPTED: 07.08.2024



Blood serum interleukins levels and their relationship with colon tissue prostanoids in experimental ulcerative colitis

Iryna Vasylieva¹, Oksana Nakonechna¹, Liudmyla Popova², Natalia Yarmysh¹, Anastasiia Bezrodna¹, Nataliia Pustova¹

¹ KHARKIV NATIONAL MEDICAL UNIVERSITY, KHARKIV, UKRAINE

² KYIV MEDICAL UNIVERSITY, KYIV, UKRAINE

ABSTRACT

Aim: To study IL-1 β , IL-6, IL-8, IL-10 blood serum levels and their relationship with colon tissue prostanoids in experimental ulcerative colitis.

Materials and Methods: Blood serum interleukins and colon tissue prostanoids were determined by enzyme immunosorbent assay on three groups of WAG population rats (1st control group – rectal saline injection; 2nd control group – 50% ethanol injection; experimental group – injection of 2,4-dinitrobenzene-sulfonic acid in 50% ethanol).

Results: The increased levels of all interleukins both in 2nd control and experimental groups versus 1st control group were found. No differences in IL-6, IL-8 levels between experimental and 2nd control groups were revealed. The relationships between interleukins and PGF2 α , between interleukins and TXB2 in all groups, and the appearance of correlations between interleukins and PGE2, between interleukins and PGI2 in experimental group were observed. Negative correlations between IL-8 and COX-2 in 1st control, between IL-8 and COX-1 in both 2nd control and experimental groups were found. Negative correlation between 8-epi-PGF2 α and IL-8, positive correlation between 8-epi-PGF2 α and PGF2 α in experimental group were revealed.

Conclusions: Results obtained testify the possible role of PGF2 α and 8-epi-PGF2 α in the development of ulcerative colitis and justify the importance of research on the link of 8-epi-PGF2 α , IL-8, PGF2 α for understanding the mechanisms of development and progression of this disease. Increasing blood serum IL-8 level may be used as marker of reducing colon tissue COX-1 content in both ethanol- and 2,4-dinitrobenzenesulfonic acid-induced ulcerative colitis.

KEY WORDS: Interleukins, prostanoids, ulcerative colitis, rats

Wiad Lek. 2024;77(9):1712-1717. doi: 10.36740/WLek/192139 DOI

INTRODUCTION

Ulcerative colitis (UC) and Crohn's disease are the most common inflammatory bowel diseases (IBD), but their pathogenetic mechanisms are not fully understood.

Immune system mediators play a significant role in IBD development but literature data regarding their changes and effects in disease progressing some times are contradictory. It is believed that proinflammatory cytokines, including IL-1 β , IL-6 and others, play significant role in upregulation, while antiinflammatory ones, including IL-10, play significant role in downregulation of disease progression [1]. According Impellizzeri D. et al. (2018) IL-1 β knockout mice were hyporesponsive to 2,4-dinitrobenzenesulfonic acid (DNBS)-induced colitis versus wild type mice [2]. However growing evidence has indicated that IL-1 β can support colonic homeostasis and attenuate colonic inflammation [3]. According results of Cominelli F. et al. (1990) pretreatment with IL-1 β low dose suppressed colonic inflammation in rabbits via PGE2 production [3]. This

is consistent with the opinion of Park Y.S. (2007) that endogenous prostanoids are involved in protecting mucous membrane from colon ulcers in dextran sodium sulfate (DSS)-induced inflammation [4]. On the contrary, according to the results of Lejeune M. et al. (2010) apical exposure of T84 colonic epithelial monolayer to PGE2 high levels diminished barrier integrity which was reversed by E-prostanoid 4 receptor antagonist [5].

According some authors IL-10 plays key role in controlling intestinal inflammation. IL-10-deficient mice and patients with mutations in IL-10 or its receptor show increased susceptibility to IBD [6]. In UC patient IL-6 and TNF- α levels were increased, while IL-10 and IL-4 levels were decreased in peripheral blood versus healthy group [7]. On the contrary, data obtained by Melger S. et al. (2003) indicate generalized activation of IL-10 producing CD4+ T cells along the gut of UC patients [8]. In the work of Carrasco A. et al. (2022) it was also revealed an increase in IL-10 messenger RNA (mRNA) in mucosa and IL-10 in blood

in UC patients versus control [9]. Moreover, according to the results of Wang S. et al. (2020) high IL-10 level at the remission phase was associated with shorter duration of remission [10].

Thus, the contradiction of some data regarding interleukines (ILs) involvement in development and course of IBD, the lack of investigation of the relationship between themselves and with prostanoids necessitate further research in this direction. The study of ILs content in systemic blood flow and ILs relationship with other inflammatory mediators particularly prostanoids in colon tissue will make it possible to evaluate the disease course state and the treatment effect without invasive methods.

AIM

The aim is to study the IL-1 β , IL-6, IL-8, IL-10 blood serum levels and their relationship with colon tissue prostanoids in experimental UC.

MATERIALS AND METHODS

The study used 42 adult WAG rats, divided into 3 equal groups. The first control group rats were rectally injected with sauline; the second control group rats were injected with a 50% ethanol solution; the experimental group rats were injected with DNBS in a 50% ethanol solution for 14 days [11]. On 15th day, the animals were removed from the experiment using a guillotine knife.

ELISA Kits for rats Interleukin 1Beta, IL-6, IL-8, IL-10 ("abcam", USA) were used to determine blood serum ILs levels. In colon homogenates, the prostanoid contents were determined by Rat PGE₂, RAT PGF₂ α , RAT PGI₂, RAT TXB₂ ELISA Kits (MyBioSource) (USA) and 8-epi-PGF₂ α ELISA Kit (Elabscience) (USA) with tissue pretreatment according the kits instructions.

Statistical data processing was carried out using GraphPad Prism 5 Software (USA). Comparisons between two independent groups of variables were performed using non-parametric Mann–Whitney U test. Results are represented as medians and interquartile ranges. Correlation analysis according Spearman was used to reveal relationship between different variables of the same group. Differences were considered significant at $p < 0.05$.

The study design was approved by the Commission of Ethics and Bioethics of Kharkiv National Medical University. The research was carried out in accordance with the EU Directive 2010/63/EU on the protection of animals used for scientific purposes and the Council of Europe Convention for the Protection of Vertebrate

Animals used for Experimental and other Scientific Purposes (ETS123).

RESULTS

According to the obtained results IL-1 β and IL-10 blood serum levels in rats with DNBS-induced UC were significantly higher versus 1st and 2nd controls. Both IL-1 β and IL-10 were also increased in 2nd control versus 1st control. Blood serum levels of IL-6 and IL-8 in rats with DNBS-induced UC were significantly higher compared with 1st control but they didn't differ from 2nd control. Both IL-6 and IL-8 levels were enhanced in 2nd control versus 1st control (Table 1). In 1st control, positive correlations between IL-1 β and IL-6 ($r = +0.64$, $p = 0.024$), between IL-1 β and IL-10 ($r = +0.58$, $p = 0.047$), and a close negative relationship between IL-8 and IL-10 ($r = -0.60$, $p = 0.041$) were revealed. In 2nd control, only positive relationship between IL-1 β and IL-6 ($r = +0.66$, $p = 0.019$) remained. In experimental group, positive relationship between IL-1 β and IL-10 ($r = +0.61$, $p = 0.035$), as well as negative relationship between IL-10 and IL-8 ($r = -0.70$, $p = 0.011$) remained.

When studying the relationships between blood serum ILs and colon tissue prostanoids the following patterns were revealed. In 1st control group, there were negative correlations between PGF₂ α and all studied ILs, except IL-6, as well as close positive correlations between TXB₂ and two ILs (IL-1 β , IL-6). On the contrary, in 2nd control and experimental groups, PGF₂ α had close negative correlation only with IL-6. In addition to this, close positive correlations between IL-1 β and PGI₂, between TXB₂ and 3 ILs (IL-1 β , IL-8, IL-10) were found in 2nd control group. Even more relationships were found in experimental group. In this group, in addition to negative correlation between IL-6 and PGF₂ α , a negative correlation between IL-8 and 8-iso-PGF₂ α was also found. For 3 ILs (IL-1 β , IL-6, IL-8), close positive associations with PGI₂ were revealed. For all ILs, except IL-8, strong relationships with PGE₂ were found (positive for IL-1 β , IL-6; negative for IL-10). For 2 ILs (IL-1 β and IL-8), close positive relationships with TXB₂ were found (Table 2).

DISCUSSION

The development of various inflammatory processes, including colitis, largely depends on inflammatory mediators. They are numerous, produced by various cells, have pleiotropic and mutually modulating effects, that difficults the results interpretation to make the real role of each of them in the disease development. We investigated 4 ILs, three of which are mostly

Table 1. The interleukins levels (pg/ml) in blood serum of rats with experimental ulcerative colitis (Me [25%; 75%])

Interleukins	1 st control group	2 nd control group	Experimental group
IL-1 β	9,67 [6,24; 14,30]	27,09 [20,43; 29,24]***	50,38 [38,07; 64,64]***, $\Delta\Delta\Delta$
IL-6	6,34 [5,29; 6,77]	25,32 [19,59; 25,91]***	25,66 [22,01; 26,97]***
IL-8	9,60 [8,56; 10,27]	32,31 [25,81; 41,05]***	35,42 [30,86; 36,52]***
IL-10	14,46[10,45; 16,63]	27,24[23,70; 31,73]***	42,87 [35,67; 48,79]***, $\Delta\Delta\Delta$

Note: *** - $p < 0,001$ versus 1st control group; $\Delta\Delta\Delta$ - $p < 0,001$ versus 2nd control group.

Table 2. The correlation coefficients between blood serum interleukins and colon tissue prostanoids in rats with experimental ulcerative colitis

Interleukins	Prostanoids				
	PGF2 α	PGE2	PGI2	TXB2	8-epi-PGF2 α
1 st control group					
IL-1 β	-0,61 *	+0,01	+0,08	+0,59*	+0,27
IL-6	+0,11	+0,04	-0,20	+0,64*	-0,55
IL-8	-0,59*	+0,17	+0,10	+0,05	-0,63
IL-10	-0,88***	-0,02	+0,10	+0,05	-0,63
2 nd control group					
IL-1 β	+0,03	+0,53	+0,65*	+0,75**	+0,47
IL-6	-0,66*	+0,56	+0,45	+0,33	-0,49
IL-8	+0,50	+0,03	+0,46	+0,86***	+0,49
IL-10	-0,50	+0,35	-0,15	+0,59*	-0,67
Experimental group					
IL-1 β	-0,43	+0,70*	+0,63*	+0,65*	+0,18
IL-6	-0,69*	+0,82**	+0,71*	+0,57	-0,69
IL-8	-0,39	+0,55	+0,72**	+0,76**	-0,84*
IL-10	-0,56	-0,58*	+0,15	+0,32	-0,56

Note: * - $p < 0,05$; ** - $p < 0,01$; *** - $p < 0,001$.

considered proinflammatory (IL-1 β , IL-6, IL-8) and one antiinflammatory and immunomodulatory (IL-10). We found an increase of all 4 ILs in serum of rats with DNBS-induced colitis versus 1st control, but only 2 of them (IL-1 β , IL-10) were enhanced versus 2nd control.

In previous works, we showed, that content changing both isoforms of cyclooxygenases (COX-1 and COX-2) and content changes of most of investigated prostanoids in colon tissue are also due to ethanol, not DNBS [12, 13]. Ethanol is used in this experimental colitis model as intestinal barrier «destroyer». It destroys intestinal barrier by two ways: by epithelial cells disruption and spaces disruption between epithelial cells [14]. Ethanol induces intestinal inflammation not only by increasing intestinal mucosa permeability, but also by dysbiosis and mucosa immune system alterations [14].

The analysis of correlations between studied ILs indicates the certain relationships loss between ILs in 2nd control and experimental groups, which may be associated with macrophage phenotypes different ratio, namely the predominance of M1 phenotype in

2nd control group and M2 phenotype in experimental group. The microenvironment in which macrophage is located provides it with various signals that divergently shift the macrophage phenotype towards «classically activated» (M1) or «alternatively activated» (M2a, M2b or M2c) [15]. M2b and M2c phenotypes secrete high levels of IL-10, which in turn suppresses production some proinflammatory factors, including IL-8 (Fiorentino DF et al., 1991) [15]. Namely the relationships between IL-10 and IL-6, as well as between IL-10 and IL-1 β , were remained in experimental group. And the only relationship between IL-1 β and IL-6 was remained in 2nd control group.

In the analysis of correlations between ILs and prostanoids, contrary to expectations, no correlations between the studied ILs and PGE2 were found in both control groups. Only in experimental group, positive correlation between PGE2 and all ILs, except IL-8, was observed. The existence of negative correlations between ILs and PGF2 α and positive correlations between ILs and TXB2 was noteworthy. While in 1st control group all ILs, except IL-6, had negative

correlations with PGF2 α , in the groups of rats exposed to either ethanol or DNBS in ethanol solution, these relationships were lost, but appeared a negative relationship between PGF2 α and IL-6. In the available literature, we did not find works related to PGF2 α role study in ulcerative colitis development, but in the work of Riaposova L. et al. (2023) it was shown that PGF2 α enhanced inflammation in myometrial cells through increased activation of NF- κ B and MAP kinases and increased COX-2 expression [16]. IL-6 is generally considered proinflammatory, but IL-6 $^{-/-}$ /IL-10 $^{-/-}$ mice were found to exhibit more pronounced intestinal inflammation and an earlier disease onset than IL-10 $^{-/-}$ mice [17], that may indicate its antiinflammatory properties. This opinion is consistent with the work of Ding Q. et al. (2023), according to which bone marrow mesenchymal stem cells pretreated with IL-6 significantly reduced colon damage score in rats with DSS-induced UC [18].

As for TXB2, a positive relationship between this prostanoid and IL-1 β was found in all groups. While positive correlation between TXB2 and IL-6 was also observed in the animals control group, in rats with inflammation provoked by both ethanol itself and ethanol dissolved DNBS, this relationship was lost, but there was relationship with IL-8. Only rats with ethanol-induced inflammation showed positive correlation between TXB2 and IL-10. TXA2 is the most abundant product of COX-1 arachidonic acid (AA) metabolism in mature human platelets (Ricciotti and FitzGerald, 2011) [19], while monocytes/macrophages synthesize TXA2 using COX-2 enzyme [20]. COX-1 participates in synthesis of TXA2 in B cells, and COX-1-derived TXA2 functions in an autocrine manner in developing B cells [21]. In the work of Sacco A. et al. (2019) was shown that specific deletion of COX-1 in platelets, i.e. inhibition of TXA2 production in platelets, resulted in milder symptoms of colitis, in exacerbation phase, and almost complete recovery from disease after withdrawal of DSS [19].

After calculating the correlation coefficients between blood serum ILs levels and colon tissue COX content, we found that only IL-8 had a close relationship with COX. This relationship was negative and observed in all 3 groups: in 1st control - between IL-8 and COX-2 ($r=-0.60$, $p=0.039$), in 2nd control and experimental groups - between IL-8 and COX-1 ($r=-0.79$, $p=0.002$ and $r=-0.63$, $p=0.046$, respectively). The synthesis of all prostanoids, including PGE2, PGF2 α , PGI2 and TXA2 (TXB2 is the stable metabolite of TXA2) is initiated by COX. It catalyzes AA conversion to PGH2. Further PGH2 conversion to respective prostanoids is provided by other specific enzymes. We didn't found any correlation COX and prostanoids amounts, except

negative correlation between COX-2 and TXB2 both in 2nd control and experimental groups ($r=-0.61$, $p=0.036$ and $r=-0.65$, $p=0.033$, respectively). The appearance of correlation between TXB2 and namely COX-2 in colonic tissue during inflammation may be related to TXB2-producing cells ratio change. The inconsistency between the correlations nature and TXB2 content may be related to changing in the functional and phenotypic properties of these cells and involving the additional factors in regulation. The possibility of changing functional and phenotypic properties of cells, and thus regulation, as a result of pathology is confirmed in the work of Charalambous S. et al. [22]. According to the work, transforming growth factor- β 1 down-regulates IL-8 production in normal brain endothelial cells (BEC), but don't inhibit IL-8 production in tumor-associated BEC [22]. One of the regulatory factors can be 8-epi-PGF2 α , formed nonenzymatically as a result of increased lipid peroxidation. It has been shown to interact with TXA2 receptors [23], so it can perform TXA2-like effects including feed-back down-regulation of IL-8 production. This is evidenced by the significant negative relationship we found between IL-8 and 8-epi-PGF2 α in experimental group.

The interpretation of data obtained is complicated by the fact that ILs can exert their effects through prostanoids, and prostanoids influence ILs release, as well as the fact that many types of cells are involved in the inflammation process and their ratio may be different in different phases of inflammation, and immunocompetent cells activation and cells response to signals depends on the microenvironment. Despite this, colon tissue prostanoids content changes are the result of the influence of all possible factors at once, including enzymes of synthesis and decay, the pool of receptors, interactions, microenvironment, etc. And the blood serum ILs content reflects the systemic processes in the body occurring in response to colon inflammation.

CONCLUSIONS

Ulcerative colitis in rats is accompanied by increase of all studied ILs in blood serum. The increase in all ILs level in 2nd control group compared to 1st control group, as well as the absence of a difference in the content of IL-6 and IL-8 between 2nd and experimental groups, are obviously conditioned with ability of ethanol to cause colon inflammation on its own.

The loss of certain relationships between ILs in the animals of 2nd control and experimental groups was found, that may be associated with a different ratio of macrophage phenotypes.

The existence of negative correlations between ILs and PGF2 α , as well as the appearance of negative correlations between PGF2 α and PGE2 in the groups of rats exposed to either ethanol or DNBS in ethanol solution, indicate the possible important role of PGF2 α in the development of UC and the need for research in this direction.

Due to strong negative correlation between the blood serum IL-8 and the colon tissue COX-1 content in both ethanol- and DNBS-induced UC, increasing blood serum

IL-8 level may be used as marker of reducing colon tissue COX-1 content in UC.

A significant negative correlation between 8-epi-PGF2 α and IL-8 and a significant positive correlation between 8-epi-PGF2 α and PGF2 α , as well as the ability of 8-epi-PGF2 α to bind to receptors to TXA2 testify to the possible role of 8-epi-PGF2 α in UC development and justify the importance of research on the link of 8-epi-PGF2 α , IL-8, PGF2 α for understanding the mechanisms of this disease development and progression.

REFERENCES

1. Tatiya-Aphiradee N, Chatuphonprasert W, Jarukamjorn K. Immune response and inflammatory pathway of ulcerative colitis. *J Basic Clin Physiol Pharmacol*. 2018;30(1):1-10. doi: 10.1515/jbcp-2018-0036. [DOI](#)
2. Impellizzeri D, Siracusa R, Cordaro M et al. Therapeutic potential of dinitrobenzene sulfonic acid (DNBS)-induced colitis in mice by targeting IL-1 β and IL-18. *Biochem Pharmacol*. 2018;155:150-161. doi: 10.1016/j.bcp.2018.06.029. [DOI](#)
3. Fan H, Zhao G, Liu L et al. Pre-treatment with IL-1 β enhances the efficacy of MSC transplantation in DSS-induced colitis. *Cell Mol Immunol*. 2012;9(6):473-81. doi: 10.1038/cmi.2012.40. [DOI](#)
4. Park YS. [COX-2 inhibitors in inflammatory bowel disease: friends or foes?]. *Korean J Gastroenterol*. 2007;50(6):350-5. (Korean).
5. Lejeune M, Leung P, Beck PL et al. Role of EP4 receptor and prostaglandin transporter in prostaglandin E2-induced alteration in colonic epithelial barrier integrity. *Am J Physiol Gastrointest Liver Physiol*. 2010;299(5):G1097-105. doi: 10.1152/ajpgi.00280.2010. [DOI](#)
6. Jofra T, Galvani G, Cosorich I et al. Experimental colitis in IL-10-deficient mice ameliorates in the absence of PTPN22. *Clin Exp Immunol*. 2019;197(3):263-275. doi: 10.1111/cei.13339. [DOI](#)
7. Su H, Kang Q, Wang H et al. Changes in expression of p53 and inflammatory factors in patients with ulcerative colitis. *Exp Ther Med*. 2019;17(4):2451-2456. doi: 10.3892/etm.2019.7253. [DOI](#)
8. Melgar S, Yeung MM, Bas A et al. Over-expression of interleukin 10 in mucosal T cells of patients with active ulcerative colitis. *Clin Exp Immunol*. 2003;134(1):127-37. doi: 10.1046/j.1365-2249.2003.02268.x. [DOI](#)
9. Carrasco A, Tristán E, Fernández-Bañares F et al. Mucosal Interleukin-10 depletion in steroid-refractory Crohn's disease patients. *Immun Inflamm Dis*. 2022;10(10):e710. doi: 10.1002/iid3.710. [DOI](#)
10. Wang S, Wang J, Ma R et al. IL-10 enhances T cell survival and is associated with faster relapse in patients with inactive ulcerative colitis. *Mol Immunol*. 2020;121:92-98. doi: 10.1016/j.molimm.2020.03.001. [DOI](#)
11. Morampudi V, Bhinder G, Wu X et al. DNBS/TNBS colitis models: providing insights into inflammatory bowel disease and effects of dietary fat. *J Vis Exp*. 2014;(84):e51297. doi: 10.3791/51297. [DOI](#)
12. Vasylyeva IM, Babenko OV, Nakonechna OA et al. Comparative analysis of two types of control in the formation of an experimental model of chronic ulcerative colitis. *Achievements of Clinscal and Experimental Medicine*. 2021;4:56-59. doi: 10.11603/1811-2471.2021.v.i4.12799. [DOI](#)
13. Vasylyeva IM, Nakonechna OA, Popova LD et al. The content of prostanoids and cyclooxygenases in colon tissue in experimental ulcerative colitis. *Clinical and Preventive Medicine*. 2023;8(30):91-97. doi: 10.31612/2616-4868.8.2023.11. [DOI](#)
14. Bishehsari F, Magno E, Swanson G et al. Alcohol and Gut-Derived Inflammation. *Alcohol Res*. 2017;38(2):163-171.
15. Arango Duque G, Descoteaux A. Macrophage cytokines: involvement in immunity and infectious diseases. *Front Immunol*. 2014;5:491. doi: 10.3389/fimmu.2014.00491. [DOI](#)
16. Riaposova L, Kim SH, Hanyaloglu AC et al. Prostaglandin F2 α requires activation of calcium-dependent signalling to trigger inflammation in human myometrium. *Front Endocrinol (Lausanne)*. 2023;14:1150125. doi: 10.3389/fendo.2023.1150125. [DOI](#)
17. Ye M, Joosse ME, Liu L et al. Deletion of IL-6 Exacerbates Colitis and Induces Systemic Inflammation in IL-10-Deficient Mice. *J Crohns Colitis*. 2020;14(6):831-840. doi: 10.1093/ecco-jcc/jjz176. [DOI](#)
18. Ding Q, Fang H, Jin P et al. Pretreating mesenchymal stem cells with IL-6 regulates the inflammatory response of DSS-induced ulcerative colitis in rats. *Transpl Immunol*. 2023;76:101765. doi: 10.1016/j.trim.2022.101765. [DOI](#)
19. Sacco A, Bruno A, Contursi A et al. Platelet-Specific Deletion of Cyclooxygenase-1 Ameliorates Dextran Sulfate Sodium-Induced Colitis in Mice. *J Pharmacol Exp Ther*. 2019;370(3):416-426. doi: 10.1124/jpet.119.259382. [DOI](#)
20. Radmark O. Formation of eicosanoids and other oxylipins in human macrophages. *Biochem Pharmacol*. 2022;204:115210. doi: 10.1016/j.bcp.2022.115210. [DOI](#)

21. Yang Q, Shi M, Shen Y et al. COX-1-derived thromboxane A2 plays an essential role in early B-cell development via regulation of JAK/STAT5 signaling in mouse. *Blood*. 2014;124(10):1610-21. doi: 10.1182/blood-2014-03-559658. [DOI](#)
22. Charalambous C, Pen LB, Su YS et al. Interleukin-8 differentially regulates migration of tumor-associated and normal human brain endothelial cells. *Cancer Res*. 2005;65(22):10347-54. doi: 10.1158/0008-5472.CAN-05-0949. [DOI](#)
23. Takahashi K, Nammour TM, Fukunaga M et al. Glomerular actions of a free radical-generated novel prostaglandin, 8-epi-prostaglandin F2 alpha, in the rat. Evidence for interaction with thromboxane A2 receptors. *J Clin Invest*. 1992;90(1):136-41. doi: 10.1172/JCI115826. [DOI](#)

CONFLICT OF INTEREST

The Authors declare no conflict of interest

CORRESPONDING AUTHOR

Iryna Vasylieva

Kharkiv National Medical University
4 Nauky avenue, 61022 Kharkiv, Ukraine
e-mail: vasilevaira@ukr.net

ORCID AND CONTRIBUTIONSHIP

Iryna Vasylieva: 0000-0002-4475-167X [A](#) [B](#) [C](#) [D](#)
Oksana Nakonechna: 0000-0002-2614-1587 [A](#) [B](#) [C](#)
Liudmyla Popova: 0000-0001-9967-8927 [A](#) [D](#) [F](#)
Natalia Yarmysh: 0000-0003-2798-4575 [B](#)
Anastasiia Bezrodna: 0000-0002-7543-7165 [B](#)
Nataliia Pustova: 0000-0002-1131-9725 [E](#)

[A](#) – Work concept and design, [B](#) – Data collection and analysis, [C](#) – Responsibility for statistical analysis, [D](#) – Writing the article, [E](#) – Critical review, [F](#) – Final approval of the article

RECEIVED: 21.05.2024

ACCEPTED: 07.08.2024



Lyme borreliosis in Ivano-Frankivsk district, Ukraine: a epidemiological and clinical characteristics (2000-2022)

Oleksandra Pryshliak, Oleksandr Boichuk, Sergii Fedorov, Victoriya Kvasniuk, Nadiya Vaskul, Andrii Protsyk, Zoriana Tylischchak

IVANO-FRANKIVSK NATIONAL MEDICAL UNIVERSITY, IVANO-FRANKIVSK, UKRAINE

ABSTRACT

Aim: To give epidemiological and clinical characteristics of the morbidity of Lyme borreliosis in Ivano-Frankivsk region for the period of 2000-2022 years.

Materials and Methods: There were used annual reports (form №1) from the State Institution "Ivano-Frankivsk Regional Center for Disease Control and Prevention of the Ministry of Health of Ukraine" and 200 of "Medical records of inpatients" (form 003/o) of the Ivano-Frankivsk Regional Clinical Infectious Diseases Hospital for 2000-2022 years.

Results: The morbidity of Lyme borreliosis in the Ivano-Frankivsk region has been permanently increasing since 2000. Natural foci have been identified, the number of which is increasing every year. There was noted late admission of patients to the Infectious Disease Hospital from the beginning of the disease, mainly at the stage of migratory annular erythema. There were almost no phenomena of intoxication and fever during the acute period. There were often observed the phenomena of hepatosis, joint damage and manifestations of the nervous system at the disseminated and chronic stages.

Conclusions: All landscape zones of Ivano-Frankivsk region are enzootic regarding Lyme borreliosis. Over the last 10 years in the region there is a tendency to a sharp increase of Lyme borreliosis morbidity. The clinical peculiarities of the disease in Ivano-Frankivsk region are: the absence of intoxication at the stage of migratory erythema, the phenomena of hepatosis. During the second and third stages of the disease there are polymorphic symptoms: recurrent erythema, damage of the retina, joints, liver, nervous system.

KEY WORDS: infectious diseases, ticks, natural foci, migratory erythema

Wiad Lek. 2024;77(9):1718-1725. doi: 10.36740/WLek/192141 DOI

INTRODUCTION

Ixodic tick-borne Lyme borreliosis – is a polyetiologic zoonotic natural-focal infection in the group of spirochetoses with a transmissible mechanism of infection, characterized by polymorphism of clinical manifestations with the skin lesion, central and peripheral nervous system, heart, musculoskeletal system and predisposition to the prolonged and chronic recurrent course [1-4]. Over the last 20 years, many epidemiological and clinical studies of this disease have been performed in Europe, the United States and Ukraine [5-9].

The causative agent of Lyme borreliosis (LB) – is a gram-negative spirochete of the *Borrelia burgdorferi sensu lato* complex [10, 11]. The reservoir of the pathogen in nature – murine rodents, wild and domestic animals, as well as birds. *Borrelia* is transmitted to humans through the bites of ixodic ticks: *I. ricinus* and *I. persulcatus*. The geographical distribution of LB is similar to natural habitat of other tick-borne infections (tick-borne encephalitis, human granular anaplasmosis, babesiosis)

[11]. With the saliva of the tick, the pathogen enters the human body, causing both a local reaction (annular erythema) and damage of the internal organs due to dissemination by lymphatic and hematogenous routes. The development of autoimmune reactions and the possibility of long-term intracellular persistence of the pathogen are the main causes of infection chronization [12-15].

Improved diagnosis of LB: serological tests using enzyme-linked immunosorbent assay, immunoblotting, detection of *Borrelia* DNA by PCR-based diagnostics. However, clinical symptoms are the leading ones in the diagnosis of LB [16, 17].

The intensity of the epidemic process and clinical peculiarities of LB course differ in various regions of the world and in regions of Ukraine [18-22], thus the observational study of local epidemiological and clinical peculiarities of LB in Ivano-Frankivsk region is important and counts for development of preventive and curative measures.

AIM

To give epidemiological and clinical characteristics of the morbidity of Lyme borreliosis in Ivano-Frankivsk region for the period of 2000-2022 years.

MATERIALS AND METHODS

There were used annual reports (form №1) from the State Institution "Ivano-Frankivsk Regional Center for Disease Control and Prevention of the Ministry of Health of Ukraine" and 200 of "Medical records of inpatients" (form 003/o) of the Ivano-Frankivsk Regional Clinical Infectious Diseases Hospital for 2000-2022 years.

The diagnosis was confirmed (until 2013) by the method of indirect immunofluorescence (IIFT), then using enzyme-linked immunosorbent assay (ELISA) there were revealed antibodies IgM, IgG to the complex *Borrelia burgdorferi sensu lato*. Since 2014, the method of immunoblotting with the detection of IgM, IgG to antigens *Borrelia burgdorferi sensu stristo*, *Borrelia garinii*, *Borrelia afzelii* was also used.

Statistical analysis of data was performed using the Microsoft Excel Statistical Package for Microsoft 365 MSO (setup 2311 of version 16.0.17029.20068) (32-bit version). License ID: EWW_58cc64b2-cc32-48b6-bd4b-cce379e20247_574357c00167ce3139.

The results obtained during the research are represented in the form of absolute numbers (quantity

of registered LB case in a particular year), rates (LB morbidity in a particular year), proportions with errors and confidence intervals (for the analysis of categorical data: part of patients with different clinical symptoms among all patients) and average values and their errors (for the analysis of quantitative data). The values were calculated according to standard formulas. To determine the long-term trend (growth, stabilization, decrease) we were used the analysis of dynamic series calculated according to standard formulas (absolute change, percentage change, relative change, percentage change from baseline, moving average). For graphic presentation of phenomena development, we used trend lines in Microsoft Excel programme.

RESULTS

Ivano-Frankivsk region is located in the West of Ukraine and borders with Lviv, Ternopil, Chernivtsi and Zakarpattia. Prykarpattia covers three different landscape zones: Prydnistrovya or forest-steppe, Peredhirya with forest-meadow landscapes, the South-west of the region is represented by the flanks of the Eastern Carpathians, covered with continuous deciduous and coniferous forests. The region is located in zone of the temperate continental climate. The peculiarity of the Ivano-Frankivsk region is determined by its physical-geographical location, favorable weather condi-

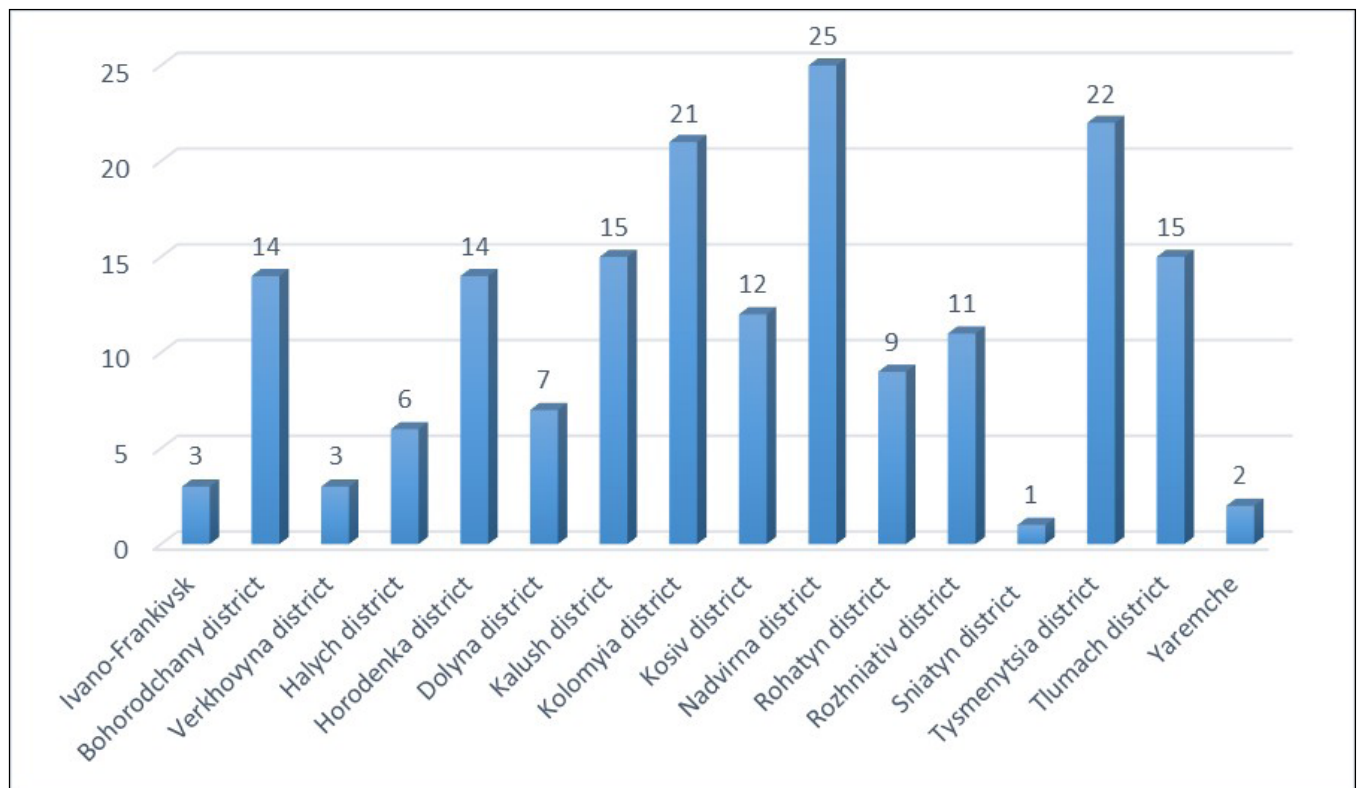


Fig. 1. The number of foci of Lyme borreliosis in administrative districts of the Ivano-Frankivsk region in 2022.

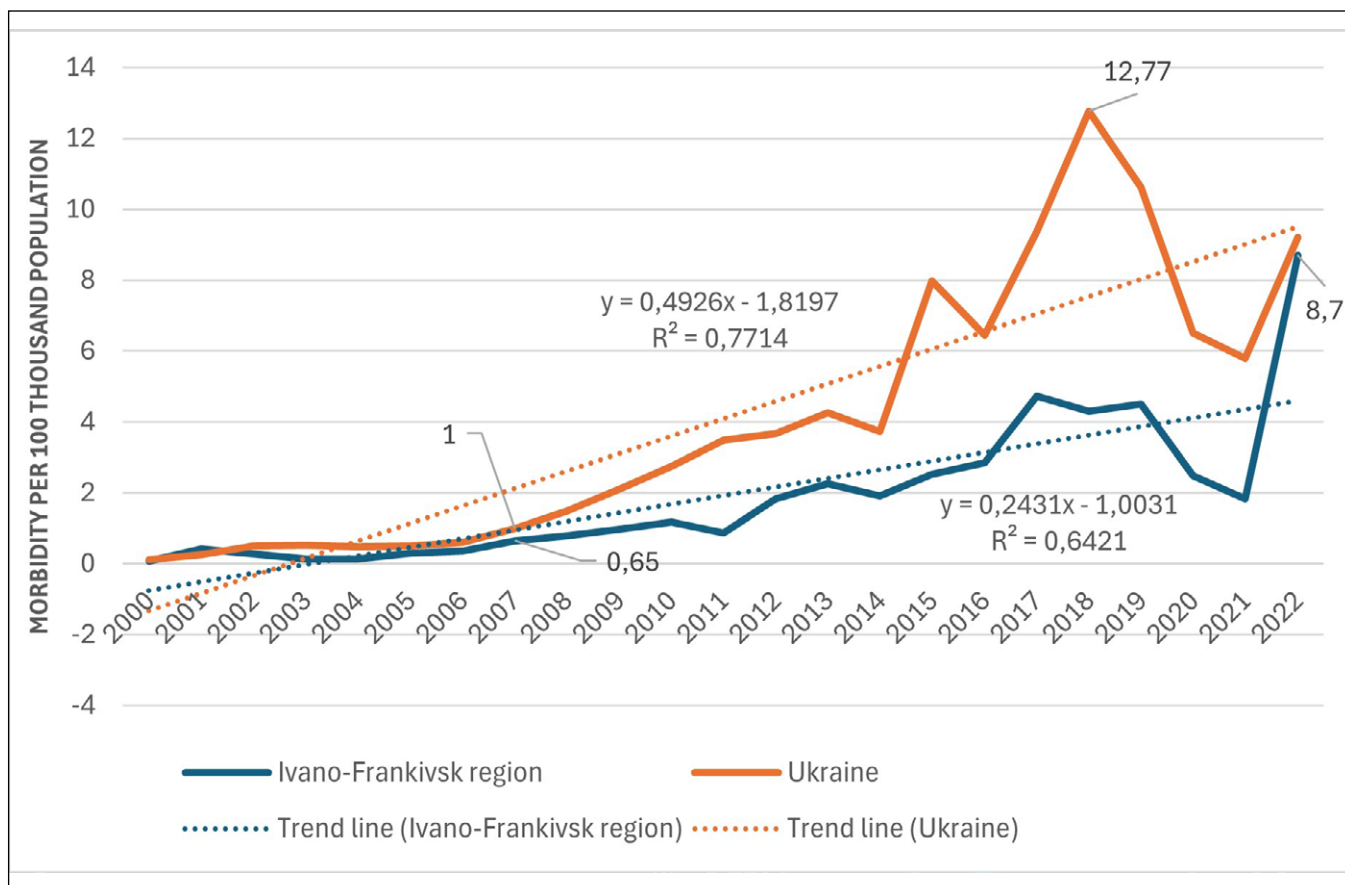


Fig. 2. Dynamics of Lyme borreliosis morbidity in Ivano-Frankivsk region and in Ukraine.

tions and composition of the fauna, which provides the prerequisites for the formation of the natural and anthropurgic foci of infectious diseases [23, 24].

Enzootic territories have been identified concerning LB in Prykarpattia: in the environs of the regional center (city and suburban villages), as well as in Prydnistrovya (Halych, Kalush, Tysmenytsia, Tlumach, Rohatyn, Horodenka districts), in Peredhirya (Bohorodchany, Dolyna, Kolomyia districts), and in the mountaneous – Kosiv and Nadvirna districts (Fig. 1).

In 2022, the number of foci has reached 199. The largest number of foci was observed in Nadvirna district, a large number was also noted in Kolomyia and Tysmenytsia districts.

To determine the layer of seropositive population in different districts of the region, there were taken blood samples in a healthy population. The study was performed on the basis of the Lviv Research Institute of Natural Focal Infections. It was found that on average $13.1 \pm 2.2\%$ of the studied healthy individuals of Nadvirna, $31.3 \pm 3.1\%$ – of Dolyna, $20.0 \pm 2,6\%$ – of Halych, $11.4 \pm 2.1\%$ – of Kolomyia, $26.2 \pm 2.9\%$ – of Sniatyn, $42.3 \pm 3.3\%$ – of Kalush districts, $14.1 \pm 2.3\%$ – of Ivano-Frankivsk have antibodies to *Borrelia burgdorferi* (IgG, IgM). Field material (ticks) was also collected.

The level of infection of ticks with *Borrelia* has reached $25.0 \pm 2.9\%$.

The morbidity (incidence) of LB since 2000 to 2022 both in Ukraine and in the region is constantly increasing. At the same time, over the last 10 years we observed significant increasing of morbidity in Ivano-Frankivsk and in Ukraine. The dynamics of the incidence of LB in Ivano-Frankivsk region and in Ukraine (2000 - 2022) is represented in Fig. 2.

According to the chart, the period since 2000 to 2007 differs in small fluctuations in morbidity, and in the indices of 0.07 per 100 thousand of population (Ivano-Frankivsk region) and 0.12 (Ukraine) have reached – 0.65 and 1.0, respectively. Intensive growth in morbidity has occurred over the past 10 years. In 2018 in Ukraine this index has increased in comparison with 2000, 100-fold (12.77 per 100 thousand of population), in Ivano-Frankivsk region the highest index was in 2022 – 8.7 that is 124 times higher, then in 2000. Over the last 10 years, 360 patients have been registered in Ivano-Frankivsk region.

According to the research aim, we also analysed dynamic of Lyme borreliosis cases in Ivano-Frankivsk region and Ukraine for the period of 2000-2022 years. Main parameters of dynamic series are presented in Table 1 and Table 2.

Table 1. Lyme borreliosis cases in the Ivano-Frankivsk region dynamic (Indicators of dynamic series analysis)

Year	LB, cases	Absolute change	Percentage Change	Relative Change	Percentage Change from baseline	Moving average
2000	1	-	-	-	100,00	-
2001	6	5,00	600,00	500,00	500,00	3,67
2002	4	-2,00	66,67	-33,33	300,00	4,00
2003	2	-2,00	50,00	-50,00	100,00	2,67
2004	2	0,00	100,00	0,00	100,00	2,67
2005	4	2,00	200,00	100,00	300,00	3,67
2006	5	1,00	125,00	25,00	400,00	6,00
2007	9	4,00	180,00	80,00	800,00	8,33
2008	11	2,00	122,22	22,22	1000,00	11,00
2009	13	2,00	118,18	18,18	1200,00	13,33
2010	16	3,00	123,08	23,08	1500,00	13,67
2011	12	-4,00	75,00	-25,00	1100,00	17,67
2012	25	13,00	208,33	108,33	2400,00	22,33
2013	30	5,00	120,00	20,00	2900,00	27,00
2014	26	-4,00	86,67	-13,33	2500,00	30,00
2015	34	8,00	130,77	30,77	3300,00	32,67
2016	38	4,00	111,76	11,76	3700,00	45,33
2017	64	26,00	168,42	68,42	6300,00	53,33
2018	58	-6,00	90,63	-9,38	5700,00	61,00
2019	61	3,00	105,17	5,17	6000,00	51,00
2020	34	-27,00	55,74	-44,26	3300,00	40,00
2021	25	-9,00	73,53	-26,47	2400,00	59,67
2022	120	95,00	480,00	380,00	11900,00	-

Moving average represent clear increasing tendency of LB both in Ivano-Frankivsk region and in Ukraine. For absolute change there is some fluctuation (decreasing in some years), but mostly we observed phenomena increasing (Table 1, Table 2). The same tendency is typical for percentage change and relative change, there for percentage change from baseline especially during last 10 years increase extremely.

There analysed 200 medical records of patients with LB who have been treated in the Ivano-Frankivsk Regional Clinical Infectious Diseases Hospital since 2000 till 2022.

The largest number of people seeking medical attention due to tick suction, was registered in May-June, the second wave was observed in September-October. Women predominated among the patients – 108 (54.0±3.5%), children were 24 (12.0±2.5%). The incubation period lasted from 1 week to 3.5 months, on average 28.7±1.9 days. Half of the patients – were urban dwellers who visited the forest in the summer or worked in country houses near the forest. Patients were admitted to the hospital, mainly in the autumn-winter period and even the next year spring, i.e. after 1.5 - 3

months and more since the onset of the disease, often in January, chronic forms even more than after 1 year. In most patients, the diagnosis of LB was determined in the early localized stage of migratory annular erythema – 142 (71.0±3.2%), in the second disseminated stage – in 30 (15.0±2.5%), in the third stage of persistent infection – in 24 (12.0±2.3%), in non-erythematous form – in 4 (2.0±0.9%) of patients.

Migratory annular erythema was observed during the first localized stage. The duration of erythema lasted from 2 weeks to 2.5 months, with an average of 53.1±4.2 days. The size of the erythema in diameter averaged 17.8±2.4 cm. Body temperature increased in 12 patients (8.22±1.9%) to subfebrile figures within 3-4 days. In 15 (10,27±2.15%) of patients at this stage, the liver size has increased, and ultrasound showed the signs of hepatosis. Some patients had had: headache, joint pain, heart pain, dizziness and others (Table 3).

During the second disseminated stage, cyanotic hyperpigmentation, the presence of additional spots, vesicles, as well as weakness, fever, headache, joint and muscle pain were observed at the site of fading erythema. There were 5 (16.67±2.64%) of patients who

Table 2. Lyme borreliosis cases in Ukraine dynamic (Indicators of dynamic series analysis)

Year	LB, cases	Absolute change	Percentage Change	Relative Change	Percentage Change from baseline	Moving average
2000	59	-	-	-	100,00	-
2001	122	63,00	206,78	106,78	106,78	141,00
2002	242	120,00	198,36	98,36	310,17	202,33
2003	243	1,00	100,41	0,41	311,86	238,00
2004	229	-14,00	94,24	-5,76	288,14	236,00
2005	236	7,00	103,06	3,06	300,00	249,00
2006	282	46,00	119,49	19,49	377,97	328,00
2007	466	184,00	165,25	65,25	689,83	479,67
2008	691	225,00	148,28	48,28	1071,19	708,67
2009	969	278,00	140,23	40,23	1542,37	974,67
2010	1264	295,00	130,44	30,44	2042,37	1277,00
2011	1598	334,00	126,42	26,42	2608,47	1512,33
2012	1675	77,00	104,82	4,82	2738,98	1736,33
2013	1936	261,00	115,58	15,58	3181,36	1767,00
2014	1690	-246,00	87,29	-12,71	2764,41	2350,67
2015	3426	1736,00	202,72	102,72	5706,78	2624,67
2016	2758	-668,00	80,50	-19,50	4574,58	3360,00
2017	3896	1138,00	141,26	41,26	6503,39	4022,00
2018	5412	1516,00	138,91	38,91	9072,88	4596,67
2019	4482	-930,00	82,82	-17,18	7496,61	4213,00
2020	2745	-1737,00	61,24	-38,76	4552,54	3223,00
2021	2442	-303,00	88,96	-11,04	4038,98	3020,67
2022	3875	1433,00	158,68	58,68	6467,80	-

had hepatitis, 3 patients (10.0±2.12%) had retinal angiopathy (spasm and sclerosis).

During the third persistent stage, the recurrent erythema persisted, sometimes up to 18 months; there were weakness, dizziness, enlargement of regional lymph nodes to the site of the tick bite up to 1.5-2 cm, joint damage – 3 (12,5±2.34%): swelling and pain (synovitis of the knee, talocrural, radiocarpal and other joints), decreased visual acuity, retinal angiopathy – 9 (37,5±3.42%), hepatitis. Rarely there were observed changes in the cardiovascular system: palpitations, pain in the heart area, systolic murmur at the apex.

There were manifestations of the nervous system at different stages of the disease in 48 (24.0±2.82%) of patients: serous meningoencephalitis 4 (2.0±0.92%), peripheral neuritis of the VII pair of the trigeminal nerve – 3 (1,3±0.75%), the phenomena of encephalomyelitis and polyneuropathy – 21 (9.13±1.90%) (vestibulo-ataxic syndrome, weakening of convergence, decreased photoreaction, Marinescu-Rodowicz's symptom, rocking in Romberg's position, eyelid tremor, diplopia), other patients had had: headache, dizziness, hearing loss, tinnitus.

Almost all patients were determined a mild form of anemia (Hb – 98.7±6.3 g/l), lymphocytosis (42.4±3.3%). In 26 patients (13.0±2.22%) there was hypoalbuminemia with the increased level of gamma-globulins (from 28.0 to 43.0%).

DISCUSSION

Long-term monitoring of LB in Ivano-Frankivsk region has shown a significant increase of morbidity over the last 10 years. Similar data are published by researchers from other European countries [25, 26]. Although in general the incidence in the region is lower than in Ukraine, but this creates a problem in terms of public health, as the actual number of patients is much higher [19]. That is also pointed out by several researchers from other countries [18, 20]. The decrease in the number of registered patients with LB in 2020-2021 years can be explained by the impact of anti-epidemic measures in case of coronavirus disease COVID-19 on population activity. Serological examination of the healthy population

Table 3. Characteristics of clinical symptoms in patients with Lyme borreliosis (first localized stage), N=146


Symptoms	Number of Patients	%	±m	95 % Confidence Interval Lower limit	95 % Confidence Interval Upper limit
Weakness	26	17,81	3,17	11,60	24,01
Fever	37	25,34	3,60	18,29	32,40
Increasing body temperature up to 38°C	12	8,22	2,27	3,76	12,67
Headache	31	21,23	3,38	14,60	27,87
Dizziness	11	7,53	2,18	3,25	11,82
Nausea	7	4,79	1,77	1,33	8,26
Catarrhal signs (sore throat, dry cough, runny nose)	12	8,22	2,27	3,76	12,67
Muscle pain	9	6,16	1,99	2,26	10,07
Neck muscle stiffness	5	3,42	1,51	0,47	6,37
Joint pain	14	9,59	2,44	4,81	14,37
Heart pain	8	5,48	1,88	1,79	9,17
Regional lymphadenitis	24	16,44	3,07	10,43	22,45
General lymphadenopathy	3	2,05	1,17	-0,25	4,36
Benign lymphocytoma of the skin	5	3,42	1,51	0,47	6,37
Hepatomegaly	15	10,27	2,51	5,35	15,20
Splenomegaly	7	4,79	1,77	1,33	8,26
Migratory annular erythema	142	97,26	1,35	94,61	991

revealed a high percentage of antibodies to *Borrelia* in almost all areas of the Ivano-Frankivsk region. These data are correlated with the authors' one on the results of a serological examination of the sera of patients from Western Ukraine [19]. The formation of new enzootic foci is associated with an increase of tick infection, favorable natural factors in the region and the lack of preventive measures. This conclusion is also consistent with the data of some authors [25, 26]. Absence of the expressed intoxication, increase in body temperature in the acute period cause late hospitalization of patients and administration of etiotropic therapy. Polymorphism of clinical manifestations during the second and third stages of the disease, the variability of laboratory studies' results create difficulties in the diagnosis of Lyme borreliosis [12, 22]. It should be based on a complex of epidemiological (the fact of ticks' sucking, being in an endemic zone in the seasonal period) and characteristic clinical data (the presence of erythema, joint damage, neurological symptoms). This is consistent with the data [19, 26].

CONCLUSIONS

1. All landscape zones of Ivano-Frankivsk region are enzootic regarding the Lyme borreliosis, seropositive healthy population in different areas of the region is from $11.4 \pm 2.1\%$ to $42.3 \pm 3.3\%$.
2. Over the last 10 years in the region there is a tendency to a sharp increase of the morbidity of Lyme borreliosis, since 2000 – it has increased 124-fold.
3. $71.0 \pm 3.2\%$ of patients are admitted to the infectious hospital in the stage of migratory erythema, without of intoxication, with short-term rise in subfebrile temperature in $8.22 \pm 1.9\%$, the phenomena of hepatosis in $10.27 \pm 2.15\%$ of patients.
4. During the second and third stages of the disease there are polymorphic symptoms: recurrent erythema, a significant frequency of retinal vascular lesions – up to $37.5 \pm 3.42\%$, joints – $12.5 \pm 2.34\%$, liver – $16.67 \pm 2.64\%$.
5. Neuroborreliosis occurs in $24.0 \pm 2.82\%$ of patients at different stages of the disease: serous meningoencephalitis, peripheral neuritis with facial nerve paresis, the phenomena of encephalomyelitis and polyneuropathy.

REFERENCES

1. Wong KH, Shapiro ED, Soffer GK. A Review of Post-treatment Lyme Disease Syndrome and Chronic Lyme Disease for the Practicing Immunologist. *Clinical reviews in allergy & immunology*. 2022;62(1):264–271. doi:10.1007/s12016-021-08906-w. 

2. Sorokman TV, Moldovan PM. Lyme disease in childhood: look at the problem and clinical case. *Actual infectology*. 2018;6(1):1-6. doi:10.22141/2312-413x.6.1.2018.125628. [DOI](#)
3. Kaczmarek KA, Szwabe K, Urbanek I et al. Prevalence of Lyme Carditis in Patients with Atrioventricular Blocks. *Int J Environ Res Public Health*. 2022;19(22):14893. doi:10.3390/ijerph192214893. [DOI](#)
4. Schoen RT. Lyme disease: diagnosis and treatment. *Curr Opin Rheumatol*. 2020;32(3):247-254. doi: 10.1097/BOR.0000000000000698. [DOI](#)
5. Sykes RA, Makiello P. An estimate of Lyme borreliosis incidence in Western Europe. *J Public Health (Oxf)*. 2017;39(1):74-81. doi: 10.1093/pubmed/fdw017. [DOI](#)
6. Weiner M, Zukiewicz-Sobczak W, Tokarska-Rodak M et al. Prevalence of *Borrelia burgdorferi sensu lato* in ticks from the Ternopil region in Ukraine. *J Vet Res*. 2018;62(3):275-280. doi:10.2478/jvetres-2018-0039. [DOI](#)
7. Carriveau A, Poole H, Thomas A. Lyme Disease. *The Nursing clinics of North America*. 2019;54(2):261-275. doi:10.1016/j.cnur.2019.02.003. [DOI](#)
8. Walter KS, Carpi G, Caccone A, Diuk-Wasser MA. Genomic insights into the ancient spread of Lyme disease across North America. *Nat Ecol Evol*. 2017;1(10):1569-1576. doi:10.1038/s41559-017-0282-8. [DOI](#)
9. Furyk OO, Pak KA, Riabokon OV et al. Clinical-epidemiologic and serologic characteristics of Lyme disease in the Zaporizhzhia region (a retrospective analysis for 2015-2019 according to the Municipal Institution "Regional Infectious Hospital" of Zaporizhzhia Regional Council). *Zaporozhye Medical Journal*. 2022;24(4):464-469. doi:10.14739/2310-1210.2022.4.256223. [DOI](#)
10. Rogovskyy A, Batool M, Gillis DC et al. Diversity of *Borrelia* spirochetes and other zoonotic agents in ticks from Kyiv, Ukraine. *Ticks Tick Borne Dis*. 2018;9(2):404-409. doi:10.1016/j.ttbdis.2017.12.006. [DOI](#)
11. MacQueen D, Centellas F. Human Granulocytic Anaplasmosis. *Infect Dis Clin North Am*. 2022;36(3):639-654. doi:10.1016/j.idc.2022.02.008.
12. Cardenas-de la Garza JA, De la Cruz-Valadez E, Ocampo-Candiani J, et al. Clinical spectrum of Lyme disease. *Eur J Clin Microbiol Infect Dis*. 2019;38(2):201-208. doi:10.1007/s10096-018-3417-1. [DOI](#)
13. Zinchuk AN, Kalyuzhna LD, Pasichna IA. Is localized scleroderma caused by *Borrelia burgdorferi*? *Vector Borne Zoonotic Dis*. 2016;16(9):577-80. doi:10.1089/vbz.2016.2004. [DOI](#)
14. Martin Y, Zimmerli S. Lyme-Borreliose; Lyme Disease - Epidemiology and Pathophysiology. *Ther Umsch*. 2022;79(9):441-447. doi:10.1024/0040-5930/a001386. [DOI](#)
15. Dersch R, Fingerle V. Lyme Borreliose und Neuroborreliose – Was ist neu? [Lyme borreliosis and Lyme neuroborreliosis - an update]. *Dtsch Med Wochenschr*. 2021;146(11):728-732. doi:10.1055/a-1265-4397. [DOI](#)
16. Branda JA, Steere AC. Laboratory Diagnosis of Lyme Borreliosis. *Clin Microbiol Rev*. 2021;34(2):e00018-19. doi:10.1128/CMR.00018-19. [DOI](#)
17. Marchesi M, Zbinden A. Lyme Borreliose. *Lyme Disease - Laboratory Diagnostics*. *Ther Umsch*. 2022;79(9):448-453. doi:10.1024/0040-5930/a001387. [DOI](#)
18. van Gorkom T, Voet W, van Arkel GHJ, et al. Retrospective Evaluation of Various Serological Assays and Multiple Parameters for Optimal Diagnosis of Lyme Neuroborreliosis in a Routine Clinical Setting. *Microbiol Spectr*. 2022;10(3):e0006122. doi:10.1128/spectrum.00061-22. [DOI](#)
19. Shkilna M, Andreychyn M, Korda M et al. Serological Surveillance of Hospitalized Patients for Lyme Borreliosis in Ukraine. *Vector Borne Zoonotic Dis*. 2021;21(4):301-303. doi:10.1089/vbz.2020.2715. [DOI](#)
20. Septfons A, Goronflot T, Jaulhac B et al. Epidemiology of Lyme borreliosis through two surveillance systems: the national Sentinelles GP network and the national hospital discharge database, France, 2005 to 2016. *Euro Surveill*. 2019;24(11):1800134. doi:10.2807/1560-7917.ES.2019.24.11.1800134. [DOI](#)
21. Zbrzeźniak J, Paradowska-Stankiewicz I. Lyme disease in Poland in 2020. *Przegl Epidemiol*. 2022;76(3). doi:10.32394/pe.76.36. [DOI](#)
22. Briciu VT, Flonta M, Țățulescu DF et al. Clinical and serological one-year follow-up of patients after the bite of *Ixodes ricinus* ticks infected with *Borrelia burgdorferi sensu lato*. *Infect Dis (Lond)*. 2017;49(4):277-285. doi:10.1080/23744235.2016.1258488. [DOI](#)
23. Pryshliak OYa, Nikiforova TO, Tylishchak ZR et al. Retrospective analysis of Leptospirosis morbidity in Ivano-Frankivsk region (epidemiological and clinical characteristics). *Wiad Lek*. 2020;73(7):1397-1401. doi:10.36740/WLek202007117. [DOI](#)
24. Moskaliuk VD, Sirota BV, Balaniuk IV et al. Tick-borne encephalitis — features of the course (literature review). *Emergency Medicine (Ukraine)*. 2022;18(7):58-61. doi:10.22141/2224-0586.18.7.2022.1533. [DOI](#)
25. Tulloch JBT, Russel JBT, Halsby JBT et al. The demographics and geographic distribution of laboratory-confirmed Lyme disease cases in England and Wales (2013-2016): an ecological study. *BMJ Open*. 2019;9(7):e028064. doi:10.1136/bmjopen-2018-028064. [DOI](#)
26. Septfons A, Goronflot T, Jaulhac B et al. Epidemiology of Lyme borreliosis through two surveillance systems: the national Sentinelles GP network and the national hospital discharge database, France, 2005 to 2016. *Euro Surveill*. 2019;24(11):1800134. doi:10.2807/1560-7917.ES.2019.24.11.1800134. [DOI](#)

CONFLICT OF INTEREST

The Authors declare no conflict of interest

CORRESPONDING AUTHOR

Oleksandr Boichuk

Ivano-Frankivsk National Medical University
2 Halytska st, 76018 Ivano-Frankivsk, Ukraine
e-mail: opboy@ukr.net

ORCID AND CONTRIBUTIONSHIP

Oleksandra Pryshliak: 0000-0002-3256-5108 **A**

Oleksandr Boichuk: 0000-0003-0646-6533 **D**

Sergii Fedorov: 0000-0002-2202-4279 **F**

Victoriya Kvasniuk: 0000-0002-1334-2339 **D**

Nadiya Vaskul: 0000-0002-5368-7948 **C**

Andrii Protsyk: 0000-0003-2041-5337 **E**

Zoriana Tylishchak: 0000-0002-7891-2849 **B**

A – Work concept and design, **B** – Data collection and analysis, **C** – Responsibility for statistical analysis, **D** – Writing the article, **E** – Critical review, **F** – Final approval of the article

RECEIVED: 01.02.2024

ACCEPTED: 07.08.2024



Genetic polymorphism of the CYP11B2 gene in an Iraqi patient with essential hypertension

Israa Mohammed Mahdy, Hussein A Saheb, Ahmed M Sultan, Bassim I Mohammad, Asma A Swadi, Sinaa Abdul Amir Kadhim

DEPARTMENT OF PHARMACOLOGY AND THERAPEUTICS, COLLEGE OF MEDICINE, UNIVERSITY OF AL-QADISIYAH, AL-QADISIYAH, IRAQ

ABSTRACT

Aim: To demonstrate the genetic variant of CYP11B2 Gen rs1799998 and rs4539 and their effect on systolic and diastolic blood pressure in Iraqi patient with essential hypertension in Al-Diwaniya province.

Materials and Methods: This is an observational cross sectional descriptive single centre study for hypertensive patients at Al-Diwaniyah province, Iraq which is diagnosed according to 2020 ISH. All candidate patients were diagnosed and recruited by specialist caregiving physician/ cardiologist. There was a total of 90 participants, 37 males and 53 women. Aldosterone and renin levels in the plasma were determined from blood samples given voluntarily by patients undergoing genetic testing.

Results: Regarding rs4539 the most frequent allele was T (112, 62%) while the most frequent genotype was TC (54, 60%). Regarding rs1799998 the most frequent allele was G (97, 54%) while the most frequent genotype was AG (49, 54%).

Conclusions: There was no significant relationship between rs1799998 (A344>G) and rs4539 (T2718C) with systolic and diastolic blood pressure in Iraqi patient with essential hypertension.

KEY WORDS: CYP11B2 gen, polymorphism, essential hypertension, Iraq

Wiad Lek. 2024;77(9):1726-1732. doi: 10.36740/WLek/191330 DOI

INTRODUCTION

Hypertension is office/clinic blood pressure consistently over 140/90 mm Hg (systolic and/or diastolic) that needs long-term management [1]. In general, human blood pressure fluctuates naturally throughout the day and is problematic if it remains constant [2]. Hypertension can be categorized as follows: 1) essential hypertension (primary) occurs in approximately 95% of patients, in which the direct causes are unknown; 2) secondary hypertension 5% to 10% of the hypertensive population have identifiable causes, such as hormonal problems, large blood vessel narrowing problem, or kidney vessel narrowing [3]. In low and middle-income nations, hypertension is a leading cause of cardiovascular illness and death worldwide [4]. Obesity, insulin resistance, excessive alcohol consumption, excessive sodium consumption (in sodium-sensitive patients), advanced age, inactivity, stress, inadequate potassium and calcium intake, and irregular heartbeat are all contributors to hypertension [5]. In the endocrine mechanism of the RAAS (renin-angiotensin-aldosterone system), renin is responsible for the conversion of angiotensinogen to angiotensin I [6], and angiotensin I is converted to angiotensin II (Ang II) under the action of

angiotensin-converting enzyme. The most potent blood artery constriction agent is angiotensin II (Ang II), which is produced from angiotensin I by angiotensin converting enzyme. Arterial smooth muscle is affected, peripheral resistance is increased, and blood pressure is increased. In addition to increasing blood volume and blood pressure, angiotensin II also induces the adrenal glands to secrete aldosterone, which stimulates the epithelial cells of the kidneys to promote sodium and water reabsorption. The possibility that mutations in genes encoding enzymes involved in aldosterone synthesis led to elevated aldosterone levels and, eventually, essential hypertension [7]. The CYP11B2 gene encodes aldosterone synthase on chromosome 8q22. The gene contains 9 exons and spans approximately 7000 base pairs of DNA [8]. Aldosterone synthase is an enzyme belonging to the cytochrome P450 superfamily. The enzyme CYP11B2 lies within the mitochondrial inner membrane. The CYP11B2 enzyme, also known as three consecutive processes are catalyzed by aldosterone synthase. In the synthesis of aldosterone from 11-deoxycorticosterone [9], there are a number of CYP11B2 polymorphisms that have been linked to elevated CYP11B2 transcription, elevated aldosterone

production, and the development of a wide variety of cardiovascular problems [10]. The 344 C/T polymorphism in the 5' promoter region of the CYP11B2 gene is the first and most extensively researched polymorphism. Increased aldosterone synthesis and secretion in serum or urine, as well as an elevated aldosterone renin ratio, have both been linked to the CYP11B2 344C/T polymorphism. The glycine-to-arginine (K173R) missense mutation in exon 3 (rs 4539) is another intriguing polymorphism linked to elevated aldosterone production [10].

AIM

The aim of this research is to demonstrate the genetic variant of CYP11B2 Gen rs1799998 and rs4539 and their effect on systolic and diastolic blood pressure in Iraqi patient with essential hypertension in Al-Diwaniyah province.

MATERIALS AND METHODS

STUDY DESIGN

This is an observational cross sectional descriptive single centre study for hypertensive patients of Iraqi nationality, which is diagnosed according to ISH 2020. All candidate patients were diagnosed and recruited by the specialist caregiving physician/cardiologist. The research was carried out at the Al-Diwaniyah Teaching Hospital and the Department of Pharmacology and Therapeutics at Al-Qadisiyah University, College of Medicine, Iraq. It extended from July 2022 through July 2023. The lab work was completed in Department of Pharmacology and Therapeutics, College of Medicine, Al-Qadisiyah University, at Al-Diwaniyah province.

SUBJECTS

The study included 90 adults (36 male and 54 female) aged 20-70 years diagnosed with essential hypertension, taking valsartan for at least two weeks.

ETHICAL CONSIDERATIONS

The study was approved by the Ethics Committee of the College of Medicine, University of Al-Qadisiyah and procedures were explained to all patients and informed consent was taken from all patients.

PRIMERS USED IN THE CURRENT STUDY

Polymerase chain reaction (PCR) primers for CYP11B2 rs1799998 and CYP11B2 rs4539 gene had been given by Bioneer Company, Korea (Table 1).

CHEMICALS USED IN THE CURRENT STUDY

In this analysis, we used a variety of chemicals have been demonstrated with the corresponding country of origin and manufacturing company (Table 2).

COLLECTION AND PREPARATION OF SAMPLES

Blood sample: 1 ml blood samples were collected from the patients that were aspirated from antecubital vein. 1 ml blood was placed until the time of DNA extraction, kept in 1 ml an EDTA tube at -20 C.

GENOTYPING

Genomic DNA was extracted by using Genaid DNA extraction kit (USA).

PCR-TETRA ARM TECHNIQUE

The PCR-TETRA ARM technique was performed for genotyping and detecting CYP11B2 (rs1799998) and CYP11B2 (rs4539) gene polymorphism in blood samples of human. PCR reactions were performed by using Accupower kit (Bioneer, Korea).

PCR PreMix preparation: PCR per-mix for the gene was prepared by using AccuPower PCR PreMix Kit according to the instructions of the company.

PCR Thermocycler condition: The PCR thermocycler conditions were done for the CYP11B2 gene according to SimpliAmp (USA), as shown in table 3.

PCR product analysis: Agarose gel electrophoresis was used to examine the PCR results as per protocol (MarLiJu, Korea) as shown in fig. 1, fig. 2.

STATISTICAL PROCESSING

A mean and standard deviation (SD) were used to represent the data. Statistical analysis was performed using SPSS version 26. Analysis of variances (one-way ANOVA) was used to compare more than two means. The Fissure exact test and the Chi-square were used to see if there was a significant difference in demographic data between the two sets of categorical data. The allele frequencies of hypertensive patients and the aldosterone level, were compared using odds ratios (ORs) and 95% confidence intervals (CIs). It was found that $p \leq 0.05$ was the statistically significant in all statistical analyses in this study. The Hardy-Weinberg law state that the allele and genotype frequencies in a population will remain constant from generation to generation in the absence of evolutionary influences.

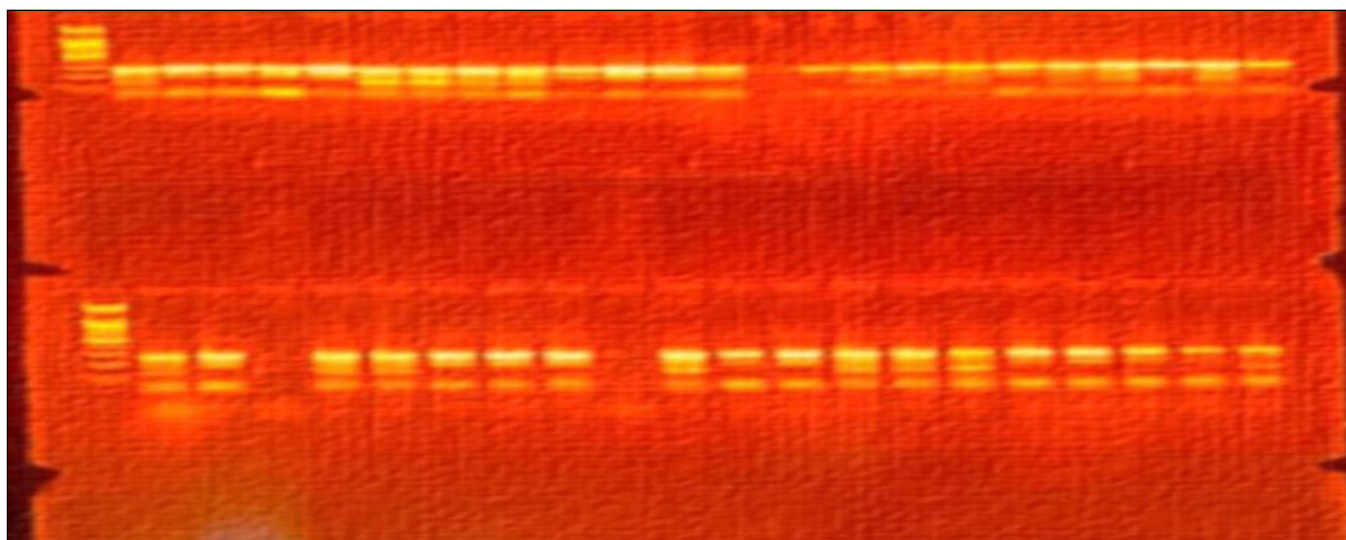


Fig. 1. The PCR product of CYP11B2 (rs1799998) gene.

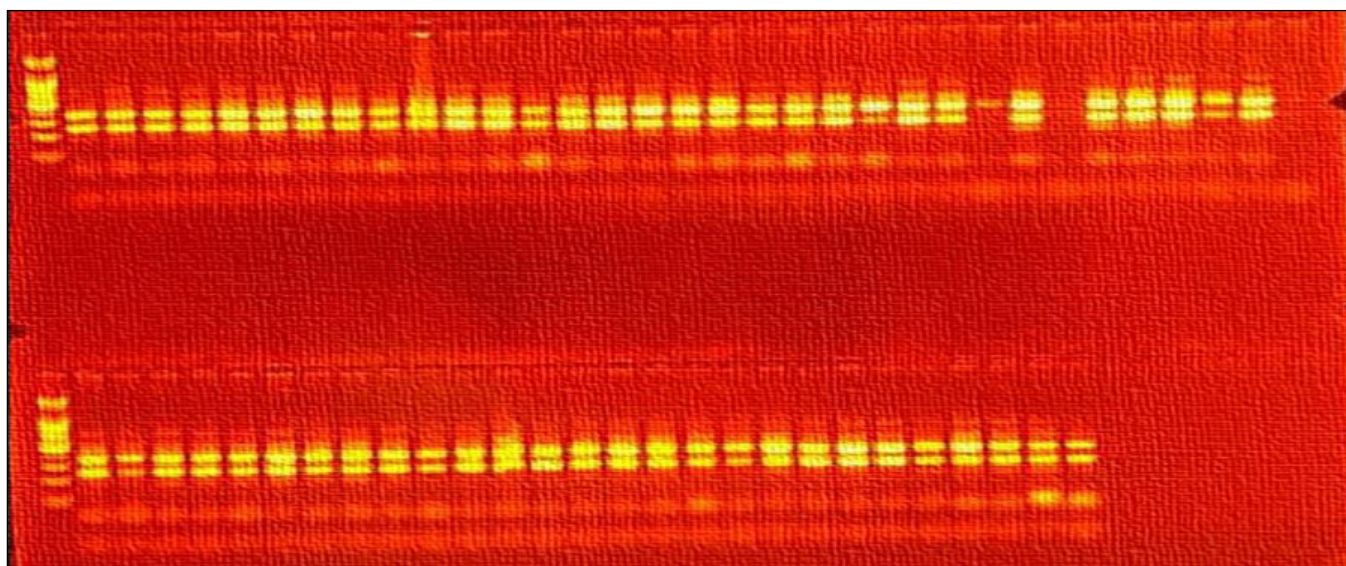


Fig. 2. The pcr product of CYP11B2 (rs 4539) gene.

RESULTS

FREQUENCY OF ALLELES AND GENOTYPES OF THE CYP11B2 GENE RS4539 AND RS1799998

The genotypes of all participants in this study and the allele frequencies of CYP11B2 are shown in table 4.

Regarding rs4539 the most frequent allele was T (112, 62%) while the most frequent genotype was TC (54, 60%). Regarding rs1799998 the most frequent allele was G (97, 54%) while the most frequent genotype was AG (49, 54%). There was no significant difference between the actual and expected frequency distribution ($P > 0.05$).

The effect of CYP11B2 rs1799998 (A344>G) and rs4539 (T2718C) polymorphism on systolic and diastolic blood pressure in Iraqi hypertensive patients taken valsartan 160 mg/day ($P > 0.05$) as shown in table 5 and table 6.

This study was investigated the polymorphism of CYP11B2 gen rs1799998 and rs4539 in Iraqi patient with essential hypertension in Al-Diwaniyah province. Regarding rs1799998 the most frequent allele was G (54%), GG (27%) while the most frequent genotype was AG (54%). The A allele have minor frequency 46% and AA genotype 19%. There was no significant difference between the actual and expected frequency distribution ($P > 0.05$). The mean \pm SE systolic blood pressure in homozygous AA, heterozygous AG and homozygous GG carrier patients was 152 ± 3.2 , 150 ± 2.2 , 144 ± 2.8 respectively. On other hand mean diastolic blood pressure in homozygous AA, heterozygous AG and homozygous GG carrier patients was 91 ± 1.7 , 89 ± 1 , 86 ± 1.1 respectively. There was no statistically significant effect of CYP11B2 rs1799998 on systolic and diastolic blood pressure.

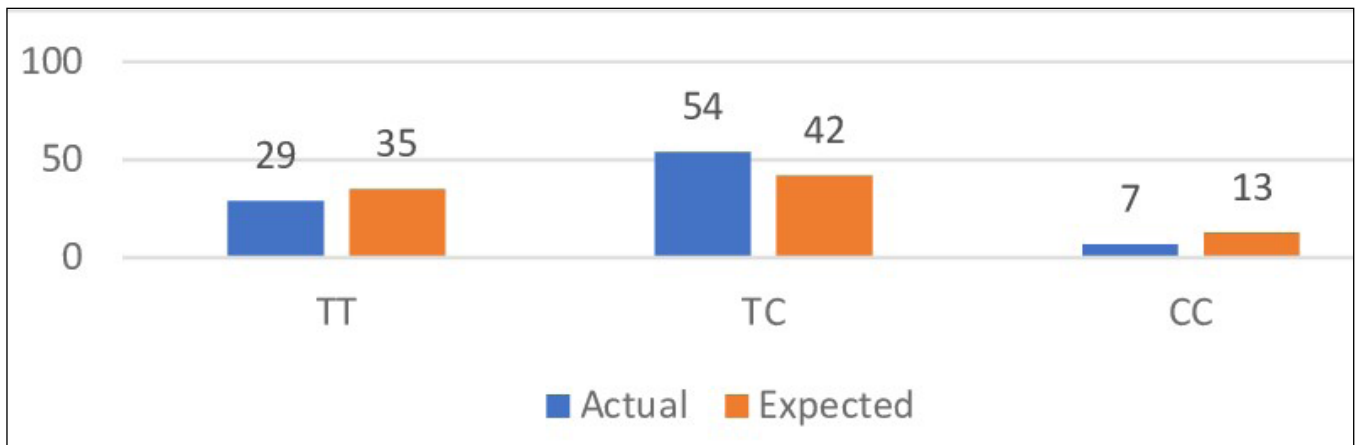


Fig 3. Genotyping frequency of CYP11B2 Gene rs4539 among Iraqi hypertensive patients taken valsartan 160 mg/day.

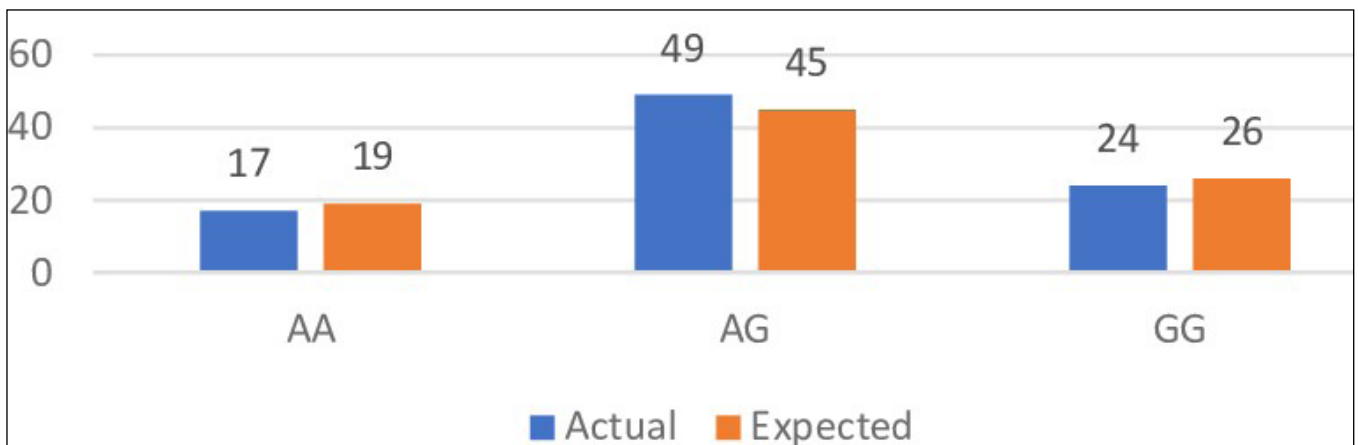


Fig. 4. Genotyping frequency of CYP11B2 Gene rs1799998 among Iraqi hypertensive patients taken valsartan 160 mg/day.

DISCUSSION

The finding of this study agrees with the study in Thailand population suggested that rs 1799998 is not associated with hypertension [11]. Also, based on the results of a meta-analysis, it appears that CYP11B2 polymorphism rs 1799998 in the RAAS have no significant effect on Bp salt sensitivity [12]. While the result of Iraqi study of Yarmouk teaching hospital in Baghdad who found that the 344G variant of CYP11B2 was not associated with hypertension in male subject they found that hypertension was associated with 344G allele CYP11B2 Gene only in female [13]. This study disagrees with many studies of Han chines where there was a positive association between Aldosterone synthase gene CYP11B2 and high blood pressure [14]. A number of studies analyzed associations between rs1799998 of CYP11B2 and hypertension with varying results [15]. Researchers found that CYP11B2 (rs179998) is significantly associated with longevity in Han Chinese participants. Japanese and European populations have also observed positive links between the rs1799998 polymorphism and HTN [16]. Another intriguing investigation found significant relationships between the CYP11B2 344G/A (rs179998) and essential HTN in South Indian Tamils (17). Niu et al. observed significant positive relationships

between CYP11B2 gene polymorphism and the onset of hypertension in a study of Japanese populations [18]. Regarding rs 4539 the most frequent allele was T (62%) while the most frequent genotype was TC (60%), TT (32%), while c allele frequency was 38% and CC genotype frequency 8% with no significant difference $P > 0.05$. The mean systolic BP and diastolic BP in homozygous TT carriers were 149 ± 2.8 mmHg, and 90 ± 1.2 mmHg respectively. In homozygous CC carriers, the mean systolic BP and diastolic BP were 144 ± 4.7 and mmHg, 88 ± 2.2 mmHg respectively while in heterozygous TC carriers the systolic BP was 152 ± 1.9 mmHg and Diastolic BP was 89 ± 0.9 mmHg. There was no statistically significant effect of CYP11B2 rs 4539 on systolic and diastolic blood pressure. This study agrees with study of Hiromichi Tanahashi et al., in Japan Gifu university that indicated no association between rs 4539 and hypertension and rs4539 associated higher CYB11B2 gene expression [19]. Also, this study agrees with Chen et al., in south west Han chines population that indicated no association between rs 4539 in CYP 11B2 Gene and Essential hypertension [20]. Also, it agrees with study of CYP11B2 gen polymorphism in Pakistan 2023 that indicate no association between rs 4539 and hypertension [21], while this study disagree with other studies that indicate, CYP11B2 (K173R) (rs 4539

Table 1. The sequencing and amplicon size of the PCR primers and annealing

Primer	Sequence	Amplicon	Annealing
CYP11B2 rs1799998	Inner forward CTTTATCTTATCGTGAGATGAGAGTGA 27	A-allele: 194 bp.	57.5 °C
	Inner reverse AAATAAAGTCTATTAAGAATCCAAGTCC 30		
	Outer forward CAGCCAAAGGTAGATGAAGGA 21	Two outer primers 370 bp.	
	Outer reverse TAACAACGTATCGAGATTCTCTCAC 24		
CYP11B2 rs4539	Inner forward CGTTCTGCAGCACCTTCTGCC 21	C-allele 164 bp.	64 °C
	Inner reverse AGGGACTTCTCCAGGCCCTTAA 23	T-allele 227 bp.	
	Outer forward GATGCACTGCTGAGACAAGGC 22	Two outer primers 347 bp.	
	Outer reverse CTCTGCCCTGGCCTCTGTAGGAAT 24		

Table 2. Chemicals with their company and country of origin

No.	Chemical	Company and Origin
1	Agarose	MarLiJu (Korea)
2	Ethidium bromide	Intron (Korea)
3	Ladder	Bioneer (Korea)
4	Primers	Macrogen (Korea)
5	TBE buffer	Intron (Korea)

Table 3. The PCR thermocycler conditions

PCR step	Temp.	Time	Repeat
Initial denaturation	95°C	5min.	1
Denaturation	95°C	1min.	35cycle
Annealing	64°C/57.5°C*	1min.	
Extension	72°C	1min.	1
Final extension	72°C	7min	

* Annealing temp 64°C for rs4539 and Annealing temp 57.5°C for rs1799998.

Table 4. Genotype frequency of CYP11B2 gen polymorphism among Iraqi hypertensive patients who took valsartan 160 mg/day

CYP11B2	Genotype	Actual		Expected by Hardy-Weinberg law		P value
		Number	Frequency	Number	Frequency	
rs1799998	AA	17	0.19	19	0.21	0.8 (NS)
	AG	49	0.54	45	0.50	
	GG	24	0.27	26	0.29	
	Total	90	1.000	90	1.00	
	Allele					
	A	83	0.46	NA	NA	-
	G	97	0.54	NA	NA	-
rs4539	Total	180	1.00			0.14 (NS)
	TT	29	0.32	35	0.39	
	TC	54	0.60	42	0.47	
	CC	7	0.08	13	0.14	
	Total	90	1.00	90	1.00	
	Allele					
	T	112	0.62	NA	NA	
C	68	0.38	NA	NA		
Total	180	1.00				

in the exon3) hypertension was discovered to be linked to polymorphisms [22]. Other study in Indian patient indicates strong synergistic effect has existed among different geno-

types of CYP11B2 G344A, IC, and T173C (rs4539) polymorphisms with the haplotype (344A-Conv-T173) associated with a higher risk for essential hypertension progression

Table 5. The effect of CYP11B2 rs1799998 (A344>G) polymorphism on systolic and diastolic blood pressure in Iraqi hypertensive patients taken valsartan 160 mg/day

Genotype rs1799998	Systolic BP means	SE	P value	Diastolic BP mean	SE	P value
AA	152	3.2	0.12 (NS)	91	1.7	0.07
AG	150	2.2		89	1	
GG	144	2.8		86	1.1	

Table 6. The effect of CYP11B2 rs4539 (T2718C) polymorphism on systolic and diastolic blood pressure in Iraqi hypertensive patients taken valsartan 160 mg/day

Genotype rs4539	Systolic BP means	SE	P value	Diastolic BP mean	SE	P value
TT	149	2.8	0.14 (NS)	90	1.2	0.781
TC	152	1.9		89	0.9	
CC	144	4.7		88	2.2	

[23]. In meta-analysis study in China 2013, there was still not enough evidence to indicate the association between rs4539T2718C with primary aldosteronism risk [24]. These variations are a reflection of the impact of demographic variables such as age and gender on populations that are geographically dispersed. Since the mechanism of the rs1799998, rs4539 variation in hypertension is unknown, large-scale studies are required to further understand the relationship between CYP11B2 polymorphism and the prevalence of hypertension.

CONCLUSIONS

Regarding rs4539 the most frequent allele was T (112, 62%) while the most frequent genotype was TC (54, 60%). Regarding rs1799998 the most frequent allele was G (97, 54%) while the most frequent genotype was AG (49, 54%). There was no significant difference between the actual and expected frequency distribution ($P > 0.05$). There was no significant relationship between rs1799998 (A344>G) and rs4539 (T2718C) with systolic and diastolic blood pressure in Iraqi patient with essential hypertension.

REFERENCES

- Unger T, Borghi C, Charchar F et al. 2020 International Society of Hypertension Global Hypertension Practice Guidelines. *Hypertension*. 2020;75(6):1334-1357. doi:10.1161/HYPERTENSIONAHA.120.15026. [DOI](#)
- Anwar A, Siddiqui A, Hafsa K et al. Prevalence of clinical signs and symptoms of hypertension: a gender and age based comparison. *Palliat Med Care Open Access*. 2018;5(2):1-8. doi:10.15226/2374-8362/5/2/00155. [DOI](#)
- Sukmaningtyas W, Utami T. Risk Factors of Hypertension in the Elderly. 1st International Conference on Community Health (ICCH 2019). *Advances in Health Sciences Research*. 2020;20(Icch 2019):215-221. doi:10.2991/ahsr.k.200204.048. [DOI](#)
- Al-Makki A, DiPette D, Whelton PK et al. Hypertension Pharmacological Treatment in Adults: A World Health Organization Guideline Executive Summary. *Hypertension*. 2022;79(1):293-301. doi:10.1161/HYPERTENSIONAHA.121.18192. [DOI](#)
- Saxena T, Ali AO, Saxena M. Pathophysiology of essential hypertension: an update. *Expert Rev Cardiovasc Ther*. 2018;16(12):879-887. doi:10.1080/14779072.2018.1540301. [DOI](#)
- Wu CH, Mohammadmoradi S, Chen JZ et al. Renin-Angiotensin System and Cardiovascular Functions. *Arterioscler Thromb Vasc Biol*. 2018;38(7):108-116. doi:10.1161/ATVBAHA.118.311282. [DOI](#)
- Moraitis AG, Rainey WE, Auchus RJ. Gene mutations that promote adrenal aldosterone production, sodium retention, and hypertension. *Appl Clin Genet*. 2013;7:1-13. doi:10.2147/TACG.S35571. [DOI](#)
- Mornet E, Dupont J, Vitek A et al. Characterization of two genes encoding human steroid 11 β -hydroxylase (P-450(11 β)). *J Biol Chem*. 1989;264(35):20961-20967. doi:10.1016/s0021-9258(19)30030-4. [DOI](#)
- Payne AH, Hales DB. Overview of steroidogenic enzymes in the pathway from cholesterol to active steroid hormones. *Endocr Rev*. 2004;25(6): 947-970. doi:10.1210/er.2003-0030. [DOI](#)
- Tarek AGM. Aldosterone synthase gene (CYP11B2) polymorphisms and enhanced cardiovascular risk. The recent topics in genetic polymorphisms. *Intech Open*. 2020. doi:10.5772/intechopen.89133. [DOI](#)
- Ji X, Qi H, Li DB et al. Associations between human aldosterone synthase CYP11B2 (-344T/C) gene polymorphism and antihypertensive response to valsartan in Chinese patients with essential hypertension. *Int J Clin Exp Med*. 2015;8(1):1173-1177.
- Charoen P, Eu-Ahsunthornwattana J, Thongmung N et al. Contribution of four polymorphisms in renin-angiotensin-aldosterone-related genes to hypertension in a Thai population. *Int J Hypertens*. 2019;2019:4861081. doi:10.1155/2019/4861081. [DOI](#)
- Sun J, Zhao M, Miao S et al. Polymorphisms of three genes (ACE, AGT and CYP11B2) in the renin-angiotensin-aldosterone system are not associated with blood pressure salt sensitivity: A systematic meta-analysis. *Blood Press*. 2016;25(2):117-122. doi:10.3109/08037051.2015.1110923. [DOI](#)

14. Kato N, Sugiyama T, Morita H et al. Comprehensive analysis of the renin-angiotensin gene polymorphisms with relation to hypertension in the Japanese. *J Hypertens.* 2000;18(8):1025-1032. doi:10.1097/00004872-200018080-00006. [DOI](#)
15. Gu D, Ge D, He J et al. Haplotypic analyses of the aldosterone synthase gene CYP11B2 associated with stage-2 hypertension in northern Han Chinese. *Clin Genet.* 2004;66(5):409-416. doi:10.1111/J.1399-0004.2004.00317.X. [DOI](#)
16. Chandra S, Saluja D, Narang R et al. Atrial natriuretic peptide and aldosterone synthase gene in essential hypertension: a case-control study. *Gene.* 2015;567(1):92–97. doi:10.1016/J.GENE.2015.04.062. [DOI](#)
17. Stowasser M. Update in primary aldosteronism. *J Clin Endocrinol Metab.* 2015;100(1):1–10. doi:10.1210/JC.2014-3663. [DOI](#)
18. Takeuchi F, Yamamoto K, Katsuya T et al. Reevaluation of the association of seven candidate genes with blood pressure and hypertension: a replication study and meta-analysis with a larger sample size. *Hypertens Res.* 2012;35(8):825-831. doi:10.1038/hr.2012.43. [DOI](#)
19. Ameer QA, Aziz IH, Salo WH. Genetic Polymorphism of (Cyp11b2) Gene in High Blood Pressure Iraqi Patients. *World Journal of Pharmacy and Pharmaceutical Sciences.* 2015;4(10).
20. Tanahashi H, Mune T, Takahashi Y et al. Association of Lys173Arg polymorphism with CYP11B2 expression in normal adrenal glands and aldosterone-producing adenomas. *J Clin Endocrinol Metab.* 2005;90(11):6226–6231. doi:10.1210/JC.2005-0299. [DOI](#)
21. Chen B, Nie S, Luo S et al. Association of the human CYP11B2 gene and essential hypertension in southwest Han Chinese population: a haplotype-based case-control study. *Clin Exp Hypertens.* 2011;33(2):106–112. doi:10.3109/10641963.2010.531835. [DOI](#)
22. Shah WA, Jan A, Khan MA et al. Association between Aldosterone synthase (CYP11B2) gene polymorphism and hypertension in pashtun ethnic population of Khyber Pakhtunkwha, Pakistan. *Genes.* 2023;14(6):1184. doi:10.3390/GENES14061184. [DOI](#)
23. Keavney B, Mayosi B, Gaukrodger N et al. Genetic variation at the locus encompassing 11-beta hydroxylase and aldosterone synthase accounts for heritability in cortisol precursor (11-deoxycortisol) urinary metabolite excretion. *J Clin Endocrinol Metab.* 2005;90(2):1072–1077. doi:10.1210/JC.2004-0870. [DOI](#)
24. Zhang GX, Wang BJ, Ouyang JZ et al. Polymorphisms in CYP11B2 and CYP11B1 genes associated with primary hyperaldosteronism. *Hypertens Res.* 2010;33(5):478-484. doi:10.1038/HR.2010.21. [DOI](#)

CONFLICT OF INTEREST

The Authors declare no conflict of interest

CORRESPONDING AUTHOR

Israa Mohammed Mahdy

University of Al-Qadisiyah

University District, Al Diwanayah, Al-Qadisiyah Governorate, Iraq

e-mail: sgahmed1331962@outlook.com

ORCID AND CONTRIBUTIONSHIP

Israa Mohammed Mahdy: 0009-0000-9813-4127 [A](#) [B](#)

Hussein A Saheb: 0000-0002-0137-8932 [B](#) [C](#)

Ahmed M Sultan: 0000-0001-6819-0208 [C](#) [D](#)

Bassim I Mohammad: 0000-0001-6732-5940 [C](#) [E](#)

Asma A Swadi: 0000-0002-7679-1596 [D](#) [E](#)

Sinaa Abdul Amir Kadhim: 0000-0001-9375-5581 [E](#) [F](#)

[A](#) – Work concept and design, [B](#) – Data collection and analysis, [C](#) – Responsibility for statistical analysis, [D](#) – Writing the article, [E](#) – Critical review, [F](#) – Final approval of the article

RECEIVED: 07.08.2023

ACCEPTED: 17.07.2024



Molecular investigate of slim and adhesion genes of *Staphylococcus saprophyticus* isolated from pregnant women with asymptomatic bacteriuria in Thi-Qar governorates

Sanaa Ghali Jabur

DEPARTMENT OF PATHOLOGICAL ANALYSIS, SCIENCE COLLAGE, THI-QAR UNIVERSITY, THI-QAR, IRAQ

ABSTRACT

Aims: to investigate and compared the frequency of biofilm formation *ica A* and adhesion genes *clf A*, *cnaA*, *fmbA* and *fmbB* in chromosome and plasmid of *S. saprophyticus*.

Materials and methods: 48 isolates about *S. saprophyticus* were selective randomly from total 1019 isolated from pregnant women with asymptomatic bacteriuria where the samples were collected in AL Habboby Hospital and Al-Hussein teaching, and bent Al-Huda hospitals from the first of April 2022 until the first of September 2023 and bacteria of study were identified depend on previous method.

Results: PCR appeared, higher existence percentage of study virulence factors genes was in chromosome that reached 399.9% of study bacteria, more than in its in plasmid 66.5%, however the frequency rate of study genes in chromosome was as following: *ica A* and *fmb A* genes were complete, 100% (48/48), while *cna A* and *clf A* genes percentage were identical and came in second grade that arrived significant rate 83.3% (40/48), the lowest results were showed 33.3% (16/48) isolates harbored *fmb B* gene, while they were decreased in its plasmid as following: *ica A* and *fmb A* genes were 12.5% (6/48) and 22.9% (11/48) respectively, the *cna A* and *clf A* genes percentage 6.2 % (3/48) and 4.1% (2/48) respectively, *fmb B* gene 20.8% (10/48).

Conclusions: Depend on above data may be *ica A*, *fmb A*, *clf A*, *cna A* genes more occurrence in comparison to *fmb B* genes among *S. saprophyticus* and plasmid may double the rate of same virulence study genes.

KEY WORDS: molecular, slim and adhesion genes, chromosome, plasmid, *S. Saprophyticus*, asymptomatic bacteriuria

Wiad Lek. 2024;77(9):1733-1739. doi: 10.36740/WLek/192862 DOI

INTRODUCTION

Staphylococcus genus is present in different clinical site as normal flor causes opportunistic infections in human. *S. saprophyticus* causes urinary tract infections, especially in girls. It is present in over 40% of all young sexually active women as part of their normal genito-urinary flor [1-4]. It represents serious to public health by its capability to give rise to infections in human and fixed in the ambience, obtain and freight plasmids, which can accentual antibiotic resistance and virulence [5, 6]. The capacity of different *Staphylococcus* species and strains to causes disease related to release a large number of virulence factors that are product of virulence gene in chromosomes. Some of these factors are importance in distinct sickness or at various phases of a pathogenesis of limited infections which may lead to morbidity and mortality [7]. Generally, many pathogenic bacteria carry genes for virulence in plasmids or other mobile genetic elements [8]. The bacteria can infected humans by virulence factors carried on virulence plasmids through a different mechanisms,

which are either toxins that caused damage and kill cells of animal, or others which introduce help to bacteria for connect and invasive cells when others act to protect bacteria from the action of immunity system [9]. Most plasmids can be transferred between different bacteria by conjugation [8]. *S. saprophyticus* can develop and carry plasmids contain antibiotic resistance and virulence genes [5, 6, 10]. Recently, attentions focused on the adhesions in staphylococcal infections. When declared, protein receptors in the cells suppose the remarkable functions in adhesion of microbe [7]. The presence of adhesions genes such as *cna*, *clf A* and biofilm formation (*ica loci*) genes in clinical *Staphylococcus* were considered important factors of virulence [11]. The *ica loci* of biofilm formation is involved polysaccharide intercellular adhesion, that called PIA and also biofilm formation that is most interest one of virulence identifiers that making easy of cohesion and settlement of bacteria [12]. Synthesis of PIA is neatly back to the manifestation of *ica A* and *ica D* genes. The substantial function of *ica A*, synthesis

of N-acetyl-Dglucosamine polymer structure [13]. All tested strains of *Staphylococcus* such as *S. saprophyticus* that can biofilms formed in vitro were contain specific locus called *ica*. Sequence analysis was found the omit of the locus of *ica* caused to loss of the capacity to biofilms formed, PIA production, or mediate activity of N-acetylglucosaminyl transferase during in vitro. The experiments of hybridization with cross-species clarified the the *ica* A found in some other species of *Staphylococcus*, proposed, cell-cell adhesion and the ability to biofilms formed is saved in the genus *Staphylococcus* [14]. The ingredients of microbe surface distinguishing, the molecules of adhesion matrix that called MSCRAMMs, are mediate adherence to the extracellular matrix ingredients of host, such as collagen, fibrinogen and fibronectin [15]. Important type of these genes is collagen adhesion gene (*cna*) encoding CNA is determinant of the ability to bind collagen. It is not present in all *Staphylococcus* types and strains. The compare between the strains of *cna*-positive *S. aureus* and its *cna*-negative strains appeared that CNA product is in *S. aureus* infection [16]. Clumping factor (Clf) is cell surface associated protein and main mediator factor of the adherence of *S. aureus* to fibrinogen and fibrin. The binding of *staphylococcal* to fibrinogen has been appeared to be important in the infection with endocarditis by invasiveness and perhaps in the attachment of bacteria to implanted biomaterials. Clf acts as a virulence agent in specific infections by repression phagocytosis. The connection of *S. aureus* with fibronectin is interposed by two neatly concerning proteins FnBPA and FnBPB, that encoded with *fnb* A and *fnb* B genes respectively. FnBPs interposed adhesion with epithelial cells of human, involving endothelial cells, airway epithelium, and fibroblasts, that are may subsequently act in these cells to the bacteria internalization [17]. Not all virulence factors that play an interest role in pathogenesis of *Staphylococcus* spp., permitting its transition from any virulence stage to other infections are produced by each type and strain, there are evidence that *Staphylococcus* strains express different virulence patterns according to isolation sources. Definition virulence factors about bacterial pathogenicity in each infection are important for treatment decision [18].

AIM

The aim of the study was to investigate the occurrence rate of virulence factors genes about slims (*ica* A) and adhesions (*cna* A, Clf A, *fnb* A and *fnb* B) genes in plasmid and chromosomes among same bacteria isolated from asymptomatic bacteriuria by molecular scanning with PCR.

MATERIALS AND METHODS

CLINICAL ISOLATES SOURCE

Forty-eight isolates about *S. saprophyticus* were selective randomly from total 1019 isolated from pregnant women with asymptomatic bacteriuria where the samples were collected in AL Habboby Hospital and Al-Hussein teaching, and bent Al-Huda hospitals from the first of April 2022 until the first of September 2023 and bacteria of study were identified depend on method of [19-21].

DETERMINE THE PRODUCTION OF SLIME

The production of a slime in *S. saprophyticus* isolates of the study was phenotypically estimated by cultured bacterial isolates on Congo red agar method as described by Ilham B [12]. Congo red agar contained: 37 gm/L brain heart infusion broth, 0.8 gm/L Congo red, 50 gm/L sucrose agar. The incubation of plates was at 37°C for 24 hrs. and incubation of whole plates accrue according on altered the color after period of incubation about 24 to 48 h. A position test result was regarded reliantly black discoloration of the colony. The colonies color of study bacteria did not altered Congo red agar, when the slim did not producing by bacteria grown in plate of culture.

MOLECULAR ANALYSIS

CYCLING PROFILES.

The assays of PCR were occurred in a 25 µl of reaction volume, and conditions of PCR amplification were in thermal cycler (Memmert, Germany) that were particular to each single primer set singly, rely on procedure of their reference which were initial denaturation temperature (94°C/30 s), elongation temperature (72°C/60 s) and extension (72°C/1min) for each gene where denaturation and annealing temperature as following:

1. *fnb*A: 94°C/30 s and 50°C/30 s respectively;
2. *fnb*B: 94°C/30 s and 50°C/30 s respectively;
3. *Ica* A: 95°C/30 s, 60°C/1 min respectively;
4. *Cna*: 90°C/30 s, and 55°C/1 min respectively;
5. Clf A: 90°C/30 s, and 57°C/1 min respectively.

EXTRACTION OF GENOMIC DNA.

The chromosomal DNA Mini Kit and plasmid DNA Mini Kit were used to extracted and purified of chromosomal and plasmid DNA from *S. saprophyticus* that was occurred rely on manufacture company instructions which was Favorgen-China. The refrigerator was

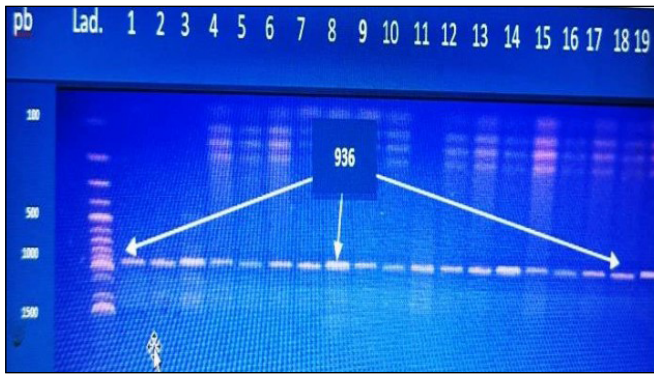


Fig. 1. Gel electrophoresis product of PCR amplification of *ica A* gene, DNA molecular size marker 1500bp ladder, TBE buffer was (1x), agarose 0.01 and 100 V for 30 min then 50 V for 45 min, red stain was used. Lanes 1-15 in chromosome and lanes 16-19 in plasmid show positive results of *S. saprophyticus*.



Fig. 4. Gel electrophoresis product of PCR amplification of *fnb A* gene, DNA molecular size marker 1500bp ladder, TBE buffer was (1x), agarose 0.01 and 100 V for 30 min then 50 V for 45 min, red stain was used. Lanes 1-9 in chromosome and lanes 10-19 in plasmid show positive results of *S. saprophyticus*.

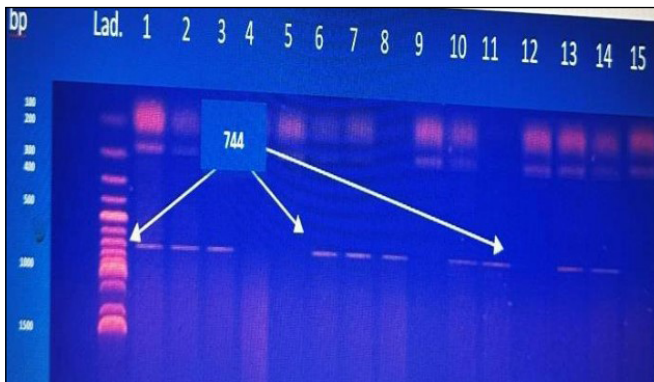


Fig. 2. Gel electrophoresis product of PCR amplification of *cna A* gene, DNA molecular size marker 1500bp ladder, TBE buffer was (1x), agarose 0.01 and 100 V for 30 min then 50 V for 45 min, red stain was used. Lanes 1,2,3,6,7,8,10 in chromosome and lanes 11,13,14 in plasmid show positive results of *S. saprophyticus*.



Fig. 5. Gel electrophoresis product of PCR amplification of *fnb B* gene, DNA molecular size marker 1500bp ladder, TBE buffer was (1x), agarose 0.01 and 100V for 30 min then 50V for 45 min, red stain was used. Lanes 3-9 in chromosome and lanes 15,16,17 in plasmid show positive results of *S. saprophyticus*.

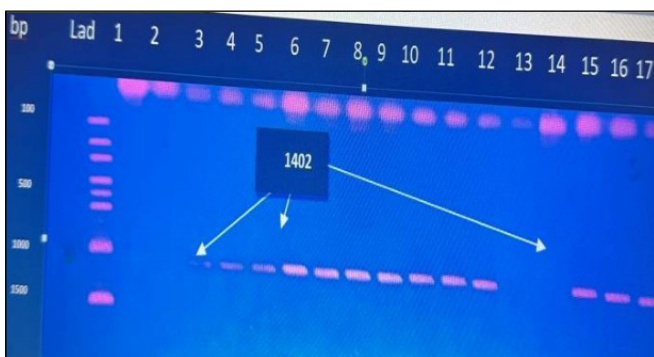


Fig. 3. Gel electrophoresis product of PCR amplification of *clf A* gene, DNA molecular size marker 1500bp ladder, TBE buffer was (1x), agarose 0.01 and 100 V for 30 min then 50 V for 45 min, red stain was used. Lanes 3-12,15 in chromosome and lanes 16-17 in plasmid show positive results of *S. saprophyticus*.

used to keep the elute production of DNA that was saved in for later until examined with PCR and gel electrophoreses.

PCR MATERIALS

Master mix used in this work was Go Tag DNA polymerase from Company Bioneer (Korea), was provided in reaction buffer that contain 2x Green Taq with pH 8.5, 400 μ m of dATP, 400 μ m of dGTP, 400 μ m of dCTP, 400 μ m of dTTP, and 3 mM of $MgCl_2$. The DNA marker of 100 bp, ladder from BioNeeer (Korea) that compose 100-1500 base pairs.

PRIMER

According to manufacturer instructions, the BioNeeer primers were prepared. The description of the primers presented in table 1.

ASSAY OF POLYMERASE CHAIN REACTION (ANALYSIS THE PRODUCT OF PCR)

AGAROSE GEL ELECTROPHORESIS

The amplified PCR products were analyzed with agarose gel electrophoresis (Lab net, U.S.A.) where

Table 1. The primers employed in the amplification of the study virulence genes with PCR assay

Gene	Orientation of primer	Primer Sequence (5'3')	Product of amplification/bp	Reference
Fnb A	F	5-TTT CCA ATA ACC ACC CGT TT-3	1279	Nashev et al., 2004
	R	3-GCG GAG ATC AAA GAC AA-5		
Fnb B	F	5-GGA GAA GGA ATT AAG GCG-3	812	Nashev et al.,2004 and Mohammadi et al.,2020
	R	3-GCC GTC GCC TTG AGC GT-5		
ica A (intracellular adhesion)	F	5TCAGACACTTGCTGGCGCAGTC -3	9936	Contreras et al., 2012
	R	3TCACGATTCTCTCCCTCTCTGCCATT -5		
cna (collagen adhesion)	F	5AGTGGTTACTAATACTG -3	7744	Kumar et al., 2009
	R	3CAGGATAGATTGGTTTA -5		
clf (clumping factor)	F	5GGCTTCAGTGCTTGTAGG-3	1402	Contreras et al., 2012
	R	3- TTTTCAGGGTCAATA TAAGC-5		

Table 2. Phenotypic Slime production in *S. saprophyticus* isolated from pregnant women with asymptomatic bacteriuria

Isolate	isolates number	Positive phenotypic slime production isolates number	Percentage (%)
S.saprophyticus	48	48	100

loaded and visualized depend on method of Ghali JS [22].

STATISTICAL ANALYSIS

The study data were statistically analyzed using SPSS version 22 software, using the chi-square test, which was applied for two or more groups compared at a significance level of 0.05.

RESULTS

PHENOTYPIC SLIME PRODUCTION

Forty eight isolates of *S. saprophyticus* appeared phenotypic black color on Congo red agar (Table 2).

MOLECULAR ANALYSIS

Molecular analysis of ica A gene showed occurrence rate 100% (48/48) in the chromosome of *S. saprophyticus*, where its frequency in plasmid was 12.5% (6/48) and the total appearance was 112.5%, (Table 3, Fig. 1), while PCR study of cna A gene showed that the chromosomal rate was 83.3% (40/48) of isolates, but decreased in plasmid

to 6.2 % (3/48), when total presence increased to 89.5%, (Table 3, Fig. 2.). The significant presence rate of Clf A gene in the whole isolates of the study was indicated as 83.33% (40/48) in chromosome and 4.16% (2/48) in plasmid, which cause the severity expression to 87.5% (42/48), (Table 3, Fig.3.), while fnb A gene in chromosome was 100% positive with a decrease in plasmid to 22.9% (11/48) and an elevated in the overall to 122.9% (59/48) (Table 3, Fig. 4.). Research data offered that only 33.33% (16/48) of the isolates had the fnb B gene in the chromosome, while 20.83% (10/48) of isolates harbored the same gene in the plasmid, which led to an increase in total gene presence, that reached 54.1% (26/48), (Table 3, Fig. 5.).

DISCUSSION

PHENOTYPIC SLIME PRODUCTION

The totally forty eight of *S. saprophyticus* isolates in research appeared phenotypic black color on Congo red agar therefore may be all isolates in study can slime production because study of Ilham B. [12] showed the black color isolates on Congo red agar were slime production isolates and Opeyemi LU et al. [23] explained the slime production was kept in the *Staphylococcus* genus.

Table 3. Frequency of some virulence slim and adhesions genes in the chromosome and plasmid of *S. saprophyticus* diagnosed with PCR assay.

Genetic site	Frequency of gene (%)					Total
	<i>ica A</i>	<i>can A</i>	<i>clf A</i>	<i>fnb A</i>	<i>fnb B</i>	
Chromosome	100%(48/48)	83.3%(40/48)	83.33% (40/48)	100%(48/48)	33.3%(16/48)	399.9
Plasmid	12.5% (6/48)	6.2 % (3/48)	4.16 % (2/48)	22.9%(11/48)	20.8%(10/48)	66.5
Total	112.5	89.5	87.5	122.9	54.1	466.4
Value=0.05	CalX ² =105.10	CabX ² = 13.95			Df = 6	

MOLECULAR ANALYSIS

The *ica A* gene showed complete occurrence rate in chromosome of *S. saprophyticus* where its rate on plasmid was lowered and total appearance was doubled to 113%. The complete prevalence of *ica A* genes in chromosome of *S. saprophyticus* isolates during the study may be because the *ica A* genes was saved in the genus *Staphylococcus* spp. as mentioned by Opeyemi LU et al. [23], who suggested that cell-to-cell adhesion and the potential to form biofilms is conserved within this genus by using cross-species hybridization technique with *Staphylococcus* species that revealed the presence of *ica A* in some other *Staphylococcus* species, lead to conclusion that cell-to-cell adhesion and the possibility to compose biofilms was maintain in same genus. The frequency of presence of the same gene in plasmid may be because acquisition of these genes by the plasmid through re-joining with the chromosome of the same bacterium or the acquisition of the plasmid carrying this gene through conjugation with other bacteria such as *S. aureus* in the same environment which may lead to double the percentage of gene in study *S. saprophyticus* isolates [8, 22] which means there were in evaluation of bacteria may be related to the role of plasmid [6, 8]. Based on the above data, the isolates in the study may be clinically responsible for slime production, this was strongly supported by phenotypically identified in above step of Phenotypic Slime production, and may be indicates all isolates of *S. saprophyticus* can colonization to causes infection in those and another location of body when can transfer to these location. Santos SV et al. [6] showed phenotype, genotype and proteome varies in *S. saprophyticus* results reflected in the capability of bacteria to survive through interaction with cells of host, because the 9325 isolates appeared highest survival average after interaction of macrophage where, about 7108 strains were possessed minimal components about proteins that related to higher ability of virulence to biofilm form suggesting, this strains can be better adjusted to preserved within the host and in nature. The possibility of protein of slime in strains of *S. saprophyticus*, can be invert in virulence and preservation, and may be more resistance to the antimicrobial action of antibi-

otics. *Staphylococci* are indicated as the most common causative agents of biofilm formation, which is associated with colonization of initiated infections, as well as mucus products that cause staphylococci to evade the host immune defense [12]. The total percentage of *ica A* gene exceeding the total percentage may be related to the role of plasmid in evaluation of bacteria [5, 24]. The results of study about *ica A* were identical to that in clinical source of several researches, the positively *ica A* were identified in whole *S. aureus* and *S. epidermidis* with 100% isolated from hemodialysis patients [12], while it differ with another research [25] shows, the slime genes average of *ica A* was about 69.6% (48/69) and 63.6% (56/88) within the isolates of *S. epidermidis* and *S. aureus* respectively. The data of study find that approximately 90% of isolates can bind to collagen of host cell and lead to infection, since CNA (product of *cna* gene) is the determinant bind ability to collagen. As mentioned by Allison GF et al. [26], when a comparison was made between strains that were positive and negative for *cna* in *S. aureus*, it significantly revealed the primary collagen binding ability by CNA. The height occurrence of this gene in *S. saprophyticus* may be resulted from the expected presence of *S. aureus* with *S. saprophyticus*, which were known to have virulence plasmid carriers of virulence genes when isolates from clinical samples in Thi-Qar- governorates that can transferred to other different bacteria by conjugation when present in same environment [22, 27]. The high occurrence of *cna A* gene in study isolates resembled to that in several clinical studies, as the *cna A* gene present 100% in all six *S. aureus* strains of hemodialysis patients [12]. Based on previous results, it is possible that a total of 87.5% of isolates can escape from host phagocytosis during infection` course, causing severity of disease, because phagocytosis of host can inhibited by *clf A* gene product during bacterial infection [14]. he significantly elevated rate of staphylococcal ClfA in clinical specimens is similar to other studies, which shows significantly higher ClfA in healthy persistent carriers than in healthy non-carriers [2], the *clf A* positive rate was confirmed in 45/88 (51.1%) of *S. aureus* isolates from hemodialysis patients [25], and in Al-Najaf city

of Iraq, the *clfA* gene was positive in all isolates of the *S. aureus* [28]. The rate of occurrence of each studied gene in the plasmid of the studied *S. saprophyticus* may be because each gene can be transferred by recombination or jumping from chromosome of same bacteria or by conjugation or transformation from chromosome or plasmid of *S. aureus*, which may be present with *S. saprophyticus* at the same clinical site of isolation, or other mobile genetic elements [8, 22]. The differences in the frequencies of *icaA*, *clfA*, *cnaA*, *fnbA* and *fnbB* in this study and other studies may be related to difference in source of isolation, this suggests that staphylococcal types and strains express different virulence patterns according to isolation sources or may be back to the environmental differences between the regions of studies or may be revert to varies between species and strains in different studies [18]. The isolates harboring the genes of investigation may represent dangerous clinical isolates and participate in increasing the distribution of slim and adhesions virulence factors by transformed genes to other different isolates of pathogenic bacteria in society, that may causes se-

verity invasive infection in carriers of pregnant women and further different infections in introduced human. The study indicated that *S. saprophyticus* isolates were more developed in relation to the study of slim and adhesions virulence factors genes.

CONCLUSIONS

Based on the above data, there is a wider distribution of *icaA*, *fnbA*, *clfA*, *cnaA* in comparison to *fnbB* genes among *S. saprophyticus* isolates of asymptomatic bacteriuria of pregnant women, therefore our study found the *S. saprophyticus* isolates harboring these genes may represent dangerous clinical isolates and participate in increase the distribution of slim and adhesions virulence factors by transformed genes to other various isolates of pathogenic bacteria in society, that may causes severity invasive infection and antibiotic resistance and fleeing host immune defenses in carriers of pregnant women and further different infections in introduced human. The study indicated *S. saprophyticus* isolates were more developed about study slim and adhesions virulence factors genes.

REFERENCES

1. Bizuwork K, Alemayehu H, Medhin G et al. Asymptomatic bacteriuria among pregnant women in Addis Ababa, Ethiopia: prevalence, causal agents, and their antimicrobial susceptibility. *Int J Microbiol.* 2021;2021:8418043. doi:10.1155/2021/8418043. [DOI](#)
2. Kooi-Pol MMVD. In vivo and in vitro profiling of global interactions between *Staphylococcus aureus* and its human host. University of Groningen. 2013. 230p. https://www.rug.nl/about-ug/latest-news/news/archief2013/promoties-oraties/promotie-mw.-m.m.-van-der-kooi-pol_-in-vivo-and-in-vitro-profiling-of-global-interactions-betwee?lang=en [Access: January 2024].
3. Nashev D, Toshkova K, Salasia SI et al. Distribution of virulence genes of *Staphylococcus aureus* isolated from stable nasal carriers. *FEMS Microbiol Lett.* 2004;233(1):45-52. doi:10.1016/j.femsle.2004.01.032 [DOI](#)
4. Ortega-Peña S, Rodríguez-Martínez S, Cancino-Díaz ME et al. *Staphylococcus epidermidis* Controls Opportunistic Pathogens in the Nose, Could It Help to Regulate SARS-CoV-2 (COVID-19) Infection? *Life (Basel).* 2022;12(3):341. doi:10.3390/life12030341. [DOI](#)
5. Lee JH, Heo S, Jeong M et al. Transfer of a mobile *Staphylococcus saprophyticus* plasmid isolated from fermented seafood that confers tetracycline resistance. *PLoS One.* 2019;14(2):e0213289. doi:10.1371/journal.pone.0213289. [DOI](#)
6. de Sousa VS, da-Silva APS, Sorenson L et al. *Staphylococcus saprophyticus* recovered from humans, food, and recreational waters in Rio de Janeiro, Brazil. *Int J Microbiol.* 2017;2017:4287547. doi:10.1155/2017/4287547. [DOI](#)
7. Cheung GYC, Bae JS, Otto M. Pathogenicity and virulence of *Staphylococcus aureus*. *Virulence.* 2021;12(1):547-569. doi:10.1080/21505594.2021.1878688. [DOI](#)
8. Ares-Arroyo M, Coluzzi C, Rocha EPC. Origins of transfer establish networks of functional dependencies for plasmid transfer by conjugation. *Nucleic Acids Res.* 2023;51(7):3001-3016. doi: 10.1093/nar/gkac1079. [DOI](#)
9. Clark DP, Pazdernik NJ, McGehee MR. *Molecular Biology (Third Edition)*, 2019. Hardback ISBN: 9780128132883.
10. Silva KCS, Silva LOS, Silva GAA et al. *Staphylococcus saprophyticus* proteomic analyses elucidate differences in the protein repertoires among clinical strains related to virulence and persistence. *Pathogens.* 2020;9(1):69. doi:10.3390/pathogens9010069 [DOI](#)
11. Peng Q, Tang X, Dong W et al. A review of biofilm formation of *Staphylococcus aureus* and its regulation mechanism. *Antibiotics (Basel).* 2022;12(1):12. doi:10.3390/antibiotics12010012. [DOI](#)
12. Bunyan I. Detection of adhesion genes and slim production among *Staphylococcus aureus* and *Staphylococcus epidermidis* isolated from hemodialysis patients. *Advances in Life Science and Technology.* 2013;15:27-33.
13. Kumar JD, Negi YK, Gaur A et al. Detection of virulence genes in *Staphylococcus aureus* isolated from paper currency. *Int J Infect Dis.* 2009;13(6):e450-e455. doi:10.1016/j.ijid.2009.02.020. [DOI](#)
14. Majumder S, Sackey T, Viau C et al. Genomic and phenotypic profiling of *Staphylococcus aureus* isolates from bovine mastitis for antibiotic resistance and intestinal infectivity. *BMC Microbiol.* 2023;23(1):43. doi:10.1186/s12866-023-02785-1. [DOI](#)

15. Afzal M, Vijay AK, Stapleton F, Willcox M. Virulence Genes of *Staphylococcus aureus* Associated With Keratitis, Conjunctivitis, and Contact Lens-Associated Inflammation. *Transl Vis Sci Technol.* 2022;11(7):5. doi:10.1167/tvst.11.7.5. [DOI](#)
16. Foster TJ, Geoghegan JA. Chapter 37 - *Staphylococcus aureus*. *Molecular medical microbiology* (2nd Edition). Science Direct Journals & Books. 2015;2:655-674. doi:10.1016/B978-0-12-397169-2.00037-8. [DOI](#)
17. Foster TJ, Geoghegan JA, Ganesh VK et al. Adhesion, invasion and evasion: the many functions of the surface proteins of *Staphylococcus aureus*. *Nat Rev Microbiol.* 2014;12(1):49-62. doi:10.1038/nrmicro3161.
18. Ionescu B, Ionescu D, Gheorghe I et al. Virulence patterns of *Staphylococcus aureus* hospital strains isolated in Bucharest, Romania. *Roman Biotechnol Lett.* 2015;20(3):10536-10546.
19. Abbas MH, Al-Mathkhury HJF. Isolation and identification of bacteria from Iraqi women with recurrent urinary tract infection. *Plant Archives.* 2020; 20(2):1838-1842.
20. Pugazhendhi A, Michael D, Prakash D et al. Antibiogram and plasmid profiling of beta-lactamase producing multidrug resistant *Staphylococcus aureus* isolated from poultry litter. *J King Saud Univer Sci.* 2020;32(6):2723-2727. doi:10.1016/j.jksus.2020.06.007. [DOI](#)
21. Rafiee M, Ghaemi EA. Detection of virulence genes among *Staphylococcus saprophyticus* isolated from women with urinary tract infections: first report from Iran. *BMC Res Notes.* 2023;16(1):206. doi:10.1186/s13104-023-06481-1. [DOI](#)
22. Jabur SG. Studying virulence plasmids and endotoxins of *Salmonella enterica* serovar Typhimurium isolated from chickens in Al-Najaf Al-Ashraf. Dissertation submitted to council of college of science /university of Kufa as partial fulfillment for the requirements of the PhD degree of philosophy in microbiology /molecular biology. 2014.
23. Lawal OU, Barata M, Fraqueza MJ et al. *Staphylococcus saprophyticus* from clinical and environmental origins have distinct biofilm composition. *Front Microbiol.* 2021;12:663768. doi:10.3389/fmicb.2021.663768. [DOI](#)
24. Billane K, Harrison E, Cameron D et al. Why do plasmids manipulate the expression of bacterial phenotypes? *Philos Trans R Soc Lond B Biol Sci.* 2022;377(1842):20200461. doi:10.1098/rstb.2020.0461 [DOI](#)
25. Duran N, Dogramaci Y, Ozer B et al. Detection of adhesin genes and slime production among *Staphylococci* in orthopaedic surgical wounds. *Afr J Microbiol Res.* 2010;4(9):708-715.
26. Gillaspay AF, Lee CY, Sau S et al. Factors affecting the collagen binding capacity of *Staphylococcus aureus*. *Infect Immun.* 1998;66(7):3170-3178. doi:10.1128/IAI.66.7.3170-3178.1998. [DOI](#)
27. Khudher KK, Jabur SG. The prevalence of some virulence plasmidic genes in *Staphylococcus aureus* infection. *Plant Archives.* 2020; 20(2): 8851-8862.
28. Al-Muaala MN, Al-Ethari SY, Al-Kraety AA et al. Molecular detection of clumping factor A gene and antibiotic susceptibility evaluation of *Staphylococcus aureus* isolated from urinary tract infections. *Archives of Razi Institute.* 2022;77(2):573-578. doi: 10.22092/ARI.2022.357153.1985. [DOI](#)

ORCID AND CONTRIBUTIONSHIP

Sanaa Ghali Jabur: 0000-0002-6043-5466 [A](#) [B](#) [C](#) [D](#) [E](#) [F](#)

CONFLICT OF INTEREST

The Author declare no conflict of interest

CORRESPONDING AUTHOR

Sanaa Ghali Jabur

Pathological Analysis, Science Collage

Thi-Qar University, Thi-Qar, Iraq

e-mail: sanaaghali@sci.utq.edu.iq

[A](#) – Work concept and design, [B](#) – Data collection and analysis, [C](#) – Responsibility for statistical analysis, [D](#) – Writing the article, [E](#) – Critical review, [F](#) – Final approval of the article

RECEIVED: 11.02.2024

ACCEPTED: 31.08.2024



Features of pregnancy and childbirth in mothers and girls suffering from abnormal uterine bleeding during puberty

Liudmyla A. Vygivska¹, Yevgenia B. Radzishavska², Olesia O. Pliekhova¹

¹DEPARTMENT OF OBSTETRICS, GYNECOLOGY, PEDIATRIC GYNECOLOGY AND MEDICAL GENETICS, KHARKIV NATIONAL MEDICAL UNIVERSITY, KHARKIV, UKRAINE

²DEPARTMENT OF MEDICAL AND BIOLOGICAL PHYSICS, MEDICAL INFORMATICS, KHARKIV NATIONAL MEDICAL UNIVERSITY, KHARKIV, UKRAINE

ABSTRACT

Aim: To determine the peculiarities of the course of pregnancy and childbirth in mothers whose children suffer from abnormal uterine bleeding during puberty.

Materials and Methods: The study involved examination of 95 girls aged 10 to 18, who were divided into clinical groups: clinical group I (main (MG)) – 65 girls with abnormal uterine bleeding during puberty, clinical group II (control (CG)) – 30 somatically healthy girls, who came to clinic for a medical checkup.

Results: Assessment of histories on the condition of mothers during pregnancy and childbirth in the MG showed existing gestational disorders. Thus, in MG, mothers were 17 times more likely to suffer from extragenital disorders, 15–20 times more likely to suffer from colds, 10 times more likely to suffer from toxicosis in the first half of pregnancy and preeclampsia, and 8 times more often to have placental dysfunction. Childbirths of mothers of MG girls were characterized by a pathological course: premature discharge of amniotic fluid, weakness of labor, preeclampsia during childbirth, fetal distress. In MG, operative deliveries were resorted to 13 times more often. In addition, birth trauma occurred in 15.38% of newborns, asphyxia at birth in 41.53%, and hypoxic-ischemic brain damage in 23.07%.

Conclusions: During the analysis of history data, peculiarities of the course of pregnancy and childbirth in mothers whose children suffer from abnormal uterine bleeding during puberty were revealed. The mothers of these girls have a complicated course of pregnancy and childbirth. Pathological effects on the fetus in the ante- and intranatal periods create the basis for the development of pathological puberty, which can manifest itself in the form of abnormal uterine bleeding.

KEY WORDS: abnormal uterine bleeding, pubertal period, gestational disorders, features of childbirth

Wiad Lek. 2024;77(9):1740-1744. doi: 10.36740/WLek/193759 DOI

INTRODUCTION

Reproductive health is one of the most important components of human health in general, and its provision, especially for adolescent girls, is one of the main steps in maintaining the health of the family and society. It is the reproductive health of teenage girls that determines population growth in the future, which is very relevant in the modern conditions of war and economic instability due to an unfavorable demographic situation [1,2].

Abnormal uterine bleeding (AUB) is defined as a significant change in the nature or volume of menstrual blood flow, caused by a number of diseases of the genital and non-genital tracts, systemic disorders, as well as taking some medications [3]. The incidence of AUB of the pubertal period in the structure of gynecological diseases of childhood and adolescence varies from 20% to 37% of all gynecological abnormalities of adolescence and makes up 50% of adolescent girls' requests for gynecological care [4]. An equally serious problem is the persistence of menstrual cycle

disorders, in particular recurrent uterine bleeding, in 38% of women in the later years of their lives. In addition, patients with AUB of the pubertal period have a history of primary infertility, miscarriage, complications during pregnancy and childbirth, and the probable development of hormone-dependent tumors [5, 6]. AUB affects all aspects of life: from study, work, sports to the performance of daily duties, that is, it significantly reduces the quality of life [7].

FIGO uses the PALM-COEIN system classification to determine the etiology of AUB (polyp, adenomyosis, leiomyoma, malignant tumor, hyperplasia – structural causes; coagulopathy, ovulatory dysfunction, endometrial, iatrogenic and not yet classified – non-structural causes) [8]. Only in 1.3–1.7% of cases, AUB occurs in adolescents due to structural problems [9]. Coagulopathy is also the leading etiology of AUB in adolescents, which accounts for 5–28%, according to various researchers, of the number of hospitalized adolescents with AUB [10, 11]. Anovulatory cycles, which manifest as amenorrhea, oligomenorrhea, or

AUB due to an immature hypothalamus-pituitary-ovary axis, are mostly the cause of AUB in the pubertal period [12, 13].

Recently, there is more and more evidence of the influence of intrauterine development on the state of the body during puberty. This is mostly related to the timing and process of puberty in teenage girls. Most studies report an association between intrauterine growth retardation and earlier pubertal development [14] or normal pubertal development but with rapid progression [15]. However, it is quite difficult to compare the results of such studies, since they use different methodologies.

It can be assumed that disorders of menstrual function are more often formed in girls born to mothers with a course of pregnancy against the background of preeclampsia, chronic fetoplacental insufficiency, which became the cause of fetal growth retardation syndrome. The triggering mechanism of these obstetric complications is the syndrome of endothelial dysfunction, which is the cause of fetal growth retardation syndrome [16, 17].

AIM

To determine the peculiarities of the course of pregnancy and childbirth in mothers whose girls suffer from abnormal uterine bleeding during puberty.

Materials and methods. The study was conducted at the department of obstetrics, gynecology, pediatric gynecology and medical genetics of KhNMU, in particular at the following clinical bases of the department: municipal non-profit enterprise "City Maternity Hospital No. 1" ("CMH No. 1") of Kharkiv City Council and a communal health care facility "Regional Children's Clinical Hospital No. 1" ("RCCH No. 1").

The study involved examination of 95 girls aged 10 to 18, who were divided into clinical groups: clinical group I (main (MG)) – 65 girls with abnormal uterine bleeding during puberty, clinical group II (control (CG)) – 30 somatically healthy girls, who came to clinic for a medical checkup. The patients of the main group were treated in the gynecological department of "CMH No. 1" and in the surgical department No. 4 of "RCCH No. 1". According to the provisions of the Helsinki Declaration of the World Medical Association of the latest revision, all girls or parents of girls involved in the study signed an informed consent for the use of examination data for scientific purposes.

Exclusion criteria were as follows: absence of bleeding during hospitalization, oncological, acute infectious diseases, pregnancy, developmental abnormalities and injuries of the reproductive system,

disorders of the blood system and acute surgical diseases, unwillingness of parents and patients (aged ≥ 14 years) to give voluntary informed consent to conduct research.

All the patients underwent a full clinical and laboratory examination. The study implied assessment of history data of the girls' mothers regarding the course of their pregnancies.

Processing of statistical data was carried out using the Statistica Basic Academic 13 for Windows general-purpose software package. Comparison of the frequencies of binary features of independent groups was carried out using the analysis of 2x2 tables ("chi-square" criterion).

RESULTS

The study showed that the age of the girls of the main group (MG) ranged from 10 to 18 years with a median of 14 years, of the control group (CG) - from 11 to 16 years with a median of 13 years. MG girls suffered from concomitant extragenital disorders (ED): overweight – 15 (23%), diseases of the cardiovascular system – 16 (25%), diseases of the respiratory system – 18 (28%), diseases of the gastrointestinal tract – 24 (37%). Combined extragenital disorders were found in 8 (12%) girls. CG was found to have the following ED: diseases of the respiratory system - 3 (10%), diseases of the gastrointestinal tract - 5 (17%).

Analysis of the course of pregnancy in the mothers of CG and MG girls showed that during pregnancy they suffered from colds, in particular in the 1st trimester in MG pregnancy - 31 (48%) women, in CG - 2 (7%); in the II trimester in MG – 25 (26%) women; in the III trimester, MG – 21 (32%) women, CG – 1 (33%) woman. Mothers of girls with AUB also had toxicosis in the first half of pregnancy, which manifested itself in the form of nausea and vomiting: in MG - 31 women (48%), in CG - in 3 (10%). The second half of pregnancy was complicated by preeclampsia of various degrees of severity in MG in 20 women (31%), in CG – in 2 (1%) women, as well as placental dysfunction in MG in 24 (37%) women, in CG – in 3 (10%). Iron deficiency anemia occurred in 19 (29%) MG women and 4 (13%) CG women. Exacerbation of chronic pyelonephritis during pregnancy occurred in 21 (32%) MG women and 3 (10%) CG women. 34 (52%) mothers of examined MG and 2 (7%) CG girls suffered from extragenital disorders. The threat of spontaneous abortion in the 1st trimester was present in 17 (26%) MG and 2 (7%) CG women. The threat of spontaneous abortion in the II trimester occurred in 10 (15%) women, and fetal growth retardation syndrome (FGR) in 8 (12%) mothers of MG girls.

Table 1. Peculiarities of pregnancy in mothers whose daughters suffer from abnormal uterine bleeding during puberty

Index	Main group, absolute number (%)	Control group, absolute number (%)	Chi-square test
A cold in the first trimester of pregnancy	31 (48)	2 (7)	p=0.0001
A cold in the second trimester of pregnancy	25 (26)	-	
A cold in the third trimester of pregnancy	21 (32)	1 (3)	p=0.0019
Toxicosis in the first half of pregnancy	31 (48)	3 (10)	p=0.0004
Preeclampsia	20 (31)	2 (7)	p=0.0096
Iron deficiency anemia	19 (30)	4 (13)	p=0.788
Exacerbation of chronic pyelonephritis	21 (32)	3 (10)	p=0.0200
Placental dysfunction	24 (36.92)	3 (10,00)	p=0.0068
Extragenital disorder	34 (52)	2 (7)	p=0.0000
A threat of spontaneous abortion in the first trimester	17 (26)	2 (7)	p=0.0273
A threat of spontaneous abortion in the second trimester	10 (15)	-	
Fetal growth retardation syndrome	8 (12.30)	-	

Table 2. Peculiarities of the course of childbirth of mothers whose girls suffer from abnormal uterine bleeding during puberty

Index	Main group, absolute number (%)	Control group, absolute number (%)	Chi-square test
Premature discharge of amniotic fluid	25 (26)	1 (3)	p=0.0004
Cesarean section	26 (40)	2 (7)	p=0.0019
Preeclampsia in childbirth	3 (5)	-	
Weakness of labor (without caesarean section)	19 (29)	1 (3)	p=0.0040
Weakness of labor (reason for caesarean section)	9 (14)	1 (3)	p=0.0665
Clinically narrow pelvis	4 (6.15)	-	
Premature birth	5 (8)	-	
Fetal distress	18 (28)	2 (7)	p=0.0195
Asphyxia at birth	27 (42)	1 (3.33)	p=0.0001
Birth trauma	10 (15.38)	-	
Hypoxic-ischemic damage of the brain	15 (23)	-	

As can be seen from the Table 1, the differences in incidence of the most indicators were statistically significant.

Labor activity of the mothers of the examined MG girls was characterized by a pathological course, in particular, preeclampsia during childbirth in 3 (5%), clinically narrow pelvis in 4 (6%) women. Mothers of the control group did not have these abnormalities. Premature discharge of amniotic fluid occurred in 25 (26%) MG women and in 1 (3%) CG woman. 26 (40%) MG mothers and 2 (7%) CG mothers had operative deliveries. Weakness of labor, which was subject to medical correction, was noted in 19 (29%) women of MG and in 1 (3%) person of CG, weakness of labor, which was not subject to medical correction (birth was completed surgically), in 9 (14%) of MG women and in

1 (3%) CG. Premature birth occurred in 5 (8%) mothers. Fetal distress was registered in 18 (28%) MG women during childbirth, while 2 (7%) women in CG had it. Birth asphyxia occurred in 27 (42%) MG newborns and in 1 (3%) CG newborn. Childbirth trauma was registered in 10 (15%) newborns, hypoxic-ischemic damage to the brain of newborns in 15 (23%) MG children; there were no such changes in CG.

As can be seen, the incidence of the most indicators was also statistically significant (Table 2).

DISCUSSION

Protection of reproductive health of children and adolescents is one of the urgent problems of modern medicine in most countries. This is due to the unfavorable

medical and demographic situation in the world and the deterioration of the health of women in the fertile period. In the structure of gynecological diseases of teenagers, the leading place is occupied by abnormal uterine bleeding during puberty. Increasingly, this abnormality takes on a protracted character and is often accompanied by relapses [18]. The formation of a young woman's reproductive health begins with the period of puberty, during which the neuroendocrine reorganization of the body and the intensive work of all organs and systems take place. The premorbid background as a set of pathological and physiological changes, which often complicate the course of the disease or create a certain basis for the development of changes in the body in the future, can also be a trigger for the development of pathological puberty in girls. The presence of chronic extragenital diseases, the unfavorable course of pregnancy and childbirth in their mothers - all this forms a negative premorbid background in the examined girls suffering from AUB during puberty. An indicator of the reproductive health of adolescent girls is a timely menarche and a regular rhythm of menstruation [19].

Assessment of history data on the condition of mothers during pregnancy and childbirth in the MG showed existing gestational disorders. Thus, in MG, mothers were 17 times more likely to suffer from extragenital disorders, 15–20 times more likely to suffer from colds, 10 times more likely to suffer from toxicosis in the first half of pregnancy and preeclampsia, and 8 times more often to have placental dysfunction.

The births of mothers of MG girls were characterized by a pathological course: premature discharge of amniotic fluid, weakness of labor, preeclampsia during childbirth, fetal distress. In MG, operative deliveries were resorted to 13 times more often. In addition, birth trauma occurred in 16% of newborns, asphyxia at birth in 41%, and hypoxic-ischemic brain damage in 23%. These data are consistent with the opinion of the authors about the possibility of the formation of pathological puberty in girls who suffered in utero, that is, whose mothers underwent a pathological period of gestation and childbirth [20, 21]. In addition, according to V.D. Markovsky et al., there is a violation of the establishment and formation of the main structural components of the female genital organs of fetuses with signs of FGSR, which in the future can lead to the development of functional insufficiency of these organs. [22]. In our study, FGSR occurred in 12% of MG fetuses.

CONCLUSIONS

During the analysis of history data, peculiarities of the course of pregnancy and childbirth in mothers whose girls suffer from abnormal uterine bleeding during puberty were revealed. The mothers of these girls have a complicated course of pregnancy and childbirth. Pathological effects on the fetus in the ante- and intranatal periods create the basis for the development of pathological puberty, which can manifest itself in the form of abnormal uterine bleeding.

REFERENCES

1. Janighorban M, Boroumandfar Z, Pourkazemi R, Mostafavi F. Barriers to vulnerable adolescent girls' access to sexual and reproductive health. *BMC Public Health*. 2022;22(1):2212. doi:10.1186/s12889-022-14687-4. [DOI](#)
2. Mehta SD, Seeley J. Grand Challenges in Adolescent Sexual and Reproductive Health. *Front Reprod Health*. 2020;2:2. doi:10.3389/frph.2020.00002. [DOI](#)
3. Alzahrani F, Hassan F. Modulation of Platelet Functions Assessment during Menstruation and Ovulatory Phases. *J Med Life*. 2019;12(3):296-300. doi:10.25122/jml-2019-0005. [DOI](#)
4. Kovalishin O. Abnormal uterine bleeding during puberty: to the pathogenesis and diagnosis. *Reproductive health of woman*. 2022; 2: 39-46. doi: 10.30841/2708-8731.2.2022.261806. [DOI](#)
5. Makarchuk O, Dziombak V. A Disorder of Menstrual Function Regularization and its Influence on a Female Reproductive Potential. *Galician medical journal*. 2017;24(3):E201739. doi: 10.21802/gmj.2017.3. [DOI](#)
6. Barrington DJ, Robinson HJ, Wilson E, Hennegan J. Experiences of menstruation in high income countries: A systematic review, qualitative evidence synthesis and comparison to low- and middle-income countries. *PLoS One*. 2021;16(7):e0255001. doi:10.1371/journal.pone.0255001. [DOI](#)
7. Robinson LB. Abnormal Uterine Bleeding Is a Quality-of-Life Issue: Clinicians Can Help Affected Women Determine the Cause and Severity, Which Are Key to Implementing a Treatment Plan. *Pharmacy Times*. 2019;85(6):71. <https://link.gale.com/apps/doc/A594180899/AONE>
8. Kahveci B, Budak MS, Ege S, Obut M, Bağlı I, Oğlak SC, Vardar MA. PALM-COEIN classification system of FIGO vs the classic terminology in patients with abnormal uterine bleeding. *Ginekolo Pol*. 2021;92(4):257-261. doi: 10.5603/GPa2021.0011. [DOI](#)
9. Pecchioli Y, Oyewumi L, Allen LM, Kives S. The Utility of Routine Ultrasound in the Diagnosis and Management of Adolescents with Abnormal Uterine Bleeding. *J Pediatr Adolesc Gynecol*. 2017;30(2):239-242. doi: 10.1016/j.jpag.2016.09.012. [DOI](#)

10. Başaran HO, Akgül S, Kanbur NO, Gümruk F, Cetin M, Derman O. Dysfunctional uterine bleeding in adolescent girls and evaluation of their response to treatment. *Turk J Pediatr.* 2013;55(2):186-9.
11. Luro K, Holopainen E. Heavy Menstrual Bleeding in Adolescent: Normal or a Sign of an Underlying Disease? *Semin Reprod Med.* 2022;40(1-02):23-31. doi: 10.1055/s-0041-1739309. DOI
12. Hernandez A, Dietrich JE. Abnormal Uterine Bleeding in the Adolescent. *Obstet Gynecol.* 2020;135(3):615-621. doi: 10.1097/AOG.0000000000003693. DOI
13. Davila J, Alderman EM. Heavy Menstrual Bleeding in Adolescent Girls. *Pediatr Ann.* 2020;49(4):e163-e169. doi: 10.3928/19382359-20200321-01. DOI
14. Suikkanen J, Nurhonen M, Cole TJ, Paalanne M, Matinolli HM, Tikanmäki M, et al. Preterm birth and subsequent timing of pubertal growth, menarche, and voice break. *Pediatr Res.* 2022;92(1):199-205. doi: 10.1038/s41390-021-01690-5. DOI
15. Wei J, Liu S, Cheng Y, Yang W, Zhu Z, Zeng L. Association of Infant Physical Development and Rapid Growth With Pubertal Onset Among Girls in Rural China. *JAMA Netw Open.* 2021;4(5):e216831. doi:10.1001/jamanetworkopen.2021.6831 DOI
16. Armengaud JB, Zydorczyk C, Siddeek B, Peyter AC, Simeoni U. Intrauterine growth restriction: Clinical consequences on health and disease at adulthood. *Reprod Toxicol.* 2021;99:168-176. doi: 10.1016/j.reprotox.2020.10.005. DOI
17. Kornacki J, Gutaj P, Kalantarova A, Sibiak R, Jankowski M, Wender-Ozegowska E. Endothelial Dysfunction in Pregnancy Complications. *Biomedicines.* 2021;9(12):1756. doi: 10.3390/biomedicines9121756. DOI
18. Kızılcan Çetin S, Aycan Z, Özsu E, Şıklar Z, Ceran A, Erişen Karaca S, Şenyazar G, Berberoğlu M. Evaluation of Abnormal Uterine Bleeding in Adolescents: Single Center Experience. *J Clin Res Pediatr Endocrinol.* 2023 Aug 23;15(3):230-237. doi: 10.4274/jcrpe.galenos.2023.2022-10-7. DOI
19. Hennegan J, Swe ZY, Than KK, Smith C, Sol L, Alberda H, Bukonya JN, Kibira SPS, Makumbi FE, Schwab KJ, Azzopardi PS. Monitoring Menstrual Health Knowledge: Awareness of Menstruation at Menarche as an Indicator. *Front Glob Womens Health.* 2022 Mar 24;3:832549. doi: 10.3389/fgwh.2022.832549. DOI
20. Saei Ghare Naz M, Farahmand M, Dashti S, Ramezani Tehrani F. Factors Affecting Menstrual Cycle Developmental Trajectory in Adolescents: A Narrative Review. *Int J Endocrinol Metab.* 2022;20(1):e120438. doi: 10.5812/ijem.120438. DOI
21. Kovalyshyn OA. Anomalni matkovi krovotechi pubertantnoho periodu: do pytan patohenezu i diahnostryky. *Reproduktyvne zdorovia zhinky.* - 2022;2:39-46.
22. Markovskiy VD, Kupriianova LS. Histolohichni osoblyvosti budovy zhinochykh statevykh orhaniv plodiv z oznakamy zatrymky vnutrishnoutrobnogo rozvytku . *Aktualni problemy suchasnoi medytsyny.* 2015;15(3):212-216.

CONFLICT OF INTEREST

The Authors declare no conflict of interest

CORRESPONDING AUTHOR

Liudmyla A. Vygivska

Kharkiv National Medical University, Kharkiv, Ukraine

4 Nauky avenue, Kharkiv, 61022, Ukraine

e-mail: liudmilavygovskaya@gmail.com

ORCID AND CONTRIBUTIONSHIP

Liudmyla A. Vygivska: 0000-0002-9389-4845 **A B D E F**

Yevgenia B. Radzishevskaya: 0000-0001-9149-7689 **A B C**

Olesia O. Pliekhova: 0000-0003-3183-8183 **A D F**

A – Work concept and design, **B** – Data collection and analysis, **C** – Responsibility for statistical analysis, **D** – Writing the article, **E** – Critical review, **F** – Final approval of the article

RECEIVED: 01.03.2024

ACCEPTED: 04.08.2024



Histopathological, immunohistochemical and physiological study for the hepatoprotective effect of melatonin against inh rifampicin-induced hepatotoxicity in mice model

Siham Mahmood Al-Rehemi¹, Rasha Hatem Dosh¹, Maha Jamal Frayyeh², Rihab Hameed Al Mudhafar³, Hussein Abdulkadhim⁴

¹DEPARTMENT OF HUMAN ANATOMY, FACULTY OF MEDICINE, UNIVERSITY OF KUFA, NAJAF, IRAQ

²AL-ABRAAR SECONDARY SCHOOL, MINISTRY OF EDUCATION, BAGHDAD, IRAQ

³DEPARTMENT OF PATHOLOGY AND FORENSIC MEDICINE, FACULTY OF MEDICINE, UNIVERSITY OF KUFA, NAJAF, IRAQ

⁴DEPARTMENT OF PHARMACOLOGY AND THERAPEUTICS, FACULTY OF MEDICINE, UNIVERSITY OF KUFA, NAJAF, IRAQ

ABSTRACT

Aim: The purpose of this study is to assess the hepatoprotective effect of melatonin against isoniazid (INH) and rifampicin (RMP) induced hepatotoxicity in albino mice.

Materials and Methods: Adult male mice were divided into four groups: saline, INH-RMP, INH-RMP+MT and MT were administered for 21 days. Biochemical analyses were performed for the determination of ALT, AST. Histopathological changes in the liver and Immunohistochemical assessment to determine the expression of Caspace3 were also examined.

Results: Biochemical analysis revealed significant increases in serum ALT and AST in INH-RMP group. Histopathological findings demonstrated severe liver damage in INH-RMP group as compared with control group. In contrast, treatment of mice with melatonin (MT) markedly mitigated the liver injury. Immunohistochemical findings demonstrated apoptotic marker caspace3 significantly higher in INH-RMP group as compared with control group.

Conclusions: Experimental findings highlight the potential benefits of melatonin in this model, prompting speculation on its potential application in human therapy.

KEY WORDS: Hepatotoxicity, Isoniazid, Rifampicin, Melatonin, caspace3, Liver damage

Wiad Lek. 2024;77(9):1745-1752. doi: 10.36740/WLek/192268 DOI

INTRODUCTION

Many medications are quite effective in treating target-directed diseases, but their usage is restricted to a brief course of treatment lasting no longer, than 1-2 weeks with a strict dosing schedule. This duration and dosage restriction is linked to their combined harmful effects, which may be caused by direct reactivity or free radicals and oxidants, which are consequences of their metabolism [1]. Tuberculosis is an extremely contagious illness that affects more than a third of the global population, leading to the deaths of over 2 million individuals annually [2]. A meta-analysis investigating the simultaneous administration of isoniazid (INH) and rifampicin (RMP), which are the primary drugs employed in tuberculosis treatment, revealed an association with hepatotoxicity ranging from 2% to 6%, severe liver damage and an elevated mortality rate [3-5], while the majority of instances involving INH

hepatotoxicity are mild and can resolve even with the continued use of INH, a small percentage of patients undergoing INH treatment experience severe hepatitis. This severe form may progress to fulminant liver failure and, if INH is not promptly discontinued, can lead to death [6]. Nevertheless, the idiosyncratic nature of INH hepatotoxicity continues to pose a significant safety concern in clinical settings. Currently, there are no specific therapies available for treating INH-induced liver injury. Although corticosteroids, which possess anti-inflammatory and immunosuppressive properties, are frequently employed, their outcomes are not consistently favourable. Consequently, there is an urgent need for mechanism-based strategies in the management of INH-induced liver injury [6]. Melatonin's hepatoprotective potential has been the subject of much interesting research in recent years, especially when it comes to drug-induced liver injury [7, 8]. A

common problem in the treatment of tuberculosis is the combination hepatotoxicity caused by isoniazid and rifampicin. This dual attack on hepatic integrity emphasizes the necessity for cutting-edge treatment approaches to lessen the resulting liver damage [9]. Although melatonin (MT) is most known for its ability to regulate circadian rhythms, it has also been shown to have a variety of other physiological effects, such as anti-inflammatory and antioxidant capabilities [9]. Research indicates that melatonin may provide defence against a range of hepatotoxic attacks, which has led to investigation into its effectiveness with regard to the hepatotoxicity caused by isoniazid-rifampicin.

AIM

The purpose of this study is to assess the hepatoprotective effect of melatonin against isoniazid and rifampicin induced hepatotoxicity in albino mice.

MATERIALS AND METHODS

EXPERIMENTAL DESIGN AND PROCEDURE

Twenty-four male albino mice weighing 18-22 g and 5 weeks old were obtained from the University of Kufa to conduct this investigation. The present study was approved by the ethics committee of the University of Kufa (Reference number: 20578). The mice were kept in a plastic cage throughout the experimentation period under typical lab conditions, which included 13-hour light cycles and 11-hour dark cycles. The mice were fed on commercial food bits and distilled water. In this study, animals were separated into four groups each of six mice. The control group was given normal saline (0.9%), and three intraperitoneal injected groups: isoniazid-rifampicin (INH-RMP) induced hepatotoxicity group were injected with 0.2 ml of INH-RMP 18 mg/kg daily for 21 days; melatonin group were injected with 0.2 ml of melatonin 0.1 mg/kg daily for 21 days; and hepatoprotective group were injected with 0.2 ml of INH-RMP 18 mg/kg and melatonin 0.1 mg/kg daily for 21 days).

PHYSIOLOGICAL AND HISTOPATHOLOGICAL EXAMINATION

On day 21, all of the mice were directly euthanized using intramuscular anaesthesia (0.25 ml xylazine (Arendonk; Belgium) per 100 g and 5 mg ketamine (Alfasan; Holland) per 100 g of the body weight). Blood was immediately aspirated from the heart and centrifuged at 1,370 × g for 10 min at 4°C, the serum was collected and stored

at –80°C until use for measurements of alanine aminotransferase (ALT) (GPT) and aspartate aminotransferase (AST) (GOT) activities (Roche diagnostics kit; Mannheim, Germany). The liver was resected after a longitudinal abdominal incision. A section of the liver from the portal hepatic was fixed in 10% neutral buffered formalin. The specimens were gradually dehydrated over a series of alcohol solutions (60%, 80%, 90%, and 100%) for two hours to prepare them for histological analysis. Then, two changes of xylene, which was easily soluble in alcohol, were added to the specimens to replace the alcohol. The specimens were then put in a dish of fresh paraffin wax, which was then moved to an oven that was continuously set at a temperature of 50 to 53°C. To replace the xylene in the tissue with paraffin, the specimens were then changed into two or three sequential plates of paraffin. Later, the specimens were embedded in the paraffin blocks and set on a microtome (Leitz; Germany), where serial sections of 5 µm thickness were cut. Finally, the specimens were stained with hematoxylin and eosin and mounted on glass slides (Leika/China) for histological analysis under a light microscope. The pathologist examined the slides in a blinded method for hepatic injury under the light microscope X100 or X400 magnification. Histopathological changes of the liver were scored as grade 0 indicates no damage, grade 1 indicates mild injury (characterized by vacuoles and focal pyknosis), grade 2 indicates moderate injury (characterized by vacuoles, ballooning, and apoptosis without necrosis), and grade 3 indicates severe injury (characterized by the presence of necrosis) [10].

IMMUNOHISTOCHEMICAL EXAMINATION OF CASPASE3

Formalin-fixed, paraffin-embedded 4 µm sections were subjected to immunohistochemical labelling using caspase3 antibodies at a 1:50 dilution (DAKO, Carpinteria, CA). In every instance, the slides were steam-heated for 30 minutes in a 1 mmol/L EDTA (pH 8.0) solution to retrieve the antigen. An automated immunostainer (DAKO) was used for staining, and a streptavidin-biotin detection system (DAKO) was used for detection. For every experiment, portions of positive and negative controls were employed. Stain intensity in the examined slide is divided into three categories: Score 0 for no stain, Score 1 for weak stain, Score 2 for moderate stain, and Score 3 for strong stain. While the proportion of stained cells and the expression of proteins in the examined slide is divided into the following categories: (Score 0: <10%, Score 1: 10-25%, Score 2: 25-50%, Score 3: 50-75%, Score 4: >75%). The outcome is expressed as a Quick H score, which is calculated by multiplying the

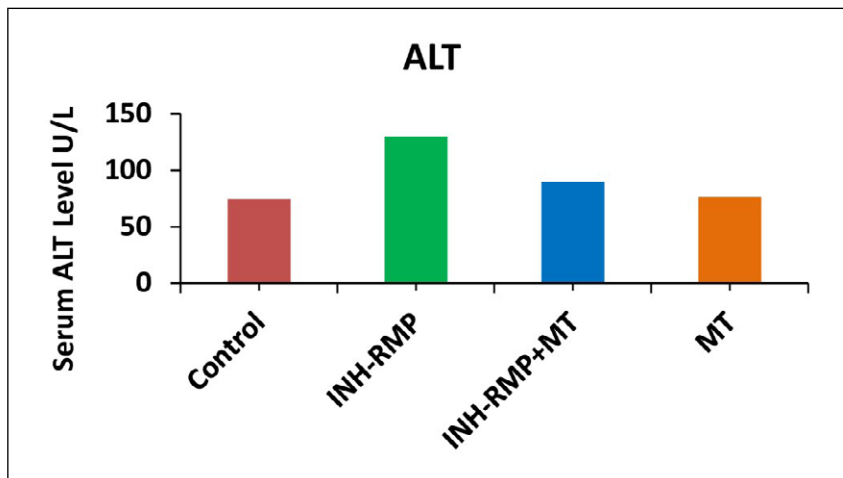


Fig. 1. Serum level of ALT in four experimental groups (six mice in each group). ($P \leq 0.05$).

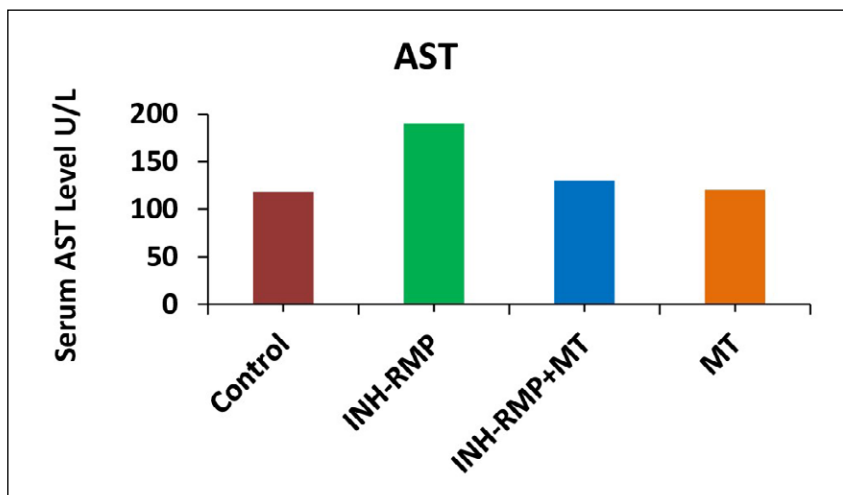


Fig. 2. Serum level of AST in four experimental groups (six mice in each group). ($P \leq 0.05$).

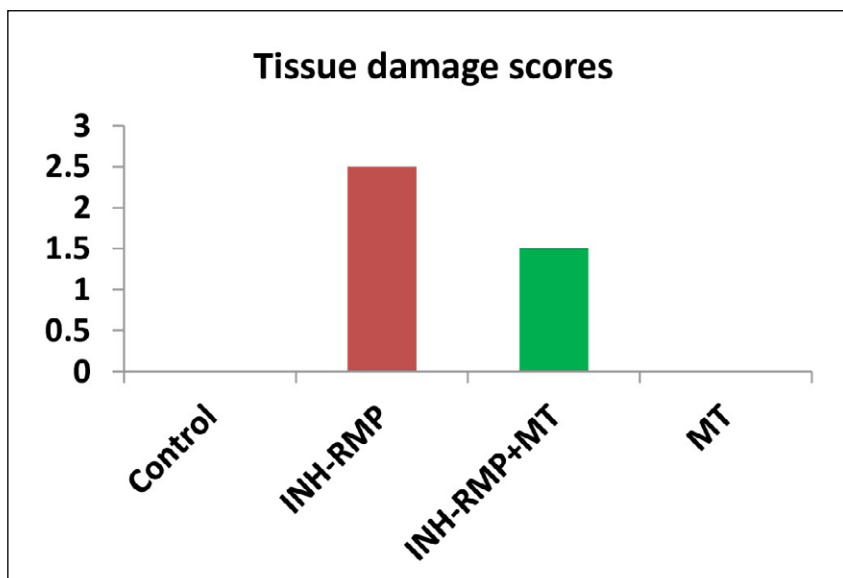


Fig. 3. Tissue damage scores in four experimental groups (six mice in each group). ($P \leq 0.05$).

stain intensity score by the proportion of stained cells on the slide under examination [11].

STATISTICAL ANALYSIS

GraphPad Prism version 8 was used to analyse the data and produce the graphics. To compare the

study groups, the Kruskal-Wallis test is a non-parametric method used to assess the levels of ALT, AST, and tissue damage between the study groups as the mean score for histopathological scoring analysis and mean quick H score for immunohistochemical results. Statistical significance was defined as a P -value ≤ 0.05 .

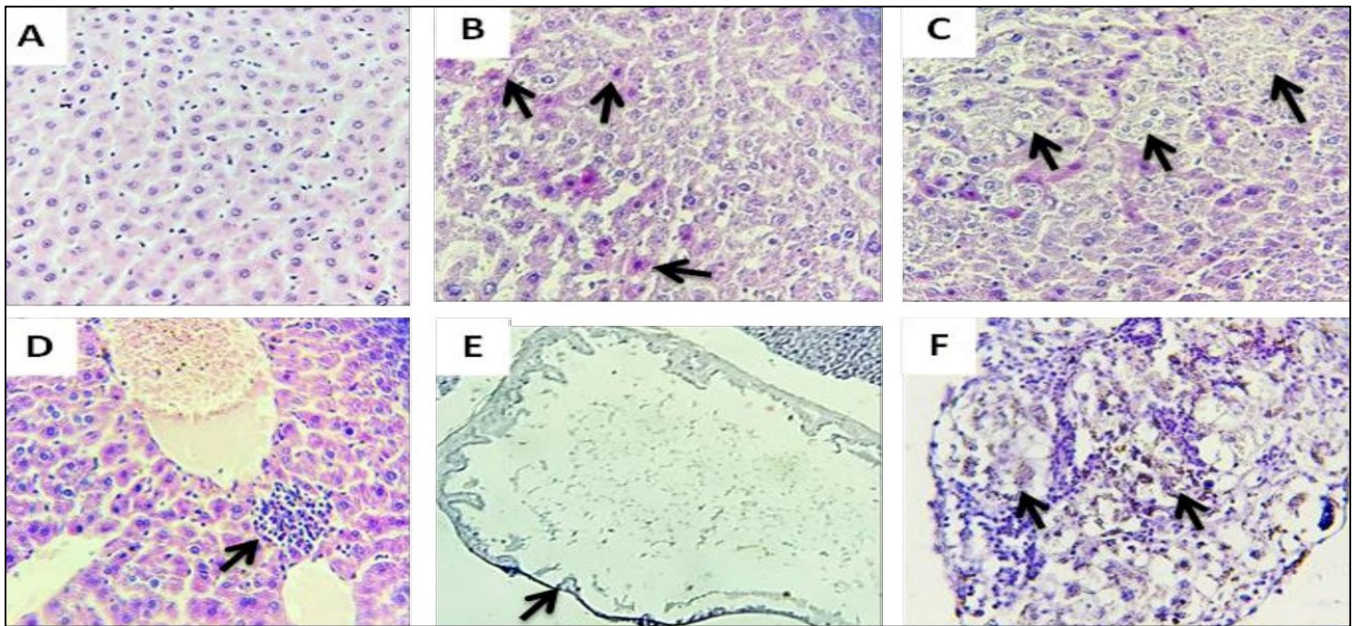


Fig. 4. (A) normal histology of the control group, (B-F) Histological images of liver sections in INH-RMP group showing moderate liver damage (score 2), (B) apoptotic cells with chromatin condensation, pyknotic nuclei, (C) hepatocytes ballooning and intracytoplasmic vacuoles, (D) mild pericentral inflammation, (E) hydatid cyst, (F) multiple granulomas, H&E stain, X400.

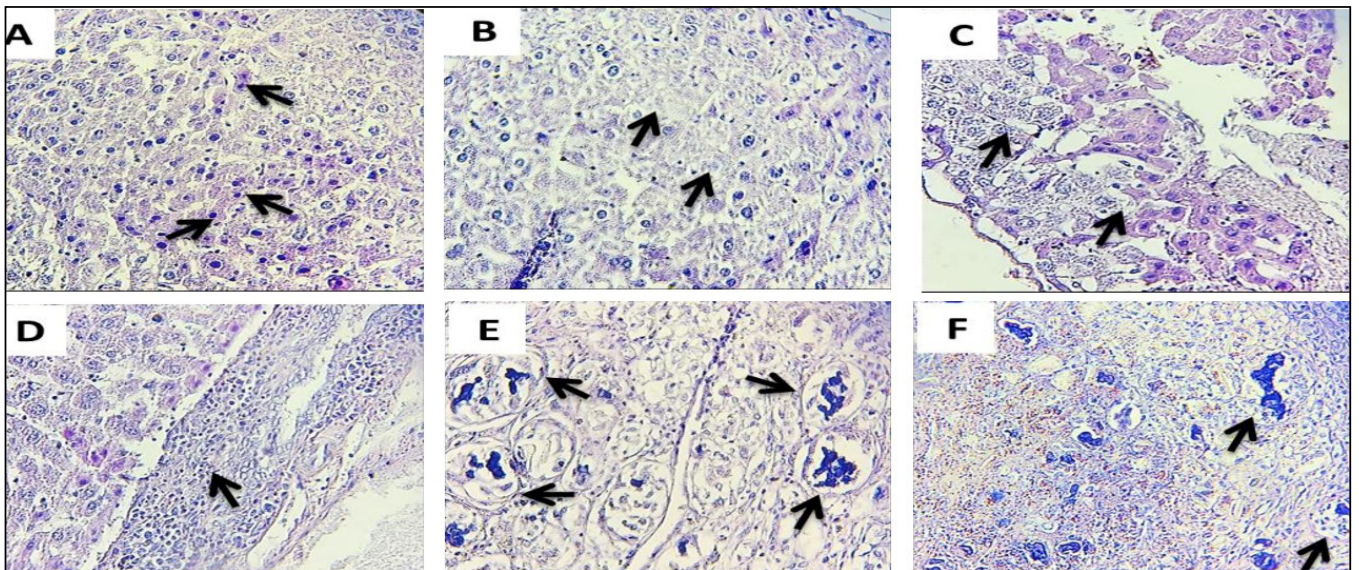


Fig. 5. Histological images of liver sections in INH-RMP group showing severe liver damage (score 3). (A) Apoptotic cells with chromatin condensation, pyknotic nuclei, (B) necrosis, (C) hepatocytes ballooning and intracytoplasmic vacuoles, (D) inflammation, (E & F) multiple granulomas, H&E stain, X400.

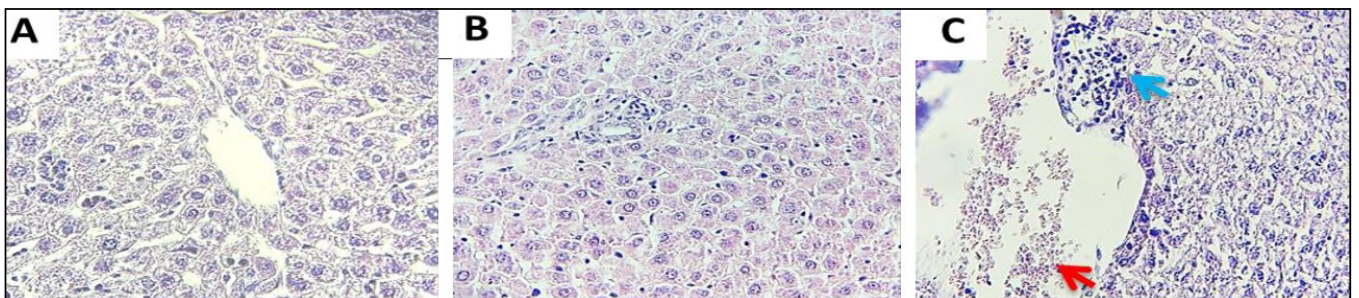


Fig. 6. Histological images of liver sections in (A) MT group showing normal histology. (B&C) INH-RMP+MT group showing: (B) liver with no damage (score 0), (C) Liver sections revealed mild liver damage (score 1) featured with pericentral Inflammation (blue arrow) and vascular congestion (red arrow). H&E stain, X400.

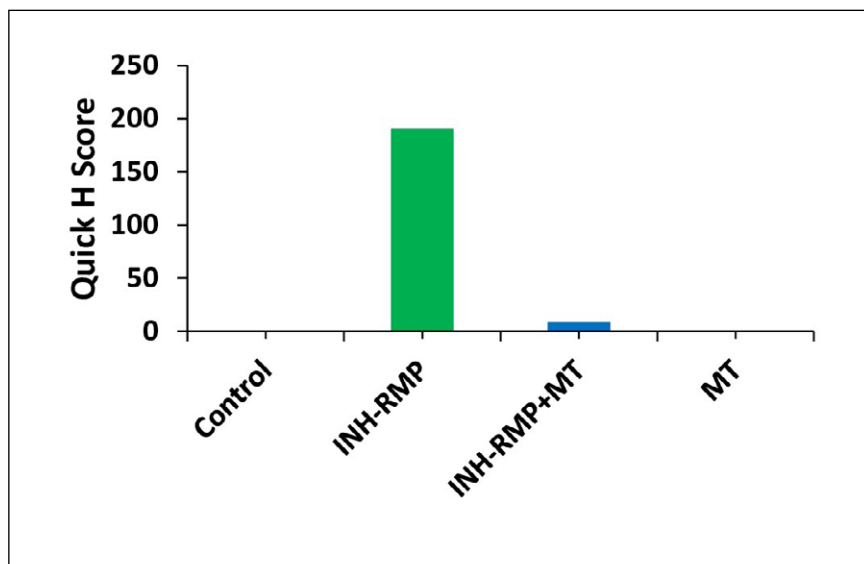


Fig. 7. Mean quick H score in four experimental groups (six mice in each group). ($P \leq 0.05$).

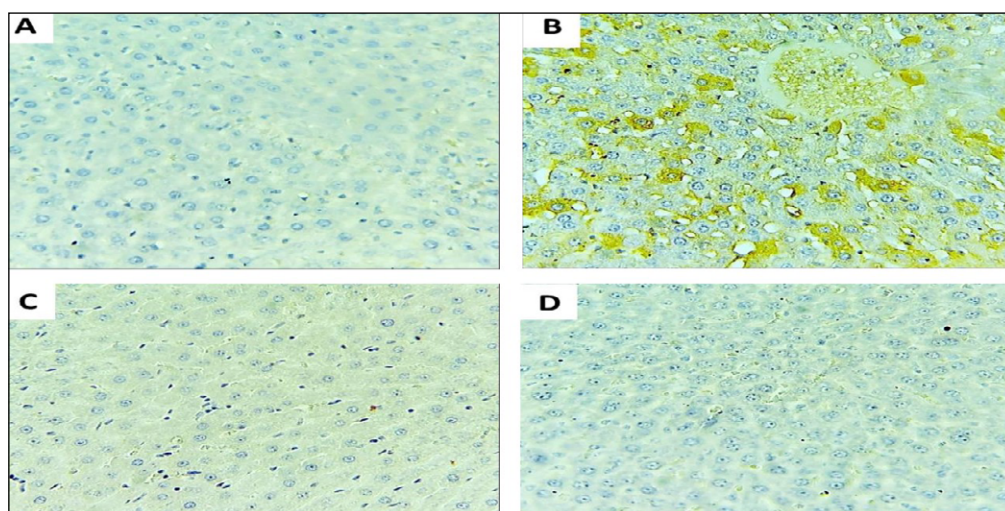


Fig. 8. Immunohistochemistry staining (brown) of Caspase3 for liver tissue: (A) control group showed negative staining, (B) INH-RMP group showed moderate to strong cytoplasmic caspase3 expression in apoptotic hepatocytes condensation in perivascular and around central veins, (C) INH-RMP+MT group showed weak cytoplasmic caspase3 expression, (D) MT group showed negative staining, X400.

RESULTS

PHYSIOLOGICAL ASSESSMENT

Serum levels of ALT and AST were utilized as markers of liver damage to examine liver function. Mice treated with INH-RMP had a significant increase in serum levels of ALT and AST when compared with the control group ($P \leq 0.05$) (Fig. 1, 2). In contrast, treatment with MT significantly reduced the serum levels of ALT and AST in the INH-RMP+MT group when compared with the INH-RMP group (Fig. 1, 2). In addition, there was a significant decrease in the serum levels of ALT and AST in the MT group when compared with the INH-RMP group (Fig. 1, 2). There was a significant decrease in the serum level of ALT in the MT group when compared with the INH-RMP+MT group (Fig. 1), whereas no significant results were found in the serum level of AST between the INH-RMP+MT group and MT group (Fig. 2).

HISTOPATHOLOGICAL SCORES OF LIVER INJURY

Histopathological study was used to investigate the severity of damage in the liver. Mice subjected to the INH-RMP group revealed moderate (score 2) and severe liver damage (score 3) compared to the control and MT groups (Fig. 3-6). By contrast, histological analysis of the liver in the INH-RMP+MT group showed a mild degree of liver damage (score 1), $P \leq 0.05$ (Fig. 3-6).

EFFECT OF INH-RMP ON APOPTOTIC MARKER (CASPACE3)

Quick H score results of cytoplasmic staining of caspase3 demonstrated normal liver tissue and absence of caspase3 (mean H score = 0) in control and MT groups (Fig. 7, 8). In contrast, the INH-RMP group showed moderate to strong positive cytoplasmic caspase3 expression in apoptotic hepatocyte condensation in

perivascular and around central veins. The H score of the INH-RMP group (H score = 190.8) was significantly (*p*-value less than 0.05) higher than the H score of the INH-RMP+MT group (H score = 8.3) (Fig. 7, 8).

DISCUSSION

The main goal of this current investigation is to provide a detailed understanding of melatonin's hepatoprotective effectiveness against liver injury caused by isoniazid-rifampicin. This research contributes to our understanding of melatonin's function in hepatic resilience and may be useful in the development of focused treatment strategies for hepatotoxicity caused by drugs. In this study, treatment with INH-RMP followed by MT was found to cause a marked reduction in levels of ALT and AST in comparison with the INH-RMP group. These results are in accordance with recent studies indicating that the levels of ALT and AST decreased in patients with liver disease when treated with melatonin [9, 12-13]. AST can be found in the liver, cardiac and skeletal muscles, pancreas, lungs, brain, kidneys, leucocytes, and red blood cells as both cytosolic and mitochondrial isoenzymes. The increase in AST may also be considered secondary to nonhepatic causes because it is not as sensitive or specific for the liver as ALT. The histological changes in hepatic tissues are shown by histopathological investigations, which also clarify the possible moderating effects of melatonin and illuminate the morphological changes caused by INH-rifampicin. Melatonin-induced immune responses can be better understood from a molecular perspective offered by immunohistochemical examination that focuses on certain protein markers. Determining the hepatoprotective mechanisms of melatonin in response to INH-rifampicin exposure requires an understanding of the cellular signaling pathways that it modulates [13]. Isoniazid is an anti-mycobacterial substance employed in the management of active or latent tuberculosis (TB). With nearly seven decades of clinical usage, INH continues to be widely employed as a primary component in anti-TB therapy. Nevertheless, the risk of liver damage and, in severe cases, fulminant liver failure associated with INH-based TB treatment poses a significant hurdle for TB control initiatives globally [14]. The primary manifestation of INH-induced hepatotoxicity is hepatocellular necrosis. Pharmaceuticals can induce liver injury in a foreseeable manner based on both the duration and dosage of their administration. Liver injury caused by INH typically manifests within weeks to months, rather than days to weeks after the onset of treatment [15]. Approximately 60% of INH hepatotoxicity cases in the United States Public Health Service (USPHS) study occurred within

the initial 3 months of treatment, with 80% of the incidents taking place in the first 6 months [16], while certain individuals may show no symptoms, others may encounter symptomatic hepatotoxicity. Asymptomatic patients may display up to a three-fold increase above the upper limit of the normal range for serum ALT and AST. The majority of INH hepatotoxicity cases are mild and generally resolve even with the continuation of INH therapy. INH, when administered orally, undergoes rapid absorption through the gastrointestinal tract and is distributed to multiple organs, including the liver, brain, and kidneys [14]. INH is primarily metabolized in the liver. The isonicotinic acyl radical has the potential to form covalent adducts with liver macromolecules, possibly prompting immune responses [17, 18]. Mass spectrometric analysis has identified INH adducts on several proteins within murine livers [19]. Nevertheless, the mechanisms underlying the formation of the INH radical and its interaction with liver proteins remain unclear. These medications facilitate the production of extremely reactive oxygen species (ROS), serving as initiators of lipid peroxidation and a mechanism for damaging the plasma membrane [20-22]. Rifampicin effectively triggers CYP2E1, a cytochrome P450 family member accountable for breaking down environmental chemicals and carcinogens. Additionally, it heightens INH-induced toxicity by promoting the generation of the toxic metabolite hydrazine through the amidase pathway [23]. Hydrazine subsequently interacts with the sulfhydryl group of glutathione (GSH), leading to a depletion of GSH levels within hepatocytes and resulting in cell death [3, 5, 24]. The combined use of INH-RIH in chemotherapy was observed to enhance the transformation of INH into isonicotinic acid, an additional hepatotoxic product. Rifampicin further accelerates the plasma half-life of acetyl hydrazine by rapidly converting it into active metabolites, thereby elevating the likelihood of liver necrosis [17, 25]. Initial research, primarily focused on its positive impact on sleep disorders, stemmed from observations highlighting melatonin's favourable outcomes in various pathological conditions affecting different organs. In the context of the liver, melatonin has been shown to bring about improvements in several experimental models of damage [26-28]. The liver plays a primary role in melatonin catabolism, accounting for 90% of the process through conventional glucuronidation-sulfation pathways. The elimination of melatonin takes place via urine, with excretion occurring in the form of either sulfated metabolites or unchanged melatonin in small quantities [29-30]. Numerous studies have investigated the impact of melatonin on liver injuries and diseases. Melatonin has demonstrated the ability to modulate various molecular pathways, including

those involved in inflammation, metastasis, apoptosis, and autophagy, across different pathophysiological conditions. These findings suggested that melatonin holds the potential for both preventing and treating liver injuries and diseases [11, 31-33].

CONCLUSIONS

In recent decades, numerous significant effects of melatonin have been uncovered. Experimental findings highlight the potential benefits of melatonin in this model, prompting speculation on its potential appli-

cation in human therapy. Physiological evaluations including liver function tests provided a thorough understanding of the systemic effects of melatonin treatment. The microscopic changes in the hepatic tissues clarified the hypothesized moderating effects of melatonin and illuminated the morphological changes caused by the drug combination. Additionally, immunohistochemistry investigations that concentrated on the Caspace3 marker revealed the molecular landscape, offering insights into the cellular signaling pathways that are modified in response to the INH-rifampicin challenge and the immune responses triggered by melatonin.

REFERENCES

1. Nieuwlaat R, Wilczynski N, Navarro T et al. Interventions for enhancing medication adherence. *Cochrane Database Syst Rev*. 2014;2014(11):CD000011. doi:10.1002/14651858.CD000011.pub4. DOI
2. Shishoo CJ, Shah SA, Rathod IS et al. Impaired bioavailability of rifampicin in presence of isoniazid from fixed dose combination (FDC) formulation. *Int J Pharm*. 2001;228(1-2):53-67. doi:10.1016/s0378-5173(01)00831-6. DOI
3. Tasduq SA, Peerzada K, Koul S et al. Biochemical manifestations of anti-tuberculosis drugs induced hepatotoxicity and the effect of silymarin. *Hepatol Res*. 2005;31(3):132-135. doi:10.1016/j.hepres.2005.01.005. DOI
4. Wang P, Pradhan K, Zhong XB et al. Isoniazid metabolism and hepatotoxicity. *Acta Pharm Sin B*. 2016;6(5):384-392. doi:10.1016/j.apsb.2016.07.014. DOI
5. Kapgade SM, Patil AB. Standardization of model of induction of hepatotoxicity with anti-tuberculosis drugs in wistar albino rats. *Asian J Pharm Clin Res*. 2017;10(6):150-153. doi:10.22159/ajpcr.2017.v10i6.11971. DOI
6. National Institute of Diabetes and Digestive and Kidney Diseases. Liver tox: Clinical and Research Information on Drug-Induced Liver Injury. 2012. <https://www.ncbi.nlm.nih.gov/books/NBK547852/>. [Accessed 15 October 2023]
7. Zhang JJ, Meng X, Li Y et al. Effects of melatonin on liver injuries and diseases. *Int J Mol Sci*. 2017;18(4):673. doi:10.3390/ijms18040673.
8. Othman MS, Fareid MA, Abdel Hameed RS et al. The protective effects of melatonin on aluminum-induced hepatotoxicity and nephrotoxicity in rats. *Oxid Med Cell Longev*. 2020;2020:7375136. doi:10.1155/2020/7375136. DOI
9. Esmaili A, Nassiri Toosi M, Taher M et al. Melatonin effect on platelet count in patients with liver disease. *Gastroenterol Hepatol Bed Bench*. 2021;14(4):356-361.
10. Li Z, Liu T, Feng Y et al. PPAR γ Alleviates Sepsis-Induced Liver Injury by Inhibiting Hepatocyte Pyroptosis via Inhibition of the ROS/TXNIP/NLRP3 Signaling Pathway. *Oxid Med Cell Longev*. 2022;2022:1269747. doi:10.1155/2022/1269747. DOI
11. Jin Z, El-Deiry WS. Overview of cell death signaling pathways. *Cancer Biol Ther*. 2005;4(2):139-163. doi:10.4161/cbt.4.2.1508. DOI
12. Mansoori A, Salimi Z, Hosseini SA et al. The effect of melatonin supplementation on liver indices in patients with non-alcoholic fatty liver disease: a systematic review and meta-analysis of randomized clinical trials. *Complement Ther Med*. 2020;52:102398. doi:10.1016/j.ctim.2020.102398. DOI
13. Terziev D, Terzieva D. Experimental Data on the Role of Melatonin in the Pathogenesis of Nonalcoholic Fatty Liver Disease. *Biomedicines*. 2023;11(6):1722. doi:10.3390/biomedicines11061722. DOI
14. Lei S, Gu R, Ma X. Clinical perspectives of isoniazid-induced liver injury. *Liver Res*. 2021;5(2):45-52. doi:10.1016/j.livres.2021.02.001. DOI
15. Mitchell JR, Zimmerman HJ, Ishak KG et al. Isoniazid liver injury: clinical spectrum, pathology, and probable pathogenesis. *Ann Intern Med*. 1976;84(2):181-192. doi:10.7326/0003-4819-84-2-181. DOI
16. Fountain FF, Tolley E, Chrisman CR et al. Isoniazid hepatotoxicity associated with treatment of latent tuberculosis infection: a 7-year evaluation from a public health tuberculosis clinic. *Chest*. 2005;128(1):116-123. doi:10.1378/chest.128.1.116. DOI
17. Metushi IG, Nakagawa T, Uetrecht J. Direct oxidation and covalent binding of isoniazid to rodent liver and human hepatic microsomes: humans are more like mice than rats. *Chem Res Toxicol*. 2012;25(11):2567-2576. doi:10.1021/tx300341r. DOI
18. Metushi IG, Sanders C, Lee WM et al. Detection of anti-isoniazid and anti-cytochrome P450 antibodies in patients with isoniazid-induced liver failure. *Hepatology*. 2014;59(3):1084-1093. doi:10.1002/hep.26564. DOI
19. Koen YM, Galeva NA, Metushi IG et al. Protein targets of isoniazid-reactive metabolites in mouse liver in vivo. *Chem Res Toxicol*. 2016;29(6):1064-1072. doi:10.1021/acs.chemrestox.6b00098. DOI
20. He X, Song Y, Wang L et al. Protective effect of pyrrolidine dithiocarbamate on isoniazid/rifampicin-induced liver injury in rats. *Mol Med Rep*. 2020;21(1):463-469. doi:10.3892/mmr.2019.10817. DOI

21. Georgieva NV, Gadjeva V, Tolekova A. New isonicotinoylhydrazones with ssa protect against oxidative-hepatic injury of isoniazid. *Trakia J Sci.* 2004;2(2):37–43.
22. Lian Y, Zhao J, Xu P et al. Protective effects of metallothionein on isoniazid and rifampicin-induced hepatotoxicity in mice. *PLoS One.* 2013;8(8):e72058. doi:10.1371/journal.pone.0072058. [DOI](#)
23. Ullah U, Badshah H, Malik Z et al. Hepatoprotective effects of melatonin and celecoxib against ethanol-induced hepatotoxicity in rats. *Immunopharmacol Immunotoxicol.* 2020;42(3):255–263. doi:10.1080/08923973.2020.1746802. [DOI](#)
24. Naji KM, Al-Khatib BY, Al-Haj NS et al. Hepatoprotective activity of melittin on isoniazid- and rifampicin-induced liver injuries in male albino rats. *BMC Pharmacol Toxicol.* 2021;22(1):39. doi:10.1186/s40360-021-00507-9. [DOI](#)
25. Tostmann A, Boeree MJ, Aarnoutse RE et al. Antituberculosis drug-induced hepatotoxicity: concise up-to-date review. *J Gastroenterol Hepatol.* 2008;23(2):192–202. doi:10.1111/j.1440-1746.2007.05207.x. [DOI](#)
26. Bona S, Fernandes SA, Moreira ACJ et al. Melatonin restores zinc levels, activates the Keap1/Nrf2 pathway, and modulates endoplasmic reticular stress and HSP in rats with chronic hepatotoxicity. *World J Gastrointest Pharmacol Ther.* 2022;13(2):11–22. doi:10.4292/wjgpt.v13.i2.11. [DOI](#)
27. Deng WS, Xu Q, Liu YE et al. Effects of melatonin on liver function and lipid peroxidation in a rat model of hepatic ischemia/reperfusion injury. *Exp Ther Med.* 2016;11(5):1955–1960. doi:10.3892/etm.2016.3160. [DOI](#)
28. Baiocchi L, Zhou T, Liangpunsakul S et al. Possible application of melatonin treatment in human diseases of the biliary tract. *Am J Physiol Gastrointest Liver Physiol.* 2019;317(5):G651–G660. doi:10.1152/ajpgi.00110.2019. [DOI](#)
29. Sankar M, Rajkumar J, Sridhar D. Hepatoprotective activity of heptoplus on isoniazid and rifampicin induced liver damage in rats. *Indian J Pharm Sci.* 2015;77(5):556–562. doi:10.4103/0250-474x.169028. [DOI](#)
30. Oztupuz O, Turkon H, Buyuk B et al. Melatonin ameliorates sodium valproate-induced hepatotoxicity in rats. *Mol Biol Rep.* 2020;47(1):317–325. doi:10.1007/s11033-019-05134-6. [DOI](#)
31. Sadoughi F, Maleki Dana P, Homayoonfal M et al. Molecular basis of melatonin protective effects in metastasis: A novel target of melatonin. *Biochimie.* 2022;202:15–25. doi:10.1016/j.biochi.2022.05.012. [DOI](#)
32. Cho JH, Bhutani S, Kim CH et al. Anti-inflammatory effects of melatonin: A systematic review and meta-analysis of clinical trials. *Brain Behav Immun.* 2021;93:245–253. doi:10.1016/j.bbi.2021.01.034. [DOI](#)
33. Sagrillo-Fagundes L, Bienvenue-Pariseault J, Vaillancourt C. Melatonin: The smart molecule that differentially modulates autophagy in tumor and normal placental cells. *PLoS One.* 2019;14(1):e0202458. doi:10.1371/journal.pone.0202458. [DOI](#)

CONFLICT OF INTEREST

The Authors declare no conflict of interest

CORRESPONDING AUTHOR

Rasha Hatem Dosh

University of Kufa

299G+HPX, Kufa Street, Kufa, Najaf Governorate, Najaf, Iraq

e-mail: sgahmed1331962@outlook.com

ORCID AND CONTRIBUTIONSHIP

Rasha Hatem Dosh: 0000-0002-2318-6608 [B](#) [C](#)

Siham Mahmood Al-Rehemi: 0000-0002-0832-7935 [A](#) [D](#)

Maha Jamal Frayyeh: 0000-0001-6202-8023 [B](#) [C](#) [D](#)

Rihab Hameed Al Mudhafar: 0000-0003-4997-5549 [E](#)

Hussein Abdulkadhim: 0009-0008-2034-2506 [A](#) [F](#)

[A](#) – Work concept and design, [B](#) – Data collection and analysis, [C](#) – Responsibility for statistical analysis, [D](#) – Writing the article, [E](#) – Critical review, [F](#) – Final approval of the article

RECEIVED: 07.06.2024

ACCEPTED: 12.08.2024



The efficacy and safety of vitamin D supplementation in women with polycystic ovarian syndrome undergoing ovulation induction using letrozole

Asma A Swadi, Hussein A Saheb, Ahmed M Sultan

DEPARTMENT OF PHARMACOLOGY AND THERAPEUTICS, COLLEGE OF MEDICINE, UNIVERSITY OF AL-QADISIYAH, IRAQ

ABSTRACT

Aim: To examine the role of vitamin D supplementation in PCOS women who failed to ovulation induction by letrozole in previous trials.

Materials and Methods: The study included 30 women diagnosed with PCOS and were complaining from primary infertility. Those women had previously been treated for 3 months with letrozole to induce ovulation, but there was failure of response to treatment. Those 30 women were selected from a pool of women who were evaluated for serum vitamin D and were proved to have vitamin D deficiency (<20 ng/ml).

Results: Daily monitoring of ovulation by transvaginal ultrasound was done starting from day 7 till day 25 of the cycle. The main outcomes were the number and the size of follicles. In addition, they were followed up for evidence of pregnancy using biochemical serum and urine examination.

Conclusions: When women with polycystic ovarian syndrome are treated with letrozole, vitamin D supplementation enhances both the result of ovulation induction and pregnancy.

KEY WORDS: polycystic ovary syndrome, ovulation, vitamin D

Wiad Lek. 2024;77(9):1753-1758. doi: 10.36740/WLek202409116 DOI

INTRODUCTION

Infertility is a common health problem in our community [1-3]. Despite the large number of articles published annually about infertility in Iraq, there is no large national population-based study to figure out the exact prevalence of infertility in Iraq population. However, the prevalence rate of infertility globally is in the range of 8% to 12% [4]. The causes of infertility are variable, but they can be grouped into 4 major categories and these are male factors, female factors, combined factors and unexplained infertility category [5]. Female infertility can be due to variety of causes affecting the structure and function of reproductive tract [6]. One of the most prevalent reasons for female infertility is polycystic ovarian syndrome [7]. It is the most common women endocrine abnormality [8]. It is characterized by anovulation, menstrual irregularities, hyperandrogenism based on clinical and biochemical evidences, and polycystic ovary based on imaging techniques, ultrasound examination in particular [9]. The disease is also associated with obesity and features of metabolic syndrome such as insulin resistance and hypertension [10]. The problem of infertility is common in women with PCOS and in a substantial proportion of them being the first cause of

presentation and seeking medical advice [11]. Anovulatory infertility is a frequent side effect of PCOS, and women who experience anovulatory infertility are more likely to develop the condition (70% to 80% of the time). As a result, addressing anovulation is the main focus of the reproductive treatments provided to these women [12]. Infertility may be negatively impacted by PCOS in a number of ways, including anovulation or irregular ovulation; a higher risk of spontaneous abortion; decreased oocyte quality; insulin resistance leading to hyperinsulinemia and an increased risk of miscarriage; and long-term intimal hyperplasia that compromises implantation [13]. PCOS is believed to be caused by a vicious cycle in which excess testosterone stimulates visceral and abdominal adipose tissue depositing, insulin resistance (IR), and compensatory hyperinsulinemia, which in turn stimulates the production of androgen by the adrenal glands and ovaries. In conjunction with hypothalamic-pituitary dysfunction, this cyclical pathogenetic interplay between IR, hyperinsulinemia, and hyperandrogenism causes further ovarian dysfunction, which can cause anovulation and infertility [14]. The first-line therapy advised for PCOS-afflicted women is lifestyle modifications that encourage weight loss [15].

Ovulation induction is the cornerstone of treatment for PCOS-related infertility in women because 70% of these women experience anovulation or oligo-ovulation. The most often employed substance is clomiphene citrate [16]. Letrozole, an aromatase inhibitor, was used as an ovulation inducer in women with anovulatory infertility who had endometrial thickness greater than 6 mm. It has also been reported that letrozole is effective in patients who are resistant to clomiphene, and that it also caused ovulation in 62% of cases and pregnancy in 14.7% of cases [17]. However, sufficient controversy existed in available published articles about the efficacy of ovulation induction alone in treating PCOS infertility that justified the search for other medical forms of intervention to treat the resistant cases [18]. Vitamin D deficiency affects PCOS patients, specially those with heavy weight. A low level of vitamin D is linked to insulin resistance and an increased chance of developing diabetes, and hypovitaminosis is a risk factor for glucose intolerance [19]. Therefore, the current study was planned and conducted aiming at exploring the role of vitamin D supplementation in PCOS women who failed to ovulation induction by letrozole in previous trials.

AIM

The current study was planned and conducted to examine the role of vitamin D supplementation in PCOS women who failed to ovulation induction by letrozole in previous trials.

MATERIALS AND METHODS

STUDY DESIGN

The current interventional study (uncontrolled clinical trial) was carried out in the department of Obsteric and Gynecology at Adiwaniyah Maternity and Pediatric Teaching Hospital, Adiwaniyah Province, Iraq during the period from March 2022 till March 2023.

INCLUSION CRITERIA

Women diagnosed with PCOS according to the Rotterdam criteria; the body mass index, which falls between 18 and 35 kg/m².

EXCLUSION CRITERIA

Exclusion of other associated causes of infertility such as tubal blockage. Pregnant PCOS women and women with hypersensitivity letrozole were also excluded from the study.

WOMEN ENROLLMENT IN THIS STUDY

The study included 30 women diagnosed with PCOS and were complaining from primary infertility. Those women were treated previously for 3 months with letrozole to induce ovulation, but there was failure of response to treatment. Those 30 women were selected from a pool of women who were evaluated for serum vitamin D and were proved to have vitamin D deficiency <20 ng/ml.

INTERVENTION

For six months, a daily dose of 4,000 IU of vitamin D₃ was administered to each of the thirty women who were selected. In addition, a course of letrozole at a dose of 2.5 mg/day at days 3-5 of the cycle for three successive months was given as an ovulation inducing agent.

FOLLOW-UP AND OUTCOME ASSESSMENT

Daily monitory for ovulation by transvaginal ultrasound was done starting from day 7 till day 25 of the cycle. The main outcomes were the number and the size of follicles. In addition, they were followed-up for evidence of pregnancy using biochemical serum and urine examination.

ETHICAL CONSIDERATIONS

The College of Medicine, University of Al-Qadisiyah's ethical approval committee granted the trial ethical approval. All enrolled women provided written consent following a thorough explanation of the current trial's methods and objectives. Formal agreements were acquired from the Iraqi Ministry of Health's official representative, the Directorate of Health.

STATISTICAL ANALYSIS

Data were transformed into an SPSS spread sheet (version 16) for purpose of statistical description and analysis. Categorical variables were expressed as percentage and number. Quantitative data were expressed as range, standard deviation, mean, median and inter-quartile range. Comparison of means was done using student t-test. Comparison of proportions was done using chi-square test. The level of significance was set at $p \leq 0.05$.

RESULTS

At the end of the study, 17 women showed positive pregnancy test and 13 women showed negative pregnancy test, thus the rate of biochemical pregnancy was 56.7% (Fig.1).

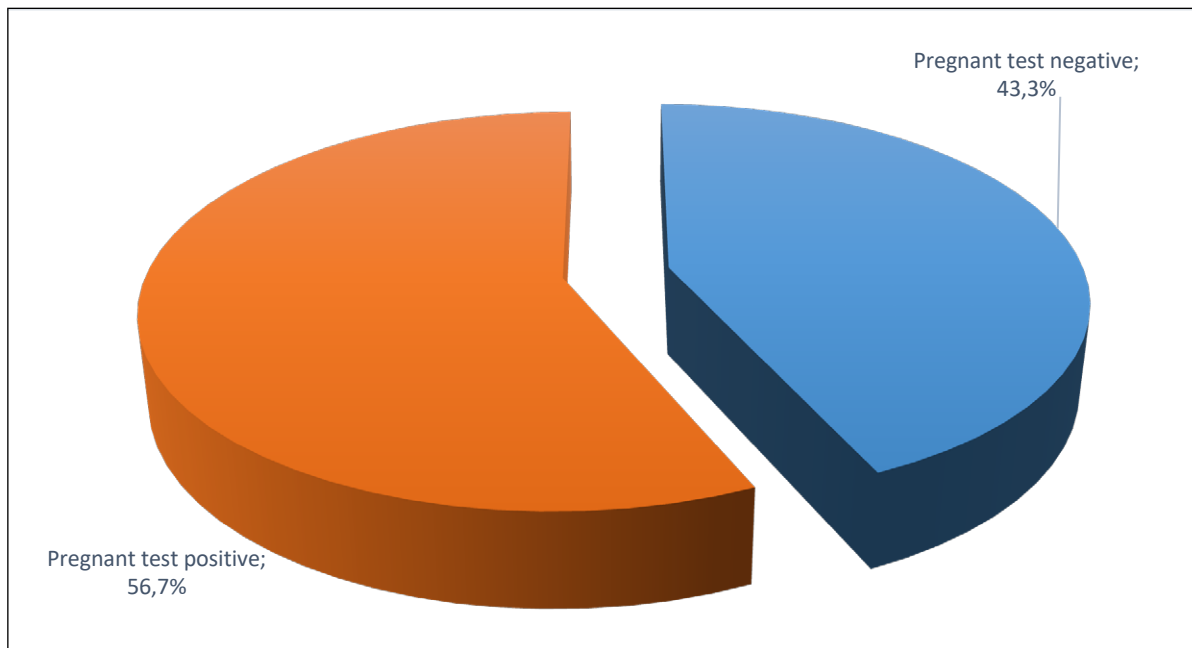


Fig. 1. Pregnancy test results among PCOS women at the end of the study.

Table 1. Comparison of characteristics of PCOS women with positive pregnancy test with those with negative pregnancy test

Characteristic	Pregnancy test positive n = 17	Pregnancy test negative n = 13	p
Age (years)			
Mean ±SD	24.05 ± 3.02	23.93 ± 4.12	> 0.05 NS
Range	20-35	19-35	
BMI (kg/m²)			
Mean ±SD	27.13 ± 7.11	29.02 ± 8.07	< 0.05 S
Range	20-35	19-35	
Duration of infertility			
Mean ±SD	2.15 ± 1.01	2.31 ± 0.92	> 0.05 NS
Range	2-5	2-5	
Size of follicles (mm)			
Mean ±SD	17.24 ± 3.05	9.02 ± 6.21	< 0.05 S
Range	15-19	7-18	
Number of follicles (>15 mm)			
Mean ±SD	4.01 ± 1.09	2.03 ± 0.97	< 0.05 S
Range	3-7	1-6	
Structure of follicles by size	<3 mm	0 (0.0%)	9 (69.2%)
	3-5 mm	10 (58.8%)	4 (30.8%)
	>5 mm	7 (41.2%)	0 (0.0%)

n: number of cases; SD: standard deviation; BMI: body mass index; NS: not significant; S: significant

The rest of results will be outlined so that characteristic of pregnant women will be contrasted to those of non-pregnant women. The mean age of pregnant and non-pregnant women did not significantly differ from one another, 24.05 ± 3.02 versus 23.93 ± 4.12 years, respectively $p > 0.05$. However, there was significant difference in mean body mass index (BMI) between pregnant

and non-pregnant women 27.13 ± 7.11 kg/m² versus 29.02 ± 8.07 kg/m², respectively $p < 0.05$; being lower in pregnant women. Between pregnant and non-pregnant women, there was no significant difference in the mean period of infertility 2.15 ± 1.01 years versus 2.31 ± 0.92 years, respectively $p > 0.05$. There was significant difference in mean size of follicles between pregnant

and non-pregnant women 17.24 ± 3.05 mm versus 9.02 ± 6.21 mm, respectively $p < 0.05$; the size being greater in pregnant women. In addition, there was significant difference in mean number of follicles > 15 mm in diameter between pregnant and non-pregnant women 4.01 ± 1.09 versus 2.03 ± 0.97 , respectively $p < 0.05$; the number being greater in pregnant women. Moreover, it was observed that none of women with positive pregnancy had follicle number > 15 mm in diameter of less than 3 and on the contrary, most of women with failure of pregnancy had mostly $<$ than 3 follicles of the size greater than 15 mm (Table 1).

DISCUSSION

The problem of infertility is the main problem facing women with PCOS in our community and the success of getting pregnant by PCOS women has dramatic impact on improving the quality of life of these women. Therefore, the medical research trying to solve this health issue in such women is of great importance. The main problem in PCOS is anovulation, thus the use of ovulation induction by medical ways is a corner stone approach in treating infertility in PCOS women. The drug of choice in this regard is clomiphene citrate; however, in substantial number of PCOS women, this approach was proved to be unsatisfactory. Therefore, it is increasingly recommended to use letrozole as a method of inducing ovulation; and yet, the results are also not so promising. It has been demonstrated that a lack of vitamin D is linked to a number of health issues. Numerous investigations have demonstrated a connection between chronic disorders such autoimmune diseases, endocrinological or tumorous states, and vitamin D insufficiency [20, 21]. Additionally, appropriate vitamin D intake has been suggested to help these patients feel better [22]. On several levels, vitamin D interacts with the epigenome, which controls around 3% of the human genome [23]. This vitamin insufficiency is prevalent in PCOS women, and vitamin D status in PCOS is associated with reproductive function, metabolic changes, and mental health [24]. The need for vitamin D is increased by obesity, PCOS, and pregnancy ϕ тв as a result, vitamin D deficiency is more prevalent and severe in people with these disorders than in healthy people [25, 26]. We suggested that the vitamin D may have a role in potentiating the effect of ovulation induction by improving ovarian response by still unknown mechanism, thus we

planned the current interventional study aiming at supplementing a sample of PCOS women, who previously failed to respond to letrozole, with vitamin D and combine this approach with another cycle of ovulation induction using letrozole. The results of our study pointed out to the substantial impact of vitamin D deficiency on ovulation response in women with PCOS and we found that 17 women out of 30 women succeeded to have pregnancy and that 21 women of them succeeded to have mature follicles of the size greater than 15 mm. The fact that vitamin D receptors (VDRs) are found in both male and female central and peripheral reproductive organs, tissues, and cells emphasizes the crucial significance of vitamin D related for fertility. VDRs are also discovered in the hypophysis, hypothalamus, granulosa cells, endometrial, placenta, decidua, testes, and cells involved in spermatogenesis in males [21, 27]. Some of the physiological effects of vitamin D include promoting follicular maturation and selection, follicular stimulation hormone (FSH) receptor gene expression, and the generation of the ovarian steroid hormones progesterone, estradiol, and estrone [28]. In line with our observations, vitamin D supplementation was included to IVF treatment for PCOS-afflicted women in a recent paper. Vitamin D levels strongly correlate with the likelihood of implantation and clinical pregnancy; they improve embryo quality-the number of high-quality embryos following vitamin D treatment equals that occurring in women with normal vitamin D levels. It was discovered that both implantation and the occurrence of clinical pregnancy were significantly higher in patients with normal vitamin D levels compared to those with decreased levels of vitamin D (20 ng/mL 25(OH)-vitamin D) [29].

CONCLUSIONS

Vitamin D supplementation improves ovulation induction and pregnancy outcome in women with polycystic ovarian syndrome treated with letrozole. Vitamin D levels strongly correlate with the likelihood of implantation and clinical pregnancy; they improve embryo quality-the number of high-quality embryos following vitamin D treatment equals that occurring in women with normal vitamin D levels. It was discovered that both implantation and the occurrence of clinical pregnancy were significantly higher in patients with normal vitamin D levels compared to those with decreased levels of vitamin D (20 ng/mL 25(OH)-vitamin D).

REFERENCES

1. Razzak AH, Wais SA. The infertile couple: a cohort study in Duhok, Iraq. *East Mediterr Health J.* 2002;8(2-3):234-238.
2. Ameen EM, Najim K, Sabir F, Mohammed SI. Relationships between semen quality and fertility in a population of infertile men in Erbil city. *Cell Mol Biol (Noisy-le-grand).* 2022;68(10):63-68. doi:10.14715/cmb/2022.68.10.9. [DOI](#)
3. Al-Kandari AM, Al-Enezi AN, Ibrahim H et al. A population-based study of the epidemiology and the risk factors for male infertility in Kuwait. *Urol Ann.* 2020;12(4):319-323. doi:10.4103/UA.UA_50_20. [DOI](#)
4. Vander Borgh M, Wyns C. Fertility and infertility: Definition and epidemiology. *Clin Biochem.* 2018;62:2-10. doi:10.1016/j.clinbiochem.2018.03.012. [DOI](#)
5. Warchol-Biedermann K. The etiology of infertility affects fertility quality of life of males undergoing fertility workup and treatment. *Am J Mens Health.* 2021;15(2):1557988320982167. doi:10.1177/1557988320982167. [DOI](#)
6. Hanson B, Johnstone E, Dorais J et al. Female infertility, infertility-associated diagnoses, and comorbidities: a review. *J Assist Reprod Genet.* 2017;34(2):167-177. doi:10.1007/s10815-016-0836-8. [DOI](#)
7. Deshpande PS, Gupta AS. Causes and prevalence of factors causing infertility in a public health facility. *J Hum Reprod Sci.* 2019;12(4):287-293. doi:10.4103/jhrs.JHRS_140_18. [DOI](#)
8. Louwers YV, Laven JSE. Characteristics of polycystic ovary syndrome throughout life. *Ther Adv Reprod Health.* 2020;14:2633494120911038. doi:10.1177/2633494120911038. [DOI](#)
9. Witchel SF, Oberfield SE, Peña AS. Polycystic ovary syndrome: pathophysiology, presentation, and treatment with emphasis on adolescent girls. *J Endocr Soc.* 2019;3(8):1545-1573. doi:10.1210/js.2019-00078. [DOI](#)
10. Chen W, Pang Y. Metabolic syndrome and PCOS: pathogenesis and the role of metabolites. *Metabolites.* 2021;11(12):869. doi:10.3390/metabo11120869. [DOI](#)
11. Melo AS, Ferriani RA, Navarro PA. Treatment of infertility in women with polycystic ovary syndrome: approach to clinical practice. *Clinics (Sao Paulo).* 2015;70(11):765-769. doi:10.6061/clinics/2015(11)09. [DOI](#)
12. Sawant S, Bhide P. Fertility treatment options for women with polycystic ovary syndrome. *Clin Med Insights Reprod Health.* 2019;13:1179558119890867. doi:10.1177/1179558119890867. [DOI](#)
13. Costello MF, Misso ML, Balen A et al. A brief update on the evidence supporting the treatment of infertility in polycystic ovary syndrome. *Aust N Z J Obstet Gynaecol.* 2019;59:867-873. doi:10.1111/ajo.13051. [DOI](#)
14. Escobar-Morreale HF. Polycystic ovary syndrome: definition, aetiology, diagnosis and treatment. *Nat Rev Endocrinol.* 2018;14:270-284. doi:10.1038/nrendo.2018.24. [DOI](#)
15. Teede HJ, Misso ML, Costello MF et al. Recommendations from the international evidence-based guideline for the assessment and management of polycystic ovary syndrome. *Fertil Steril.* 2018;110:364-379. doi:10.1016/j.fertnstert.2018.05.004. [DOI](#)
16. Cunha A, Póvoa AM. Infertility management in women with polycystic ovary syndrome: a review. *Porto Biomed J.* 2021;6(1):e116. doi:10.1097/j.pbj.000000000000116. [DOI](#)
17. Guang HJ, Li F, Shi J. Letrozole for patients with polycystic ovary syndrome: A retrospective study. *Medicine (Baltimore).* 2018;97(44):e13038. doi:10.1097/MD.00000000000013038. [DOI](#)
18. Vyrides AA, El Mahdi E, Giannakou K. Ovulation induction techniques in women with polycystic ovary syndrome. *Front Med (Lausanne).* 2022;9:982230. doi:10.3389/fmed.2022.982230. [DOI](#)
19. Morgante G, Darino I, Spanò A et al. PCOS pathophysiology and vitamin D deficiency: biological insights and perspectives for treatment. *J Clin Med.* 2022;11(15):4509. doi:10.3390/jcm11154509. [DOI](#)
20. Muscogiuri G, Altieri B, Annweiler C et al. Vitamin D and chronic diseases: The current state of the art. *Arch. Toxicol.* 2017;91:97-107. doi:10.1007/s00204-016-1804-x. [DOI](#)
21. Muscogiuri G, Altieri B, de Angelis C et al. Shedding new light on female fertility: The role of vitamin D. *Rev. Endocr. Metab. Disord.* 2017;18:273-283. doi:10.1007/s11154-017-9407-2. [DOI](#)
22. Rak K, Bronkowska M. Immunomodulatory effect of vitamin D and its potential role in the prevention and treatment of type 1 diabetes mellitus - a narrative review. *Molecules.* 2018;24:53. doi:10.3390/molecules24010053. [DOI](#)
23. Bouillon R, Carmeliet G, Verlinden L et al. Lessons from Vitamin D receptor null mice. *Endocr. Rev.* 2008;29:726-776. doi:10.1210/er.2008-0004. [DOI](#)
24. Mu Y, Cheng D, Yin T-L et al. Vitamin D and polycystic ovary syndrome: a narrative review. *Reprod. Sci.* 2021;28:2110-2117. doi:10.1007/s43032-020-00369-2. [DOI](#)
25. Holick MF. The vitamin D deficiency pandemic: Approaches for diagnosis, treatment and prevention. *Rev. Endocr. Metab. Disord.* 2017;18:153-165. doi:10.1007/s11154-017-9424-1. [DOI](#)
26. Takács I, Dank M, Majnik J et al. Magyarországi konszenzusajánlás a D-vitamin szerepéről a betegségek megelőzésében és kezelésében [Hungarian consensus recommendation on the role of vitamin D in disease prevention and treatment]. *Orv Hetil.* 2022;163(15):575-584. doi:10.1556/650.2022.32463. [DOI](#)

27. Frasiak JM, Lara-Molina EE, Pellicer A. Vitamin D in human reproduction. *Curr. Opin. Obstet. Gynecol.* 2017;29:189–194. doi:10.1097/GCO.0000000000000375. [DOI](#)
28. Voulgaris N, Papanastasiou L, Piaditis G et al. Vitamin D and aspects of female fertility. *Hormones.* 2017;16:5–21. doi:10.14310/horm.2002.1715. [DOI](#)
29. Zhao J, Liu S, Wang Y et al. Vitamin D improves in-vitro fertilization outcomes in infertile women with polycystic ovary syndrome and insulin resistance. *Minerva Med.* 2019;110:199–208. doi:10.23736/S0026-4806.18.05946-3. [DOI](#)

CONFLICT OF INTEREST

The Authors declare no conflict of interest

CORRESPONDING AUTHOR

Asma Swadi

University of Al-Qadisiyah

University District, Al Diwaniyah, Al-Qadisiyah Governorate, Iraq

e-mail: sgahmed1331962@outlook.com

ORCID AND CONTRIBUTIONSHIP

Asma Swadi: 0000-0002-7679-1596 [B](#) [C](#) [D](#)

Hussein Saheb: 0000-0002-0137-8932 [C](#) [D](#) [E](#)

Ahmed Sultan: 0000-0001-6819-0208 [A](#) [D](#) [E](#) [F](#)

[A](#) – Work concept and design, [B](#) – Data collection and analysis, [C](#) – Responsibility for statistical analysis, [D](#) – Writing the article, [E](#) – Critical review, [F](#) – Final approval of the article

RECEIVED: 27.11.2023

ACCEPTED: 12.08.2024



The study of the hypoxia markers against the background of prolonged hyperglycemia in experimental animals

Nataliya I. Preys¹, Ivan V. Savvitskyi¹, Olga Yu. Denisiuk¹, Vasyl M. Sarakhan²

¹INTERNATIONAL ACADEMY OF ECOLOGY AND MEDICINE, KYIV, UKRAINE

²ODESA NATIONAL MEDICAL UNIVERSITY, ODESA, UKRAINE

ABSTRACT

Aim: The aim of article is to investigate the energetic functions of retinal mitochondria under conditions of chronic hyperglycemia to understand the pathogenic mechanisms involved in the development of this diabetic complication.

Materials and Methods: The experimental study was carried out on non-linear rats which were divided into 2 groups: intact animals and rats with diabetic retinopathy. We investigated the level of lactate, pyruvate and adenine nucleotides.

Results: The increase in lactate and pyruvate levels may indicate a reduction in the energy potential of the retina under conditions of experimental diabetic retinopathy, while the elevation of adenine nucleotides activity suggests the activation of energy processes and the development of adaptation to hypoxia in retinal cells.

Conclusions: The analysis of lactate and pyruvate levels, as well as adenine nucleotides, may serve as prognostic markers in predicting the severity of diabetic retinopathy in the context of prolonged hyperglycemia.

KEY WORDS: diabetic retinopathy, hyperglycemia, pathogenesis, energy markers, experimental investigation

Wiad Lek. 2024;77(9):1759-1762. doi: 10.36740/WLek/194081 DOI

INTRODUCTION

Nowadays the problem of diabetes mellitus is one of the most pressing issues globally, given its prevalence, severity, and complications. The International Diabetes Federation reports that in 2023, diabetes was diagnosed in 463 million individuals, with 91% having type 2 diabetes. By 2045, the incidence of diabetes is projected to rise to 700 million people, accounting for over 10% of the entire population. The relentless increase in diabetes prevalence is linked to urbanization, an aging population, stress, a higher percentage of individuals with obesity, sedentary lifestyles, changes in food quality, and the rising availability of products containing hidden fats and carbohydrates, as well as genetically modified components [1, 2].

It is crucial to note that diabetes mellitus disrupts most metabolic processes, leading to an increased risk of tissue damage in the body, and potentially causing serious secondary complications. Due to the lack of timely patient consultations and late diagnosis of type 2 diabetes, by the time the diagnosis is established, 50% of patients already have complications associated with the development of micro- and macroangiopa-

thies, among which diabetic retinopathy (DR) is quite common. This pathology is increasingly widespread globally, taking on the characteristics of a non-communicable epidemic [2, 3].

Vascular pathologies are characterized by tissue hypoxia, leading to a deficit in energy status. DR is marked by disruptions in metabolic processes with pathological implications. Therefore, energy supply processes in retinal cells play a crucial role. Mitochondria serve as the "powerhouse" of the cell, participating in metabolic processes and respiration. Mitochondrial dysfunction significantly impacts tissue homeostasis. One of the primary functions of mitochondria is the production of adenosine triphosphate (ATP) – a molecule that acts as an "energy reservoir" for cells and the entire organism. There are two main pathways through which cells produce ATP: glycolysis and oxidative phosphorylation [3, 4, 5].

The retina is one of the most metabolically active tissues in the body, consuming more oxygen than the brain. Significant changes in mitochondrial bioenergetics can disrupt the functioning of the electron transport chain in mitochondria [4].

AIM

Study the features of the energetic functions of retinal mitochondria under conditions of chronic hyperglycemia to expand the understanding of the pathogenic mechanisms involved in the development of DR.

MATERIALS AND METHODS

The experimental study was carried out on non-linear rats. Controls were intact rats that received distilled water intragastrically. A streptozotocin model was used to reproduce type 2 diabetes. This model makes it possible to reproduce the main pathogenetic links of type 2 diabetes in humans – impaired secretion and action of insulin and is characterized by the development of intolerance to carbohydrates, relative insufficiency of insulin secretion in response to elevated glucose levels, and preservation of the secretory response to non-glucose secretogens. For this purpose, streptozotocin (SigmaAldrich Chemie GmbH, Germany) was administered to rats once intravenously at a dose of 65 mg/kg. Streptozotocin solution was prepared in 0.1 M citrate buffer (pH 4.5). In order to reduce the diabetogenic effect of streptozotocin, 15 minutes before its administration, nicotinamide (Afton Pharma, India) was administered intraperitoneally at a dose of 230 mg/kg, which allows preserving up to 40% of pancreatic insulin reserves in experimental rats, due to which the animals develop a stable basal hyperglycemia [6].

Lactate activity was determined using a kinetic method based on the reduction of pyruvate in the presence of NADH. The lactate content was measured using a spectrophotometric method, which relies on the formation of a lactate-iron complex with a maximum absorption at 390 nm [7].

Pyruvate content was assessed using the Umbreit method, which is based on the formation of a hydrazone when pyruvic acid reacts with 2,4-dinitrophenylhydrazine, expressed in mmol/mg of protein [6, 7].

The levels of adenine nucleotides (ATP, ADP) were determined using high-voltage paper electrophoresis followed by spectrophotometry at wavelengths of 260 and 290 nm [7].

In working with animals we adhered to the International Code of Medical Ethics (Venice, 1983), the “European Convention for the Protection of Vertebrate Animals Used for Experimental and Other Scientific Purposes” (Strasbourg, 1986), the “General Ethical Principles of Animal Experiments” adopted at the First National Congress on Bioethics (Kyiv, 2001), Directive 2010/63/EU of the European Parliament and Council on the protection of animals used for scientific purposes, and the Law of Ukraine “On the Protection of Animals from Cruel Treatment” No. 440-IX dated January 14, 2020.

Statistical processing of the obtained results was carried out with the help of the “Statistica 10.0” program. The probability of differences between the indicators of the control and experimental groups was determined by Student’s and Fisher’s tests. The level of reliability was accepted at $p < 0.05$.

RESULTS AND DISCUSSION

A significant increase in lactate levels in serum was observed: on day 60 there was in 1.2 times ($p < 0.05$), and on day 120 – in 1.8 times ($p < 0.05$) compared to intact animals (Table 1). Additionally, significant differences were noted between the results obtained on days 60 and 120 of the experiment.

The level of pyruvate on day 60 also increased significantly in 1.2 times ($p < 0.05$) compared to intact rats (0.245 ± 0.016 mmol/L vs. 0.294 ± 0.019 mmol/L); on day 120 this parameter rose in 1.4 times ($p < 0.05$) respectively (0.352 ± 0.026 mmol/L vs. 0.294 ± 0.019 mmol/L).

We found that ATP concentration in serum on day 60 was 704.8 ± 42.7 nmol/L, which was in 1.1 times lower than that of intact animals; on day 120 it was in 1.4 times lower ($p < 0.05$). ATP levels also showed significant differences over the course of the study.

ADP levels on the day 60 decreased in 1.2 times ($p < 0.05$) compared to the intact group (305.72 ± 14.6 nmol/L vs. 361.06 ± 17.4 nmol/L); on day 120 – in 1.3 times ($p < 0.05$) respectively (270.8 ± 15.2 nmol/L vs. 361.06 ± 17.4 nmol/L).

When studying these parameters in the retina, similar changes were found as in serum (Table 2). The lactate level on day 60 increased in 1.4 times ($p < 0.05$) compared to intact animals (7.98 ± 0.73 mmol/g vs. 5.67 ± 0.51 mmol/g); on day 120 – in 2.0 times ($p < 0.05$) respectively (11.2 ± 0.9 mmol/g vs. 5.67 ± 0.51 mmol/g).

On day 60 the level of pyruvate was 0.241 ± 0.018 mmol/g, which was in 1.2 times ($p < 0.05$) higher than that of intact rats; on day 120 this parameter increased in 1.5 times ($p < 0.05$) to 0.288 ± 0.018 mmol/g compared to 0.198 ± 0.016 mmol/g in the control group.

The concentration of ATP and ADP in the retina showed the following changes: a significant decrease in ATP and ADP was noted on day 60 with reductions in 1.3 times ($p < 0.05$) and in 1.2 times ($p < 0.05$), respectively, compared to the intact group (2.51 ± 0.16 μ mol/g vs. 3.33 ± 0.21 μ mol/g; 0.725 ± 0.050 μ mol/g vs. 0.847 ± 0.067 μ mol/g). On day 120 ATP and ADP levels were 1.84 ± 0.14 μ mol/g and 0.641 ± 0.035 μ mol/g, which were lower in 1.8 times ($p < 0.05$) and in 1.3 times ($p < 0.05$), respectively, compared to the intact group.

We experimentally established that under conditions of prolonged hyperglycemia, rats with diabetic retinopathy develop a hypoxic state in the retina, with

Table 1. Study of the mitochondria energy profile of in the serum of rats with experimental diabetic retinopathy ($\bar{X} \pm Sx$)

Indicator	Intact group (n=10)	Control group (n=20)	
		On day 60	On day 120
Lactate, mmol/L	2,61±0,19	3,25±0,21*	4,57±0,30*/**
Pyruvate, mmol/L	0,245±0,016	0,294±0,019*	0,352±0,026*
ATP, nmol/L	807,61±60,3	704,8±42,7	576,9±35,8*/**
ADP, nmol/L	361,06±17,4	305,72±14,6*	270,8±15,2*/**

Notes:

1. * – $p < 0.05$ compared to the intact group of animals;
2. ** – $p < 0.05$ relative to the values obtained on day 60;
3. n – number of animals in the group.

Table 2. Study of the mitochondria energy profile of in the retina of rats with experimental diabetic retinopathy ($\bar{X} \pm Sx$)

Indicator	Intact group (n=10)	Control group (n=20)	
		On day 60	On day 120
Lactate, mmol/g	5,67±0,51	7,98±0,73*	11,2±0,9*/**
Pyruvate, mmol/g	0,198±0,016	0,241±0,018*	0,288±0,018*
ATP, μ mol/g	3,33±0,21	2,51±0,16*	1,84±0,14*/**
ADP, μ mol/g	0,847±0,067	0,725±0,050*	0,641±0,035*/**

Notes:

1. * – $p < 0.05$ compared to the intact group of animals;
2. ** – $p < 0.05$ relative to the values obtained on day 60;
3. n – number of animals in the group.

increased levels of biochemical markers such as lactate and pyruvate compared to intact animals [8]. At the same time, a significant decrease in ATP and ADP was observed in the animals with the modeled pathology.

Lactate is an indicator of bioenergetic hypoxia and one of the primary markers of mitochondrial dysfunction. It is considered an early prognostic marker, as its levels rise before other signs of oxygen deprivation. The accumulation of lactic acid occurs when glycolytic breakdown of glucose surpasses the oxidation of pyruvate in mitochondria, typically due to reduced oxygen availability and mitochondrial dysfunction. In this case, the organism "switches" to a less efficient (anaerobic) energy production pathway through glucose breakdown, generating ATP. Lactate is the main byproduct of this anaerobic process. A significant increase in lactate in the plasma indicates mitochondrial dysfunction [2, 4, 9].

Furthermore, the lactate/pyruvate ratio reflects the balance between glycolytic and oxidative metabolism of carbohydrates [10].

In our study, alongside identifying hypoxia in the retinas of rats with modeled DR, we observed a decrease in the levels of adenine nucleotide metabolites ATP and ADP in both the retina and serum of experimental animals. These nucleotides serve as markers of cellular energy potential. As known, ATP and ADP levels are important regulators of insulin secretion, which is

stimulated by glucose levels. In aerobic cells, phosphorylation potential is regulated by mechanisms typical of mitochondrial metabolism, leading to compensatory changes in electron transport. Alterations in mitochondrial energy function can result in damage to the entire mitochondrial electron transport chain [4, 7, 10].

Thus, the results obtained from the DR model regarding the likely metabolic mechanisms underlying the protective action of the eye against the development of diabetic complications in the retina will be significant for further understanding the pathogenesis of diabetic retinopathy.

CONCLUSIONS

1. The increase in lactate and pyruvate levels may indicate a reduction in the energy potential of the retina under conditions of experimental diabetic retinopathy, while the elevation of ATP and ADP activity suggests the activation of energy processes and the development of adaptation to hypoxia in retinal cells.
2. The analysis of lactate and pyruvate levels, as well as ATP and ADP, may serve as prognostic markers in predicting the severity of diabetic retinopathy in the context of prolonged hyperglycemia. These markers play an important role in understanding the pathogenic mechanisms underlying the development of retinopathy.

REFERENCES

1. Shani M, Eviatar T, Komaneshter D, et al. Diabetic Retinopathy - Incidence and Risk Factors in A Community Setting- A Longitudinal Study. *Scand. J. Prim. Health Care.* 2018;36:237-241.
2. Wong TY, Cheung CM, Larsen M, et al. Diabetic retinopathy. *Nature Reviews Disease Primers.* 2016;2:e16012.
3. Ansari P, et al. Diabetic retinopathy: an overview on mechanisms, pathophysiology, and pharmacotherapy. *Diabetology.* 2022;3(1):159-175.
4. Hammes HP, Lemmen KD, Bertram B. Diabetic Retinopathy and Maculopathy. *Experimental and clinical endocrinology & diabetes : official journal, German Society of Endocrinology [and] German Diabetes Association.* 2023;131(1-02):66-71.
5. Coughlin BA., Feenstra DJ., Mohr S. Müller cells and diabetic retinopathy. *Vision Res.* 2017;139:93-100.
6. Sirman YaV., Savytskyi IV, Preys NI. Prediction model for severity of diabetic retinopathy derived from review of endothelial dysfunction and hypoxia markers. *Mižnarodnij endokrinologičnij žurnal.* 2021;17(1):76-80.
7. Gao Y, Xue M, Dai B, et al. Identification of immune associated potential molecular targets in proliferative diabetic retinopathy. *BMC ophthalmology.* 2023;23(1):27.
8. Kaštelan S, Orešković I, Biščan F, et al. Inflammatory and angiogenic biomarkers in diabetic retinopathy. *Biochemia medica.* 2020;30(3):e030502.
9. Peng W, Zhang M, Yi X. Systemic Inflammatory Mediator Levels in Non-Proliferative Diabetic Retinopathy Patients with Diabetic Macular Edema. *Current eye research.* 2025;49(1):80-87.
10. Spencer BG, Estevez JJ, Liu E, et al. Pericytes, inflammation, and diabetic retinopathy. *Inflammopharmacology.* 2020;28(3):697-709.

CONFLICT OF INTEREST

The Authors declare no conflict of interest

CORRESPONDING AUTHOR

Ivan Savytskyi

International Academy of Ecology and Medicine

121 Kharkivske Avenue, Kyiv, Ukraine

e-mail: prof_S.I.V@ukr.net

ORCID AND CONTRIBUTIONSHIP

Nataliya I. Preys: 0000-0002-0026-6218 **A** **B** **C** **D**

Ivan V. Savytskyi: 0000-0002-5841-9993 **A** **B** **C** **F**

Olga Yu. Denisiuk: 0000-0001-5648-5228 **E** **F**

Vasyl M. Sarakhan: 0000-0002-6773-5672 **D** **E**

A – Work concept and design, **B** – Data collection and analysis, **C** – Responsibility for statistical analysis, **D** – Writing the article, **E** – Critical review, **F** – Final approval of the article

RECEIVED: 04.06.2024

ACCEPTED: 27.08.2024



Problems of diagnostic of the state of pulp and pulpal diagnoses in children

Lyudmyla Kaskova, Nataliia Yanko, Iryna Vashchenko, Olena Khmil

POLTAVA STATE MEDICAL UNIVERSITY, POLTAVA, UKRAINE

ABSTRACT

Aim: To analyze diagnostic methods of the pulp status in children and align pulpal diagnoses with international and Ukrainian classifications.

Materials and Methods: The authors searched for articles via Google using keywords such as «pulpitis classification», «pulp diagnostic in children», «reversible pulpitis», «irreversible pulpitis», «pulp necrosis» combined with «primary teeth», «permanent immature teeth». Also evidence of primary data was evaluated by levels of evidence statements and grades of recommendations for questions relating to diagnosis.

Results: Level of evidence of primary data about methods of pulpal state diagnosis varies from 2 to expert opinion, grade of recommendation is C-D. Sensibility tests can be used for pulp diagnosing in primary and immature permanent teeth, in conjunction with other clinical diagnostic aids. Such conditions of pulp as complete pulp necrosis, pulpless and infected root canal system, previously treated pulpitis, and previously initiated therapy could be included in the Ukrainian classification. Pulp hyperplasia only partially corresponds pulpitis chronica hypertrophica and may be associated with any form of reversible and irreversible pulpitis. In international classifications, partial pulp necrosis includes pulpitis chronica gangraenosa and pulpitis acuta purulenta from the Ukrainian variant.

Conclusions: Pulpal diagnosis in children relies on observation of clinical and periapical radiographic findings. While the Ukrainian classification covers various forms of pulpitis, it could be expanded to include pulp conditions, but only some of them completely correspond diagnoses of the Ukrainian classification. Therefore, the development of new classification of the status of the pulp in children is promising and challenging task.

KEY WORDS: pulp, children, diagnosis

Wiad Lek. 2024;77(9):1763-1768. doi: 10.36740/WLek/191319 DOI

INTRODUCTION

Nature of different pulp conditions is complicated. For example, it has been found that not only oxidative stress plays role in periodontal inflammation [1], but and the caries-related inflammation alters the oxidative stress cycle in dental pulp tissue [2]. Also different bacterial species have been found in deep caries cavities [3,4], making diverse pulp inflammation.

Diagnostic tools to make endodontic diagnosis in adults have less value for primary teeth and limited in their use in immature permanent teeth. Ukrainian classification of pulpitis in children [5] has serious differences with international classifications [6,7]. Due to the use of international classifications at private dental practice in Ukraine, and the need to make standard treatment protocols, we have focused on the methods of pulpitis diagnostic in primary and permanent teeth in children and the international classifications of pulp diseases. The aim of this article is to analyze diagnostic methods of the status of the pulp in children and align

pulpal diagnoses with international and Ukrainian classifications.

AIM

The aim was to analyze diagnostic methods of the pulp status in children and align pulpal diagnoses with international and Ukrainian classifications.

MATERIALS AND METHODS

The authors searched for articles and scientific publications via Google using keywords such as «pulpitis classification», «pulp diagnostic in children», «reversible pulpitis», «irreversible pulpitis», «pulp necrosis» combined with «primary teeth», «permanent immature teeth». Additional publications were identified by checking the references of review and original articles. Also evidence of primary data was evaluated by levels of evidence statements and grades of recommendations for questions relating to diagnosis [8].

REVIEW AND DISCUSSION

METHODS OF PULPAL STATE DIAGNOSIS

The ideal technique for the evaluation of the dental pulp status in children needs to be non-invasive, objective, painless, reliable, reproducible, standardized, easy to employ (a simple technique) and fast [9].

The American Academy of Pediatric Dentistry (AAPD) recommends to use diagnostic criteria for pulpitis in children, which were described by Camp [10] (grade of recommendation - D). The clinical diagnosis of pulpitis is based on:

- medical history;
- review of past and present dental history and treatment, including current symptoms;
- subjective evaluation of the area associated with current symptoms by questioning the patient/parent on the location, intensity, duration, stimulus, relief, and spontaneity;
- objective extraoral and intraoral examination;
- radiographs to diagnose periapical or periradicular changes;
- clinical tests such as palpation, percussion, and mobility; electric pulp and thermal tests are considered as unreliable in immature permanent and primary teeth.

In order to avoid behavior management problems, when performing percussion and palpation tests in children, the fingertip should be gently used in combination with Tell, Show, and Do (TSD) technique [11]. The dentist should start the test with a contralateral non-affected tooth to familiarize the patient with a normal response to the stimuli. Comparing the mobility of a suspicious tooth with its opposite equivalent can be helpful for differential diagnosis [12].

There are two groups for pulp testing – tests for pulp sensibility and vitality. Sensibility pulp tests include thermal, electric pulp testing, selective anesthesia, and test cavity (preparation). The test of cavity preparation may prove tooth vitality, but is not suitable for children; selective anesthesia is also considered unappropriated.

Cold and electric pulp testing in primary teeth are to be applied only in children who can understand the instructions and provide an adequate response to the stimuli. These tests may yield unreliable data due to fear, management problems, and inability to understand or communicate accurately [13]. Moreover, International Association of Dental Traumatology considers pulp sensitivity tests and percussion as unreliable in primary teeth (grade of recommendation – D) [14].

If a dentist uses cold or electric pulp test, control teeth should be tested first. The cold test should be applied to the tooth for 10 seconds or until the patient responds

definitively. Electric pulp test helps to differentiate caries and its complications in permanent teeth, however, it could not be used to distinguish between reversible pulpitis from an irreversible one (level of evidence 3) [15]. Hori et al. [16] reported about 73.3% and 80% sensitivity of the cold test and electric pulp in primary teeth, accordingly (level of evidence 3). The diagnostic accuracy of the electric pulp test was 76.2% and 92.5%, the cold test had a diagnostic accuracy of 85% and 92.5% in the incomplete and complete central incisors (level of evidence 2, grade of recommendation C) [17]. Therefore, sensibility tests can be used for diagnosing of the status of the pulp in primary and immature permanent teeth, in conjunction with other clinical diagnostic aids.

Tests for pulp vitality (laser doppler flowmetry, pulse oximetry, etc.) are limited to teeth containing pulp tissue within the coronal part of the tooth [18]. Despite this limitation, they are considered useful for diagnosing pulpitis in primary and immature permanent teeth [19]. Unfortunately, these tests are mostly unavailable in everyday clinical practice. In Brazilian survey, only a few pediatric dentists reported about using of laser doppler flowmetry; also 93.7% of them reported about using sensibility tests routinely and cold and electric pulp tests equally (level of evidence 2) [20].

Consequently, most diagnoses in pediatric dentistry rely on observation of clinical symptoms and evidence of periapical radiographic changes [11]. Level of evidence of primary data about methods of pulpal state diagnosis varies from 2 to expert opinion, grade of recommendation is C-D.

PULPAL DIAGNOSES IN PRIMARY TEETH

The authors aligned Ukrainian classification of pulpitis in children [5], pulpal diagnoses approved by American Association of Endodontics (AAE), which is the recommended best practice based on the clinical experience of the guideline development group (level of recommendation - D) [6], and Abbott's classification of the conditions of the pulp and root canal system (expert opinion, level of recommendation – D) [7]. A complete endodontic diagnosis includes both a pulpal and a periapical diagnosis for each tooth evaluated.

Normal pulp and periodontium (AAE and Abbott's classifications). No pain, tooth has a small caries cavity or a part of crown is absent due trauma. Pulp chamber is close, probing is painless. In a case of dental trauma, temporary loss of pulp sensitivity is possible for 4-6 weeks (grade of recommendation – D) [14]. The cold test gives the response which disappears with stimulus removal. Percussion is painless, palpation of oral mu-

cosa about roots is painless. There are no radiographic changes.

Reversible pulpitis (with normal periodontium) from AAE and Abbott's classifications. Diagnosis is made on observation of several subjective and objective symptoms. Patient complains of provoked short-time pain upon removal of the stimulus (cold or sweet food, tooth brushing, chewing) – acute reversible pulpitis, or no complains – chronic reversible pulpitis. Asymptomatic manifestation with pulp exposure corresponds pulpitis chronica fibrosa in Ukrainian classification. The history of pain presented for a few hours to days. There is no spontaneous and nighttime pain. Tooth has a deep caries lesion without pulp exposure; pulp exposure could be revealed only after dentin excavation [21]. Pulpal exposure may be clinical or radiographic; the thickness of circumpalpal dentin on roentgenogram for reversible pulpitis is not less 1 mm [12]. Probing of exposed pulp is painful, light red small drop of pulp is found, with bleeding that can be controlled within five minutes. The tooth also may have filling or crown fracture. The cold test causes pain for a few seconds. There are no such symptoms of apical periodontitis as painful percussion, painful palpation of mucosa about roots, a sinus tract, inflammation of oral mucosa not resulting from periodontal disease, excessive mobility not associated with trauma or exfoliation, furcation/apical radiolucency, or radiographic evidence of internal/ external resorption [10].

Such diagnosis is available until the period of physiological resorption of roots in primary teeth. Dentist may make such provisional diagnosis if stimuli induce a short-time pain, no spontaneous pain and periapical inflammation. In this case the tooth needs vital therapy and follow-ups for 3 months, and pulp sensitivity could get over or pulp necrosis becomes evident [7].

Irreversible pulpitis (same in AAE and Abbott's classifications, no such diagnosis in the Ukrainian classification). It includes cases with and without apical periodontitis. A radiograph may show intra-root resorption. The cold test provokes a long-time pain for minutes. Profuse dark pulp bleeding is a symptom of irreversible pulpitis [20]. Pain provoked by eating for a short duration (5-10 minutes). The diagnosis of irreversible pulpitis cannot be solely rely on pulpal bleeding that be controlled more five minutes without other clinical symptoms. However, there are no evident recommendations for irreversible pulpitis in primary teeth [22].

Symptomatic (acute) irreversible pulpitis (same in AAE an Abbott's classifications, pulpitis acuta serosa diffusa in the Ukrainian classification) is characterized by spontaneous, paroxysmal pain and provoked pain in response to cold, heat stimuli. The tooth has a deep

caries lesion without pulp exposure or filling. Probing of bottom of caries cavity is painful. The tooth may be tender to biting pressure and/or percussion and, if present, this usually indicates spread of the inflammatory process to the periapical tissues.

Asymptomatic (chronic) irreversible pulpitis (pulpitis chronica fibrosa in Ukrainian classification) is characterized by provoked pain to cold, heat stimuli. No pain [18] or provoked/spontaneous pain in past [17]. Tooth has a deep caries lesion with or without pulp exposure, or filling. If no pulp exposure, probing of bottom of caries cavity is painful. Probing of exposed pulp is painful and provokes bleeding.

Pulp hyperplasia is a kind of degenerative changes in the pulp (Abbott's classification) which may exhibit symptoms of irreversible pulpitis [3]. It is pulpitis chronica hypertrophica in the Ukrainian classification. Caries cavity united with pulp chamber and filled by pulp polyp. If there are no complains or provoked pain, probing of polyp is painless, and it can be chronic irreversible pulpitis, if a patient experiences pain when eating, probing of polyp is painful, provoked bleeding, it can be acute irreversible pulpitis. Pulp polyp is not connected with gums. The cold test may elicit a response for minutes. It may be associated with chronic apical periodontitis.

Partial pulp necrosis (pulp condition in Abbott's classification). Similar symptoms with pulpitis chronica gangraenosa in the Ukrainian classification: sensitivity to hot stimuli that persists after the stimulus is removed; deep caries cavity connected with pulp chamber; tooth may have filling or grey crown; halitosis. Also probing of pulp chamber is painless, root canals – painful. May be associated with acute or chronic apical periodontitis.

Complete pulp necrosis (AAE and Abbott's classifications). There is complete pulp necrosis with and without apical periodontitis. Asymptomatic pulpitis. History of provoked pain, trauma or filling. Deep caries cavity united with pulp chamber, or tooth has filling or grey crown. No reaction to the cold test. Preparation test is negative. Unfortunately, there are no clear recommendations for diagnostic of pulp necrosis in primary teeth (grade of recommendation – D) [22]. The authors disagree with Mohammad et al. [23] who did not divide pulp necrosis in primary teeth on partial and complete, emphasizing that pain may or may not be spontaneous, pain is elicited by various stimuli, and response to various testing modalities is usually absent.

Pulpless and infected root canal system is considered by Abbott as a pulp condition which develops after pulp necrosis. No pulp sensitivity. Obligatory sign is periapical radiolucency (sign of chronic apical periodontitis). Only this pulp condition might be associated with symptoms of exacerbation of chronic apical periodon-

titis. No such diagnosis in the Ukrainian classification.

Previously Treated Pulpitis (AAE and Abbott's classifications). Root canals are filled or not, with or without symptoms of apical chronic periodontitis [6]. If endodontic treatment was adequate, the tooth does not respond to stimulation. Symptoms may or may not be present, indicating chronic apical periodontitis.

Previously Initiated Therapy (AAE and Abbott's classifications) [7] the tooth has been previously treated by endodontic therapy such as pulpotomy or pulpectomy. Depending on the level of therapy, the tooth may or may not respond to pulp testing modalities. Symptoms may or may not be present, indicating chronic apical periodontitis.

THE STATUS OF THE PULP DIAGNOSIS IN PERMANENT TEETH

Normal pulp and periodontium. No pain, tooth has a small caries cavity or a part of crown is absent due trauma. The pulp chamber is close, probing is painless. The pulp responds to thermal and electrical tests in a manner similar to that of a corresponding control tooth. The reaction to the cold test in mature permanent teeth up to 2 seconds [18]. In a case of dental trauma, temporary loss of pulp sensitivity can occur for 6-8 weeks [14]. Percussion is painless, palpation of oral mucosa about roots is painless. There are no radiographic changes.

Reversible pulpitis (with normal periodontium). It is diagnosed based on observation of several subjective symptoms. Patient complains of provoked short-time pain upon removal of the stimulus (cold or sweet food, tooth brushing) – acute reversible pulpitis, or no complains – chronic reversible pulpitis. There is no spontaneous and nighttime pain [7]. History of pain presents for few hours-days.

The tooth exhibits a deep caries lesion without pulp exposure or pulp exposure is revealed after dentin excavation [7]. The tooth also may have filling or crown fracture. Probing of the exposed pulp is painful, light red small drop of pulp is found. The cold test provokes a long-time pain for a few seconds, this test is longer in immature permanent teeth (level of evidence 4) [12]. Pain is typically triggered by extreme temperature changes (ice cream and cold drink from the fridge) [7]. There are no symptoms of apical periodontitis [10]. Dentist may make such provisional diagnosis if stimuli induce a short-time pain, no spontaneous pain and periapical inflammation. In this case the tooth needs vital therapy and follow-ups for 3 months, and pulp sensitivity could get over or pulp necrosis becomes evident [7]. However, the symptoms of pulp hyperaemia and pulpitis acuta limita (from the Ukrainian classification) do not correspond symptoms of reversible pulpitis.

Irreversible pulpitis. There is irreversible pulpitis with and without apical periodontitis. A radiograph may have intra-root resorption. One of the criteria that is commonly used to "con-

sider" irreversible pulpitis is the 10 seconds of lingering pain after conducting a cold test on tooth.

Symptomatic (acute) irreversible pulpitis is characterized by spontaneous, paroxysmal pain which lasts for a few seconds to a few hours, irradiation pain, waking at night, and worse lying down. The patient typically has a history of pain for a few days. The tooth has a deep caries lesion without pulp exposure and a recent restoration. Probing of the bottom of the caries cavity is painful. The tooth may be tender to biting pressure and/or percussion and, if present, this usually indicates spread of the inflammatory process to the periapical tissues.

Asymptomatic (chronic) irreversible pulpitis is characterized by provoked pain to cold, heat stimuli. Occasionally, there may be pain when exposed to heat, cold, and/or biting for a few months, often preceded by a restoration procedure. Sharp provoked pain, then a dull ache that lingers (more than five minutes). The tooth has a deep caries lesion with or without pulp exposure. If there is no pulp exposure, probing of bottom of caries cavity is painful. Probing of exposed pulp is painful and provokes bleeding.

Pulp hyperplasia. Caries cavity connected with pulp chamber and filled by a pulp polyp which is not connected with gums. The pulp polyp may bleed on probing, may or may not be sensitive to probing. This pulp condition may have clinical manifestations of acute and chronic reversible and irreversible pulpitis [7]. The tooth will respond to pulp sensibility tests depending on the type of pulpitis present. It may be associated with chronic apical periodontitis.

Partial pulp necrosis. The pain has only been present for a short time (a few days or less); triggered by heat, cold or biting; if temperature changes cause pain then usually only minor temperature changes required (tap water); pain lingers for a long time; pain may be spontaneous. Patient may have had a recent restoration; crown is grey, deep caries cavity, united with pulp chamber. If the pulp chamber is close, a "bead" of pus may emerge when the pulp chamber is opened, relieving the pain. If the pulp chamber is open, its probing is painless, but probing of the root canals is painful. Halitosis might be present. Sometimes, pulp sensibility test results may be mixed and frequently inconclusive or inconsistent with the patient's description of symptoms [7]. Chronic apical periodontitis may be associated with this condition. The authors suggest that these symptoms both correspond pulpitis chronica gangraenosa, which reacts only to hot stimulus and develops over time, and pulpitis acuta purulenta from the Ukrainian classification, which presents with spontaneous pain, close pulp chamber, and pus upon opening.

Complete pulp necrosis. It may or may not be associated with apical periodontitis. Asymptomatic pulpitis [18]. History of provoked pain, trauma or filling. Deep caries cavity united with pulp chamber, or tooth has filling or grey crown. Test cavity (preparation) is negative. Negative cold test proves pulp necrosis if tooth has caries cavity (level of evidence 2)

[23]. However, a negative cold test is not necessarily indicative of pulp necrosis in cases of trauma [12].

Pulpless and Infected Root Canal System is considered by Abbott as a pulp condition which develops after pulp necrosis. No pulp sensitivity. Obligatory sign is periapical radiolucency (sign of chronic apical periodontitis). Symptoms of exacerbation of chronic apical periodontitis may occur in this pulp condition.

Previously Treated Pulpitis. Root canals are filled, with or without symptoms of apical chronic periodontitis [6]. The tooth's response to pulp testing modalities depends on the level of therapy received. There are symptoms or no symptoms of chronic apical periodontitis.

Previously Initiated Therapy. The tooth has been previously treated by endodontic therapy such as pulpotomy or pulpectomy [6]. Depending on the level of therapy, the tooth may or may not respond to pulp testing modalities. There are symptoms or no symptoms of apical chronic periodontitis. 94,7% of the permanent teeth react to electric pulp test 1 year after pulpotomy, and 13,5% - to cold test (level of evidence 3b) [24]. There are symptoms or no symptoms of chronic apical periodontitis.

Pulp canal calcification is considered by Abbott as a «condition» rather than as a «disease» [7] with radiographic observation of the appearance of the root canals, emphasizing that all pulpal diagnoses could be associated with such calcification. Therefore, pulp canal calcification does not align with pulpitis chronica concrementosa from the Ukrainian

classification. This pulp condition does not respond to pulp sensibility tests by the symptoms and other clinical findings, and may be associated with periapical conditions.

To sum up, reversible and irreversible pulpitis have the respondents in Ukrainian classification. Such conditions of pulp as complete pulp necrosis, pulpless and infected root canal system, previously treated pulpitis, and previously initiated therapy could be included in the Ukrainian classification. Pulp hyperplasia only partially corresponds pulpitis chronica hypertrophica and may be associated with any form of reversible and irreversible pulpitis. In international classifications, partial pulp necrosis includes pulpitis chronica gangraenosa and pulpitis acuta purulenta from the Ukrainian variant. Therefore, the development of new classification of the status of the pulp in children is promising and challenging task.

CONCLUSIONS

Pulpal diagnosis in children relies on observation of clinical and periapical radiographic findings. While the Ukrainian classification covers various forms of pulpitis, it could be expanded to include pulp conditions. Such pulp conditions as pulp hyperplasia and partial pulp necrosis only partially correspond diagnoses of the Ukrainian classification. Therefore, the development of new classification of the status of the pulp in children is promising and challenging task.

REFERENCES

1. Dogan Buzoglu H, Ozcan M, Bozdemir O et al. Evaluation of oxidative stress cycle in healthy and inflamed dental pulp tissue: a laboratory investigation. *Clin Oral Investig*. 2023. doi: 10.1007/s00784-023-05203-y. [DOI](#)
2. Yelins'ka AM, Akimov OY, Kostenko VO. Role of AP-1 transcriptional factor in development of oxidative and nitrosative stress in periodontal tissues during systemic inflammatory response. *Ukrainian Biochemical Journal*. 2019;91(1): 80-85. doi: 10.15407/ubj91.01.080. [DOI](#)
3. Faustova MO, Ananieva MM, Basarab YO et al. Bacterial factors of cariogenicity (literature review). *Wiad Lek*. 2018;71(2):378-382.
4. Ananieva MM, Faustova MO, Basarab IO et al. *Kocuria rosea*, *kocuria kristinae*, *leuconostoc mesenteroides* as caries-causing representatives of oral microflora. *Wiad Lek*. 2017;70(2): 296-298.
5. Khomenko LO et al. *Terapevtychna stomatolohiia dytiachoho viku. Kariies zubiv ta yoho uskladnennia* [Pediatric therapeutic dentistry. Dental caries and its complications]. Kyiv: Knyha-plius. 2016, p.432. (Ukrainian)
6. Gerald N, Glickman L, Jordan L et al. *Endodontic diagnosis*. Chicago: American Association of Endodontists. 2013. www.aae.org/colleagues. [Accessed 20 December 2023]
7. Abbott PV. Examination and diagnosis of pulp, root canal, and periapical/periradicular conditions. In: I Rotstein, JI Ingle (Eds.) *Ingle's endodontics 7*, 7th edition. Raleigh, NC: PMPH-USA Ltd. 2019, pp. 215–266.
8. SIGN 50: a guideline developer's handbook. https://www.sign.ac.uk/assets/sign50_2011.pdf. [Accessed 20 December 2023]
9. Igna A, Mircioagă D, Boariu M, Stratul Ş-I. A Diagnostic Insight of Dental Pulp Testing Methods in Pediatric Dentistry. *Medicina*. 2022;58(5):665. doi:10.3390/medicina58050665. [DOI](#)
10. Camp JH. Diagnosis dilemmas in vital pulp therapy: Treatment for the toothache is changing, especially in young, immature teeth. *Pediatr Dent*. 2008;30(3):197-205.
11. American Academy of Pediatric Dentistry. Pulp therapy for primary and immature permanent teeth. *The Reference Manual of Pediatric Dentistry*. Chicago, Ill.: American Academy of Pediatric Dentistry. 2021:415-23. https://www.aapd.org/media/Policies_Guidelines/BP_PulpTherapy.pdf. [Accessed 20 December 2023]
12. Fuks AB, Peretz B. *Pediatric endodontics: current concepts in pulp therapy for primary and young permanent teeth*. Switzerland: Springer International Publishing, 2016. <https://link.springer.com/book/10.1007/978-3-319-27553-6>. [Accessed 20 December 2023]

13. Waterhouse P, Whitworth J, Camp J et al. Pediatric Endodontics. In: Hargreaves KM, Cohen S, Berman LH. Cohen's Pathways of the Pulp; St. Louis: Mosby Elsevier. 2011, pp. 809–818.
14. Malmgren B, Andreasen JO, Flores MT et al. Guidelines for the management traumatic dental injuries: 3. Injuries in the primary dentition. Dent Traumatol. 2012;28:174–82. doi: 10.1111/edt.12576. [DOI](#)
15. Sui H, Lv Y, Xiao M et al. Relationship between the difference in electric pulp test values and the diagnostic type of pulpitis. BMC Oral Health. 2021;21:339. doi:10.1186/s12903-021-01696-9. [DOI](#)
16. Hori A, Poureslami HR, Parirokh M et al. The ability of pulp sensibility tests to evaluate the pulp status in primary teeth. Int J Paediatr Dent. 2011;21(6):441-5. doi: 10.1111/j.1365-263X.2011.01147.x. [DOI](#)
17. Molaasadolah F, Zargar N, Bargrizan M et al. Comparison of pulse oximeter, cold test, and electric pulp test for assessment of pulp vitality in permanent immature teeth. Folia Med (Plovdiv). 2022;64:134-142. doi: 10.3897/folmed.64.e66573. [DOI](#)
18. Mejàre IA, Axelsson S, Davidson T et al. Diagnosis of the condition of the dental pulp: A systematic review. Int Endod J. 2012;45:597–613. doi: 10.1111/j.1365-2591.2012.02016.x. [DOI](#)
19. Sharma A, Madan M, Shahi P et al. Comparative Study of Pulp Vitality in Primary and Young Permanent Molars in Human Children with Pulse Oximeter and Electric Pulp Tester. Int J Clin Pediatr Dent. 2015;8:94–98. doi:10.5005/jp-journals-10005-1291. [DOI](#)
20. Ghouth N, Duggal MS, Nazzal H. The use of dental pulp tests in children with dental trauma: a national survey of the British Society of Paediatric Dentistry's members. Br Dent J. 2019. doi: 10.1038/sj.bdj.2019.99. [DOI](#)
21. Milcheva N, Kabaktchieva R, Gateva N. Direct pulp capping in treatment of reversible pulpitis in primary teeth- clinical protocol. Journal of IMAB. 2016;222:1348-1351. doi:10.5272/jimab.2016224.1348. [DOI](#)
22. Coll JA, Dhar V, Vargas K et al. Use of Non-Vital Pulp Therapies in Primary Teeth. Pediatr Dent. 2020;42(5):337-49.
23. Mohammad G, Jerin F, Jebin S. Pulpal Diagnosis of Primary Teeth: Guidelines for Clinical Practice. Bangladesh J Dent Res Educ. 2012;2:65–68. doi:10.3329/BJDRE.V2I2.16248. [DOI](#)
24. Aravind A, Rechithra R, Sharma R et al. Response to Pulp Sensibility Tests after Full Pulpotomy in Permanent Mandibular Teeth with Symptomatic Irreversible Pulpitis: A Retrospective Data Analysis. J Endod. 2022;48(1):80-86. doi: 10.1016/j.joen.2021.10.005. [DOI](#)

The work is a fragment of the scientific research work «Improvement of methods of prevention and treatment of diseases of hard dental tissues and periodontal diseases on the background of somatic pathology in children, taking into account socio-economic factors and psycho-emotional state», state registration number 0119U102852.

CONFLICT OF INTEREST

The Authors declare no conflict of interest

CORRESPONDING AUTHOR

Nataliia Yanko

Poltava state medical university
24 Shevchenko st., 36000 Poltava, Ukraine
e-mail: latned@ukr.net

ORCID AND CONTRIBUTIONSHIP

Lyudmyla Kaskova: 0000-0003-0855-2865 [D](#) [E](#) [F](#)
Nataliia Yanko: 0000-0002-3752-4110 [A](#) [B](#) [D](#) [E](#) [F](#)
Iryna Vashchenko: 0000-0002-5025-8005 [E](#) [F](#)
Olena Khmil: 0000-0001-5390-9099 [E](#) [F](#)

[A](#) – Work concept and design, [B](#) – Data collection and analysis, [C](#) – Responsibility for statistical analysis, [D](#) – Writing the article, [E](#) – Critical review, [F](#) – Final approval of the article

RECEIVED: 07.10.2023

ACCEPTED: 17.07.2024



Advancements in preventing post-contrast acute kidney injury in EVAR: clinical strategies and future directions

Bartłomiej Antoń¹, Piotr Kaszczewski¹, Sławomir Nazarewski¹, Jolanta Małyszko², Zbigniew Gałązka¹

¹DEPARTMENT OF GENERAL, VASCULAR, ENDOCRINE AND TRANSPLANT SURGERY, MEDICAL UNIVERSITY OF WARSAW, WARSAW, POLAND

²NEPHROLOGY, DIALYSIS AND INTERNAL MEDICINE, WARSAW MEDICAL UNIVERSITY, WARSAW, POLAND

ABSTRACT

Abdominal Aortic Aneurysm (AAA) represents a significant global health issue with a high risk of rupture, resulting in substantial mortality rates. Endovascular Aneurysm Repair (EVAR) has emerged as the preferred treatment method due to its minimally invasive nature. However, the procedure carries a risk of acute kidney injury (AKI), particularly post-contrast acute kidney injury (PC-AKI), which can adversely affect patient outcomes. This review examines the incidence, pathophysiology, and prevention strategies for PC-AKI in the context of EVAR. It synthesizes current research on the mechanisms underlying PC-AKI, such as renal vasoconstriction, oxidative stress, and tubular toxicity. The effectiveness of various preventive measures, including pre-procedural hydration, use of low-osmolality contrast agents, and alternative imaging techniques, is evaluated. Additionally, the review explores patient-specific risk factors and the potential of novel pharmacologic interventions. The incidence of PC-AKI in EVAR varies based on procedural complexity and patient-specific factors like preexisting renal insufficiency, diabetes, and hypertension. Preventive strategies such as intravenous hydration and the use of less nephrotoxic contrast agents have shown effectiveness. Advances in imaging technology and innovative pharmacologic interventions, including antioxidants and vasodilatory drugs, present promising approaches to reducing the risk of PC-AKI. Effective management of PC-AKI in EVAR necessitates a comprehensive and multifaceted approach that considers both procedural and patient-specific factors. Future research should aim to standardize diagnostic criteria, refine preventive strategies, and explore novel therapies. Enhanced understanding of PC-AKI pathophysiology and personalized preventive measures can improve patient safety and outcomes in EVAR procedures.

KEY WORDS: nephrotoxicity, acute kidney injury, abdominal aortic aneurysm, endovascular aneurysm repair, post-contrast acute kidney injury, preventive strategies

Wiad Lek. 2024;77(9):1769-1774. doi: 10.36740/WLek/193211 DOI

INTRODUCTION

Abdominal Aortic Aneurysm (AAA) remains a pressing global health issue characterized by the abnormal dilation of the aorta, posing a significant risk of life-threatening rupture if left untreated [1]. The Global Burden of Disease (GBD) study in 2019 highlighted its severity, reporting approximately 170,000 deaths annually attributed to aortic aneurysms, underscoring the critical need for effective management strategies [2]. Endovascular Aneurysm Repair (EVAR) has emerged as the preferred treatment for AAA due to its minimally invasive nature, associated with reduced 30-day mortality, shorter hospital stays, and quicker recovery compared to traditional open surgical repair [3]. However, EVAR is not without its complications, notably including acute kidney injury (AKI), which significantly impacts both short-term outcomes and long-term renal function [4].

AIM

This review examines the incidence, pathophysiology, and prevention strategies for PC-AKI in the context of EVAR. It synthesizes current research on the mechanisms underlying PC-AKI, such as renal vasoconstriction, oxidative stress, and tubular toxicity. The effectiveness of various preventive measures, including pre-procedural hydration, use of low-osmolality contrast agents, and alternative imaging techniques, is evaluated. Additionally, the review explores patient-specific risk factors and the potential of novel pharmacologic interventions.

MATERIALS AND METHODS

The review was performed in the period from 01.2024 to .07.2024. The materials for the literature review were publications on research from January 2001 to July

2024. Relevant articles were identified by two authors (BA, PK) searching PubMed's, Scopus, Web of Science, Embase databases, and Cochrane Library using advanced search and keywords: [[PC-AKI] OR [AKI]] AND [EVAR]].

REVIEW AND DISCUSSION

ACUTE KIDNEY INJURY (AKI) AND EVAR

Acute kidney injury following AAA repair, whether through EVAR or open surgical approaches, presents a substantial clinical challenge. The incidence varies widely and is influenced by procedural complexity, the type of repair performed, and patient-specific risk factors such as preexisting renal insufficiency, diabetes mellitus, hypertension, and overall cardiovascular health.[5,6] Studies indicate that up to 20% of patients undergoing elective EVAR may experience AKI, which has been linked to increased morbidity, prolonged hospital stays, and higher mortality rates.[7,8] Effective management of AKI in this context necessitates rigorous perioperative surveillance and optimization of renal function to attenuate adverse outcomes [9].

POST CONTRAST ACUTE KIDNEY INJURY (PC-AKI) IN EVAR

Iodinated contrast media are indispensable for accurate imaging during EVAR procedures but carry a significant risk of nephrotoxicity, commonly referred to as post-contrast acute kidney injury (PC-AKI) or formerly termed contrast-induced nephropathy (CIN). [10] The exact pathophysiology of PC-AKI involves multifactorial mechanisms, including renal vasoconstriction, oxidative stress, and direct tubular toxicity. The reported incidence of PC-AKI varies widely across studies, influenced by factors such as the volume and type of contrast used, procedural characteristics, and patient-specific factors like baseline renal function and comorbidities [11]. The lack of standardized diagnostic criteria for PC-AKI contributes to inconsistencies in its diagnosis and management across clinical settings [12].

CHALLENGES AND CURRENT UNDERSTANDING

Current research underscores the intricate interplay between contrast media properties, procedural factors, and patient susceptibility in the development of PC-AKI [11]. Despite advancements in preventive strategies, including intravenous hydration and the

use of less nephrotoxic contrast agents, uncertainties persist regarding the precise impact of contrast media on renal function and the optimal management of PC-AKI in EVAR patients. The variability in study designs and diagnostic criteria further complicates efforts to establish definitive guidelines for the prevention and management of PC-AKI in this vulnerable patient population [10, 13].

PATHOPHYSIOLOGICAL INSIGHTS INTO PC-AKI

The pathophysiology of PC-AKI in EVAR involves complex mechanisms contributing to renal injury. Iodinated contrast media induce renal vasoconstriction through endothelin-mediated pathways, leading to decreased renal blood flow and subsequent ischemia. Additionally, contrast agents generate reactive oxygen species (ROS) within renal tubular cells, promoting oxidative stress and cellular damage. Direct tubular toxicity results from the accumulation of contrast media within renal tubules, disrupting cellular integrity and function. These multifaceted mechanisms underscore the complexity of PC-AKI pathophysiology and highlight the need for targeted preventive strategies [14].

PREVENTIVE STRATEGIES AND CLINICAL MANAGEMENT

Efforts to mitigate PC-AKI risk in EVAR patients focus on several key strategies. Pre-procedural hydration remains a cornerstone intervention, aiming to maintain adequate renal perfusion and enhance contrast media excretion. Intravenous administration of isotonic saline solutions has shown efficacy in reducing PC-AKI incidence by optimizing intravascular volume and promoting renal blood flow [15]. Additionally, the selection of low-osmolality or iso-osmolality contrast agents, which exhibit reduced nephrotoxicity profiles compared to high-osmolality agents, represents another preventive approach [16]. Clinical decision-making regarding contrast media volume and type is crucial, with current guidelines recommending the use of minimal contrast volumes necessary for diagnostic accuracy and procedural success. Tailoring contrast media protocols to patient-specific factors, such as baseline renal function and comorbidities, further optimizes PC-AKI prevention [17]. Advances in imaging technology, including the development of non-contrast imaging modalities and the utilization of magnetic resonance angiography (MRA), provide alternative strategies to minimize contrast exposure in high-risk patients [18].

FUTURE DIRECTIONS IN RESEARCH

Future research endeavours in PC-AKI associated with EVAR should focus on advancing diagnostic criteria and refining preventive strategies. Prospective multicenter studies incorporating standardized definitions and robust outcome measures will facilitate a comprehensive understanding of PC-AKI epidemiology and risk factors across diverse patient populations [19]. Personalized preventive measures can be enabled by biomarker research's potential to identify early predictors of renal injury and stratify PC-AKI risk. Novel treatment approaches, such as antioxidant therapy and vasodilatory drugs, that target certain pathways implicated in PC-AKI development should be investigated in order to minimize renal damage and improve clinical outcomes [20].

DETAILED ANALYSIS OF PROCEDURAL FACTORS

One of the primary procedural factors influencing PC-AKI incidence is the volume of contrast media used during EVAR. While minimal contrast volume is recommended, achieving optimal imaging quality and procedural success often requires a delicate balance. Studies have shown that high volumes of contrast media correlate with a higher risk of renal impairment, necessitating a strategic approach to contrast administration [21]. Techniques such as contrast dilution, selective angiography, and the use of adjunctive imaging modalities can help minimize contrast volume without compromising procedural efficacy [16,17]. Another critical procedural consideration is the type of contrast media employed. Low-osmolality and iso-osmolality contrast agents have been shown to have a reduced nephrotoxic profile compared to high-osmolality agents. This difference is attributed to their lower propensity to cause renal vasoconstriction and tubular toxicity. The selection of contrast media should be tailored to individual patient risk profiles, considering factors such as preexisting renal insufficiency and comorbidities [16].

PATIENT-SPECIFIC RISK FACTORS AND THEIR MANAGEMENT

Following EVAR, patient-specific variables are crucial in the development of PC-AKI. One known risk factor is preexisting renal insufficiency; patients with impaired renal function at baseline are especially vulnerable to further renal injury from contrast exposure. Pre-procedural renal optimizing techniques, including as hydration and medication therapies, are essential in these situations [22]. Diabetes mellitus and hypertension are examples of comorbidities that increase the risk of PC-AKI by causing

underlying renal vascular and tubular damage. In the perioperative phase, strict blood pressure and glucose management can help reduce these risks. Additionally, patient-specific risk stratification algorithms that take into account variables like age, renal function, and comorbidities might help identify patients who are at a higher risk and adjust preventative measures accordingly [23]. Recently, HALP score calculated with the formula "hemoglobin \times albumin \times lymphocyte count/platelet count" was reported to be used to predict PC-AKI and medium-long-term mortality in EVAR patients [24].

INNOVATIVE IMAGING MODALITIES AND TECHNIQUES

Advancements in imaging technology offer promising alternatives to traditional contrast-based methods. Non-contrast imaging techniques, such as duplex ultrasound and magnetic resonance angiography (MRA), provide valuable diagnostic information without the nephrotoxic risk associated with iodinated contrast media. These modalities can be particularly beneficial in high-risk patients, reducing the overall burden of contrast exposure [25]. Furthermore, improvements in intraoperative imaging, including as the use of intraoperative ultrasonography and carbon dioxide angiography, have demonstrated the potential to reduce the need for contrast material while preserving procedural accuracy. While not always applicable, these strategies are useful for lowering the risk of PC-AKI.[26]

PHARMACOLOGIC INTERVENTIONS AND NOVEL THERAPIES

Research on pharmacologic treatments to prevent PC-AKI has been conducted extensively. Some agents have demonstrated varying degrees of efficacy in mitigating contrast-induced kidney impairment, including bicarbonate, statins, and N-acetylcysteine. Although these medicines' antioxidative and vasodilatory qualities theoretically help to mitigate kidney damage, the outcomes of varied clinical trials have made routine use of them contentious [27, 28]. Prospective treatments aimed at particular pathophysiological pathways connected to PC-AKI appear promising. Reactive oxygen species (ROS) produced by contrast media can be neutralized by antioxidant therapy, which may lessen oxidative stress and tubular injury [29]. Another possible treatment option is to use vasodilatory drugs to offset the renal vasoconstriction caused by contrast. Those drugs are: prostaglandins, calcium channel blockers, theophylline. Prostaglandins are naturally occurring vasodilators that can improve renal blood flow. Pros-

taglandin analogues, such as misoprostol, have been investigated for their potential to prevent PC-AKI by counteracting the vasoconstrictive effects of contrast media [30, 31]. Calcium channel blockers, such as diltiazem, can dilate blood vessels and potentially improve renal perfusion. However, their role in preventing PC-AKI has not been well-established [32]. Theophylline, a methylxanthine derivative, has vasodilatory properties and can increase renal blood flow. Some studies have indicated that theophylline may help prevent PC-AKI, but like other agents, its use is not universally endorsed due to inconsistent evidence [33].

CONCLUSIONS

In order to fully address the pressing problem of PC-AKI within the framework of EVAR, more research must be done on the various factors that contribute to this ill-

ness as well as new approaches to care and prevention. A complicated web requiring a nuanced approach to patient care is created by the combination of procedural variables, patient-specific factors, and the inherent nephrotoxicity of contrast media.

The prevention and management of PC-AKI in the context of EVAR require a comprehensive and multifaceted approach. Procedural factors, patient-specific risk profiles, and the inherent nephrotoxicity of contrast media must all be carefully considered to optimize renal outcomes. Advancements in imaging technology, innovative pharmacologic interventions, and a deeper understanding of pathophysiological mechanisms will continue to shape the landscape of PC-AKI prevention and management. Through continued research and the implementation of evidence-based strategies, clinicians can enhance patient safety, reduce renal complications, and improve overall outcomes in EVAR procedures.

REFERENCES

1. Shaw PM, Loree J, Gibbons RC. Abdominal Aortic Aneurysm. 2024 Feb 27. In: StatPearls [Internet]. Treasure Island (FL): StatPearls Publishing; 2024 Jan.
2. Krafčik BM, Stone DH, Cai M, et al. Changes in global mortality from aortic aneurysm. *J Vasc Surg*. 2024 Jul;80(1):81-88.e1. doi: 10.1016/j.jvs.2024.02.025. [DOI](#)
3. Daye D, Walker TG. Complications of endovascular aneurysm repair of the thoracic and abdominal aorta: evaluation and management. *Cardiovasc Diagn Ther*. 2018 Apr;8(Suppl 1):S138-S156. doi: 10.21037/cdt.2017.09.17. [DOI](#)
4. Zarkowsky DS, Hicks CW, Bostock IC, Stone DH, Eslami M, Goodney PP. Renal dysfunction and the associated decrease in survival after elective endovascular aneurysm repair. *J Vasc Surg*. 2016 Nov;64(5):1278-1285.e1. doi: 10.1016/j.jvs.2016.04.009. [DOI](#)
5. Yokoyama N, Nonaka T, Kimura N, et al. Acute Kidney Injury Following Elective Open Aortic Repair with Suprarenal Clamping. *Ann Vasc Dis*. 2020 Mar 25;13(1):45-51. doi: 10.3400/avd.oa.19-00095. [DOI](#)
6. Saratzis A, Nduwayo S, Sarafidis P, Sayers RD, Bown MJ. Renal Function is the Main Predictor of Acute Kidney Injury after Endovascular Abdominal Aortic Aneurysm Repair. *Ann Vasc Surg*. 2016 Feb;31:52-9. doi: 10.1016/j.avsg.2015.10.010. [DOI](#)
7. Antoń B, Nazarewski S, Małyżko J. Kidney Function, Male Gender, and Aneurysm Diameter Are Predictors of Acute Kidney Injury in Patients with Abdominal Aortic Aneurysms Treated Endovascularly. *Toxins (Basel)*. 2023 Feb 4;15(2):130. doi: 10.3390/toxins15020130. [DOI](#)
8. Saratzis A, Melas N, Mahmood A, Sarafidis P. Incidence of Acute Kidney Injury (AKI) after Endovascular Abdominal Aortic Aneurysm Repair (EVAR) and Impact on Outcome. *Eur J Vasc Endovasc Surg*. 2015 May;49(5):534-40. doi: 10.1016/j.ejvs.2015.01.002. [DOI](#)
9. Rodriguez JD, Hashmi MF, Hitte CC. Perioperative Acute Kidney Injury. 2023 Sep 12. In: StatPearls [Internet]. Treasure Island (FL): StatPearls Publishing; 2024 Jan-. PMID: 32491609.
10. Davenport M, Perazella M, Yee J, et al. Use of Intravenous Iodinated Contrast Media in Patients with Kidney Disease: Consensus Statements from the American College of Radiology and the National Kidney Foundation. *Radiology*. 2020;294(3):660-8. doi:10.1148/radiol.2019192094 [DOI](#)
11. Mandurino-Mirizzi A, Munafò A, Crimi G. Contrast-Associated Acute Kidney Injury. *J Clin Med*. 2022 Apr 13;11(8):2167. doi: 10.3390/jcm11082167. PMID: 35456260; PMCID: PMC9027950. [DOI](#)
12. Makris K, Spanou L. Acute Kidney Injury: Diagnostic Approaches and Controversies. *Clin Biochem Rev*. 2016 Dec;37(4):153-175. PMID: 28167845; PMCID: PMC5242479.
13. Obed M, Gabriel MM, Dumann E, Vollmer Barbosa C, Weißenborn K, Schmidt BMW. Risk of acute kidney injury after contrast-enhanced computerized tomography: a systematic review and meta-analysis of 21 propensity score-matched cohort studies. *Eur Radiol*. 2022 Dec;32(12):8432-8442.
14. Vlachopoulos G, Schizas D, Hasemaki N, Georgalis A. Pathophysiology of Contrast-Induced Acute Kidney Injury (CIAKI). *Curr Pharm Des*. 2019;25(44):4642-4647. doi: 10.2174/1381612825666191210152944. PMID: 31820694. [DOI](#)
15. Kanbay M, Copur S, Mizrak B, Ortiz A, Soler MJ. Intravenous fluid therapy in accordance with kidney injury risk: when to prescribe what volume of which solution. *Clin Kidney J*. 2022 Dec 16;16(4):684-692. doi: 10.1093/cjk/sfac270. PMID: 37007689; PMCID: PMC10061428. [DOI](#)

16. Lee T, Kim WK, Kim AJ, et al. Low-Osmolar vs. Iso-Osmolar Contrast Media on the Risk of Contrast-Induced Acute Kidney Injury: A Propensity Score Matched Study. *Front Med (Lausanne)*. 2022 Apr 29;9:862023. doi: 10.3389/fmed.2022.862023. [DOI](#)
17. Zebrauskaite A, Ziubryte G, Mackus L, Lieponyte A, Kairyte E, Unikas R, Jarusevicius G. A Simple Strategy to Reduce Contrast Media Use and Risk of Contrast-Induced Renal Injury during PCI: Introduction of an "Optimal Contrast Volume Protocol" to Daily Clinical Practice. *J Cardiovasc Dev Dis*. 2023 Sep 19;10(9):402. doi: 10.3390/jcdd10090402. [DOI](#)
18. Summerlin D, Willis J, Boggs R, Johnson LM, Porter KK. Radiation Dose Reduction Opportunities in Vascular Imaging. *Tomography*. 2022 Oct 21;8(5):2618-2638. doi: 10.3390/tomography8050219. [DOI](#)
19. Jamme M, Legrand M, Geri G. Outcome of acute kidney injury: how to make a difference? *Ann Intensive Care*. 2021 Apr 15;11(1):60. doi: 10.1186/s13613-021-00849-x. [DOI](#)
20. van Duijl TT, Soonawala D, de Fijter JW, Ruhaak LR, Cobbaert CM. Rational selection of a biomarker panel targeting unmet clinical needs in kidney injury. *Clin Proteomics*. 2021 Feb 22;18(1):10. doi: 10.1186/s12014-021-09315-z. [DOI](#)
21. Mun JH, Kwon SK, Park JH, Chu W, Kim DH, Jung HJ, Lee SS. Renal function-adjusted contrast medium volume is a major risk factor in the occurrence of acute kidney injury after endovascular aneurysm repair. *Medicine (Baltimore)*. 2021 Apr 9;100(14):e25381. doi: 10.1097/MD.00000000000025381. [DOI](#)
22. Vandenberghe W, Hoste E. Contrast-associated acute kidney injury: does it really exist, and if so, what to do about it? *F1000Res*. 2019 May 29;8:F1000 Faculty Rev-753. doi: 10.12688/f1000research.16347.1. [DOI](#)
23. Kaur A, Sharma GS, Kumbala DR. Acute kidney injury in diabetic patients: A narrative review. *Medicine (Baltimore)*. 2023 May 26;102(21):e33888. doi: 10.1097/MD.00000000000033888. PMID: 37233407; PMCID: PMC10219694. [DOI](#)
24. Özderya A, Şahin S, Koşmaz T, et al. Can HALP score predict post-contrast acute kidney injury and 6-year mortality in patients undergoing endovascular abdominal aneurysm repair? *Vascular*. 2024 Apr 12:17085381241246905. doi: 10.1177/17085381241246905. Epub ahead of print. [DOI](#)
25. Thurman J, Gueler F. Recent advances in renal imaging. *F1000Res*. 2018 Nov 29;7:F1000 Faculty Rev-1867. doi: 10.12688/f1000research.16188.1 [DOI](#)
26. Young M, Mohan J. Carbon Dioxide Angiography. 2023 Jul 3. In: *StatPearls [Internet]*. Treasure Island (FL): StatPearls Publishing; 2024 Jan.
27. Li Y, Wang J. Contrast-induced acute kidney injury: a review of definition, pathogenesis, risk factors, prevention and treatment. *BMC Nephrol*. 2024 Apr 22;25(1):140. doi: 10.1186/s12882-024-03570-6. [DOI](#)
28. Sharp AJ, Patel N, Reeves BC, Angelini GD, Fiorentino F. Pharmacological interventions for the prevention of contrast-induced acute kidney injury in high-risk adult patients undergoing coronary angiography: a systematic review and meta-analysis of randomised controlled trials. *Open Heart*. 2019 Jan 25;6(1):e000864. doi: 10.1136/openhrt-2018-000864. [DOI](#)
29. Gyurászová M, Gurecká R, Bábíčková J, Tóthová L. Oxidative Stress in the Pathophysiology of Kidney Disease: Implications for Noninvasive Monitoring and Identification of Biomarkers. *Oxid Med Cell Longev*. 2020 Jan 23;2020:5478708. doi: 10.1155/2020/5478708. [DOI](#)
30. Gurkowski L, MacDougall M, Wiegmann T. Effects of Misoprostol on Contrast-Induced Renal Dysfunction. *Am J Ther*. 1995 Nov;2(11):837-842. doi: 10.1097/00045391-199511000-00003. [DOI](#)
31. Li Y, Xia W, Zhao F, Wen Z, Zhang A, Huang S, Jia Z, Zhang Y. Prostaglandins in the pathogenesis of kidney diseases. *Oncotarget*. 2018 May 29;9(41):26586-26602. doi: 10.18632/oncotarget.25005. [DOI](#)
32. Robles NR, Fici F, Grassi G. Dihydropyridine calcium channel blockers and renal disease. *Hypertens Res*. 2017 Jan;40(1):21-28. doi: 10.1038/hr.2016.85. [DOI](#)
33. Dai B, Liu Y, Fu L, Li Y, Zhang J, Mei C. Effect of theophylline on prevention of contrast-induced acute kidney injury: a meta-analysis of randomized controlled trials. *Am J Kidney Dis*. 2012 Sep;60(3):360-70. doi: 10.1053/j.ajkd.2012.02.332. [DOI](#)

ORCID AND CONTRIBUTIONSHIP

Bartłomiej Antoń: 0000-0002-3983-2096 [A](#) [B](#) [C](#) [D](#) [E](#) [F](#)

Piotr Kaszczewski: 0000-0002-8461-1049 [A](#) [B](#) [C](#) [D](#) [E](#) [F](#)

Sławomir Nazarewski: 0000-0003-1195-9252 [A](#) [E](#) [F](#)

Jolanta Małyszko: 0000-0001-8701-8171 [A](#) [D](#) [E](#) [F](#)

Zbigniew Gałązka: 0000-0001-5542-3404 [E](#) [F](#)

CONFLICT OF INTEREST

The Authors declare no conflict of interest

CORRESPONDING AUTHOR

Jolanta Małyszko

Nephrology, Dialysis and Internal Medicine,
Warsaw Medical University
Banacha 1 a, 02-097, Warszawa, Poland
e-mail: jolmal@poczta.onet.pl

A – Work concept and design, **B** – Data collection and analysis, **C** – Responsibility for statistical analysis, **D** – Writing the article, **E** – Critical review, **F** – Final approval of the article

RECEIVED: 30.06.2024

ACCEPTED: 30.08.2024



Multimodal management of breast architectural distortion: an analytical literature review

Andrii Kovtun¹, Andrii Gurando², Vadym Telniy¹, Tetiana Kozarenko²

¹MEDICAL CENTER "VERUM EXPERT CLINIC", KYIV, UKRAINE

²SI "INSTITUTE OF NUCLEAR MEDICINE AND DIAGNOSTIC RADIOLOGY OF NAMS OF UKRAINE", KYIV, UKRAINE

ABSTRACT

Aim: The objective of this literature review was to determine the optimal diagnostic algorithm for breast cancer detection associated with architectural distortion.

Materials and Methods: The Pubmed, Google Scholar, Web of Science, and Scopus databases was used to search for materials on architectural distortion, associated pathologies, and radiological imaging methods.

Conclusions: Architectural distortions may represent both benign and malignant pathology, but ultrasound, magnetic resonance, and roentgenological signs may not always with confidence determine the etiology of these changes. Therefore, the correct diagnostic algorithm which uses contrast imaging methods and digital breast tomosynthesis can prevent potentially exceeding radiation exposure, and unnecessary biopsies, change surgical operation volumes, decrease patient stress from procedures, and reduce the number of resources spent. After analyzing a number of scientific sources, we recommend morphological verification of all architectural distortions that are not the result of surgery, trauma, or that accumulate contrast media during breast imaging.

KEY WORDS: breast cancer, digital breast tomosynthesis, breast magnetic resonance imaging, breast ultrasound, contrast-enhanced mammography

Wiad Lek. 2024;77(9):1775-1781. doi: 10.36740/WLek/191324 DOI

INTRODUCTION

Architectural distortion (AD) is a deformity of normal breast parenchyma without an obvious visualized mass [1-3]. AD is the third most common manifestation of non-palpable breast cancer (BC), and 12–45% of them are missed BC on full-field digital mammography (FFDM) [4-9]. An AD can be main or associated finding that is combined with signs of an underlying mass [3]. Interpretation of the data and further tactics for AD is challenging due to the large number of pathologies associated with AD, including both benign and malignant processes, such as sclerosing adenosis, radial scar, various types of breast cancer, fat necrosis, and other changes associated with surgery, biopsy, or trauma [1, 4, 5, 10-12]. Correctly chosen diagnostic tactics, the use of modern diagnostic methods, such as contrast-enhanced mammography (CEM) and digital breast tomosynthesis (DBT), can prevent potential radiation exposure, unnecessary biopsies, change the scope of surgery, or determine the feasibility of surgery in general, which reduces the amount of stress for women.

AIM

The objective of this literature review was to determine the optimal diagnostic algorithm for breast cancer detection associated with architectural distortion.

MATERIALS AND METHODS

The Pubmed, Google Scholar, Web of Science, and Scopus databases was used to search for materials on architectural distortion, associated pathologies, and radiologic research methods.

REVIEW AND DISCUSSION

In this article, in addition to diagnostic methods in radiology, we will consider the main benign and malignant findings that can be represented by AD. Among the malignant findings represented by AD the most common were invasive lobular carcinoma (ILC), invasive ductal carcinoma (IDC), and ductal carcinoma in situ (DCIS) [1, 10-12]. Invasive cancer forms account

for 78–90% of malignant pathology [9, 13–15]. The most frequent benign findings associated with AD include radial scar, sclerosing adenosis, parenchymal changes, and fat necrosis after surgery, biopsies, and trauma [1, 4, 5, 10–12, 16].

MAMMOGRAPHY

AD accounts for about 6% of pathological findings visualized during FFDM [4,5]. Most often, AD and all the related pathologies are incidental asymptomatic mammographic findings and less often palpable lumps [1, 4, 5, 10, 17–19]. The average age of patients with an AD that hides a malignant pathologies is 59 years and 55 years for a benign pathology [1]. AD is the most commonly missed pathology in false-negative results, which may be related to diagnostic errors or reduced sensitivity of FFDM due to the density of the breast parenchyma, peculiarities of glandular tissue distribution, and tumor type [2, 20]. During the data collection, no correlation was found between the AD detection and age, race, family history, and individual history of BC treatment, which would help to correlate AD pathologies.

According to the Breast Imaging-Reporting and Data System (BI-RADS) Atlas, radiologically, AD is most often presented as an area with radial spicules emanating from a single point and localized retraction or distortion of the parenchymal margin [3]. It is worth noting that no sonographic, radiologic, or magnetic resonance (MR) signs can be used with certainty to identify the pathology hidden by an AD [10, 21–23]. It has been suggested that AD with concomitant findings such as calcifications increases the risk of BC; therefore, it is important to report the location and concomitant findings, although some authors consider these data to be statistically insignificant [3, 24, 25].

DIGITAL BREAST TOMOSYNTHESIS

In recent years, DBT has become a highly sensitive method for detecting AD and generally increases sensitivity and accuracy compared to FFDM, and reduces the patient recall rate [6, 7, 24, 26, 27]. DBT is the most informative for breasts with dense parenchyma, it helps to partially eliminate summation artifacts and detect findings hidden in the dense parenchyma [7, 24, 28, 29]. DBT improves the AD visualization and also detects from 9.2% to 74% of ADs that are mammographically occult [6, 8, 10, 20, 27, 28, 30, 31]. Lee [21] argues that in addition to AD, DBT has the advantage of visualizing human epidermal growth factor receptor 2 (HER-2) negative bulky masses with a low histologic differentiation

grade. The percentage of BC after core-needle biopsy (CNB) or surgery was lower (10.2%) if the AD was seen only on DBT compared to the AD on FFDM (43.4%) [32]. DBT-only ADs were malignant in 33–68% of cases [22, 28] with positive predictive value (PPV) accounting for 9.8–50% [10, 14, 22, 30, 31].

The disadvantages of DBT includes a higher radiation exposure compared to conventional FFDM and an increase in the number of false-positive results [7, 28].

Difficulties in interpreting AD on FFDM can be caused by linear anatomical structures such as ligaments, vessels, ducts that simulate AD in cross-sections [9]. For example, Langman [33] describes an AD area on FFDM caused by an additional axillary muscle present in 7% of population. To improve the visualization of AD visualized in two or only one projection, the use of a targeted image or new full-field images in other projections is recommended [6, 7, 12].

ILC is the most common malignant pathology visualized on FFDM as AD and accounts for 16–20% of cases [34]. Due to late diagnosis, it most often manifests clinically as a palpable lump area, and as diffuse lesions, the breast is retracted, wrinkled, with thickened skin and nipple retraction [1, 7, 11]. An AD with or without a central hypo- or isodense mass is a classic FFDM sign of ILC [34, 11]. Much less commonly, ILC is presented as a mass with even or distinct edges, a developing asymmetry area [35]. IDC on FFDM is presented as a mass with uneven or distinct even contours, with the “white star” signs, AD with concomitant grouped amorphous, pleomorphic, fine linear calcifications [1, 11, 34]. DCIS is a precancerous condition with a tendency to transform into an invasive tumor that develops in the terminal ducts [5]. With the development of FFDM and the spread of screening programs, the pathology has become a common group of BC [5, 36]. FFDM usually detects it as grouped or segmental pleomorphic, powdery, or rarely coarse heterogeneous calcifications, in 10–15% of cases as calcification-free masses, and in 2–10% as AD [4, 5, 11, 36].

The most common benign process is radial scar, which occurs as a result of idiopathic processes not associated with trauma or surgery and is visualized as an AD on FFDM in 50–74.4% [4, 21, 18, 37]. On FFDM, it is presented as an area with a radiolucent central core and radiating contours, which may contain calcifications [4, 5, 18]. It is believed that the increase in the number of detected radial scar and AD is associated with the widespread use of DBT [11]. Radial scar detected on DBT is associated with BC in almost a third of the cases on the post-surgery material [7, 34, 38]. It is still unclear whether radial scar is a marker of the increased risk of BC or a precancerous condition in itself [18]. The asso-

ciation between radial scar and BC may be the cause of insufficiently informative CNB, due to the small amount of material collected or failure to reach the malignancy site [34, 37]. To establish a more accurate diagnosis, it is suggested that vacuum-assisted breast biopsy (VABB) with 8G and 11G needles be performed, if possible, as an alternative to excisional biopsy in some cases [18]. The highest diagnostic accuracy is achieved with 12 columns of material collected by VABB, but accuracy does not increase with increasing amounts of material [37]. The rate of upgrade of radial scar to BC on the post-surgery material was 8–19.5% [18, 34, 37]. Interestingly, the presence of calcifications in the histologic material increased the risk of BC threefold, and the risk of atypia—almost 10 times [18]. Williams [39] observed in the case of atypical ductal hyperplasia that the upgrade was detected on the post-surgery material in 17.7% of cases, and Villa-Camacho [23] reported an upgrade on AD with atypia in 28.2% of cases. Given the high risk of radial scar upgrade on the post-surgery material after CNB, especially in the presence of atypia in the histologic material, surgical removal of radial scar or VABB is recommended to establish the definitive diagnosis [12, 18, 37, 38]. In patients with benign concordant findings, annual FFDM is recommended [15].

Sclerosing adenosis is a benign proliferative pathology that is usually detected in perimenopausal women [5, 19]. Core-needle biopsy is recommended after cytologic diagnosis, as sclerosing adenosis can coexist with various forms of cancer and other benign processes [8, 19, 34]. On FFDM, it is represented by calcifications (grouped, punctate, powdery, or amorphous, rarely pleomorphic) and masses, and some studies indicate that AD is the most common FFDM finding in case of sclerosing adenosis [5, 8, 34].

AD often occurs at the site of surgery; therefore, it is important to look at whether architectural changes are detected along with the site of surgery [11]. After reduction mammoplasty, the FFDM shows downward displacement of glandular tissue, fat necrosis, skin thickening, paraareolar skin calcifications, and the AD has a characteristic vortex-like appearance [8, 11].

Changes after biopsies may disappear within weeks to months and rarely progress [11]. Rarely, they can be presented on FFDM as AD, seromas, or dystrophic calcifications [5]. Miner [40] describes the formation of AD at the site of a large cyst aspiration.

A special mention should be made of fat necrosis, which is a benign inflammatory process of adipose tissue that represents almost 3% of all breast masses [4, 16]. The clinical manifestation of fat necrosis is a lump, usually in the subareolar area [16]. Mammographically, it is visualized as an oil cyst with a clear center and a thin

capsule with even or wavy contours, large rod-like calcifications, rarely focal asymmetries, microcalcifications, and concomitant changes with skin deformation on the subcutaneous fat tissue around the area of interest [4, 16]. Fat necrosis may appear as a mass with radiating contours if the inflammatory process is dominated by fibrous changes [4, 16].

Post-surgery and post-radiation changes in the breast parenchyma (skin and breast edema) should stabilize or decrease in size within 1–3 years after surgery and radiation therapy [5, 7, 11]. Increased size, new masses, or a change in appearance should raise suspicion of BC [5]. If AD is found to be associated with post-surgery changes, routine annual screening is recommended [11]. A thorough history and breast examination for scarring, skin and areola changes are important for this [5, 7, 11, 12]. If in doubt whether the surgical site coincides with the area of interest, we use cutaneous markers [5].

MAGNETIC RESONANCE IMAGING (MRI)

The diagnostic value of MRI is higher than FFDM for AD detection [2, 25]. Mei [2] found that with the additional application of MRI to FFDM, the sensitivity and specificity increased from 86.3% and 41.7% to 98.1% and 97.5%, respectively. MRI signs of AD are an area of localized retraction and distortion of the parenchyma without obvious signs of a mass and without contrast agent (CA) accumulation [3]. malignant pathology in the form of AD on MRI can be defined as an irregularly shaped mass with indistinct contours or non-mass enhancement (NME) [17, 20, 25]. In the Amitai study [17], out of 175 women, 61% of AD did not demonstrate CA accumulation, and none of these patients were subsequently diagnosed with malignancy. In 30% of women with contrast-enhanced masses, BC was diagnosed after biopsy [17]. ADs associated with BC were characterized by plateau and washout kinetics in most cases [17]. The most common pathology that accumulated CA was radial scar [17]. If the MRI results are negative, we continue to monitor the AD without additional invasive interventions, but we should pay attention to the low specificity of MRI [17, 20]. Samreen [12] suggests that the next DBT should be performed in 6 months if there is no MRI correlation of the pathology.

ILC on MRI is most often defined as a single mass with uneven radiating contours, sometimes, as with IDC, smaller masses or contrasting foci are present around, AD, focal or regional heterogeneous CA accumulation, NME are observed [1, 35]. The late-phase washout is achieved much more rarely than with IDC,

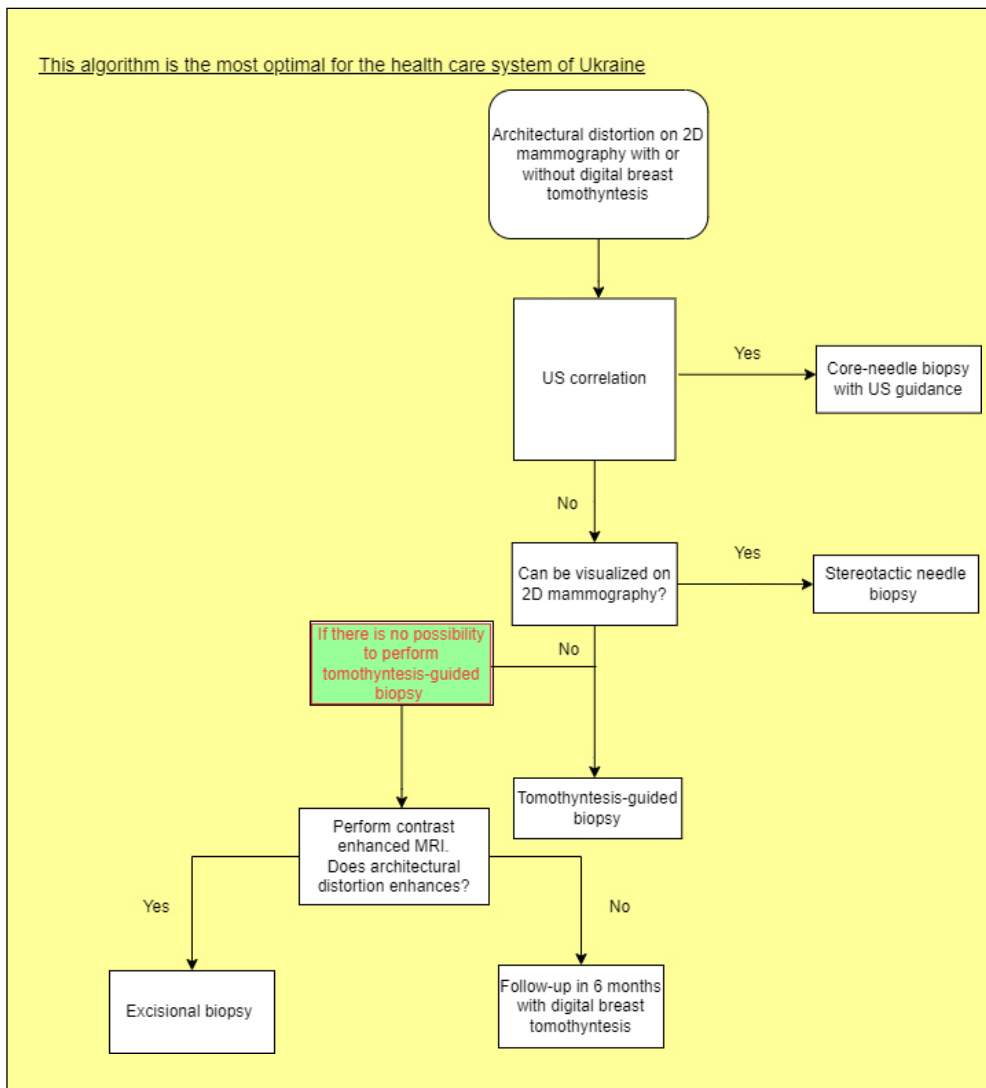


Fig. 1. This algorithm is the most optimal for the health care system of Ukraine.

but it more often has a kinetic plateau [1]. MR-findings representing IDC are characterized by a mass with uneven or radiating contours that accumulates CA in the periphery as a rim in 40% of cases and less commonly as a rounded mass with lobulated contours, NME [1]. Plateau or washout kinetics are present in 76–91% of cases and are more characteristic of masses with a higher differentiation grade [1].

Radial scar has a wide range of findings: enhanced bulky mass and NME, AD, almost all the findings had type 1 and type 2 kinetic curve, and most had uneven or radiating edges, which makes differential diagnosis with BC difficult [19].

A post-surgery scar on MRI can normally be contrasted in the first 12 months after surgery [5]. Any MRI CA accumulation at the site of surgery for BC after 18 months should be evaluated with caution and require further verification [5]. There may be a signal void in the operation location due to surgical marks and large rod-like dystrophic calcifications, which can be correlated with by means of FFDM [5].

The MRI signs of fat necrosis are characterized by a predominance of fat density in the mass, although a significant amount of variation is possible depending on the amount of inflammatory changes, fat content, and fibrosis stage [4, 16]. The most common MRI sign of fat necrosis is a rounded or oval fat cyst with a hypointense T1 signal on fat saturation images [16]. Kinetic analysis is not helpful in the evaluation, as fat necrosis has a whole range of kinetic curve signs for benign and malignant findings [16]. Short tau inversion recovery (STIR) mode visualizes the characteristic “black hole” sign, which appears as a central hypointense mass [16].

CONTRAST-ENHANCED MAMMOGRAPHY

A new method that expands the diagnostic capabilities of FFDM is CEM, an alternative to MRI when the latter is not possible. This method uses the principle of dual-energy subtraction to evaluate contrast enhancement of breast masses [8]. Similar to MRI, CEM

helps to define pathology characteristics, perform local staging, and assess response to neoadjuvant chemotherapy, but at a lower cost [8, 13]. Goh [8] found that ADs with little or no contrast enhancement have a lower risk of malignancy, as opposed to more obvious contrast enhancement, and the negative predictive value (NPV) of masses without suspicious CA accumulation was 100%. At the same time, CEM has a high sensitivity to AD contrast enhancement, reaching 96.7%, specificity of 57.9%, and NPV for BC up to 91.7% on the example of 49 ADs, which suggests mandatory verification of all contrasted masses [13]. The phenomenon of background parenchymal enhancement remains a diagnostic problem, which can mask BC and complicates the assessment of masses [8]. If the AD on CEM is contrasting but the biopsy shows benign findings with no signs of increased risk, the next FFDM can be performed routinely [31].

ULTRASOUND (US)

The ultrasound correlation of AD on FFDM is present in 40–87.6% of cases, and the presence of correlation increases the risk of detecting BC [13, 14, 17, 21–23, 31]. Wadhwa [12] found that the risk of BC is three times higher if the AD has US correlation compared to a finding without US correlation (63.1% v 17.7%). AD on US is defined as compression of the tissue around the tumor, obliteration of the tissue planes by an infiltrating lesion, straightening or thickening of Cooper's ligaments, and an echogenic rim around the finding [3]. The authors' opinions and study results differed on what to do with AD without US correlation. Thus, some argue that in the absence of US correlation with an FFDM finding, it is more likely to assume that the AD is a benign process [6, 24]. Other studies indicate that 17.7–27.9% of BCs were without US correlation, indicating that the absence of US correlation cannot completely exclude BC [21, 31].

US visualizes ILC as a hypoechoic mass with uneven and indistinct radiating contours, with posterior shadowing, and rarely as a rounded hypoechoic mass [1, 35]. The best correlation with US is present when AD is visualized in two standard mammographic planes [34]. IDC is most often present as a hypoechoic mass with uneven contours and posterior shadowing [1].

US findings of radial scar are characterized by a hypoechoic mass or AD that visually mimics a malignant mass [4]. AD represents radial scar in 44.2% of cases on US [18]. Sclerosing adenosis on ultrasound looks like a solid hypoechoic heterogeneous nodule, which can be clinically manifested as a mass [19]. Other signs on US include both distinct and indistinct contours, and mild to moderate blood flow [19].

US is used as an additional method for detecting post-surgery seromas, hematomas, and abscesses, but it should be remembered that post-surgery findings can mimic BC due to hypoechoic areas with indistinct margins [4, 5]. A fat necrosis is visualized as a cystic mass with septa or a solid mass with distinct or indistinct edges in the background of the AD, and posterior acoustic shadowing [4, 16].

Although a significant number of malignant and benign pathologies hidden under the AD, the frequency and improvement of AD visualization only increased over the years. But radiologists still have difficulties in identifying this radiological sign and choosing further tactics for patients, against the background of the emergence of new sensitive diagnostic methods (CEM and DBT) and already existing ones (MRI, FFDM, US). We aimed to systematize signs visualized by various radiological methods to give a better understanding of what AD can look like and what to do with it. The acquired knowledge will have a positive effect on medical algorithms, minimizing the number of unnecessary surgical and minimally invasive interventions for patients, can change the tactics of surgical intervention and more systematically assessing the risks and benefits for the patient.

ALGORITHM

If AD is present on the FFDM and we cannot be sure about previous surgery, biopsy, or trauma than ultrasound should be used for targeting and performing CNB [3, 21]. When ultrasound-guided CNB is not possible, radiology-guided CNB (stereotactic or DBT) is recommended, with postbiopsy marker placement and repeat mammography to ensure the correct biopsy site, and further marking before surgery if necessary [7, 12].

If AD is visualized only on tomosynthesis scans and it is not possible to perform a CNB, MRI or CEM may be additionally recommended as an alternative to tomosynthesis-guided core biopsy. Excisional biopsy is recommended in the presence of accumulation of contrast media, and follow-up in 6 months is recommended in the absence of accumulation [7] (Fig. 1).

CONCLUSIONS

Because architectural distortion represents a significant amount of benign and malignant pathologies, and ultrasound, MRI, and mammographic signs cannot determine the etiology of architectural distortion with certainty. We recommend that all architectural distortions that are not due to surgery, trauma, or biopsy and have contrast agents accumulation on MRI or CEM must be verified.

REFERENCES

1. Berg WA, Leung JWT. *Diagnostic Imaging: Breast*, 3rd Edition. Philadelphia, PA, Elsevier. 2019, pp.342-347.
2. Mei H, Xu J, Yao G et al. The diagnostic value of MRI for architectural distortion categorized as BI-RADS category 3-4 by mammography. *Gland Surg.* 2020;9(4):1008-1018. doi:10.21037/gs-20-505. DOI
3. D'Orsi CJ, Sickles EA, Mendelson EB et al. *ACR BI-RADS® Atlas, Breast Imaging Reporting and Data System*. Reston, VA, American College of Radiology. 2013, pp.127-128.
4. Gaur S, Dialani V, Slanetz PJ et al. Architectural distortion of the breast. *AJR Am J Roentgenol.* 2013;201(5):W662-70. doi: 10.2214/AJR.12.10153. DOI
5. Shaheen R, Schimmelpenninck CA, Stoddart L et al. Spectrum of diseases presenting as architectural distortion on mammography: multimodality radiologic imaging with pathologic correlation. *Semin Ultrasound CT MR.* 2011;32(4):351-62. doi: 10.1053/j.sult.2011.03.008. DOI
6. Partyka L, Lourenco AP, Mainiero MB. Detection of mammographically occult architectural distortion on digital breast tomosynthesis screening: initial clinical experience. *AJR Am J Roentgenol.* 2014;203(1):216-22. doi: 10.2214/AJR.13.11047. DOI
7. Durand MA, Wang S, Hooley RJ et al. Tomosynthesis-detected Architectural Distortion: Management Algorithm with Radiologic-Pathologic Correlation. *Radiographics.* 2016;36(2):311-21. doi: 10.1148/rg.2016150093. DOI
8. Goh Y, Chan CW, Pillay P et al. Architecture distortion score (ADS) in malignancy risk stratification of architecture distortion on contrast-enhanced digital mammography. *Eur Radiol.* 2021;31(5):2657-2666. doi:10.1007/s00330-020-07395-3. DOI
9. Suleiman WI, McEntee MF, Lewis SJ et al. In the digital era, architectural distortion remains a challenging radiological task. *Clin Radiol.* 2016;71(1):e35-40. doi: 10.1016/j.crad.2015.10.009. DOI
10. Vijayaraghavan GR, Newburg A, Vedantham S. Positive Predictive Value of Tomosynthesis-guided Biopsies of Architectural Distortions Seen on Digital Breast Tomosynthesis and without an Ultrasound Correlate. *J Clin Imaging Sci.* 2019;9:53. doi: 10.25259/JCIS_134_2019. DOI
11. Young JJ, Joines MM. Benign to Malignant Spectrum of Architectural Distortions on Digital Breast Tomosynthesis. *Contemporary Diagnostic Radiology.* 2016;39(23):1-5. doi:10.1097/01.CDR.0000504575.58842.27. DOI
12. Samreen N, Moy L, Lee CS. Architectural Distortion on Digital Breast Tomosynthesis: Management Algorithm and Pathological Outcome. *J Breast Imaging.* 2020;24(5):424-435. doi: 10.1093/jbi/wbaa034. DOI
13. Patel BK, Naylor ME, Kosiorek HE et al. Clinical utility of contrast-enhanced spectral mammography as an adjunct for tomosynthesis-detected architectural distortion. *Clin Imaging.* 2017;46:44-52. doi: 10.1016/j.clinimag.2017.07.003. DOI
14. Choudhery S, Johnson MP, Larson NB et al. Malignant Outcomes of Architectural Distortion on Tomosynthesis: A Systematic Review and Meta-Analysis. *AJR Am J Roentgenol.* 2021;217(2):295-303. doi: 10.2214/AJR.20.23935. DOI
15. Ambinder EB, Plotkin A, Euhus D et al. Tomosynthesis-Guided Vacuum-Assisted Breast Biopsy of Architectural Distortion Without a Sonographic Correlate: A Retrospective Review. *AJR Am J Roentgenol.* 2021;217(4):845-854. doi: 10.2214/AJR.20.24740. DOI
16. Kerridge WD, Kryvenko ON, Thompson A et al. Fat Necrosis of the Breast: A Pictorial Review of the Mammographic, Ultrasound, CT, and MRI Findings with Histopathologic Correlation. *Radiol Res Pract.* 2015;2015:613139. doi: 10.1155/2015/613139. DOI
17. Amitai Y, Scaranelo A, Menes TS et al. Can breast MRI accurately exclude malignancy in mammographic architectural distortion? *Eur Radiol.* 2020;30(5):2751-2760. doi: 10.1007/s00330-019-06586-x. DOI
18. Ferreira AI, Borges S, Sousa A et al. Radial scar of the breast: Is it possible to avoid surgery?. *European Journal of Surgical Oncology (EJSO).* 2017;43(7):1265-1272.
19. Tan H, Zhang H, Lei Z et al. Radiological and clinical findings in sclerosing adenosis of the breast. *Medicine (Baltimore).* 2019;98(39):e17061. doi:10.1097/MD.00000000000017061. DOI
20. Taskin F, Durum Y, Soyder A et al. Review and management of breast lesions detected with breast tomosynthesis but not visible on mammography and ultrasonography. *Acta Radiol.* 2017;58(12):1442-1447. doi: 10.1177/0284185117710681. DOI
21. Bahl M, Baker JA, Kinsey EN et al. Architectural Distortion on Mammography: Correlation With Pathologic Outcomes and Predictors of Malignancy. *American Journal of Roentgenology.* 2015;205(6), 1339-1345. doi:10.2214/AJR.15.14628. DOI
22. Pujara AC, Hui J, Wang LC. Architectural distortion in the era of digital breast tomosynthesis: outcomes and implications for management. *Clin Imaging.* 2019;54:133-137. doi: 10.1016/j.clinimag.2019.01.004. DOI
23. Villa-Camacho JC, Bahl M. Management of Architectural Distortion on Digital Breast Tomosynthesis With Nonmalignant Pathology at Biopsy. *AJR Am J Roentgenol.* 2022;28:1-9. doi: 10.2214/AJR.21.27161. DOI
24. Vijapura C, Yang L, Xiong J et al. Imaging Features of Nonmalignant and Malignant Architectural Distortion Detected by Tomosynthesis. *AJR Am J Roentgenol.* 2018;211(6):1397-1404. doi: 10.2214/AJR.18.19658. DOI
25. Si L, Zhai R, Liu X et al. MRI in the differential diagnosis of primary architectural distortion detected by mammography. *Diagn Interv Radiol.* 2016;22(2):141-150. doi:10.5152/dir.2016.15017. DOI

26. Dykan IM, Bozhok YeM, Gurando AV. Pershyi dosvid vykorystannia 3D mamohrafi v Ukraini. Luhevaja diagnostika. Luhevaja Terapija [The first experience of using 3D mammography in Ukraine]. 2018;2:40-8. (Ukrainian)
27. Babkina TM, Gurando AV, Kozarenko TM et al. Detection of breast cancers represented as architectural distortion: a comparison of full-field digital mammography and digital breast tomosynthesis. *Wiad Lek.* 2021;74(7):1674–1679.
28. Ray KM, Turner E, Sickles EA et al. Suspicious Findings at Digital Breast Tomosynthesis Occult to Conventional Digital Mammography: Imaging Features and Pathology Findings. *Breast J.* 2015;21(5):538-42. doi: 10.1111/tbj.12446. [DOI](#)
29. Lee SH, Jang MJ, Kim SM et al. Factors Affecting Breast Cancer Detectability on Digital Breast Tomosynthesis and Two-Dimensional Digital Mammography in Patients with Dense Breasts. *Korean J Radiol.* 2019;20(1):58-68. doi: 10.3348/kjr.2018.0012. [DOI](#)
30. Freer PE, Niell B, Rafferty EA. Preoperative Tomosynthesis-guided Needle Localization of Mammographically and Sonographically Occult Breast Lesions. *Radiology.* 2015;275(2):377-83. doi: 10.1148/radiol.14140515. [DOI](#)
31. Wadhwa F, Majidi SS, Cherian S et al. Architectural Distortion on Screening Digital Breast Tomosynthesis: Pathologic Outcomes and Indicators of Malignancy. *Journal of Breast Imaging.* 2020;3(1):34-43. doi:10.1093/jbi/wbaa099. [DOI](#)
32. Alshafeiy TI, Nguyen JV, Rochman CM et al. Outcome of Architectural Distortion Detected Only at Breast Tomosynthesis versus 2D Mammography. *Radiology.* 2018;288(1):38-46. doi: 10.1148/radiol.2018171159. [DOI](#)
33. Langman EL, Georgiade GS. Architectural Distortion Caused by an Accessory Axillary Muscle. *Journal of Breast Imaging.* 2019;1(3):272–273. doi:10.1093/jbi/wbz030. [DOI](#)
34. Boyer B, Russ E. Anatomical-radiological correlations: Architectural distortions. *Diagnostic and Interventional Imaging.* 2014;95(2):134-140. doi:10.1016/j.diii.2014.01.003. [DOI](#)
35. Lopez JK, Bassett LW. Invasive lobular carcinoma of the breast: spectrum of mammographic, US, and MR imaging findings. *Radiographics.* 2009;29(1):165-76. doi: 10.1148/rg.291085100. [DOI](#)
36. Sekine K, Tsunoda-Shimizu H, Kikuchi M et al. DCIS showing architectural distortion on the screening mammogram - comparison of mammographic and pathological findings. *Breast Cancer.* 2007;14(3):281-4. doi: 10.2325/jbcs.14.281. [DOI](#)
37. Linda A, Zuiani C, Furlan A et al. Radial scars without atypia diagnosed at imaging-guided needle biopsy: how often is associated malignancy found at subsequent surgical excision, and do mammography and sonography predict which lesions are malignant? *AJR Am J Roentgenol.* 2010;194(4):1146-51. doi: 10.2214/AJR.09.2326. [DOI](#)
38. Freer PE, Niell B, Rafferty EA. Preoperative Tomosynthesis-guided Needle Localization of Mammographically and Sonographically Occult Breast Lesions. *Radiology.* 2015;275(2):377-83. doi: 10.1148/radiol.14140515. [DOI](#)
39. Williams KE, Amin A, Hill J et al. Radiologic and Pathologic Features Associated With Upgrade of Atypical Ductal Hyperplasia at Surgical Excision. *Acad Radiol.* 2019;26(7):893-899. doi: 10.1016/j.acra.2018.09.010. [DOI](#)
40. Miner N, Meng K. Mammographic architectural distortion caused by cyst aspiration. *Acta Radiol Open.* 2019;8(6):2058460119859353. doi:10.1177/2058460119859353. [DOI](#)

CONFLICT OF INTEREST

The Authors declare no conflict of interest

CORRESPONDING AUTHOR

Andrii Kovtun

Medical Center "Verum Expert Clinic"

13 Demiivska st, office 3, 03039 Kyiv, Ukraine

e-mail: andriikvtn17@gmail.com

ORCID AND CONTRIBUTIONSHIP

Andrii Kovtun: 0000-0001-9471-3252 [A](#) [B](#) [D](#)

Andrii Gurando: 0000-0002-2708-3040 [A](#) [B](#) [D](#) [F](#)

Vadym Telniy: 0000-0001-9860-9663 [A](#) [E](#)

Tetiana Kozarenko: 0000-0002-0838-9773 [E](#) [F](#)

[A](#) – Work concept and design, [B](#) – Data collection and analysis, [C](#) – Responsibility for statistical analysis, [D](#) – Writing the article, [E](#) – Critical review, [F](#) – Final approval of the article

RECEIVED: 23.10.2023

ACCEPTED: 17.07.2024



Features of the proteo-peptidome composition and the influence of the scorpion venom toxins on the structure of the heart of mammals (review)

Andrii Yanchyshyn¹, Inha Samborska², Oleksandr Maievskiy³, Iryna Dzevulska¹

¹BOGOMOLETS NATIONAL MEDICAL UNIVERSITY, KYIV, UKRAINE

²NATIONAL PIROGOV MEMORIAL MEDICAL UNIVERSITY, VINNYTSYA, UKRAINE

³CLINICAL MEDICINE DEPARTMENT, EDUCATIONAL AND SCIENTIFIC CENTER "INSTITUTE OF BIOLOGY AND MEDICINE" OF TARAS SHEVCHENKO NATIONAL UNIVERSITY OF KYIV, KYIV, UKRAINE

ABSTRACT

Aim: To determine the profound influence of scorpion venom toxins on the intricate structure of the heart of mammals, a topic of utmost importance in toxicology and cardiovascular health.

Materials and Methods: A meticulous and comprehensive literature analysis was conducted using PubMed, Google Scholar, Web of Science, and Scopus databases. We meticulously selected the newest publications up to 5 years old or the most thorough publications that vividly described our topic's essence, ensuring our findings' credibility and reliability.

Conclusions: Scorpion venom is a complex of biologically active substances that have a wide range of effects on the vital systems of the victim's body. Violations of the normal functioning of the cardiovascular system occur both as a result of disorders of the conduction system of the heart and as a result of pronounced morphological changes in the tissues of the organ. In particular, the development of inflammatory processes of the myocardium, the formation of blood clots in the heart vessels, degeneration of myofibrils, fragmentation of fibres, haemorrhages, etc., are characteristic under these conditions. In addition, these changes are accompanied by the production of pro-inflammatory cytokines, apoptosis factors, and the development of OS.

KEY WORDS: scorpions, toxins, heart, inflammation, oxidative stress

Wiad Lek. 2024;77(9):1782-1788. doi: 10.36740/WLek/191323 DOI

INTRODUCTION

Poisoning due to scorpion bites is one of the current medical problems that pose a threat to the health and life of people, especially children and older people with a severe medical history [1]. The epidemiology of scorpionism worldwide is staggering. Every year, about 1.2-1.5 million people suffer from the bites of these animals, which leads to 2,600 deaths. Until recently, it was believed that poisoning due to scorpion bites is characteristic mainly of poorly developed tropical and subtropical countries, namely Africa, India, the Middle East, Mexico, and Latin America. However, the significant expansion of their usual distribution area is currently well known, so fatal cases are also recorded in countries with a high standard of living [2, 3]. Data from scientific sources testify to more than 1,500 different species of scorpions, among which 50 are poisonous subspecies [4]. It has been established that the toxic

components of their venom cause the appearance of not only local symptoms (redness at the site of bites, pain, swelling) but also the development of severe neurological and haematological disorders, disorders of the cardiovascular, respiratory, excretory systems, etc. Clinical manifestations, as indicated, depend on the dose of toxin that entered the victim's body, age, season, when the case occurred, the time between the actual bite, and the speed of providing medical assistance. The results of experimental studies show that among the leading causes of death under these conditions are heart failure and pulmonary oedema [5]. In modern sources of scientific literature, it is stated that among all arthropods, the genome of scorpions contains the most significant number of genes (almost 32,016) encoding proteins. The last ones are essential structural components of their venom and have extremely toxic properties [6].

AIM

This crucial research aimed to determine the profound influence of scorpion venom toxins on the intricate structure of the heart of mammals, a topic of utmost importance in toxicology and cardiovascular health.

MATERIALS AND METHODS

A thorough literature analysis was conducted using PubMed, Google Scholar, Web of Science, and Scopus databases. When searching for information on the features of the scorpion venom composition peculiarities of the influence of scorpion venom toxins on the structure and functions of the organs and systems of the mammalian body, we used the following combinations of keywords: "scorpions", "toxins", "heart", "inflammation", "oxidative stress". When processing the search results, we chose the newest publications up to 5 years old or the most thorough publications that vividly described the essence of our topic. After conducting a detailed review of the abstracts of the articles and getting acquainted with their entire content, 36 sources were selected that fully corresponded to the results of the request.

REVIEW AND DISCUSSION

Even though more than 800 peptides have been identified to date, the composition of scorpion venom is considered poorly researched. In addition, it can vary significantly even within a species. Therefore, the variables are the features of biological action, impact on target organs, and morphological changes in body systems. Therefore, a detailed study of the structural elements of scorpion toxins is a promising area of toxicology, molecular biology, morphology, etc. Expanding ideas about the influence of scorpion venoms will make it possible to establish the pathogenetic mechanisms of the development of certain complications and patterns of histological and biochemical changes in target organs. It may also be essential in developing treatment methods, prevention, and producing medicines and antidotes.

Scorpion venom contains a whole arsenal of biologically active substances, including polypeptides, enzymes (phospholipases A, B, acid phosphatase, phosphodiesterase, acetylcholinesterase, 5'-nucleotidase, hyaluronidase, ribonucleases, metalloproteinases), mono- and polysaccharides, lipids, nucleotides, biogenic amines, in particular, histamine and serotonin. Scientists know the classification of the peptides of their venom into those containing disulfide bridges (disulfide-bridged peptides – DBP) and those without

them (non-disulfide bridged peptides – NDBP) [7]. Most DBPs exhibit neurotoxic activity, having the ability to change the permeability of ion channels and block or reduce the action potential. Among these peptides, toxins of Na⁺, K⁺, Ca²⁺, and Cl⁻ channels are distinguished [8]. Blockers of Na⁺ channels contain 58 to 76 amino acid residues in the structure and are stabilised by four disulfide bridges. They are classified into α and β -toxins. α -Na toxins (α -NaTx) affect the nervous system of victims by prolonging the depolarisation time of ion channels, while β -Na toxins (β -NaTx) cause changes in their activation threshold [9].

DBPs acting on K⁺ channels comprise 20-70 amino acid residues and 3-4 disulfide bridges. According to the molecular weight and the number of disulfide bridges, α -KTx, β -KTx, γ -KTx, κ -KTx are distinguished. As a result of the blockade of K⁺ channels, there is a delay in their repolarisation, a prolongation of the action potential, and an increase in the refractory period [10].

Inhibitors of Cl⁻ channels are currently less studied than the previously mentioned types. However, 30-40 amino acid residues and four disulfide bridges in their composition have been established. The interaction of toxins with low-conductance chlorine channels leads to suppression or complete inhibition of their activity. In the body of the victims, it becomes the cause of the development of convulsions and paralysis. The latter mainly affects the respiratory muscles, sometimes leading to severe respiratory dysfunction [11].

Scientists have established that the enzymatic activity of scorpion venom is much lower than the venom of snakes and vipers. Still, most of them have adverse effects on the victim's body. In particular, hyaluronidase is involved in the rapid systemic distribution of toxins. This property is characterised by enzyme degradation of the extracellular matrix, vessel walls, and poison entering the bloodstream. A high content of hyaluronidase was found in the venom of scorpions *Tituys serrulatus* and *Tituys stigmurus* [12]. Metalloproteinases (MMPs) have demonstrated the ability to cleave neuropeptides and affect synaptic vesicles of the presynaptic membranes of neuromuscular junctions. Scorpion venom phospholipases belong to the III class of secretory phospholipases. These have a particular heterodimeric structure built from a long polypeptide chain connected to a short one by a disulfide bridge. Neurotoxic, myotoxic, hemolytic, anticoagulant, anticarcinogenic, and antiangiogenic activities are among their biological effects on the human body [13].

Experimental studies of recent years prove that the toxins of almost all species of scorpions have a high tropism to the cardiovascular system [14, 15]. A series of cardiac conduction disturbances occur in approximate-

ly one-third of patients in case of systemic distribution of venom components. The most common conditions are atrial tachycardia, ventricular extrasystole, T-wave inversion, ST segment changes, and bundle branch block (bundle of His) [16]. Probable causes of the appearance of these complications are pronounced sympathetic stimulation. Hypertension is also a common consequence. Hypotension, on the other hand, is rare and is associated with a severe course of poisoning characterised by vasodilatation, hypovolemia, and suppression of the contractility of the heart [17].

Abroug F. et al. [18] studied cardiomyopathy associated with scorpionism. Cardiac dysfunction occurring in the early stages of poisoning is associated, according to the researchers, with the so-called "vascular phase". It is characterised by catecholamine-induced vasoconstriction, which leads to an increase in the afterload of the left ventricle, an increase in the filling pressure, a violation of its emptying and a critical rise in pressure in the capillaries, leading to the development of pulmonary oedema, an increase in the afterload of the right ventricle. In response to increased production of vasoconstrictors – epinephrine, norepinephrine, neuropeptide B, and endothelin, the contractility of the myocardium of the left ventricle and, accordingly, oxygen consumption increases, temporarily maintaining cardiac output at an acceptable level. Subsequently, the "myocardial" phase occurs, accompanied by a decrease in the contractile ability of the heart muscle, low cardiac output, and hypotension. Among scientists, there are various hypotheses regarding the mechanisms of cardiomyopathy in scorpion bites. Considering the reversibility of pathological changes and the main pathophysiological pathways of development, most hold opinions regarding the development of Takotsubo cardiomyopathy or stress cardiomyopathy. Recent clinical observations have shown that under these conditions, stress cardiomyopathy occurs more often in children and is characterised by spasms of small myocardial vessels, ischemia of the heart muscle, and microvascular vasomotor dysfunction.

A careful and comprehensive study of literature sources made it possible to establish that myocardial infarction is a frequent complication of poisoning by scorpion toxins. It is known that the active components of their venom stimulate the production and release of vasoactive pro-inflammatory and thrombogenic substances, such as histamine, serotonin, bradykinins, leukotrienes, and thromboxane. These compounds can induce spasms of coronary arteries and stimulate the aggregation of platelets and the formation of blood clots in the vessels of the heart. In addition, there is data on the possible mechanism of myocardial infarction

due to IgE-induced hypersensitivity of the immediate type, which was described for the first time by Kunis and is accompanied by damage of the heart muscle and severe eosinophilia [19].

Reis M. B. et al. [20], studying the mechanisms of the cardiovascular system damage during intoxication with *Tityus serrulatus* scorpion venom, established the induction of the inflammatory reaction in heart tissue. Thus, flow cytometric analysis of the organ revealed an increase in neutrophils and a decrease in macrophages. This process was accompanied by activating genes that regulate the innate immune system and produce eicosanoids. The venom of *Tityus serrulatus* stimulated the activation of the inflammasome – NLRP3, apoptosis-associated proteins and caspase 1/11, the release of IL-1 β and the production of PGE₂ in experimental animals' heart and blood serum. During the experiment, it was possible to determine that in the mechanisms of triggering inflammatory reactions, the leading role belongs to the fibroblasts of the organ and, to a lesser extent, to cardiomyocytes. Stimulation of the culture of these cells for 24 hours showed that only fibroblasts could release IL-1 β and both cell types PGE₂. Cardiac fibroblasts showed higher expression of pro-inflammatory genes and CD14 and TLR₄ receptors on the surface of cell membranes. It is known that for NLRP3 and increasing of the of IL-1 β , activation of pattern recognition receptors (PRR), increased release of K⁺ ions from the cell, synthesis and release of PGE₂, increased levels of 3'-5'-cAMP, activation of protein kinase A and nuclear factor-kB (NF-kB) are necessary conditions. Cardiac fibroblasts treated with *Tityus serrulatus* scorpion venom-induced IL-1 β release through the PGE₂/cAMP/PKA signalling pathway. cAMP levels increased in these cells after the addition of exogenous PGE₂. Increased expression of the total and phosphorylated form of PKA was also observed in the heart lysates of poisoned mice. Therefore, the authors indicated that the fibroblasts of the heart participate in the processes of triggering the inflammatory cascade in the heart of rats after intoxication with *Tityus serrulatus* scorpion venom by stimulating the production of IL-1 β and PGE₂.

Single studies were found in scientometric databases, accompanied by histological examination of heart samples of experimental rats exposed to the venom of various types of scorpions. *Androctonus mauretanicus* and *Buthus occitanus* were found to cause degeneration of cardiac muscle myofibrils 60 minutes after venom injection in rats. Further observations under the specified conditions revealed a deepening of the myocardial damage. The venom of *Buthus lienhardi* scorpions within 3 hours after administration causes significant myocardial fibres and haemorrhage frag-

mentation. Inoculation of animals with toxins from scorpions *Androctonus australis hector* led to dystrophy of cardiomyocytes, infiltration of the myocardium with polymorphonuclear cells, macrophages, lymphocytes, the appearance of oedema, acute haemorrhage, and necrosis [21].

Bakir F. et al. [22] studied the effect of *Androctonus crassicauda* venom on rat heart tissue when administered intravenously to animals. Examination of the morphological state of the organ was carried out after 1, 3, 6, and 24 hours. Microscopic studies revealed hydropic degeneration of cardiomyocytes; their cytoplasm contained many vacuoles of various shapes and sizes, and pyknosis of the nuclei was characteristic. However, cardiomyocytes with signs of necrosis containing homogeneous eosinophilic granules rarely occurred among degenerated myofibrils. Some muscle fibres lost transverse striation. Myocardial capillaries had signs of whole blood and included many erythrocytes. Erythrocytes between myofibrils in many fields of view and phenomena of haemorrhages were also noted. Infiltration of heart tissue by leukocytes and macrophages was observed. Biochemical studies confirmed organ damage, as an increase in the level of cardiac troponin I (cTnI) was recorded.

Yazdkhasti M. et al. [23] proved the cardiotoxic effect of *Hemiscorpius lepturus* venom. Morphological studies revealed signs of multifocal fragmentation of myocardial muscle fibres, between which foci of haemorrhages were noted. In some fields of vision, the characteristic transverse striation of the heart muscle disappeared. After 3-6 hours of observation, acute myocytolysis and interstitial necrosis were characteristic. The results of parallel studies confirmed these findings and, in addition, demonstrated the development of oedema and hypertrophy of myocardial muscle fibres with their massive infiltration by leukocytes. In the blood serum of laboratory animals under these conditions, the levels of LDH, AST, CPK-MB and cTnI increased after 1, 3 and 24 hours of the study [24].

Scorpion venom leads to the activation of inflammatory processes and excess production of free radicals in the heart tissue of victims, leading to organ damage. As a rule, venom components bind to pattern recognition receptors, namely Toll-like receptors TLR₂ and TLR₄, activate the transcription factor NF- κ B, stimulate the production of pro-inflammatory mediators and reactive oxygen species (ROS), which leads to the development of oxidative stress in the heart (OS) [25, 26]. Recently, it has been established that endothelin-1, the production of which increases significantly under the conditions of poisoning with scorpion toxins, also stimulates the production of superoxide anion and pro-inflammatory

cytokines, including IL-1, TNF- α , IL-6 [27, 28]. In experiments on rats, Sifi A. et al. [29, 30] established that the introduction of venom from the scorpion *Androctonus australis hector* was associated with increased expression of TNF- α and IL-17 in animals. In addition, the pronounced activity of myeloperoxidase (MPO) (the main enzyme of azurophilic granules of neutrophils), matrix metalloproteinases (MMP-2 and MMP-9) was found in homogenates of rat heart and aorta. According to the authors, MPO, under these conditions, is a marker of neutrophil activation. MMPs are involved in the degradation of the extracellular matrix of the myocardium and components of the aorta walls. Scientists have proven the development of OS in the heart of experimental animals by injecting them with the venom of the specified species of scorpions. OS was characterised by an increase in the levels of H₂O₂, malondialdehyde (MDA), and NO₂ in the supernatants of the myocardium. At the same time, a decrease in the activity of antioxidant protection enzymes – catalase and glutathione peroxidase was recorded. Microscopic studies revealed damage to the myocardium, degeneration of muscle fibres, foci of haemorrhages, and oedema. Zones of myonecrosis and pronounced leukocyte infiltration were noted. The aorta was characterised by thickening of its tunica media, and in some places, signs of the development of an aneurysm of its wall were observed.

Naserzadeh P. and co-authors [31], studying the venom of scorpions *Hemiscorpius lepturus*, established that the last exhibits a cardiotoxic effect. Thus, the authors, through experiments on rats, demonstrated that the indicated effect of the toxins of these animals consists in the death of cardiomyocytes by apoptosis. The venom of *Hemiscorpius lepturus* causes the activation of caspase-3 and the development of mitochondrial dysfunction. Mitochondrial dysfunction was associated with significant production of ROS, swelling of organelles, a decrease in the potential of their membranes, activity of cytochrome c oxidase (respiratory chain complex IV), ATP levels, and ruptures of the mitochondrial outer membrane. In addition, inhibition of the activity of the II complex of the respiratory chain (succinate-CoQ-oxidoreductase) and the formation of apoptosomes – cytosolic factors of apoptosis, in response to the release of cytochrome c due to the opening of the pores of the mitochondrial membranes were recorded.

Studying the sources of scientific literature showed that some components of scorpion venom have a positive effect on the structures of the heart muscle under certain conditions. Ahmed L. A. et al. [32] found that bradykinin-potentiating peptides isolated from *Leiurus quinquestriatus* scorpion venom protect myocardial












structures and significantly reduce the adverse effects of doxorubicin-induced acute cardiotoxicity. In their experiments, the researchers isolated a fraction of the venom and treated it by γ -irradiation to weaken the peptides' toxicity and potentiate the pharmacological activity. Pretreatment of the myocardium with bradykinin-potentiating peptides from *Leiurus quinquestriatus* scorpion venom before treatment of experimental rats with doxorubicin significantly reduced the degree of heart tissue damage and manifestations of OS, inflammation, and apoptosis. Bradykinin-potentiating peptides showed antioxidant, anti-inflammatory and immunomodulatory properties. The realisation of these effects is possible through antigen-receptor signalling pathways. Activation of bradykinin B2 receptors leads to increased production of NO, increased expression of antioxidant defence enzymes, in particular SOD (MnSOD, Cu/Zn-SOD), and reduction of NADPH oxidase, which prevents excessive production of ROS. It should be noted that the histological structure of the myocardium significantly improved under these conditions. Thus, doxorubicin led to the formation of areas of necrosis, foci of infiltration by mononuclear cells, the development of nuclear pyknosis, intercellular oedema, and hyalinosis. During preliminary treatment of heart tissue with bradykinin-potentiating peptides from *Leiurus quinquestriatus* scorpion venom,

cardiomyocytes had an organisation similar to that of intact rats; only sporadic cases of moderate degenerative changes were recorded.

CONCLUSIONS

Scorpion venom is a complex of biologically active substances that have a wide range of effects on the vital systems of the victim's body. The toxins of their venom are tropic to the organs of the nervous, respiratory, skeletal, excretory, and cardiovascular systems. Violations of the normal functioning of the cardiovascular system occur both as a result of disorders of the conduction system of the heart and as a result of pronounced morphological changes in the tissues of the organ. In particular, the development of inflammatory processes of the myocardium, the formation of blood clots in the heart vessels, degeneration of myofibrils, fragmentation of fibres, haemorrhages, etc., are characteristic under these conditions. In addition, these changes are accompanied by the production of pro-inflammatory cytokines, apoptosis factors, and the development of OS. These data point to the need for an in-depth study of the structure, biological action, and functional activity of scorpion toxins of various species since a significant part of them remains unknown.

REFERENCES

- Almeida ACC, Carvalho FM, Mise YF. Risk factors for fatal scorpion envenoming among Brazilian children: a case-control study. *Trans R Soc Trop Med Hyg.* 2021;115(9): 975-983. doi: 10.1093/trstmh/traab120. DOI 
- Cid-Urbe JI, Veytia-Bucheli JI, Romero-Gutierrez T et al. Scorpion venomomics: a 2019 overview. *Expert Rev Proteomics.* 2020;17(1):67-83. doi: 10.1080/14789450.2020.1705158. DOI 
- Torrez PPQ, Dourado FS, Bertani R et al. Scorpionism in Brazil: exponential growth of accidents and deaths from scorpion stings. *Rev Soc Bras Med Trop.* 2019;52:e20180350. doi: 10.1590/0037-8682-0350-2018. DOI 
- El-Aziz FEA A, El Shehaby DM, Elghazally SA, Hetta HF. Toxicological and epidemiological studies of scorpion sting cases and morphological characterization of scorpions (*Leiurusquin questriatus* and *Androctonus crassicauda*) in Luxor, Egypt. *Toxicol Rep.* 2019;6:329-335. doi: 10.1016/j.toxrep.2019.03.004. DOI 
- Abroug F, Ouanes-Besbes L, Tilouche N, Elatrous S. Scorpion envenomation: state of the art. *Intensive Care Med.* 2020;46(3):401-410. doi: 10.1007/s00134-020-05924-8. DOI 
- Amorim FG, Longhim HT, Cologna CT et al. Proteome of fraction from *Tityus serrulatus* venom reveals new enzymes and toxins. *J Venom Anim Toxins Incl Trop Dis.* 2019;25:e148218. doi: 10.1590/1678-9199-JVATITD-1482-18. DOI 
- Batista CVF, Martins JG, Restano-Cassulini R et al. Venom characterization of the Amazonian scorpion *Tityus metuendus*. *Toxicon.* 2018;143:51-58. doi: 10.1016/j.toxicon.2018.01.006. DOI 
- Dueñas-Cuellar RA, Santana CJC, Magalhães ACM et al. Scorpion Toxins and Ion Channels: Potential Applications in Cancer Therapy. *Toxins (Basel).* 2020;12(5):326. doi: 10.3390/toxins12050326. DOI 
- Furtado AA, Daniele-Silva A, Silva-Júnior AAD, Fernandes-Pedrosa MF. Biology, venom composition, and scorpionism induced by brazilian scorpion *Tityus stigmurus* (Thorell, 1876) (Scorpiones: Buthidae): A mini-review. *Toxicon.* 2020;185:36-45. doi: 10.1016/j.toxicon.2020.06.015. DOI 
- Díaz-García A, Varela D. Voltage-Gated K⁺/Na⁺ Channels and Scorpion Venom Toxins in Cancer. *Front Pharmacol.* 2020;11:913. doi: 10.3389/fphar.2020.00913. DOI 
- Cohen G, Burks SR, Frank JA. Chlorotoxin-A Multimodal Imaging Platform for Targeting Glioma Tumors. *Toxins (Basel).* 2018;10(12):496. doi: 10.3390/toxins10120496. DOI 

12. Guerra-Duarte C, Rebello Horta CC, Ribeiro Oliveira-Mendes BB et al. Determination of hyaluronidase activity in *Tityus* spp. Scorpion venoms and its inhibition by Brazilian antivenoms. *Toxicon*. 2019;167:134-143. doi: 10.1016/j.toxicon.2019.06.019. [DOI](#)
13. Krayem N, Gargouri Y. Scorpion venom phospholipases A2: A minireview. *Toxicon*. 2020;184:48-54. doi: 10.1016/j.toxicon.2020.05.020. [DOI](#)
14. Khalaf MA, El-Deen MAB, Hishmat AM. Scorpion sting: N-terminal fragment of proB-type natriuretic peptide as an early predictor of pediatric cardiotoxicity. *Hum Exp Toxicol*. 2021;40(5):754-760. doi: 10.1177/0960327120968863. [DOI](#)
15. Ratnayake RM, Kumanan T, Selvaratnam G. Acute myocardial injury after scorpion (*Hottentotta tamulus*) sting. *Ceylon Med J*. 2016;61(2):86-87. doi: 10.1177/0960327120968863. [DOI](#)
16. Prasad R, Kumar A, Jain D et al. Echocardiography versus cardiac biomarkers for myocardial dysfunction in children with scorpion envenomation: An observational study from tertiary care center in northern India. *Indian Heart J*. 2020;72(5):431-434. doi: 10.1016/j.ihj.2020.07.020. [DOI](#)
17. Costal-Oliveira F, Guerra-Duarte C, Oliveira MS et al. Cardiorespiratory alterations in rodents experimentally envenomed with *Hadruroides lunatus* scorpion venom. *J Venom Anim Toxins Incl Trop Dis*. 2016;23:2. doi: 10.1186/s40409-016-0076-5. [DOI](#)
18. Abroug F, Souheil E, Ouanes I et al. Scorpion-related cardiomyopathy: Clinical characteristics, pathophysiology, and treatment. *Clin Toxicol (Phila)*. 2015;53(6):511-518. doi: 10.3109/15563650.2015.1030676. [DOI](#)
19. Baykan AO, Gür M, Acele A et al. Scorpion envenomation-induced acute thrombotic inferior myocardial infarction. *Turk Kardiyol Dern Ars*. 2016;44(1):82-86. doi: 10.5543/tkda.2015.88590. [DOI](#)
20. Reis MB, Rodrigues FL, Lautherbach N et al. Interleukin-1 receptor-induced PGE2 production controls acetylcholine-mediated cardiac dysfunction and mortality during scorpion envenomation. *Nat Commun*. 2020;11(1):5433. doi: 10.1038/s41467-020-19232-8. [DOI](#)
21. Darkaoui B, Lafnoue A, Chgoury F et al. Induced pathophysiological alterations by the venoms of the most dangerous Moroccan scorpions *Androctonus mauretanicus* and *Buthus occitanus*: A comparative pathophysiological and toxic-symptoms study. *Hum Exp Toxicol*. 2022;41:9603271211072872. doi: 10.1177/09603271211072872. [DOI](#)
22. Bakir F, Ozcan O, Alcigir ME, Vural SA. Effects of *Androctonus crassicauda* scorpion venom on the heart tissue. *J Anim Vet Adv*. 2012;11(14):2594-2599. doi:10.3923/javaa.2012.2594.2599. [DOI](#)
23. Yazdkhasti M, Jalali MR, Khadjeh GH et al. Cardiotoxic effects of *Hemiscorpius lepturus* scorpion venom fractions in rats. *Iran J Toxicol*. 2021;15(1):27-36.
24. Ait Laaradia M, El Hidan MA, Marhoume F et al. *Buthus lienhardi* venom and pathophysiological effects at the histological, hematological, biochemical and motor skills levels. *Toxicon*. 2018;146:106-113. doi: 10.1016/j.toxicon.2018.03.001. [DOI](#)
25. Ahmed AE, Hassan MH, Rashwan NI et al. Myocardial injury induced by scorpion sting envenoming and evidence of oxidative stress in Egyptian children. *Toxicon*. 2018;153:72-77. doi: 10.1016/j.toxicon.2018.08.008. [DOI](#)
26. Zoccal KF, Bitencourt Cda S, Paula-Silva FW et al. TLR2, TLR4 and CD14 recognize venom-associated molecular patterns from *Tityus serrulatus* to induce macrophage-derived inflammatory mediators. *PLoS One*. 2014;9(2):e88174. doi: 10.1371/journal.pone.0088174. [DOI](#)
27. Al-Asmari AK, Riyasdeen A, Islam M. Scorpion Venom Causes Apoptosis by Increasing Reactive Oxygen Species and Cell Cycle Arrest in MDA-MB-231 and HCT-8 Cancer Cell Lines. *J Evid Based Integr Med*. 2018;23:2156587217751796. doi: 10.1177/2156587217751796.
28. Corzo G, Espino-Solis GP. Selected scorpion toxin exposures induce cytokine release in human peripheral blood mononuclear cells. *Toxicon*. 2017;127:56-62. doi: 10.1016/j.toxicon.2017.01.007. [DOI](#)
29. Sifi A, Adi-Bessalem S, Laraba-Djebari F. Involvement of the Endothelin Receptor Type A in the Cardiovascular Inflammatory Response Following Scorpion Envenomation. *Toxins (Basel)*. 2020;12(6):389. doi: 10.3390/toxins12060389. [DOI](#)
30. Sifi A, Adi-Bessalem S, Laraba-Djebari F. Role of angiotensin II and angiotensin type-1 receptor in scorpion venom-induced cardiac and aortic tissue inflammation. *Exp Mol Pathol*. 2017;102(1):32-40. doi: 10.1016/j.yexmp.2016.11.006. [DOI](#)
31. Naserzadeh P, Mehr SN, Sadabadi Z et al. Curcumin Protects Mitochondria and Cardiomyocytes from Oxidative Damage and Apoptosis Induced by *Hemiscorpius lepturus* Venom. *Drug Res (Stuttg)*. 2018;68(2):113-120. doi: 10.1055/s-0043-119073. [DOI](#)
32. Ahmed LA, Abdou FY, El Fiky AA et al. Bradykinin-Potentiating Activity of a Gamma-Irradiated Bioactive Fraction Isolated from Scorpion (*Leiurus quinquestriatus*) Venom in Rats with Doxorubicin-Induced Acute Cardiotoxicity: Favorable Modulation of Oxidative Stress and Inflammatory, Fibrogenic and Apoptotic Pathways. *Cardiovasc Toxicol*. 2021;21(2):127-141. doi: 10.1007/s12012-020-09602-5. [DOI](#)

CONFLICT OF INTEREST

The Authors declare no conflict of interest

CORRESPONDING AUTHOR

Inga Samborska

National Pirogov Memorial Medical University

56 Pirogov st, 21018, Vinnytsya, Ukraine

e-mail: samborska1990@gmail.com

ORCID AND CONTRIBUTIONSHIP

Inga Samborska: 0000-0002-6812-489X **B** **D**

Oleksandr Maievskiy: 0000-0002-9128-1033 **A** **E**

Andrii Yanchyshyn: 0000-0003-1598-8106 **F**

Iryna Dzevelska: 0000-0002-8043-6626 **A** **E**

A – Work concept and design, **B** – Data collection and analysis, **C** – Responsibility for statistical analysis, **D** – Writing the article, **E** – Critical review, **F** – Final approval of the article

RECEIVED: 11.12.2023

ACCEPTED: 17.07.2024



Advancements and applications of laser technology in modern dentistry

Agnieszka Rolek¹, Piotr Pławecki²

¹PRIVATE DENTAL PRACTICE - AGNIESZKA ROLEK, WROCLAW, POLAND

²DEPARTMENT OF CRANIO-MAXILLO-FACIAL SURGERY, PROVINCIAL SPECIALIST HOSPITAL NO. 5 IN SOSNOWIEC, SOSNOWIEC, POLAND

ABSTRACT

The use of lasers in dentistry has revolutionized dental procedures, providing significant advantages over traditional techniques. Lasers offer enhanced precision, reduced bleeding, faster healing times, and improved patient comfort. This review explores CO₂ lasers, diode lasers, Er, and Er, Cr lasers, and Photobiomodulation and Low-Level Laser Therapy (LLLT). CO₂ Lasers: Introduced in the 1970s, CO₂ lasers are effective for soft tissue surgeries such as gingivectomy and frenectomy due to their high water absorption, which allows for precise cutting with minimal damage. They also enhance enamel and dentin resistance, treat gingival hyperpigmentation, and manage peri-implantitis. Diode Lasers: These are suitable for soft tissue procedures, emitting wavelengths of 800-980 nm. Diode lasers are widely used for periodontal therapy and peri-implantitis management due to their antimicrobial properties, offering benefits like reduced bleeding and faster healing. Er and Er, Cr Lasers: Emitting at 2940 nm and 2780 nm respectively, these lasers are absorbed by water and hydroxyapatite, making them ideal for caries removal and bone contouring. They provide precise ablation with minimal thermal damage. Photobiomodulation and LLLT: These therapies use low-level lasers or LEDs to stimulate cellular function, promote healing, and reduce pain without thermal damage, making them effective for managing pain and inflammation. Overall, lasers offer significant benefits in precision, patient comfort, and healing, making them a valuable tool in modern dentistry.

KEY WORDS: coagulation, lasers, non invasive surgery

Wiad Lek. 2024;77(9):1789-1792. doi: 10.36740/WLek202409121 DOI

INTRODUCTION

The utilization of lasers in dentistry has revolutionized various dental procedures, offering significant advantages over traditional techniques. Lasers provide unparalleled precision, reduced bleeding, faster healing times, and enhanced patient comfort, making them a preferred choice for many dental applications. This document delves into the different types of dental lasers, including CO₂ lasers, diode lasers, Er, and Er,Cr lasers, as well as the emerging fields of Photobiomodulation and Low-Level Laser Therapy (LLLT), outlining their specific applications and benefits in modern dental practice.

AIM

The aim of this study is to describe and discuss the use of lasers in modern dentistry, highlighting their advantages and disadvantages compared to conventional methods.

MATERIALS AND METHODS

This study is based on a review of scientific literature on laser therapy. It includes articles from the past 25 years,

encompassing original research, systematic reviews, and meta-analyses. The focus is on the use of lasers for aiding in healing as well as their broad application in soft and hard tissue surgery.

REVIEW

TYPES AND APPLICATIONS OF DENTAL LASERS
CO₂ laser has been a significant tool in dentistry since its introduction in the 1970s, primarily for soft tissue applications. It is a gas mixture (primarily carbon dioxide) which is used in its mechanism. CO₂ laser emits at a wavelength of 10,600 nm [1]. These are primarily used for soft tissue surgeries due to their high water absorption, leading to efficient cutting and coagulation with minimal damage to surrounding tissues. It is effective for both soft and hard tissues due to its high absorption in water and hydroxyapatite. Provides precise cutting and vaporization with minimal thermal damage to surrounding tissues when used properly [2]. These lasers can be used not only in surgery, including gingivectomy, frenectomy, and treatment of oral lesions such as leukoplakia, erythroplakia, and lichen

planus as they offer precise cutting with minimal bleeding due to their excellent hemostatic properties [3, 4] but also in caries prevention. CO₂ lasers enhance the resistance of enamel and dentin to acid demineralization. They can also inhibit the progression of existing carious lesions and improve the longevity of composite restorations by reducing caries around them [3, 5]. The laser is also effective in treating gingival hyperpigmentation. Provides a non-invasive method to achieve aesthetic improvements in patients with excessive melanin deposits in their gums. Studies show significant patient satisfaction with minimal pain and quick healing [6]. CO₂ lasers are increasingly used in the treatment of peri-implantitis due to their precise ablation properties and ability to disinfect implant surfaces. The high absorption of CO₂ lasers in water and hydroxyapatite makes them effective for soft tissue debridement and bone contouring around implants. CO₂ lasers are a versatile and valuable tool in modern dentistry, offering numerous benefits for both soft and hard tissue procedures. Their precise control, reduced patient discomfort, and enhanced healing make them a preferred choice for various dental applications, although they require proper training and careful handling to avoid potential risks.

Diode Laser is suitable for soft tissue procedures and uses semiconductor diodes. Emission wavelengths typically range from 800-980 nm and is primarily absorbed by melanin and hemoglobin [7]. Diode Lasers are widely used for soft tissue procedures, including gingivectomy, frenectomy, and periodontal therapy. They offer benefits like reduced bleeding, pain, and faster healing times [8, 9] and have become increasingly popular in dentistry due to their versatility, ease of use, and relatively low cost compared to other types of lasers. As well as CO₂ lasers, diode lasers are frequently used for soft tissue surgeries such as gingivectomy, frenectomy, and tissue contouring. They are effective in cutting and coagulating soft tissues with minimal bleeding [8, 9]. As well as CO₂ lasers they are used in caries and gingival depigmentation treatment. Diode lasers also play a crucial role in the management of peri-implantitis due to their antimicrobial properties and ability to decontaminate implant surfaces. The laser energy helps to remove bacterial biofilms from the implant surfaces, which is essential for the successful treatment of peri-implantitis [10, 11]. The anti-inflammatory properties of diode lasers help to reduce inflammation in the peri-implant tissues. This can result in improved healing and regeneration of the tissues around the implant [8].

Er and Er, Cr Lasers (Erbium-doped Yttrium Aluminium Garnet) and Er, Cr (Erbium, Chromium-doped Yttrium Scandium Gallium Garnet) lasers operate by emitting high-intensity light at specific wavelengths, primarily targeting water and hydroxyapatite in dental tissues. Er Laser emits light at a wavelength of 2940 nm, while Er, Cr Laser emits light at

a wavelength of 2780 nm. These wavelengths are highly absorbed by water, making them effective for both hard and soft tissue procedures. The laser energy is absorbed by the water content in the tissues, causing rapid heating and vaporization of water molecules. This results in micro-explosions that precisely ablate the target tissue with minimal thermal damage to surrounding areas [12]. The lasers are also absorbed by hydroxyapatite, a mineral found in teeth and bone. This allows for effective cutting and reshaping of hard dental tissues without excessive heat buildup, which could damage surrounding tissues [13]. They are widely used in dentistry for various applications due to their specific wavelength characteristics and interactions with dental tissues. These are effective for caries removal, cavity preparation, and etching. The ablation process removes diseased or unwanted tissue through precise vaporization. The coagulative effect helps in controlling bleeding by sealing small blood vessels, making it particularly useful for soft tissue procedures. These lasers often incorporate a cooling system, such as a water spray or air cooling, to manage the heat generated during the procedure and to further minimize thermal damage to adjacent tissues [12]. The precise ablation capabilities make Er and Er, Cr lasers suitable for removing caries and preparing cavities without the need for anesthesia in many cases. Their ability to cut and coagulate makes them ideal for procedures like gingivectomy, frenectomy, and periodontal debridement. They are perfectly effective for bone contouring and other hard tissue modifications due to their interaction with hydroxyapatite.

Photobiomodulation and Low-Level Laser Therapy (LLLT): are therapeutic techniques that utilize low-level lasers or light-emitting diodes (LEDs) to stimulate cellular function and promote healing, pain relief, and tissue regeneration without causing thermal damage. These therapies have found increasing applications in dentistry due to their non-invasive nature and efficacy. LLLT works by delivering photons to the cells, which are absorbed by the mitochondria. This process enhances ATP (adenosine triphosphate) production, leading to increased cellular energy and metabolic activity. LLLT promotes vasodilation, which increases blood flow to the treated area, facilitating the delivery of oxygen and nutrients, and removal of waste products. This accelerates the healing process [10]. The therapy reduces the levels of pro-inflammatory cytokines and increases anti-inflammatory cytokines. This helps in reducing inflammation and pain in the treated area. LLLT is effective in reducing pain associated with various dental procedures, including tooth extractions, implant placements, and orthodontic adjustments. It is also used for managing temporomandibular joint disorders (TMD) and myofascial pain [9]. Numerous oral disorders have shown significant improvement with the use of low-intensity lasers. When combined with antibiotics, these lasers can

enhance the treatment outcomes for patients suffering from bisphosphonate-related osteonecrosis of the jaw (BRONJ) and medication-related osteonecrosis of the jaw (MRONJ), effectively reducing clinical symptoms [8].

DISCUSSION

Studies have shown mixed results regarding the effectiveness of lasers as an adjunct to mechanical therapy. Some studies indicate significant improvements in clinical and microbiological parameters when lasers are used, while others suggest no additional benefits over conventional methods [1, 7]. However, the precision and disinfection properties of lasers make them a promising option. The coagulative properties minimize bleeding, improving visibility and reducing the need for sutures [8, 9]. Faster healing times due to reduced inflammation and less trauma to tissues has been observed [8]. In a review of current literature authors noticed less postoperative pain and swelling, leading to higher patient comfort for the patient [10]. Laser-Assisted Treatment for Gingival Melanin Hyperpigmentation has been also more satisfying for patients, healing time has been shortened [6]. In the study presented by Romeo U., et al. in the evaluation of the effectiveness of using diode lasers as a protocol to excise leukoplakia, patients experienced a light burning sensation during the procedure [8]. The previous limitations of using CO₂ lasers in surgery due to the bulky delivery arm have been resolved with the introduction of Photonic Band Gap Fiber Assembly (PBFA). This innovation allows for flexible fiber delivery of CO₂ lasers, enhancing the surgeon's ability to effectively visualize and access the head and neck areas during procedures [8]. A study by Xue VW et al. demonstrated that a carbon dioxide laser with a wavelength of 10,600 nm effectively inhibited biofilm growth and decreased bacterial viability. However, there is a lack of research on the use of a 9,300 nm carbon dioxide laser for similar purposes, indicating a need for future studies to explore its potential [14]. The same group of researchers says that laser-activated fluoride therapy lowered the critical pH level at which enamel dissolves, suggesting a synergistic effect in caries prevention when combining laser irradiation with fluoride treatment. The research indicated that the beneficial effects span across visible and near-infrared wavelengths, including those of carbon dioxide lasers. Additionally, a clinical trial demonstrated that using a 9,600 nm carbon dioxide laser in conjunction with fluoride varnish application promoted remineralization and prevented the development of fissure caries in molars [14]. Laser techniques have been found more effective in reducing bacterial load in periodontal pockets [9]. Significant reduction in gingival inflammation, improving overall periodontal health has also been noticed [10]. Cavity preparation using Er and Er,Cr lasers are effective in precisely removing decayed tissue without affecting the

surrounding healthy structure which is a big advantage comparing to traditional drilling technique. Lasers also create micro-retentive surfaces that enhance the bonding strength of restorative materials, while mechanical drills are effective but less precise, potentially removing more healthy tissue than necessary. The fracture mode was examined separately for laser irradiation and thermocycling procedures using a Chi-Square test. The analysis showed no statistically significant differences, with a p-value of 0.136 for laser irradiation and 0.091 for thermocycling [12]. A meta-analysis by Schwarz et al. showed that lasers, particularly Er, improved clinical parameters such as probing depth and attachment levels in periodontal therapy compared to traditional scaling and root planing (SRP) [1]. In a retrospective analysis by Mettraux, the effectiveness of using adjunctive laser irradiation in non-surgical peri-implant therapy was examined. The study involved treating 23 infected implant sites with probing pocket depths (PPD) greater than 5 mm using conventional mechanical debridement and sterile saline rinsing. Additionally, diode laser irradiation was applied around the implant pockets. This protocol was conducted at the start and repeated after 7 and 14 days. After a 2-year observation period, the researchers observed significant improvements in peri-implant health, including notable reductions in clinical attachment level (CAL), probing pocket depth (PPD), bleeding on probing (BOP), and sulcular suppuration [1, 15]. Renvert conducted a randomized controlled trial with 42 patients divided equally into control and test groups to compare the effectiveness of abrasive air-flow therapy versus Er laser therapy. After six months, the study found no statistically significant differences between the two groups in terms of bleeding on probing and probing depth [9]. In many dental fields the fact that procedures using lasers generally result in less pain and discomfort during and after treatment is beneficial for pediatric and anxious patients.

CONCLUSIONS

While traditional methods are still effective and widely used, the benefits of laser treatments make them an increasingly popular choice in modern dental practice. Traditional techniques such as mechanical drills and scalpels are effective but often involve more extensive tissue damage, longer healing times, and greater discomfort for patients. The choice between laser and traditional methods should be based on the specific clinical situation, the dentist's expertise, and the patient's preferences. Factors such as the type of procedure, the patient's medical history, and their comfort level with different treatment options should be considered when determining the best approach. For instance, while lasers are highly effective for soft tissue procedures, traditional methods may still be preferred for certain types of hard tissue work where mechanical precision is paramount.

REFERENCES

1. Pisano M, Amato A, Sammartino P, Iandolo A, Martina S, Caggiano M. Laser Therapy in the Treatment of Peri-Implantitis: State-of-the-Art, Literature Review and Meta-Analysis. *Appl Sci.* 2021;11:5290. doi: 10.3390/app11115290 [DOI](#)
2. Mostafa D. Different laser approaches in treatment of peri-implantitis: a review. *Laser Dent Sci.* 2019;3:71-82. doi: 10.1007/s41547-019-00063-w [DOI](#)
3. Luk K, Yu OY, Mei ML, et al. Effects of carbon dioxide lasers on preventing caries: a literature review. *Laser Dent Sci* 2019;3:83-90. doi: 10.1007/s4:1547-019-00065-8 [DOI](#)
4. Condor D, Culciçchi C, Blum R, Baru O, Buduru S, Kui A, Țig I. A Review of CO2 Laser-Mediated Therapy for Oral Mucosal Lesions. *Appl Sci.* 2021;11:7744. doi: 10.3390/app11167744 [DOI](#)
5. Luk K, Zhao IS, Gutknecht N, et al. Use of carbon dioxide lasers in dentistry. *Laser Dent Sci.* 2019;3;1-9 doi: 10.1007/s41547-018-0047-y [DOI](#)
6. Tran TH, Nguyen QLD, Do TT, Truong KN, Dang QV, Bui MTN. Evaluation of Carbon Dioxide Laser-Assisted Treatment for Gingival Melanin Hyperpigmentation. *Dent J.* 2022;10:238. doi: 10.3390/dj10120238 [DOI](#)
7. AlMarzooqi AMA, Kukreja BJ, Reddy S, Lawrence D'Souza J, Eid Abdelmagyd HA. Treatment of Peri-implant Diseases using Lasers: A Systematic Review. *Open Dent J.* 2023 doi: 10.2174/18742106-v17-e230517-2022-143 [DOI](#)
8. Malcangi G, Patano A, Trilli I, et al. Therapeutic and Adverse Effects of Lasers in Dentistry: A Systematic Review. *Photonics.* 2023;10(6):650. doi: 10.3390/photonics10060650 [DOI](#)
9. Lazić MC, Puletić M, Radović N, Vuković B, Zarić S, Biočanin V. Clinical applications of lasers in conventional periodontal care. *J Laser Appl.* 1 February 2023;35(1):011201. doi: 10.2351/7.0000816 [DOI](#)
10. Strakas D, Franzen R. The blue wavelengths in laser dentistry: a review of current literature. *Laser Dent Sci* 2023;7:97-99. doi: 10.1007/s41547-023-00182-5 [DOI](#)
11. Deppe H, Horch HH. Laser applications in oral surgery and implant dentistry. *Lasers Med Sci.* 2007;22, 217-221. doi: 10.1007/s10103-007-0440-3 [DOI](#)
12. Nahas P, Nammour S, Gerges E, Zeinoun T. Comparison between Shear Bond Strength of Er:YAG and Er,Cr:YSGG Lasers-Assisted Dentinal Adhesion of Self-Adhering Resin Composite: An Ex Vivo Study. *Dent J.* 2020;8:66. doi: 10.3390/dj8030066 [DOI](#)
13. Sun G, Chen X, Wei F, et al. Effects of Er:YAG, Er, Cr:YSGG, and Nd:YAG laser irradiation and adhesive systems on the immediate and long-term bond strength of dentin: a systematic review and meta-analysis. *Lasers Med Sci.* 2023;38:32. doi: 10.1007/s10103-022-03699-6 [DOI](#)
14. Xue VW, Zhao IS, Yin IX, Niu JY, Lo ECM, Chu CH. Effects of 9,300 nm Carbon Dioxide Laser on Dental Hard Tissue: A Concise Review. *Clin Cosmet Investig Dent.* 2021 Apr 30;13:155-161. doi: 10.2147/CCIDE.S304273 [DOI](#)
15. Mettraux GR, Sculean A, Bürgin WB, Salvi GE. Two-Year Clinical Outcomes Following Non-Surgical Mechanical Therapy of Peri-Implantitis with Adjunctive Diode Laser Application. *Clin Oral Implant Res.* 2016;27:845-849

CONFLICT OF INTEREST

The Authors declare no conflict of interest

CORRESPONDING AUTHOR

Agnieszka Rolek
 Prywatna Praktyka Stomatologiczna Agnieszka Rolek,
 Wrocław, Poland
 e-mail: aga.rolek@gmail.com

ORCID AND CONTRIBUTIONSHIP

Agnieszka Rolek: 0009-0007-2880-2055 [A](#) [B](#) [D](#) [E](#) [F](#)
 Piotr Pławecki: 0000-0003-2550-8452 [A](#) [B](#) [D](#) [E](#) [F](#)

[A](#) – Work concept and design, [B](#) – Data collection and analysis, [C](#) – Responsibility for statistical analysis, [D](#) – Writing the article, [E](#) – Critical review, [F](#) – Final approval of the article

RECEIVED: 01.07.2024

ACCEPTED: 02.09.2024



Pulmonotoxic xenobiotics and methods of their determination in ambient air of nuclear power plant equipment

Andrii S. Zaitsev¹, Oleksandr R. Pulyk², Rooslan S. Vastyanov¹, Oleksandr M. Stoyanov¹, Yaroslav V. Biesieda¹, Volodymyr P. Maidanyuk¹, Serhii V. Zaitsev³

¹ODESA NATIONAL MEDICAL UNIVERSITY, ODESA, UKRAINE

²JAN DLUGOSZ UNIVERSITY IN CZESTOCHOWA, POLAND

³NATIONAL UNIVERSITY «ODESA POLYTECHNIC», ODESA, UKRAINE

ABSTRACT

Aim: To identify appropriate methods for determining the content of radioactive and non-radioactive pulmonotoxic xenobiotics in the ambient air of NPP equipment to ensure its reliability, radiation and environmental safety, as well as to reduce the risks of occupational pathologies for workers and protect people's health.

Materials and Methods: Analytical methods of analysis of modern methods of determining the content of radioactive and non-radioactive pulmonary toxic xenobiotics in the ambient air of NPP equipment.

Conclusions: a) during operation of NPP equipment, pulmonotoxic xenobiotics enter the surrounding air, which can then enter the human respiratory system in the form of radioactive or non-radioactive substances; b) significant methods of determining the content of pulmonotoxic xenobiotics in the air are: gas chromatography; gas chromatography-mass spectrometry; liquid scintillation; photometric, ionometric, polarographic, titrimetric, turbidimetric, atomic absorption, radiometric and γ -spectrometric measurements; c) radioactive pulmonotoxic xenobiotics cause radiation pathologies in the respiratory organs as a result of internal radioactive irradiation of the body; d) the effects of non-radioactive pulmonotoxic xenobiotics are accompanied by irritation and inflammatory processes in the respiratory organs, as well as toxic swelling of the lungs; e) there is a connection between the presence of pulmonotoxic xenobiotics in the air and the course of human respiratory diseases as a result of breathing such air.

KEY WORDS: pulmonotoxic xenobiotics, pulmonology, occupational pathology, ambient air, environmental monitoring, nuclear energy, measurement methods

Wiad Lek. 2024;77(9):1793-1801. doi: 10.36740/WLek/193760 DOI

INTRODUCTION

The main nuclear power facilities are nuclear power plants (NPP) using controlled nuclear reactions in nuclear reactors. Emissions from NPP equipment into the atmosphere have a negative impact on the environment and human health. Ukraine has a developed nuclear power industry, which is based on NPP – Khmelnytskyi, Rivne, Zaporizhzhia and South-Ukrainian NPP. These NPP are high-risk facilities, and therefore the prospects for their development are related to their safe operation and protection of territories, civilians and the environment in the area where the plant is located; under various negative factors (violation of technological processes, limits and conditions of safe operation, man-made accidents and incidents, natural phenomena, sabotage for terrorist purposes, hostilities, etc.), emergencies may occur at NPP that pose a significant risk to the natural environment, the health of personnel and the population of the surrounding areas [1].

NPP due to the accumulation of significant amounts of radioactive products during operation and the possibility of their release beyond the prescribed limits in case of accidents represent a source of potential hazard or a source of risk of radiation exposure to personnel, the public and the environment [2].

It is known that: a) to ensure continuous operation of NPP, various auxiliary man-made facilities are located and operate on their territory, which emit and discharge non-radiation pollutants into the environment; b) during the entire period of NPP operation, under various negative technical and natural circumstances (disruption of the technological process, explosion of equipment due to lightning, adverse meteorological conditions, unauthorized emissions, etc. c) The most chemically hazardous man-made facilities on the territory of the NPP are the start-up and backup boiler house, diesel generator stations, oil and fuel facilities, welding sites, metalworking sites, chemical reagent

tanks, a gas station, as well as equipment containing ozone-depleting refrigerants (freons), and others [3]. As a result of their operation, various pollutants are generated and released into the atmosphere through chimneys. The main pollutants are: nitrogen oxides, sulfur compounds, carbon oxides, suspended particulate matter, chlorine compounds, fluorine compounds, soot, non-methane volatile organic compounds, CH_4 , NH_3 , metals and their compounds, freons, etc. [3].

Thus, during normal operation or accidents of Rivne NPP equipment, the sources of pulmonotoxic xenobiotics (PTXs) emissions into the atmosphere are: reactor compartment with nuclear power units; systems of the installation for holding gas blowdowns during nuclear fuel overload; special ventilation systems; unit for thermo-catalytic combustion of hydrogen gas flows; technical systems for ensuring water-chemical regimes of circulating cooling of equipment of the first and second circuits of nuclear power units; special sewage system; reactor circuit water treatment system; reactor circuit purge water treatment system and organized leaks; ladder water treatment system; water treatment system for pools and emergency boric acid storage tanks; steam generator purge water treatment system; a boric acid regeneration system; a wastewater treatment system for special laundries; an atmospheric air liquefaction unit for producing oxygen and nitrogen with the use of CFCs for cooling; a hydrogen cooling unit in a hydrogen-cooled turbine generator with the use of CFCs; a maintenance and repair unit with sections for machining, gas and electric cutting or welding of metal and plastic structures (welding, cutting, surfacing, spraying); equipment for ventilation units; a road transport support unit; a power plant for NPP's own needs using liquid fuel oil; diesel power plants for emergency power supply to NPP; technical systems for drinking water supply; technical systems for wastewater treatment for discharge into water bodies; chemical laboratories; dosimetric control laboratories; warehouses with solid and liquid radioactive waste of decommissioned NPPs with ventilation systems; installation for production of gaseous H_2 and O_2 by electrolysis of aqueous solutions; facilities for solid and liquid radioactive waste management with ventilation systems; chemical warehouse with ventilation systems; warehouse with mineral energy oils; warehouse with synthetic fire-resistant energy oils; warehouse with diesel fuel [4-6].

One of the priority areas of national security in Ukraine is to ensure radiation-safe living conditions for citizens and society, environmental protection and rational use of natural resources, and this goal can be achieved, among other things, by monitoring the content of radioactive and non-radioactive harmful substances,

such as PTXs, in the air surrounding NPP equipment [7]. Pulmonotoxicity is the ability of chemicals, including xenobiotics, to cause structural and functional disorders of the respiratory system, and selective effects on different parts of the respiratory system can occur both through local and resorptive action of toxicants [8]. In this case, acute lesions of PTXs are accompanied by the formation of a number of pathological processes: irritation and inflammation in the respiratory tract (acute laryngitis and tracheobronchitis), lung parenchyma (acute pneumonia), and toxic pulmonary edema [8].

PTXs are often in the air in the form of aerosols, including radioactive ones, and have a fibrogenic effect, which increases the risk of developing occupational respiratory diseases. It is known that there is a connection between the presence of PTXs in the ambient air of NPP equipment in concentrations exceeding the established standards and the course of human respiratory diseases due to breathing such air [8]. Thus, there is a need for continuous research of the sources of PTXs and methods for their determination in the ambient air of NPP equipment.

AIM

The aim of the present work was the identification of appropriate methods for determining the content of radioactive and non-radioactive pulmonotoxic xenobiotics in the ambient air of nuclear power plant equipment to ensure its reliability, radiation and environmental safety, as well as to reduce the risks of occupational pathologies for workers and protect human health.

MATERIALS AND METHODS

Analytical methods for analyzing modern methods for determining the content of radioactive and non-radioactive PTXs in the ambient air of NPP equipment.

REVIEW AND DISCUSSION

Even with absolute reliability and trouble-free operation, any NPP significantly affects the environment through gas and aerosol (including radioactive) emissions into the atmosphere [9]. Most of the radionuclides contained in gas and aerosol emissions are retained by purification filters or rapidly decay, losing radioactivity, but there is still a significant amount that enters the environment and contaminates it, for example, with tritium (T (or ^3H) compounds: T compounds include T_2 , NT, NTO, T_2O , DTO, DT, CH_3T .

In addition to the usual gas and aerosol emissions, any NPP periodically releases aerosols into the atmosphere, which are formed as a result of corrosion of the nuclear

reactor and its first circuit. These aerosols contain radionuclides that are the product of uranium nuclear fission. The most significant radionuclides are: ^{51}Cr ; ^{54}Mg ; ^{60}Co ; ^{95}Nb ; ^{106}Ru ; ^{144}Ce , etc. Once in the biosphere, radioactive isotopes or their decay products are eventually involved in biochemical and biophysical processes that occur inside every living organism.

Some of these isotopes or their decay products are dangerous for all living things, as they can disrupt metabolic processes. In [9]: the necessity of creating new technologies and technical means for detecting aerosol radioactive emissions from NPPs and establishing radioecological monitoring and control over them in real time is substantiated; the main technical characteristics of the created complex for monitoring α - and β -radiation of radioactive aerosols are presented. References [10, 11] note the use of such xenobiotics as NH_3 , H_3BO_3 , KOH , $\text{C}_2\text{H}_7\text{NO}$ (monoethanolamine), $\text{C}_4\text{H}_9\text{NO}$ (morpholine), N_2H_4 (hydrazine) to ensure water-chemical conditions of equipment, including Zaporizhzhya NPP. During the operation of NPP equipment, these substances can be released into the surrounding air in the form of vapor, gas or aerosol, and then can enter the human respiratory system. Accidents involving spills of liquid radioactive media, such as the coolant of the first circuit of a WWER reactor, lead to increased concentrations of radionuclides such as ^{51}Cr ; ^{54}Mg ; ^{60}Co ; ^{95}Nb ; ^{106}Ru ; ^{144}Ce in the air of the process room and in ventilation emissions [12, 13]. It is shown in [14] that xenobiotics such as $\text{C}_2\text{H}_8\text{O}_7\text{P}_2$ (oxyethylidene diphosphonic acid) and NaOCl were used to ensure the water-chemical regime of the technical water supply system for responsible consumers of the reactor department and backup diesel power plants of the Rivne NPP. Reference [15] proposes a technology for the treatment of industrial water waste from NPPs based on the use of a natural mineral sorbent, bentonite. The paper shows the possibility of liquid radioactive waste (LRAW) treatment on the example of gangway water with a significant salt content, as well as energy oils and surfactants. To implement such a technology, ozone (O_3) and ultrasonic irradiation are required.

In [16] discusses the processes of industrial wastewater treatment by treating it with ozone. Reference [17] proposes a technology for the treatment of industrial water radioactive waste NPP using O_3 and ultrasonic cavitation or electric discharge at high pH values of liquid waste. Paper [18]: provides a critical analysis of existing experimental and practically implemented oxidative methods for the destruction of LRAW metal-organic complexes; highlights the results of combined oxidation (ultraviolet and O_3), supercritical oxidation in the presence of hydrogen peroxide (H_2O_2), cavitation

discharge using ozone). It is shown that today the main source of radioactive waste (RAW) in Ukraine is NPP. The largest and most hazardous part of the total amount of RAW is LRAW, which is characterized by significant volumes, activity and the potential for uncontrolled release into the environment [18]. In the process of NPP operation, radioactively contaminated waste water is generated and accumulated from various sources.

The main sources of gangway water formation include: leakage of the water coolant of the first NPP circuit and nuclear fuel pools; decontamination water solutions; drainage of special laundries and showers. It has been shown that the most effective way to destroy highly stable LRAW complexes today is their oxidative decomposition or removal of organic compounds using physicochemical processes, such as ozonation, cavitation (electro-hydro-discharge method), supercritical water oxidation (hydrothermal treatment), addition of H_2O_2 to aqueous solutions, or the use of reagents capable of forming oxidants in the course of chemical reactions, such as KMnO_4 or Fenton's reagent [18].

It is known that radioactive iodine is one of the dose-forming radionuclides in public exposure from nuclear reactor releases [19]. Work [20] shows the possibility of controlling the individual effective dose of internal radioactive exposure when PTXs in the form of radioactive compounds NTO, DTO, T_2O , NT, DT, T_2 , CH_3T enter the human body by measuring the volumetric activity in body secretions: in the condensate of water vapour from exhaled air and in urine. Iodine isotope ^{131}I is considered as an important factor of radiation exposure from nuclear reactor releases, and a feature of controlling emissions of radioactive iodine isotope ^{131}I is to take into account the variety of physical forms and chemical compounds of radioactive iodine, since 150 to 246 products of radioactive iodine interaction can be formed when ^{131}I interacts with water coolant and structural materials [21]. It is noted in [5, 6] that gaseous radioactive waste is gaseous or aerosolized radioactive products in the air.

The gas-air mixture removed directly from the NPP process equipment contains a significant amount of caustic, toxic and radioactive substances. The impurities include: a) inert radioactive gases – ^{41}Ar , ^{85}Kr , $^{85\text{m}}\text{Kr}$, ^{87}Kr , ^{88}Kr , ^{133}Xe , $^{133\text{m}}\text{Xe}$, ^{135}Xe , $^{135\text{m}}\text{Xe}$; b) iodine nuclides ^{131}I , ^{133}I , ^{135}I c) radioactive aerosols as a mixture of nuclear fuel fission products – ^{131}I , ^{89}Sr , ^{90}Sr , ^{91}Sr , ^{103}Ru , ^{137}Cs , ^{141}Ce , ^{144}Ce , ^{51}Cr , ^{54}Mn , ^{55}Mn , ^{59}Fe , ^{58}Co , ^{60}Co , ^{95}Zr , $^{110\text{m}}\text{Ag}$, ^{22}Na , ^{24}Na , ^{88}Rb , ^{99}Mo , ^{140}Ba , ^{140}La , etc. d) corrosion products of structural materials activated in the neutron flux – ^{58}Co , ^{60}Co , ^{54}Mn , ^{110}Ag , ^{59}Fe , ^{51}Cr , ^{95}Zr , ^{95}Nb , etc. e) activation products of corrective impurities in nuclear reactor water coolant – ^{13}N , ^{16}N , ^{17}N , ^{18}F , ^7Li ,

^{24}Na , ^1H , ^2H , ^3H , ^{14}C , etc. e) ^{14}C compounds in gaseous emissions – CO , CO_2 , CH_4 , C_2H_6 , C_4H_{10} , etc. It is proposed to determine the content of gaseous and vaporous radioactive and non-radioactive substances in the air – H_2O , H_2 , N_2 , O_2 , Ar , CO , CH_4 , CO_2 , C_2H_4 , C_2H_6 , C_2H_2 , C_3H_8 , C_3H_8 , C_4H_8 , C_4H_{10} , CH_3I , Kr , Xe , H_2O_2 (some of which are PTXs), using gas chromatography (GCh) methods [21, 22]. In [23] considers the results of research in the field of radiation physicochemical processes occurring in the air under the influence of various types of radioactive radiation, including in NPP air.

Thus, during radioactive irradiation of air, O_3 (ozone) is formed in it, which is chemically aggressive, easily enters into chemical reactions, including with organic compounds, and, if inhaled into the human body, can lead to respiratory diseases [24]. Thus, it has been shown in [24] that, depending on the concentration of O_3 in the air, the direct effect of O_3 on the human body causes fatigue, headache, irritation of the respiratory tract and related respiratory disorders, cough, vomiting, exacerbation of chronic bronchitis, asthma, pulmonary emphysema, pulmonary edema, i.e., O_3 is a pulmonotoxic xenobiotic. Indirectly, O_3 acts on the blood similarly to ionizing radiation: at an O_3 concentration of 0.8 g/m^3 , half-hour inhalation of O_3 is equivalent to radioactive exposure of 100 R. In addition to its general toxic effects, O_3 has carcinogenic, mutational, genotoxic effects on humans and significantly reduces immunity to infections, and it is toxic by inhalation and irritates the mucous membranes of the eyes and respiratory tract, damaging lung surfactant [25].

The sequence of painful manifestations when O_3 is inhaled: first, drowsiness occurs, then breathing changes – it becomes deep, irregular; at the end, there are breaks in breathing; death occurs, apparently, as a result of respiratory paralysis. Pathological and anatomical studies show a characteristic picture of poisoning: the blood does not clot, the lungs are permeated with many hemorrhages. In the presence of nitrogen oxides in the air, the toxicity of O_3 increases 20 times [26].

Thus, the concentration of O_3 in the air of 2 mg/dm^3 causes coughing, burning of the larynx, weakness if a person inhales such air for several seconds, inhalation for 5 minutes develops pulmonary edema, and inhalation for 10 mins can be fatal [26].

Paper [27] presents the results of a study of the sources of harmful radioactive and nonradioactive substances and methods for determining their content in the air during the operation of double-circuit NPP equipment in Ukraine; proves that during the operation of NPP equipment, harmful substances enter the ambient air, which can then enter the human respiratory

system in the form of radioactive or nonradioactive substances; proposes an improved structural diagram of a 7-channel gas chromatograph for determining the content of radioactive and nonradioactive substances in the ambient air of NPP equipment.

Paper [28] describes the complex for solid radioactive waste treatment at the Rivne NPP using plasma processing: this produces pyrolysis gases containing a toxic component in the form of CO , NO , NO_2 , SO_2 , SO_3 , HCN , which can enter the ambient air and further into the human respiratory system. Work [29] show that during the operation of NPP electrical gas equipment, gas (SF_6) and toxic products of its degradation can enter the surrounding air: gaseous – SOF_2 , F_2 , SOF_4 , SO_2F_2 , SO_2 , HF , CF_4 , SF_4 , WF_6 ; solid – S_2 , CuF_2 , AlF_3 , FeF_3 .

Work [30] show that when performing electric welding using metal structures, welding aerosols accumulate in the atmospheric air, including the following individual substances or their compounds with other individual substances, such as solids – Al , Si , B , V , W , Fe , Cd , Ca , Co , Mn , Cu , Ni , Mo , Sn , Pb , Ti , Cr , Zn , Zr , fluorine salts; gaseous – CO , CO_2 , O_3 , NO ; NO_2 , HF . Work [31] show that during welding operations in the repair of equipment, phosphine (PH_3) is released into the ambient air, which is a toxic substance with a general toxic effect, and during inhalation, it disrupts metabolism and affects the central nervous system and skeletal system, corrodes/irritates the skin, damages/irritates the eyes, liver, kidneys, spleen, ureters, bladder.

During welding operations with the use of plastic structures, the following substances accumulate in the air: CO ; HCl ; HCN ; COCl_2 ; CH_2O (formaldehyde); C_4H_6 (1,3-butadiene); $\text{C}_2\text{H}_6\text{O}$ (ethanol); $\text{C}_3\text{H}_6\text{O}$ (acetone); white spirit; $\text{C}_2\text{H}_4\text{O}_2$ (acetic acid); $\text{C}_2\text{H}_2\text{O}_4$ (oxalic acid); C_6H_6 (benzene); C_7H_8 (toluene); C_8H_{10} (xylenes); $\text{C}_6\text{H}_6\text{O}$ (phenol); carboxylic acid chlorohydrates; unsaturated hydrocarbons; $\text{C}_2\text{H}_4\text{O}$ (acetaldehyde); $\text{C}_{16}\text{H}_{22}\text{O}_4$ (dibutyl phthalate); $\text{C}_{10}\text{H}_{10}\text{O}_4$ (dimethyl phthalate); $\text{C}_{24}\text{H}_{38}\text{O}$ (di-(2-ethylhexyl)-phthalate); $\text{C}_2\text{H}_3\text{Cl}$ (vinyl chloride); CHCl_3 (chloroform); CH_2Cl_2 (dichloromethane); $\text{C}_4\text{H}_8\text{O}_2$ (dichloroethane); $\text{C}_4\text{H}_8\text{O}_2$ (dioxane); C_4F_8 (perfluoroisobutylene); CS_2 [32]. In [33] show that fluoroplastics are widely used in NPP equipment. When such fluoroplastics are heated, they are destroyed with the release of such toxic components as HF , C_4F_8 (perfluoroisobutylene); COF_2 (carbonyl fluoride); C_2F_4 (tetrafluoroethylene) into the surrounding air.

Paper [34] describes the main mechanisms and syndromes of PTXs exposure to the respiratory system. At the same time, PTXs can be transformed in the human body. It is noted that the syndromes of respiratory damage under the influence of PTXs can be: asphyxiation; bronchospasm; hypoxia; acute pul-

monary edema; myasthenic syndrome. When PTXs are exposed to the respiratory system, the following consequences are possible: irritation of the upper respiratory tract; burns; tissue decomposition under the influence of ionizing α -, β -, and γ -radiation from radioactive substances that have entered the respiratory system. Thus, the asphyxiating effect of PTXs is based on their ability to penetrate the lungs and cause damage to alveolar endothelial cells, resulting in filling the alveolar space with transudate coming from the capillary pulmonary network. When cauterizing PTXs affect the respiratory system, the pathogenesis of shock is dominated by severe pain, as well as extensive hemolysis of erythrocytes (hemolytic shock) or an allergic reaction (anaphylactic shock) [34].

The adult lung is a stable organ with low proliferative activity, so the effects of radioactive lung exposure do not appear immediately [35, 36]. At the same time, localized exposure may result in radiation pneumonia, which is accompanied by the death of epithelial cells, inflammation of the airways, pulmonary alveoli, and blood vessels. These effects can cause pulmonary insufficiency and even death within a few months after chest irradiation. The respiratory organs contain cellular structures that differ significantly in their resistance to radiation. Thus, the cartilaginous tissue of the airways and pleura are radioresistant, lymphatic tissue and the vascular system of the lungs, as well as bronchiolar epithelium and cells lining the alveoli, are radiosensitive. As a result of radiation exposure, changes occur in the respiratory system that are in full compliance with the development of clinical and anatomical signs of radiation pathology.

For example, in the first 3–4 days of acute radiation sickness, swelling and partial disintegration of argyrophilic fibers are observed; hyperemia, red blood cell diapedema and edema in the alveoli, subpleural emphysema. After the latent period, a new phase begins, characterized by increased vascular permeability, perivascular blood loss, hemorrhage, necrosis, which are often observed, bacterial infection, neutropenic bronchopneumonia. Survivors undergo resorption and regeneration with proliferation of connective tissue and sclerotic phenomena. Respiratory changes develop against a background of sharply suppressed cellular reactions, so in the midst of the disease there is no phagocytosis of bacteria and tissue decay products. Doses that do not have a significant effect on the epithelium cause only mild fibrosis.

Pneumonias, which are secondary infectious complications, can be a decisive link in the fatal outcome of radiation damage to the body. Although the lungs are classified as radioresistant organs, information

on radiosensitivity is very controversial. At sublethal doses, no special effects are observed. But after exposure to relatively higher doses, there is a change in the frequency and depth of respiratory movements. Congestion and emphysema occur in the lungs. It is assumed that the main factor in this process is the destruction of capillaries, followed by erythropedesis and collagenosis, and then sclerotization of lung tissue. Various forms of pneumonia occur: from local, mild, serous to severe hemorrhagic. Recovery processes are slow. In the mechanism of pulmonary pathology development, the occurrence of increased vascular permeability and hemicirculatory disorders in the lung tissue is important.

The pathology develops along the following chain: bronchial lesions lead to impaired air permeability \rightarrow decreased gas exchange, development of atelectasis \rightarrow pneumonia \rightarrow pleurisy \rightarrow in the long term - radiation fibrosis [35, 36].

Paper [37] shows that in NPP technological processes, when using fire-resistant synthetic turbine oils (based on triphenyl phosphates) in hydrogen-cooled turbine generators [38], these oils can produce the toxic substance P_2O_5 , which, when interacting with water, can in turn produce the toxic acid H_3PO_4 . These substances are released from these oils into the surrounding air. It can be assumed that in the event of thermal defects in the bearings of a hydrogen-cooled turbine generator, the toxic substance PH_3 [39] can be formed in the fire-resistant synthetic turbine oil and released into the surrounding air.

The process of PH_3 formation can take place along the following chain: 1) $P_2O_5 + H_2O = 2HPO_3$; 2) $P_2O_5 + 3H_2O = 2H_3PO_4$; 3) $2P_2O_5 \rightarrow P_4O_{10} + 2O_2$; 4) $P_4O_{10} + 6H_2O = 4H_3PO_4$; 5) $4H_3PO_3 \rightarrow 2H_3PO_4 + PH_3$ [39]. In the presence of dissolved hydrogen gas in fire-resistant synthetic turbine oil, a chemical reaction is possible with the formation of PH_3 according to the scheme $P_2O_5 + 8H_2 = 2PH_3 + 5H_2O$.

Table 1 provides information on the most significant radioactive and non-radioactive PTXs and methods for their determination in NPP air.

Thus, the results of the study show that during the operation of NPP equipment, radioactive and non-radioactive PTXs can enter the ambient air in the form of steam, gas or aerosol, which can then enter the human respiratory system and cause damage to them; allow to improve methods and technical means of environmental monitoring of the ambient air of NPP equipment to ensure radiation and environmental safety, reduce the risks of occupational pathologies for workers, protection of human health during accidents or normal operation of NPP equipment.

Table 1. Radioactive and non-radioactive PTXs and methods for their determination in the air NPP

PTXs in the air; (methods for determining PTXs)
Radioactive pulmonary toxic xenobiotics
⁴¹ Ar, ⁸⁵ Kr, ^{85m} Kr, ⁸⁷ Kr, ⁸⁸ Kr, ¹³³ Xe, ^{133m} Xe, ¹³⁵ Xe, ^{135m} Xe, ¹³¹ I, ¹³³ I, ¹³⁵ I, HTO, DTO, T ₂ O, HT, DT, T ₂ , CH ₃ T; (RGSM); (LSM) [IEC 60761-3. Equipment for continuous monitoring of radioactivity in gaseous effluents, Part 3, Specific requirements for radioactive noble gas monitors; IEC 60761-4, Equipment for continuous monitoring of radioactivity in gaseous effluents, Part 4, Specific requirements for radioactive iodine monitors]; [20]
Elements, organic and inorganic compounds of elements; ¹³⁷ Cs, ¹³⁴ Cs, ²³⁸ Pu, ²³⁹ Pu, ²⁴⁰ Pu, ⁹⁰ Sr, ⁸⁹ Sr, ⁹⁰ Sr, ⁹¹ Sr, ⁵¹ Cr, ⁵⁴ Mn, ⁵⁵ Mn, ⁵⁹ Fe, ⁵⁸ Co, ⁶⁰ Co, ^{110m} Ag, ⁹⁵ Nb; (RGSM; RCR for ⁹⁰ Sr); [IEC 60761-2. Equipment for continuous monitoring of radioactivity in gaseous effluents, Part 2, Specific requirements for radioactive aerosol monitors including transuranic aerosols]
Non-radioactive pulmonary toxic xenobiotics
HCN; (GCh); [MU 4775-88. Guidelines for gas chromatographic measurement of the concentrations of hydrogen cyanide and acrylic acid nitrile in the air of the working area]
N ₂ H ₄ (hydrazine); (PhMM); [MU 1657-77. Guidelines for the photometric determination of hydrazine in air]
NO, NO ₂ ; (PhMM); [MU 4187-86. Methodological guidelines for the photometric measurement of nitrogen oxide and dioxide concentrations in workplace air]
HNO ₃ ; (ICh); [ISO 21438-2:2009. Workplace atmospheres – Determination of inorganic acids by ion chromatography – Part 2: Volatile acids, except hydrofluoric acid (hydrochloric acid, hydrobromic acid and nitric acid) (IDT)]; PND F 13.1:2:3.19-98. Quantitative chemical analysis of atmospheric air and air emissions. Methods for measuring the mass concentrations of nitrogen dioxide and nitric acid (total), nitrogen oxide, sulfur trioxide and sulfuric acid (total), sulfur dioxide, hydrogen chloride, hydrogen fluoride, phosphoric acid and ammonia in industrial emissions samples, ambient air and working area air by ion chromatography]
C ₂ H ₂ O ₄ (oxalic acid); (PhMM); [MUK 4.1.1732-03. Spectrophotometric measurement of mass concentrations of ethanedonic acid dihydrate (oxalic acid dihydrate) in working area air. Methodical instructions]
C ₂ H ₄ O ₂ (acetic acid); (GCh); [MU 5904-91. Methodological guidelines for gas chromatographic measurement of monochloroacetic and acetic acid concentrations in workplace air]
C ₂ H ₇ NO (monoethanolamine); (PhMM); [MU 2568-82. Methodological guidelines for the photometric measurement of concentrations of primary aliphatic amines (methylamine, ethylamine, propylamine, butylamine, hexylamine, monoethanolamine) in working area air]
Freons; (PhMM); [MU 1699-77. Methodological guidelines for the photometric determination of organofluorine compounds (diethyl ester of perfluorodipic acid, diethyl ester of perfluoroglutaric acid, perfluorodibutyl ester, freons, benzotrifluoride, hexafluoropropylene, perfluoroacetone dihydrate, trifluoroethyl alcohol, trifluorobutyl alcohol, tetrafluoropropyl alcohol, octafluoromethyl alcohol, trifluorochloropropane) in air]
H ₂ O ₂ ; (PhMM); [MU 4586-88. Methodological guidelines for the photometric measurement of hydrogen peroxide and organic peroxides concentrations in workplace air]
H ₂ , CO, CH ₄ , CO ₂ , C ₂ H ₄ , C ₂ H ₆ , C ₂ H ₂ , C ₃ H ₈ , C ₃ H ₆ , C ₄ H ₈ , C ₄ H ₁₀ ; (GCh); [ASTM D 3612-012. Standard Test Method for Analysis of Gases Dissolved in Electrical Insulating Oil by Gas Chromatography. ASTM International]
COCl ₂ ; (PhMM); [MU 4768-88. Methodological guidelines for the photometric measurement of phosgene concentrations in workplace air]
CS ₂ ; (GCh); [MU 3973-85. Methodological guidelines for gas chromatographic measurement of concentrations of carbon disulfide in working area air]
CH ₂ O (formaldehyde); (PhMM); [MU 4595-85. Methodological instructions for gas chromatographic measurement of formaldehyde concentrations in working area air]
C ₁₆ H ₂₂ O ₄ (dibutyl phthalate); (GCh); [MU 2222-80. Methodological guidelines for gas chromatographic determination of dibutyl phthalate and dioctyl phthalate in air]
SF ₆ ; (GCh); [MU 2697-83. Methodological guidelines for gas chromatographic determination of sulfur hexafluoride in air]
CCl ₄ ; (GCh); [MU 1577-77. Methodological guidelines for gas chromatographic determination of allyl chloride, carbon tetrachloride and 1,2-dichloropropane in air]
NaOH, KOH; (PhMM); [MU 5937-91. Methodical instructions for photometric measurement of caustic alkali aerosol concentrations in workplace air]
Cl ₂ ; (PhMM); [MU 1644a-77. Methodological guidelines for the photometric determination of chlorine in air]
H ₂ S; (GCh); [MU 5304-90. Methodological guidelines for gas chromatographic measurement of hydrogen sulfide concentrations in working area air]
HCl; (IMM); [MU 5932-91. Methodological guidelines for the ionometric measurement of hydrogen chloride concentrations in workplace air]
NH ₃ ; (PhMM); [MU 4785-88. Methodological guidelines for the photometric measurement of concentrations of MU and formaldehyde in the combined presence in workplace air]
I ₂ ; (PhMM); [MU 16446-77. Methodological guidelines for the photometric determination of iodine in air]
CH ₃ I; (GCh); [22]

PH₃; (LC); [A guide to Dräger indicator tubes and CMS chips. Analysis of soil, water and air as well as technical gases. 17th edition. Dräger Safety AG & Co. KGaA. Lübeck, 2015, 458 p.]

C₄F₈ (perfluorooctylene); (GCh); [40]

SO₂, SO₃; (PhMM); [MU 4588-88. Methodological guidelines for the photometric measurement of sulfuric acid and sulfur dioxide concentrations in the presence of sulfates in workplace air]

H₂SO₄; (TDA); [MU 08-47/355-2014. Working area air. Turbidimetric method for measuring the mass concentration of sulfuric acid]

P₂O₅+H₃PO₄; (ICh); [ISO 21438-1:2022. Workplace atmospheres – Determination of inorganic acids by ion chromatography – Part 1: Non-volatile acids (sulfuric acid and phosphoric acid, ISO/TC 146/SC 2, ICS Classification: 13.040.30 Workplace atmospheres, Edition 2022, 22 p.]

CH₂Cl₂ (dichloromethane); C₂H₄Cl₂ (dichlorethane), C₆H₆ (benzene); C₇H₈ (toluene), C₆H₆O (phenol); (GCh-MS); [GOST R ISO 16017-1-2007. Atmospheric air, working area and confined spaces. sampling of volatile organic compounds using a sorption tube followed by thermal desorption and gas chromatographic analysis on capillary columns. Part 1. Sampling by pumping; ISO 16017-1:2000. Indoor, ambient and workplace air — Sampling and analysis of volatile organic compounds by sorbent tube/thermal desorption/capillary gas chromatography — Part 1: Pumped sampling (IDT)]

Elements, organic and inorganic compounds of elements: Al, Si, B, V, W, Fe, Cd, Ca, Co, Mn, Cu, Ni, Mo, Sn, Pb, Ti, Cr, Zn, Zr, fluoride salts, HF, O₃; (PhMM, IMM, PGA, AAA, GCh, TMA, AES); [ISO 15202-3:2004. Workplace air – Determination of metals and metalloids in airborne particulate matter by inductively coupled plasma atomic emission spectrometry – Part 3: Analysis (IDT); MU 4945-88. Methodological guidelines for the determination of harmful substances in welding aerosol (solid phase and gases)]

Notes: LSM – liquid scintillation method; RGSM – radiometric and gamma spectrometric measurements; RCR – radiation and chemical removal; GCh – gas chromatography; GCh-MS – gas chromatography-mass spectrometry; PhMM – photometric measurements; IMM – ionometric measurements; TDA – turbidimetric analysis; TMA – titrimetric analysis; PGA – polarographic analysis; AAA – atomic absorption analysis; ICh – ion chromatography; AES – atomic emission spectrometry; LC – linear and colourful.

CONCLUSIONS

1. It is shown that: a) during the operation of NPP equipment, PTXs can be released into the surrounding air in the form of vapor, gas or aerosol, which can then enter the human respiratory system in the form of radioactive or non-radioactive substances – ⁴¹Ar, ⁸⁵Kr, ^{85m}Kr, ⁸⁷Kr, ⁸⁸Kr, ¹³³Xe, ^{133m}Xe, ¹³⁵Xe, ^{135m}Xe, ¹³¹I, ¹³³I, ¹³⁵I, HTO, DTO, T₂O, HT, DT, T₂, CH₃T, ¹³⁷Cs, ¹³⁴Cs, ²³⁸Pu, ²³⁹Pu, ²⁴⁰Pu, ⁸⁹Sr, ⁹⁰Sr, ⁹¹Sr, ⁵¹Cr, ⁵⁴Mn, ⁵⁵Mn, ⁵⁹Fe, ⁵⁸Co, ⁶⁰Co, ^{110m}Ag, ⁹⁵Nb, NO, NO₂, HNO₃, SO₂, SO₃, H₂SO₄, SF₆, N₂H₄, H₂O₂, Cl₂, HCl, H₂S, CS₂, CCl₄, NH₃, NaOH, KOH, HCN, COCl₂, acetic acid, formaldehyde, perfluoroisobutylene, freons; elements, organic and inorganic compounds of elements – Al, Si, B, V, W, Fe, Cd, Ca, Co, Mn, Cu, Ni, Mo, Sn, Pb, Ti, Cr, Zn, Zr, fluoride salts, HF, O₃; b) Significant methods for determining the content of PTXs in NPP air include: gas chromatography; gas chromatography-mass spectrometry; liquid scintillation; photometric, ionometric, polarographic, titrimetric, turbidimetric, atomic absorption, radiometric, and γ-spectrometric measurements; c) exposure to radioactive PTXs due to radioactive irradiation of the body in the respiratory system leads to the development of clinical and anatomical signs of radiation pathology; d) exposure to non-radioactive PCBs leads to pathological processes: irritation and inflammation in the respiratory system, as well as toxic pulmonary edema; e) there is a link between the presence of PTXs in the ambient air of NPP equipment in concentrations exceeding the established standards and the course of human respiratory diseases caused by breathing such air.
2. The prospects of the obtained research results lie in the possibility of using them to improve the systems of ensuring: reliability, radiation and environmental safety of NPP equipment; health protection and reduction of risks of occupational pathologies in case of respiratory diseases of people under the influence of PTXs during the operation of NPP equipment.

REFERENCES

1. Popov OO, Yatsyshyn AV, Kovach VO, Artemchuk VO, et al. Analysis of possible causes of emergencies at NPPs in order to minimize the risk of their occurrence. Nuclear and radiation safety. 2019;1(81):75-80. doi:10.32918/nrs.2019.1(81).13. [DOI](#)
2. Odinets VV. Assessment of NPP personnel safety in case of accidental release of toxic chemicals. Modern problems of scientific support of energy: materials of the XVIII International Scientific and Practical Conference of Young Scientists and Students 2020. In 2 vols. K.: Ihor Sikorskyi Kyiv Polytechnic Institute. 2020;1:45.
3. Popov OO, Yatsyshyn AV, Kovach VO, Artemchuk VO, et al. Physical features of the distribution of pollutants in the atmospheric air under conditions of an emergency at a nuclear power plant. Nuclear and radiation safety. 2019;4(84):88-98. doi:10.32918/nrs.2019.4(84).11. [DOI](#)
4. Kishnevskiy VA, Chichenin VA, Pavlyshin PYa, Bondarenko VN, Tikhomirov AYu. Water-chemical regimes of circulating cooling systems of large power facilities. Odesa: Astroprint. 2018:250.

5. Kovalchuk VI, Kozlov IL, Dorozh AA. Fundamentals of radioactive waste management at nuclear power plants. Principles, technologies, equipment. Odesa: Astroprint. 2020:372.
6. Kliuchnikov AA, Pazukhin EM, Shigera VM, Shigera .Yu. Radioactive waste of nuclear power plants and methods of handling them. K.: Institute for NPP Safety Problems of the National Academy of Sciences of Ukraine. 2005:487.
7. Azarov SI, Popovych OV, Sydorenko VL. Conceptual directions of implementation of radiation safety culture. Nuclear energy and the environment. 2015;2(6):53-60.
8. Bagdasarian AS, Pukhniak DV, Kamalyan ZhA, Staritskiy AG, et al. Selected Issues of Disaster Medicine in Practical Healthcare. Krasnodar: Kuban State Medical University. 2011:256.
9. Alekseeva OV, Lisichenko GV, Zabulonov YuL, Burtniak VM, Odukalets LA. Monitoring and control of aerosol radioactive emissions from nuclear power plants. Science and innovation. 2012;6(8):19-25.
10. Maltseva TV, Zinchenko SA, Dobrovolskaia IY, Arkhipenko AV. Influence of Correction Chemical Treatment of the Primary Circuit Coolant and Secondary Circuit Working Medium at NPP with Water-Cooled Water Reactor, PWR on Radiation Safety. Nuclear and Radiation Safety. 2012;4(56):37-43.
11. Report on periodic safety reassessment of ZNPP Units 3,4. Comprehensive safety analysis of power unit No.3 (21.3.59.OPPB.00. September 2017). Analytical materials State Enterprise National Nuclear Energy Generating Company "Energoatom", "Zaporizhzhya NPP". 2017:387. <https://www.npp.zp.ua/Content/docs/prolong/kab-znpp-3-170926-2.pdf>
12. Kyrylenko YuO, Kameneva IP. Mathematical modeling of the release source in accidents with liquid radioactive media spills. Collection of abstracts of the XXXVII Scientific and Technical Conference of Young Scientists and Specialists of the H. Ye. Pukhov Institute for Modeling Problems in Energy of the National Academy of Sciences of Ukraine, Kyiv. May 15, 2019. H. Ye. Pukhov Institute for Modeling Problems in Energy of the National Academy of Sciences of Ukraine. 2019:19-24.
13. Kyrylenko YuO. Features of radiation exposure in accidents with liquid radioactive media spills. Collection of abstracts of the scientific and technical conference of young scientists and specialists of the H. Ye. Pukhov Institute for Modeling Problems in Energy of the National Academy of Sciences of Ukraine. Kyiv. May 16, 2018, H. Ye. Pukhov Institute for Problems of Modeling in Energy of the National Academy of Sciences of Ukraine. 2018:23-26.
14. Kuznetsov PM, Bedunkova OO. Experimental tests of biocidal treatment of cooling water for safety systems of Rivne NPP power units. Nuclear and radiation safety. 2023;1(97):30-40. doi:10.32918/nrs.2023.1(97).04 [DOI](#)
15. Gerliga VA, Kravchenko VP, Prityka IA, Ganem Hussam. Purification of Water Solutions from Salts and Radionuclides. Nuclear and Radiation Safety. 2018;1(77):47-51.
16. Jiahao Luo, Xin Jin, Yadong Wang, Pengkang Jin. Advanced Treatment of Laundry Wastewater by Electro-Hybrid Ozonation-Coagulation Process: Surfactant and Microplastic Removal and Mechanism. Water. 2022;14(4138):1-16. doi:10.3390/w14244138. [DOI](#)
17. Ganem Hussam, Gerliga VA, Kravchenko VP, Makedon VV, Shulga OV. Purification of liquid radioactive waste from surfactants and organic compounds. Nuclear and radiation safety. 2019;1(81):62-67. doi:10.32918/nrs.2019.1(81).11. [DOI](#)
18. Shabalin BH, Lavrinenko OM. Destruction of organic substances of radioactively contaminated waters of NPPs with Water-Cooled Water Reactor (analytical review). Nuclear energy and the environment. 2020;3(18):65-78. doi:10.31717/2311-8253.20.3.8. [DOI](#)
19. INPRO Methodology for Sustainability Assessment of Nuclear Energy Systems: Environmental Impact. Vienna: IAEA. 2016;12(13):40-44. (IAEA Nuclear Energy Series; № NG-T-3.15).
20. ISO 27048:2011. Radiation protection – Dose assessment for the monitoring of workers for internal radiation exposure, TC 85/SC 2, ICS 13.280, Publication Date 07-Jan-2011, 76 p.
21. Dickinson S, Bowskill S, Sims H. The iodair model for radiolysis of gaseous iodine species in air: data comparisons and predictions. Proceedings of the International OECD-NEA/NUGENIA-SARNET Workshop on the Progress in Iodine Behaviour for NPP Accident Analysis and Management Paper. 2015;3:243-255.
22. Zaitsev S, Kishnevsky V, Oborsky G, Tikhomirov A, Tikhenko V. Improvement of Quality Control Methods for Filters' Adsorbents in Purification of Gas Emissions of Nuclear Power Plants. Lecture Notes in Mechanical Engineering. Advanced Manufacturing Processes III Selected Papers from the 3rd Grabchenko's International Conference on Advanced Manufacturing Processes (InterPartner-2021). September 7-10. 2021. Odessa. Ukraine. Springer. Switzerland. 720 p.
23. Pshezhitskiy SYa, Dmitriev MT. Radiation physical and chemical processes in the air environment. Moscow: Atomizdat. 1978:184.
24. Borisova SV. Ozone in the atmosphere. Odesa: Odesa State Ecological University. 2011:113.
25. The effect of ozone on the body, bacteria and viruses. https://dentaum.com.ua/index.php?route=product/product&path=93&product_id=348
26. Galetich IK. Lecture notes on the discipline "Ecology". Kharkiv: Kharkiv National University of Municipal Economy. 2012:88.
27. Zaitsev SV, Zaitsev AS. Methods of determining hazardous substances in the air during operation of nuclear power plant equipment. International Scientific-technical journal «Measuring and computing devices in technological processes». 2023;3:31-39. doi:10.31891/2219-9365-2023-75-3. [DOI](#)

28. Kornilov AA, Barbashev SV. On the Inclusion of the Plasma Processing Complex for Solid Radioactive Waste into the Radioactive Waste Processing Complex at the Rivne NPP. Nuclear energy and the environment. 2018;1(11):18-26.
29. Kuzin PV, Yakobson IA. Gas-insulated equipment adjustment. Moscow: Energoatomizdat. 1990:112.
30. Pokhodnya IK, Yavdoshchin IR, Gubanya IP. Welding aerosol. Influence factors, physical properties, methods of analysis (Review). Automatic Welding. 2011;6:39-42.
31. Berezuckyi V, Hondak I. Welding of metal products and safety. Bulletin of NTU "KhPI". Series: Innovative technologies and equipment for materials processing in mechanical engineering and metallurgy. 2018;41(1317):91-102.
32. Kataev RF. Plastics Welding. Ekaterinburg: Ural State Technical University-Ural Polytechnic Institute. 2008:138.
33. Dickerman DN, Kunegin VS. Wires and cables with fluoroplastic insulation. Moscow: Energoizdat. 1982:144.
34. Golikov SN. Emergency Care for Acute Poisonings. Handbook of Toxicology. Moscow: Medicine. 1978:312.
35. Vizir VA, Poplionkin EI. Radiation injuries. Clinical characteristics of ionizing radiation. Clinical classification of radiation damage, acute radiation sickness. The concept of radiation trauma, medical care at the stages of medical evacuation. Zaporizhzhia city: Zaporizhzhia State Medical University. 2015:63.
36. Ovcharenko OP, Lazar AP, Matiushko RP. Basics of radiation medicine. Odesa city: Odesa State Medical University. 2002:208.
37. RD 153-34.1-43.106-2001 Standard Instruction on acceptance, storage and operation of fire-resistant turbine oils of OMTI type. Moscow: JSC "VTI". 2002:56.
38. RD 153-34.0-45.512-97 Standard instruction on operation of gas-oil system of hydrogen cooling of generators. Moscow: JSC "ORGRES" 1997:77.
39. Van Weser John. Phosphorus and its compounds. Translation from English, edited by A.I. Shereshevsky, Candidate of Technical Sciences. Moscow: Foreign Literature Publishing House. 1962:688.
40. Kochetkova NV, Pavlova PI, Soboleva GI. Generation and determination of microquantities of perfluoroisobutylene by gas chromatography with electron-capture detector. Magazine of Analytical Chemistry. 1987;52(12):2227-2231.

The work is fragments of scientific-research investigation "Development of modern methods of diagnosis and treatment of purulent-septic complications in combat surgical trauma", state registration No 0120U101834

CONFLICT OF INTEREST

The Authors declare no conflict of interest

CORRESPONDING AUTHOR

Andrii S. Zaitsev

Odesa National Medical University
2 Valikhovsly lane, 65082, Odesa, Ukraine
e-mail: zaitsevandrii1@gmail.com

ORCID AND CONTRIBUTIONSHIP

Andrii S. Zaitsev: 0000-0002-6467-5168 **A** **F**
 Oleksandr R. Pulyk: 0000-0002-8717-047X **B** **D**
 Rooslan S. Vastyanov: 0000-0001-8585-2517 **A** **E** **F**
 Oleksandr M. Stoyanov: 0000-0002-3375-0452 **D** **F**
 Yaroslav V. Biesieda: 0009-0004-1683-0292 **B** **F**
 Volodymyr P. Maidanyuk: 0000-0002-3351-1515 **A** **B**
 Serhii V. Zaitsev: 0000-0002-1166-3243 **A** **B**

A – Work concept and design, **B** – Data collection and analysis, **C** – Responsibility for statistical analysis, **D** – Writing the article, **E** – Critical review, **F** – Final approval of the article

RECEIVED: 11.03.2024

ACCEPTED: 01.08.2024



Choking in children: causes, prevention and intervention strategies

Klaudia Korycka¹, Agata Mormul¹, Michał Korab², Joanna Smalira¹


¹DEPARTMENT OF INTERNAL MEDICINE, PRASKI HOSPITAL IN WARSAW, POLAND

²DEPARTMENT OF GENERAL SURGERY, DISTRICT HOSPITAL IN SOCHACZEW, POLAND

ABSTRACT

Choking episodes in children are a significant public health problem that can lead to serious consequences if not addressed quickly and effectively. Early diagnosis, appropriate treatment and prevention are key to ensuring the safety of children. This review article aims to comprehensively examine the causes, symptoms, diagnosis, and intervention methods of choking in the pediatric population. The review methods included the analysis of scientific publications located in databases such as PubMed and scientific journals, including meta-analyses, randomized trials and systematic reviews regarding the scope of the problem of choking in children, excluding case reports. Choking is most often caused by the aspiration of foreign objects such as small toys, food (e.g. grapes, nuts, pieces of meat) and other small objects that children often put into their mouths out of curiosity. Children aged 1 to 4 are particularly vulnerable as they have a natural tendency to explore their surroundings using their mouths. Symptoms of choking may include sudden difficulty breathing, intense coughing, wheezing, cyanosis and loss of consciousness. Quick recognition of symptoms is crucial to prevent serious consequences, such as cerebral hypoxia or cardiac arrest. In diagnostics, it is also important to take a thorough history and use imaging tests, such as X-ray or bronchoscopy, to locate and remove the foreign body. This article seeks to better understand the factors contributing to choking in children and provide the latest evidence-based recommendations for prevention and intervention.

KEY WORDS: foreign body, choking, obstruction

Wiad Lek. 2024;77(9):1802-1807. doi: 10.36740/WLek202409123 

INTRODUCTION

Choking incidents in the pediatric population constitute a pressing public health issue, demanding attention due to their potential for severe consequences on children's well-being. Each year, it is approximated that tens of thousands of deaths are attributed to choking, with an incidence rate of 0.66 per 100,000 population [1]. While the majority of Foreign Body Airway Obstruction (FBAO) events are nonfatal, FBAO is a major cause of coincidental death in children less than one year old and accounts for 7% of deaths in children under four years old [2]. The vulnerability of children to choking hazards is heightened by their developmental stages, dietary habits, and exploratory behaviors, making it imperative to understand the causes, assess preventative measures, and develop effective interventions [3].

The World Health Organization (WHO) estimates that unintentional injuries, including choking, are a leading cause of mortality and morbidity among children globally. Choking, specifically, arises from the inhalation or ingestion of foreign objects, primarily food items, toys,

or small objects, posing a significant risk to the respiratory and cardiovascular systems of young children [4].

Choking incidents are not only a result of physical hazards but also a consequence of inadequate supervision and knowledge. Parental and caregiver education about the risks and preventive measures are crucial components of a comprehensive approach to reducing pediatric choking incidents.

Despite advances in medical care and emergency response, the timely and effective management of choking incidents remains a critical challenge. Basic life support training for caregivers, educators, and healthcare professionals is crucial in alleviating the consequences of such incidents and enhancing overall community preparedness.

AIM

This review article aims to comprehensively examine the causes, symptoms, diagnosis, and intervention methods of choking in the pediatric population.

MATERIAL AND METHODS

The review methods included the analysis of scientific publications located in databases such as PubMed and scientific journals, including meta-analyses, randomized trials and systematic reviews regarding the scope of the problem of choking in children, excluding case reports.

REVIEW AND DISCUSSION

CAUSES OF CHOKING IN CHILDREN

AGE-RELATED RISK FACTORS

Instances of Foreign Body Airway Obstruction (FBAO) are frequent among children, especially in the pre-school age group, most commonly occurring between the ages of one and four years [5, 6]. This is due to a number of factors, including underdeveloped chewing abilities, immature dentition, narrower airways, and specific behaviors such as heightened activity levels, playfulness, and distractibility, all of which elevate the risk of choking [3, 7].

While there is some variation in the literature, an overwhelming amount of data suggests that the highest risk is observed in young males [3, 8]. The majority of these choking events involving children occur either at home or at preschool, where parents or kindergarten teachers typically provide care and supervision, given that these are the primary settings where children spend their time [9].

Age plays a crucial role in the susceptibility of children to choking incidents. Infants, with their limited motor skills and reflexes, are particularly vulnerable, while toddlers and older children may face different risks associated with their developmental stages. Understanding the age-related factors contributing to choking incidents is pivotal for tailoring prevention and intervention strategies to specific age groups [3, 7].

PRIMARY CAUSES OF CHOKING IN CHILDREN

Numerous objects and substances prevalent in children's environments have been identified as common choking hazards. Choking incidents in children often involve small and hard foods like nuts, seeds, popcorn, candies, and raw vegetables, as well as small toys, coins, tooth fragments, buttons, and batteries [3, 8]. In the study conducted by Chiu et al., nuts and peanuts were identified as the most frequently aspirated foreign bodies, accounting for 59% of cases [10]. Additionally, the lack of awareness among caregivers regarding these hazards further compounds the risk. Analyzing the types of objects and foods associated with choking

incidents provides insights into effective educational campaigns and childproofing strategies.

SYMPTOMS OF FOREIGN BODY ASPIRATION

Symptoms of foreign body aspiration depend on the degree of airway obstruction, the child's age, the type of foreign body aspirated, and the time elapsed since the event. Delayed diagnosis of foreign body aspiration is common. Data suggest that diagnosis within 24 hours of the event occurs in only 50-60% of cases [11, 12]. The duration between presentation and diagnosis, as well as the time between an FBA and seeking medical assistance, seem to be influenced by a number of factors. These variables include the severity of airway obstruction, whether or not a witnessed choking episode was present, the patient's age, and the kind of foreign body obstructing the airway [3]. To avoid delayed diagnosis and associated mortality, medical personnel should exhibit a high suspicion for this condition.

Most often, children with foreign body aspiration present symptoms of partial airway obstruction. The most common symptom is cough, followed by tachypnea and stridor. An important sign in physical examination aiding in the diagnosis of foreign body aspiration is regional diminishment of breath sounds and the presence of wheezing. The classical triad of symptoms, including cough, wheezing, and diminished breath sounds, is not present in every case. In a description of 135 cases of foreign body aspiration in children, the classical triad of symptoms occurred in only 57% of cases [11].

Symptoms of foreign body aspiration vary depending on its location in the airways. Only 3% of aspirated foreign bodies typically become lodged in the larynx, often characterized by their bulkiness, irregular shape, or sharp, penetrating nature [13]. The majority of aspirated foreign bodies (75%) typically lodge in the lower section of the airway. According to studies 13% of these are lodged in the trachea, 60% in the right lung, and 23% in the left lung. Bilateral foreign body occurrences are rare, accounting for only 2% of cases [14, 15].

Location in the larynx or trachea – foreign bodies in the larynx and trachea are rare but particularly life-threatening. Symptoms include wheezing, cough, drooling, dyspnea, and voice change. Foreign bodies in this location most commonly manifest as acute respiratory distress [16, 17].

Location in the large bronchi – typical symptoms for this location include cough and wheezing. Hemoptysis, dyspnea, difficulty breathing, diminished breath sounds, fever, and cyanosis may also occur [14, 15, 18]. Foreign bodies most commonly lodge in the right bronchus.

Lower airways – children with a foreign body lodged in this part of the airways may have few or no symptoms in the initial period after choking.

DIAGNOSIS

The diagnostic process for children suspected of foreign body aspiration involves a systematic approach, encompassing clinical evaluation, imaging studies, and, if necessary, endoscopic procedures. The steps typically include:

1. Clinical assessment

Gathering information on the patient's medical history, including details about the choking episode, type of object or food involved, and the duration of symptoms is essential for an accurate diagnosis. According to Yadav et al. study the duration of symptoms ranged from ≤ 6 hours to 3 months [19].

Aspiration of foreign bodies might not be suspected initially due to nonspecific symptoms. A sizable foreign body can lead to complete airway obstruction, resulting in sudden and potentially fatal outcomes. Sharp objects can directly injure the airway. However, in the majority of cases, symptoms of tracheobronchial foreign body aspiration are nonspecific. This underlines the significance of assessing symptoms such as coughing, wheezing, respiratory distress, dysphagia and fever [8, 20].

2. Imaging studies and endoscopic evaluation

In the assessment of airway foreign bodies in pediatric patients, whether radiopaque or non-radiopaque, radiography, serves a crucial role in both initial detection and subsequent follow-up evaluations [20]. Magnetic resonance imaging (MR) and computed tomography (CT) are additional imaging techniques that may be beneficial, but usually aren't required to make the diagnosis [13].

The majority of foreign bodies are radiolucent, primarily composed of organic material, such as food. Only around 10% of aspirated foreign bodies appear radiopaque [13]. In many cases, particularly when the foreign body doesn't completely obstruct the airway, chest radiographs may show no abnormalities. Radiographic findings are influenced by the location and characteristics of the obstruction, whether it is partial or complete. For upper airway obstruction caused by foreign bodies, indirect signs may be observed, including hypopharynx overdistention and prevertebral soft-tissue swelling. In cases of partial airway obstruction, which is most common, there might be evidence of unilateral hy-

perinflation, atelectasis, or mediastinal shift. Due to the typical delay in clinical manifestations (averaging 24 hours), careful examination is crucial for identifying complications such as pneumomediastinum and pneumothorax [13].

CT is usually not indicated because it will delay diagnosis. However CT is recommended to examine for any remaining foreign body post-bronchoscopy or when there is concern about severe complications, such as aortic perforation. Esophageal foreign bodies might also lead to airway obstruction due to mass effect and inflammation [13].

Bronchoscopy stands as the definitive standard for both the diagnosis and management of aspirated foreign bodies, even in cases where radiographs show no abnormalities [13]. Shlizerman et al. reported that the occurrence of positive bronchoscopies for foreign bodies was notably higher in children aged ≤ 2 years (82.6%) in comparison to older children (57.1%) ($p = 0.001$) [21].

3. Additional tests and follow-up assessments

Additional tests may be ordered to further assess specific aspects of foreign body aspiration cases. Pulmonary function tests are conducted when there is suspicion of compromised airway function, providing valuable insights into lung performance. Blood tests are also utilized to check for signs of infection or inflammation, aiding in the overall diagnostic evaluation and differential diagnosis of respiratory failure [3].

Continuous monitoring of the patient's clinical status is vital in foreign body aspiration cases. This includes regular observation of symptoms and respiratory condition, with the possibility of repeat imaging for resolution confirmation or complication identification. This proactive monitoring strategy ensures timely responses to any changes in the patient's condition, enhancing overall management effectiveness [13].

Recognition of esophageal, tracheal or bronchial lodging of disc batteries is crucial due to the risk of serious complications, including perforation. After removal, bronchoscopy and an upper gastrointestinal examination is essential to assess for potential issues like strictures, erosions, tracheoesophageal, or aorto-esophageal fistulas [13].

The diagnosis process involves a collaborative effort among healthcare professionals, including pediatricians, pulmonologists, and otolaryngologists, to ensure a comprehensive and accurate assessment. Timely and precise diagnosis is crucial for initiating appropriate management, which may include bronchoscopic removal of the foreign body and addressing any associated complications.

MANAGEMENT

In cases of partial airway obstruction, characterized by audible breathing and the ability to produce sound, children should be encouraged to cough and observed. For complete airway obstruction, where the child cannot speak or cough but remains conscious, attempts should be made to remove the obstruction using back blows and chest thrusts in infants and the abdominal thrusts in older children. However, these interventions should be avoided in children who can speak or cough, as they may convert partial obstruction into complete obstruction [11].

Recommendations from the American Heart Association differ for children under 1 year of age and older.

Management in children under 1 year of age

The child should be placed on the caregiver's forearm with the head lowered, using the index finger and thumb to grip the chin, taking care not to grasp the child's neck. The caregiver should deliver five back blows with the heel of their other hand between the shoulder blades and check if the foreign body has been dislodged.

If five back blows are unsuccessful, the child should be laid on their back, and the caregiver should use two fingers to perform chest compressions at a rate of 100-120 per minute to a depth of about $\frac{1}{3}$ of the anterior-posterior diameter of the chest. Up to five chest compressions should be performed, checking if the foreign body has been expelled from the child's mouth. If there is no improvement, repeat the back blows and chest compressions until successful.

If the child loses consciousness, resuscitation should be initiated.

Management in older children

The caregiver should sit and place the child bent forward over their knees. In this position, the child should receive five back blows between the shoulder blades. If there is no improvement, five abdominal thrusts should be performed. The caregiver should stand behind the child, wrap their arms around the child's armpits, place their left hand in a fist just below the xiphoid process, grasp with their right hand, and vigorously pull their hands towards themselves and upwards to increase pressure in the chest. This action should be repeated five times, alternating with back blows.

In the oldest children and adults, place the left hand on the chest in front and bend the person down with the right hand. Then, five vigorous thrusts should be delivered with the heel of the hand between the shoulder blades, checking if the foreign body has been expelled from the mouth. If unsuccessful, the caregiver should

stand behind the patient, wrap their arms around them under the armpits, place their left hand in a fist just below the xiphoid process, grasp with their right hand, and vigorously pull their hands towards themselves and upwards. This action should be repeated five times, alternating with back blows.

Pre-hospital procedures

Pre-hospital care is critical in stabilizing pediatric patients with airway obstructions before hospital arrival. Emergency medical teams should aim to partially clear the airway to enable safe transport. If the child can maintain minimal respiration, transport to the hospital can proceed, where advanced procedures, like bronchoscopy, can be performed. Pre-hospital interventions may include suction, manual clearance, or intubation, depending on the severity of the obstruction. Timely action significantly improves outcomes and reduces the risk of complications.

Hospital Management

If airway obstruction persists despite the above measures, attempts may be made to remove the foreign body through direct laryngoscopy using Magill forceps. However, this method is only applicable to foreign bodies located above the vocal cords.

If the foreign body is not visible during laryngoscopy, surgical airway clearance or attempts to push the foreign body into the right main bronchus with an intubation tube may be considered. Additionally, rigid bronchoscopy may be utilized.

When obstruction caused by a foreign body is below the larynx and recommended measures are ineffective, intubation and ventilation of the patient should be considered until rigid bronchoscopy can be performed.

Complications of foreign body aspiration

Foreign body aspiration can lead to acute and life-threatening obstruction. Over 300 deaths of children annually in the United States result from foreign body aspiration. Undiagnosed foreign bodies can also cause serious complications such as pneumonia, wheezing, bronchiectasis, or atelectasis.

High vigilance is necessary to avoid significant morbidity and mortality [22-24]

Most children recover completely after the removal of a foreign body following an aspiration incident. However, some, particularly with delayed diagnosis, may experience a complicated recovery course characterized by persistent respiratory symptoms such as cough and wheezing or require prolonged hospitalization. Many of these events are associated with inflammatory processes initiated by the foreign body [24, 25].

A study conducted by Karakoc, F. et al. involved long-term observation of 110 patients, in which no persistent symptoms such as cough or wheezing or bronchiectasis were found after removal of inorganic foreign bodies. However, it was noted that organic foreign bodies were associated with an increased risk of persistent symptoms and bronchiectasis, as confirmed by computer tomography [26].

The frequency of distant complications after aspiration of an organic foreign body was associated with the time elapsed from aspiration to diagnosis. The risk of distant complications increased with the duration from aspiration to diagnosis. No complications occurred in children diagnosed within the first 24 hours, while the complication rate reached 60% in children diagnosed after 30 days ($p = 0.0035$). Bronchiectasis was a serious complication in 25% of patients with a delay in diagnosis of more than 30

days ($p = 0.0001$). Persistent respiratory symptoms such as cough and wheezing were found in 25% of patients not diagnosed within the first 24 hours [26].

CONCLUSIONS

By addressing the causes, diagnosis strategies, and intervention methods associated with choking incidents in children, this research paper aims to contribute to the development of effective public health initiatives and policies to safeguard the well-being of the pediatric population. Detailed discussion of these issues enables a deeper understanding of the mechanisms leading to choking, identification of the most effective diagnostic procedures, and implementation of interventions that can prevent or minimize the risk of choking in the pediatric population.

REFERENCES

1. Mittleman RE, Wetli CV. The fatal cafe coronary. Foreign-body airway obstruction. *JAMA*. 1982 Mar 5;247(9):1285-8.
2. Brkic F, Umihanic S, Altumbabic H, et al. Death as a Consequence of Foreign Body Aspiration in Children. *Med Arch*. 2018 Jun;72(3):220-223.
3. Sidell DR, Kim IA, Coker TR, et al. Food choking hazards in children. *Int J Pediatr Otorhinolaryngol*. 2013 Dec;77(12):1940-6.
4. Kumar A, Varshney S, Tyagi AK, et al. Choking – A Public Health Problem- Are We Prepared?. *Indian J Comm Health*. 2019 Jun; 31(2): 284-286.
5. Committee on Injury, Violence, and Poison Prevention. Prevention of choking among children. *Pediatrics*. 2010 Mar;125(3):601-7.
6. Hayes NM, Chidekel A. Pediatric choking. *Del Med J*. 2004 Sep;76(9):335-40.
7. Denny SA, Hodges NL, Smith GA. Choking in the Pediatric Population. *Am J Lifestyle Med*. 2015;9(6):438-441.
8. Passàli D, Lauriello M, Bellussi L, et al. Foreign body inhalation in children: an update. *Acta Otorhinolaryngol Ital*. 2010 Feb;30(1):27-32.
9. American Academy of Pediatrics. Committee on School Health. American Academy of Pediatrics: Guidelines for emergency medical care in school. *Pediatrics*. 2001 Feb;107(2):435-6.
10. Chiu CY, Wong KS, Lai SH, et al. Factors predicting early diagnosis of foreign body aspiration in children. *Pediatr Emerg Care*. 2005 Mar;21(3):161-4.
11. Tan HK, Brown K, McGill T, et al. Airway foreign bodies (FB): a 10-year review. *Int J Pediatr Otorhinolaryngol*. 2000;56(2):91.
12. Laya BF, Restrepo R, Lee EY. Practical Imaging Evaluation of Foreign Bodies in Children: An Update. *Radiol Clin North Am*. 2017 Jul;55(4):845-867.
13. Darras KE, Roston AT, Yewchuk LK. Imaging Acute Airway Obstruction in Infants and Children. *Radiographics*. 2015 Nov-Dec;35(7):2064-79.
14. Burton EM, Brick WG, Hall JD, et al. Tracheobronchial foreign body aspiration in children. *South Med J*. 1996 Feb;89(2):195-8.
15. Eren S, Balci AE, Dikici B, et al. Foreign body aspiration in children: experience of 1160 cases. *Ann Trop Paediatr*. 2003 Mar;23(1):31-7.
16. Lima JA. Laryngeal foreign bodies in children: a persistent, life-threatening problem. *Laryngoscope*. 1989 Apr;99(4):415-20.
17. Esclamado RM, Richardson MA. Laryngotracheal foreign bodies in children. A comparison with bronchial foreign bodies. *Am J Dis Child*. 1987 Mar;141(3):259-62.
18. Laks Y, Barzilay Z. Foreign body aspiration in childhood. *Pediatr Emerg Care*. 1988 Jun;4(2):102-6.
19. Yadav SP, Singh J, Aggarwal N, et al. Airway foreign bodies in children: experience of 132 cases. *Singapore Med J*. 2007 Sep;48(9):850-3.
20. Hegde SV, Hui PK, Lee EY. Tracheobronchial foreign bodies in children: imaging assessment. *Semin Ultrasound CT MR*. 2015 Feb;36(1):8-20.
21. Shlizerman L, Ashkenazi D, Mazzawi S, et al. [Foreign body aspiration in children: ten-years experience at the Ha'Emek Medical Center]. *Harefuah*. 2006 Aug;145(8):569-71, 631.
22. Mu L, He P, Sun D. The causes and complications of late diagnosis of foreign body aspiration in children. Report of 210 cases. *Arch Otolaryngol Head Neck Surg*. 1991 Aug;117(8):876-9.
23. Al-Majed SA, Ashour M, al-Mobeireek AF, et al. Overlooked inhaled foreign bodies: late sequelae and the likelihood of recovery. *Respir Med*. 1997 May;91(5):293-6.

24. Friedman EM. Tracheobronchial foreign bodies. *Otolaryngol Clin North Am.* 2000 Feb;33(1):179-85.
25. Reilly J, Thompson J, MacArthur C, et al. Pediatric aerodigestive foreign body injuries are complications related to timeliness of diagnosis. *Laryngoscope.* 1997 Jan;107(1):17-20.
26. Karakoç F, Karadağ B, Akbenlioğlu C, et al. Foreign body aspiration: what is the outcome? *Pediatr Pulmonol.* 2002 Jul;34(1):30-6.

CORRESPONDING AUTHOR

Klaudia Korycka

Department of Internal Medicine, Praski Hospital in Warsaw, Poland

e-mail: klaudia@korycka.com

ORCID AND CONTRIBUTIONSHIP

Klaudia Korycka: 0009-0006-2542-6915 **A B C D E F**

Agata Mormul: 0009-0008-7793-4799 **A B C D E F**

Michał Korab: 0009-0003-0908-3033 **A D F**

Joanna Smalira: 0009-0003-7207-1393 **A D**

A – Work concept and design, **B** – Data collection and analysis, **C** – Responsibility for statistical analysis, **D** – Writing the article, **E** – Critical review, **F** – Final approval of the article

RECEIVED: 02.07.2024

ACCEPTED: 05.09.2024



Challenges and opportunities in implementing telemedical solutions for COPD management in the Polish healthcare sector: a presenting own experience

Wojciech Tański^{1,2}, Andrzej Teplicki³, Anna Stapkiewicz⁴, Adrianna Szalonka⁵, Izabela Kulas⁶, Beata Jankowska-Polańska^{2,7}

¹DEPARTMENT OF INTERNAL MEDICINE, 4TH MILITARY TEACHING HOSPITAL IN WROCLAW, WROCLAW, POLAND

²FACULTY OF MEDICINE, WROCLAW UNIVERSITY OF SCIENCE AND TECHNOLOGY, POLAND

³CLINICAL DEPARTMENT OF PULMONOLOGY-ALLERGOLOGY AND INTERNAL DISEASES, 4TH MILITARY CLINICAL HOSPITAL IN WROCLAW, WROCLAW, POLAND

⁴DEPARTMENT OF FUNDS ACQUISITION, 4TH MILITARY CLINICAL HOSPITAL IN WROCLAW, WROCLAW, POLAND

⁵CLINICAL RESEARCH SUPPORT CENTRE, 4TH MILITARY CLINICAL HOSPITAL IN WROCLAW, WROCLAW, POLAND

⁶DEPARTMENT OF FAMILY MEDICINE, HEALTHCARE NORWAY IN NORWAY, FORNEBU, NORWAY

⁷CENTRE FOR RESEARCH AND INNOVATION, 4TH MILITARY CLINICAL HOSPITAL IN WROCLAW, WROCLAW, POLAND

ABSTRACT

Aim: The aim of this article is to present and discuss the conclusions of a finalized pilot project implementing telemedical solutions for COPD management within the senior population in Wrocław and the Lower Silesian Voivodeship during 2022-2023. It also aimed to contribute to the development of innovative strategies to improve care for individuals with COPD through the use of telemedical technologies.

Materials and methods: An interdisciplinary and comprehensive pilot project in pulmonology was applied, dividing it into health, organizational, and technological areas. The steps and data collection strategy were presented, enabling the implementation of telemedical solutions among COPD patients in Poland.

Results: The implementation of telemedical solutions in COPD represented an innovative approach to improving care. Among the main goals of the project were to reduce patient waiting times, enhance disease progress monitoring, and provide access to specialized healthcare through the use of modern telemedical technologies. Various telemedical solutions were implemented, including remote monitoring of health parameters, online consultations with pulmonology specialists, and patient education on self-monitoring of symptoms. The final summary of the materials collected within the described methodology allowed for a holistic view of the implementation of telemedicine in pulmonary healthcare in Poland, using the discussed pilot project as an example.

Conclusions: The analysis of the pilot project implementing telemedical solutions in the field of pulmonology in the Polish healthcare sector has shown that telemedicine can improve care for COPD patients. The project's outcomes indicate the potential for reducing patient waiting times and better monitoring of disease progression. However, these aspects require improvement and refinement, particularly in terms of systemic solutions.

KEY WORDS: telemedicine, pulmonology, chronic obstructive pulmonary disease, opportunities, challenges

Wiad Lek. 2024;77(9):1808-1817. doi: 10.36740/WLek/192865 DOI

INTRODUCTION

The rising incidence of chronic obstructive pulmonary disease (COPD) necessitates innovative approaches to patient care [1]. Telemedicine has emerged as a crucial tool for improving COPD management by enabling continuous health monitoring and remote consultations [2,3]. Telemedical solu-

tions offer significant potential in monitoring and managing COPD by enabling continuous tracking of lung function through self-administered spirometry tests. Patients can use specialized spirometric devices linked to telemedical platforms to measure their lung capacity regularly [4]. These measurements are then transmitted to healthcare providers, allowing

for real-time assessment and individualized treatment adjustments. This approach not only facilitates timely medical interventions but also empowers patients to actively participate in their health management [5, 6].

Telemedical platforms also enable remote pulmonology consultations, where specialists can analyze spirometry results, provide advice, and adjust treatment based on current data. This eliminates the need for frequent visits to medical facilities, especially for patients with limited mobility, allowing for effective healthcare in the comfort of their own homes [7]. The self-performance of spirometry by patients aligns with the trend of health education and motivation for self-care. Telemedicine offers interactive educational tools that allow patients with COPD to understand the importance of regularly monitoring lung function [8]. Moreover, access to personalized information about spirometry results can motivate patients to adhere to medical recommendations, reinforcing their engagement in the treatment process [9–11].

The introduction of telemedicine and e-health for monitoring patients with COPD, with an emphasis on self-performing spirometry, not only improves the quality of care but also increases the accessibility of medical services [12]. Thanks to these innovations, COPD patients can actively engage in managing their health, while enabling doctors to monitor the progress of the disease and quickly respond to any deterioration in health [13]. This contemporary approach to caring for COPD patients integrates modern technologies into the daily management of the disease, contributing to an improvement in their quality of life [14].

The seamless integration of telemedicine not only enhances accessibility to healthcare but also fosters a proactive and informed patient-doctor partnership, fostering a holistic and patient-centered model of care [15, 16]. This collaborative approach empowers patients to take an active role in disease management, providing them with valuable insights into their health and promoting a sense of control [17]. Additionally, it allows healthcare providers to deliver personalized and timely interventions, ultimately leading to more effective and patient-tailored care [18–20].

Considering the ongoing challenges related to the care and rehabilitation of patients with COPD, the implementation of modern solutions becomes imperative for improving pulmonary care and rehabilitation [21, 22]. This article summarizes a pilot project aimed at implementing and testing innovative tele-

medicine solutions in the field of chronic diseases. This project, conducted in 2022–2023 in Wrocław and the Lower Silesian Voivodeship, represents a step forward in the transformation of healthcare, focusing on adapting modern technologies to the specific needs and challenges associated with caring for patients with COPD.

By focusing on the practical implementation of telemedicine solutions, this project not only explores the potential of modern technologies but also emphasizes the tangible benefits they can bring to patients, medical staff, and the healthcare system as a whole. Encompassing areas such as the analysis of pulmonary needs, selection of appropriate technologies, staff training, testing effectiveness, and acceptance assessment, this project sheds light on the comprehensive process of adapting telemedicine in COPD.

However, despite the benefits, there are several potential disadvantages and challenges associated with the use of telemedical platforms for COPD patients such as (1) patient compliance: ensuring that patients consistently use the telemedical devices and adhere to monitoring protocols can be challenging; (2) data security concerns: the transmission and storage of sensitive health data over digital platforms raise concerns about data privacy and security; (3) technical support: patients may require ongoing technical support to effectively use telemedical devices, which can be a barrier, especially for elderly patients who may not be technologically savvy; (4) limited access: not all patients have access to the necessary technology or reliable internet connections, which can limit the reach and effectiveness of telemedicine interventions; and (5) integration with existing systems: integrating telemedical data into existing healthcare systems and workflows can be complex and may require significant changes to current practices. Addressing these challenges is crucial for the successful implementation and sustainability of telemedical solutions in COPD care.

In this article, a closer look will be taken at the key stages of the project, with the obtained results, conclusions, and prospects for further development being analyzed. The introduction of telemedicine into the field of pulmonology is not only opening up new diagnostic and therapeutic possibilities but also raising the question of how to best tailor these modern tools to the unique needs of COPD patients. Acting as a bridge between traditional care and innovative technologies, this project contributes to the creation of a more accessible, effective, and personalized pulmonary care for COPD patients.

AIM

The aim of this article is to present and discuss the conclusions of a finalized pilot project implementing telemedical solutions for COPD management within the senior population in Wrocław and the Lower Silesian Voivodeship during 2022-2023. The article intends to analyze the challenges and opportunities associated with the implementation of these innovative solutions in the Polish healthcare sector. By delving into the project's experiences and evaluating the effectiveness of telemedical technologies in the context of COPD, this article aims to provide practical insights that may support the further development of pulmonary care in Poland.

RESULTS

To achieve the goals set for this article, an interdisciplinary and comprehensive research framework was applied. The steps and data collection strategy that enabled the goal of analyzing the implementation of telemedical solutions in chronic diseases, using COPD as an example in the Polish healthcare sector, are presented below. For each project, the goal, scope, applied telemedical technologies, and gathered data were thoroughly analyzed. This information served as a starting point for identifying key issues related to the implementation of telemedicine in the care of individuals diagnosed with COPD. The effectiveness of patient health monitoring was assessed, clinical benefits were identified, and potential challenges related to the interpretation and management of health data in pulmonary healthcare were evaluated. The level of acceptance of telemedical technologies by patients, their understanding of experiences, and expectations regarding modern e-health solutions in healthcare were identified. The final summary of the materials collected within the described methodology allowed for a holistic view of the implementation of telemedicine in pulmonary healthcare in Poland, using the discussed pilot project as an example.

MATERIAL AND METHODS

An attempt was made to identify challenges and draw conclusions to contribute to the development of innovative strategies to improve care for patients with COPD. The implementation of the project was summarized in the health, organizational, and technological areas. Key indicators from the implementation of the pilot project were also presented in relation to the assumptions of the project proposal within the Polish healthcare system.

The project involved individuals above 18 years old who have given informed consent to participate and have been diagnosed with COPD. The target group included not only the patients themselves but also Primary Health Care (PHC) doctors, nurses, specialist pulmonologists, and, to some extent, caregivers of patients (legal or actual). Patients received health support and education, while the medical staff will gain additional knowledge and qualifications related to caring for patients with COPD, including the use of telemedicine solutions. Caregivers of patients received information about the functioning of the telemedicine platform, which is the basis for the provided services, and acquired knowledge in the field of health education directed to both them and the patients [23].

The main goal of the project was to conduct tests aimed at confirming the effectiveness of a solution that could later be implemented on a larger scale, such as nationwide. The project focused on monitoring the progress of COPD and predicting exacerbations of the disease through constant monitoring of health and performance parameters using self-administered spirometry. It is assumed that the number of patients covered by the project will be 520 individuals, with an equal distribution of gender, taking into account the standard distribution in the population. The estimated number of caregivers is around 20% of this figure, or about 100 individuals. The medical team will consist of 10 specialists, 9 PHC doctors, and 9 community nurses [23].

The project does not favor any of the groups, allowing testing the model as a universal solution applied in the general healthcare system without any access limitations. Nevertheless, following the program's objectives, priority in participation will be given to individuals from municipalities in excluded areas, i.e., those with income per capita below the national average. This approach aims to ensure the achievement of the set indicators and direct support primarily to residents in areas that are challenging for private or public healthcare, especially in locations distant from major cities, where the healthcare service market may be limited [23].

RESULTS AND DISCUSSION

HEALTHCARE FIELD

The summary includes an assessment of the project's impact on the health domain, focusing on clinical and health outcomes. The effectiveness of telemedicine in improving diagnosis, monitoring,

and treatment efficiency for patients with COPD was analyzed. Potential health benefits for patients, such as improved quality of life, reduced waiting time for medical assistance, and decreased hospitalizations, were also considered.

The project aims to increase access to healthcare services, especially through telemedicine, which is a key objective. However, the primary goal is to improve the quality of life for patients and enhance their sense of security, regardless of their place of residence. The telemedicine platform enables early medical interventions, which are crucial for the effectiveness of patient care. In the context of COPD, the project focuses on telemonitoring symptoms at the patient's home, allowing the anticipation of exacerbations. This is an important tool in managing the health of patients with this chronic disease. By early detection of COPD exacerbations, the project contributes to reducing adverse health effects for patients, which can have a significant impact on improving their quality of life.

The project focuses on efficiently organizing the appointment system, adapting it to the individual needs of patients suffering from COPD. As part of a three-month telemedicine-based medical care, individuals registered to participate in the project have access to various services. The process begins with registration at the project promoter's headquarters or partner locations, as well as during organized medical events. Subsequently, patients respond to their managing physician's proposal or contact the project through a special phone number. During the three-month care period, patients have access to two consultations or teleconsultations with a primary care physician, one educational consultation with a nurse or physiotherapist, and one consultation or teleconsultation with a pulmonology specialist. This comprehensive appointment system aims to ensure effective medical and educational care through the use of telemedicine for individuals with COPD.

The project offers patients broad access to education through electronic and printed materials, providing essential information and recommendations regarding health and lifestyle management recommended for individuals at risk of COPD exacerbation. Patients use a dedicated application installed on their own phone or provided free of charge during the initial project participation visit, especially if they do not have internet access. A key element is the user-friendly spirometer, allowing independent measurement of respiratory parameters at home. Spirometry results are transmitted to the project staff through the telemedicine platform, and if necessary, patients receive support from an assistant during home spirometric

measurements, with the option to report alerts by phone in case of deteriorating health. The project concludes with a summary of participation in the form of a document that patients can share with their managing physician after the project ends, including the spirometry results obtained during the project. This comprehensive approach aims to provide patients with comprehensive care, education, and monitoring of their health in a home setting.

The project provides patients with extensive access to education through electronic and printed materials, delivering essential information and recommendations regarding health and lifestyle management recommended for individuals at risk of COPD exacerbation. Patients use a dedicated platform on their own phone or a tablet provided free of charge during the initial project participation visit, especially if they do not have internet access. A key element is the user-friendly spirometer, allowing independent measurement of respiratory parameters at home. Spirometry results are transmitted to the project staff through the telemedicine platform, and if necessary, patients receive support from an assistant during home spirometric measurements, with the option to report alerts by phone in case of deteriorating health. The project concludes with a summary of participation in the form of a document that patients can share with their managing physician after the project ends, including the spirometry results obtained during the project. This comprehensive approach aims to provide patients with comprehensive care, education, and monitoring of their health in a home environment.

Based on the conducted pilot, pulmonary recommendations indicate that the Program may be too advanced for patients with mild obstruction. It is recommended that such patients receive information from their primary care physician (PCP) to be aware of when their condition may exacerbate. Potential inclusion in the Project should occur after assessment in the PCP, conducted due to exacerbation, with spirometric examination. The PCP, using the guidelines provided on the platform, should decide on the possible participation of the patient in the Program. In case of doubts, the PCP should consult their decision with a pulmonologist available on the telemedical platform. For patients with severe obstruction, continuous spirometric monitoring is not recommended, as such patients should be under the constant care of the attending pulmonologist. The pulmonologist, familiar with the specificity of the measurement results and relevant examinations for the specific patient, can effectively oversee their health. Patients with severe obstruction are usually aware of the deterioration of

their condition, and any issues related to actions in such a situation should be discussed with the attending pulmonologist.

The patient with moderate obstruction would benefit the most from inclusion in the telemedical care program. In the case of such a patient, the PCP or pulmonologist should suggest participation in the Program and initiate training on using the spirometer. Individuals with moderate obstruction, at risk of exacerbation, should receive, in addition to the password for the telemedical platform account assigned to the attending physician, a pulse oximeter and educational materials on monitoring health through the platform. After several health monitoring visits (monthly or after an exacerbation) in the PCP, the patient may receive a simple spirometer for home use. The condition is that the patient, after several spirometry tests performed in the presence of the PCP, will be able to independently conduct a reliable spirometric examination. Including spirometry in the PCP visit for a patient with suspected COPD is in line with the Ministry of Health's strategy, which aims to expand the competencies of primary care physicians, reflecting in legal regulations.

ORGANIZATIONAL FIELD

The focus was on the impact of the project on healthcare organization, identifying changes in the organizational structure and workflow of medical staff. The adaptation of administrative and logistical systems to the implementation of telemedicine was also analyzed, paying attention to potential time and resource savings.

In terms of project management, procedures were conducted to select members of the Project Management Team; members of the project team were hired, and their responsibilities were defined; the project regulations and documents for the Leader and partners were created. Difficulties encountered in the project implementation included a lack of widespread interest among physicians, who showed little enthusiasm for participating in competitions for medical roles in the pilots. This resulted in the need to primarily involve the potential of the Promoter and Partners, responsible for creating the funding application. Another challenge was the significant workload on physicians in the Polish healthcare system, requiring the organization of their participation in the pilot in a way that allowed for the automation or delegation of the most time-consuming organizational tasks to assistants.

In the area of preventive and promotional activities in public health, comprehensive promotional materi-

als were developed as part of the Project Promotion Strategy, including leaflets, posters, public transport displays, radio banners, and a radio spot. Additionally, promotional activities were initiated during the project's opening conference, and a dedicated website was created. To increase the effectiveness of the promotion, a request was made to include a sub-measure related to advertising during a trip to Norway. During the project implementation, the emphasis of promotion was shifted from scattered print publications to organized promotion during the closing conference of the project. However, difficulties were encountered, mainly related to the financing of the pilot project, which necessitated adherence to competitiveness principles when selecting providers of promotional services. The diversity of promotional activities and the internal conditions of the beneficiaries made the application of competitive procedures for promotional activities time-consuming. Furthermore, the limited project implementation schedule created additional challenges in coordinating efforts on promotional elements.

In the scope of testing model solutions in partnership with primary care entities, cooperation was established through the signing of partnership agreements with 9 entities. The change in the project schedule had a significant impact on the possibility of cooperation due to changes in employment and the involvement of partners in other tasks. As a result, it was necessary to involve new partners in the project. Within the project implementation, medical staff were hired, and project staff were trained in the operation of the telemedical platform, as well as the principles and documents used in the project. Progress in project work was regularly presented, and any risks were discussed during the meetings of the pilot assessment and supervision team. However, difficulties were encountered, especially regarding the digital competencies of doctors, which proved crucial for the effective assumption of roles by doctors in the project. Lower levels of digital competencies among doctors resulted in a lower number of conducted patient visits. Additionally, the lack of the ability to verify the impact of the incentivizing fee for visits for primary care and specialist doctors posed a significant problem in the pilot's implementation.

Regarding the informational and promotional activities of the project, diverse promotional materials were developed as part of the strategy for promoting project results, including brochures, posters, public transportation displays, broadcast banners, and a closing conference for the project, along with the creation of a dedicated website. Efforts were also

Table 1. Key indicators of the geriatric project

Indicator	Achieved Value (n)	Target Value (n)	Performance Indicator (%)
Number of beneficiaries (female)	143	260	55%
Number of beneficiaries (male)	110	260	42%
Number of individuals expressing satisfaction with services received through new e-health methods according to the implemented model	253	520	49%
Number of healthcare services provided with the assistance of purchased modern equipment	271	1560	17%
Number of primary healthcare units covered by telemedical service	9	9	100%
Number of organizations (primary healthcare units, foreign partners, patient organizations, domestic partners) collaborating with the Leader in the implementation and validation of the project	12	12	100%
Territorial scope of the project: Number of counties whose residents participate in the project	4	4	100%
Experience of the Applicant and Partners: Number of entities with experience in implementing at least one project in the field of e-health or telemedicine	5	5	100%
Project management: Number of entities that will apply PRINCE2 project management methodology and an approach in line with the principles of equality management and equal opportunities policy in project management	12	12	100%
Number of patients diagnosed with geriatric conditions: sarcopenia, malnutrition, frailty syndrome based on online consultations and questionnaires conducted with the patient	0	520	0%
Increase in the level of knowledge about using medical services online among project participants	253	520	49%
Increase in the level of knowledge about geriatric diseases according to the model, the way they are diagnosed, principles of prevention and treatment involving telemedicine, among project participants (verification based on a sample of participants in the focus group)	253	520	49%

made to promote the project's results during a trip to Norway. Significant changes involved coordinating the promotion of project outcomes, shifting the focus from scattered print publications to an organized promotion during the conference concluding the project. However, difficulties were encountered due to the funding of the pilot project, where 85% of the funds came from Norwegian Funds and 15% from the State Budget. This necessitated the selection of promotional service providers while adhering to competitive principles. Competitive procedures for promotional activities proved time-consuming due to the diversity of planned actions and internal conditions of the beneficiaries. The rigid project implementation schedule, which was not flexible and allowed too little time for task completion in relation to their complexity, was also a limitation (Table 1).

TECHNOLOGICAL FIELD

Regarding the purchase of equipment for testing model solutions, the project procured necessary equipment for testing model solutions, including tablets with internet access for digitally excluded patients, laptops for medical and administrative staff, spirometers, and ensured the operation of a help desk. However, the tight schedule of project implementation resulted in increased financial risk, especially due to the need to announce procurement even at the stage of processing the project financing agreement. Additionally, patients showed reluctance to use tablets borrowed from the Program Implementers, preferring to use their own phones or computers. In the context of spirometers, difficulties arose related to the availability of devices meeting the requirements for transmitting spirometry results to the telemedical

platform, as well as patients' ability to independently perform spirometry at home, which does not guarantee the correct execution of this test.

Regarding the action related to building the platform for telemedical services, the project selected a telemedical platform provider and conducted training for doctors on its use, as well as substantive support for workshops for patients. Effective manuals and operating procedures were developed, and technical support for conducting visits with patients was also provided. However, difficulties arose due to time constraints. The time needed to conduct the procurement procedure for selecting a spirometer supplier affected the timing of starting this process. The inflexible project schedule required simultaneous training for doctors, implementing recruitment, and working on the tool, which should have been separated in time. Lack of time also prevented the full development of procedures for emergencies or the improvement of technological solutions. The need for ongoing collaboration between the telemedical platform provider and the spirometer supplier was demanding and excessively engaged Project Coordinators and Assistants.

CONCLUSIONS

The implementation project and testing of pilot telemedical solutions in COPD represented an innovative approach in the Polish healthcare system. Among the main goals of the project were reducing patient waiting times, improving disease progress monitoring, and ensuring access to specialized healthcare through the use of modern telemedical technologies. During the project implementation, the focus was on identifying risks associated with COPD and implementing effective management strategies. Various telemedical solutions were introduced, such as remote monitoring of health parameters, online consultations with pulmonology specialists, and patient education on self-monitoring of symptoms.

The integration of the program with the telemedical platform proved effective in patient monitoring. It was indicated that patients with moderate obstruction expecting exacerbations constitute an optimal group for inclusion in the program. Early stages of the disease do not require frequent spirometric measurements, and patient motivation to provide information is low. The program's effectiveness increases during exacerbations, requiring intervention by a pulmonology specialist. Recommendations include precise guidelines for PCP and training patients in the independent use of devices, especially spirometers. Communication

between physicians plays a crucial role, and patient recruitment must be individualized and coordinated over time. The conclusions emphasize the need for flexible adaptation of the program to the disease's severity and active collaboration between medical entities.

However, several challenges and disadvantages were encountered during the project:

- *Patient Compliance:* Ensuring consistent use of telemedical devices by patients was challenging. Many patients, especially the elderly, faced difficulties in adhering to the monitoring protocols due to a lack of familiarity with the technology or forgetfulness. Regular follow-ups and reminders, as well as caregiver involvement, were implemented to address this issue.
- *Data Security Concerns:* The transmission and storage of sensitive health data over digital platforms raised significant concerns about data privacy and security. Robust encryption methods and secure data storage protocols were employed to mitigate this risk, and patients were educated about data security measures.
- *Technical Support:* The need for ongoing technical support was another challenge, as some patients struggled with the operation of the devices. A dedicated technical support team was established to provide assistance, and detailed user manuals and instructional videos were made available.
- *Limited Access:* Not all patients had access to the necessary technology or reliable internet connections. The project provided devices and internet access to digitally excluded patients, and community centers were set up to facilitate access for those who could not have the technology at home.
- *Integration with Existing Systems:* Integrating telemedical data into existing healthcare systems and workflows proved complex, requiring significant adjustments to current practices and additional training for healthcare providers. Collaborative workshops and training sessions were organized to ease this integration process.

PRACTICAL IMPLICATIONS

Implementing telemedical solutions in the treatment of patients with COPD can have specific practical implications. Firstly, continuous monitoring of patients' health parameters enables doctors to react quickly to any deterioration in health, contributing to a reduction in hospitalizations and shorter recovery times. Additionally, remote online consultations with pulmonology specialists eliminate time and geographical barriers, allowing patients easier access to experts.

This can lead to more effective care, especially in urgent situations or those requiring rapid intervention. Patient education on self-monitoring of symptoms can increase health awareness and patient activity in managing their health. In the longer term, this may contribute to improving the quality of life for COPD patients. The insights from this project can serve as inspiration for further developing innovative care strategies for patients with chronic diseases, leveraging the potential of telemedical technologies in the Polish healthcare sector.

LIMITATIONS

While the pilot project demonstrated promising results, several limitations should be acknowledged. First, the sample size was relatively small and may not be representative of the broader COPD patient population. Second, the study was conducted within a specific geographic region (Wrocław and the Lower Silesian Voivodeship), which may limit the generalizability of the findings to other regions with different healthcare infrastructures. Third, patient compliance with telemedical monitoring varied, which could

impact the consistency and reliability of the data collected. Fourth, the project primarily relied on self-reported data, which is subject to bias and inaccuracies. Lastly, the integration of telemedical data into existing healthcare systems posed significant challenges, and the effectiveness of these integrations was not fully evaluated.

FURTHER RESEARCH/VVW

Based on your recommendation, the expansion of the telemonitoring system in future projects to include these additional features should be considered. Incorporating parameters such as the COPD Assessment Test (CAT), information on sputum volume and content, self-reported exacerbations, and exercise capacity will ensure a more comprehensive approach to monitoring COPD. This will not only enhance the accuracy and relevance of patient monitoring but also align more closely with the current guidelines and endpoints established by COPD GOLD. Such enhancements are expected to improve patient outcomes and provide more detailed insights into disease progression and management.

REFERENCES

1. Watson A, Wilkinson TMA. Digital healthcare in COPD management: a narrative review on the advantages, pitfalls, and need for further research. *Ther Adv Respir Dis*. 2022;16:17534666221075493. doi:10.1177/17534666221075493 [DOI](#)
2. Tomasic I, Tomasic N, Trobec R, Krpan M, Kelava T. Continuous remote monitoring of COPD patients—justification and explanation of the requirements and a survey of the available technologies. *Med Biol Eng Comput*. 2018;56(4):547-569. doi:10.1007/s11517-018-1798-z [DOI](#)
3. Compton M, List R, Starheim E, et al. Home spirometry utilisation in telemedicine clinic for cystic fibrosis care during COVID-19 pandemic: a quality improvement process. *BMJ Open Qual*. 2021;10(3):e001529. doi:10.1136/bmj-2021-001529 [DOI](#)
4. Doumit M, Ledwos R, Plush L, et al. Telehealth application of an ultrasonic home spirometer. *Arch Dis Child*. 2022;107(8):752-754. doi:10.1136/archdischild-2021-322536 [DOI](#)
5. Congrete S, Metersky ML. Telemedicine and Remote Monitoring as an Adjunct to Medical Management of Bronchiectasis. *Life (Basel)*. 2021;11(11):1196. doi:10.3390/life11111196 [DOI](#)
6. Kołtowski Ł, Basza M, Bojanowicz W, et al. Remotely supervised spirometry versus laboratory-based spirometry during the COVID-19 pandemic: a retrospective analysis. *Respir Res*. 2024;25:39. doi:10.1186/s12931-023-02586-0 [DOI](#)
7. Morais A, Bugalho A, Drummond M, et al. Teleconsultation in respiratory medicine – A position paper of the Portuguese Pulmonology Society. *Pulmonology*. 2023;29(1):65-76. doi:10.1016/j.pulmoe.2022.04.007 [DOI](#)
8. Barbosa MT, Sousa CS, Morais-Almeida M. Telemedicine in the Management of Chronic Obstructive Respiratory Diseases: An Overview. In: Linwood SL, ed. *Digital Health*. Exon Publications; 2022. Accessed January 26, 2024. <http://www.ncbi.nlm.nih.gov/books/NBK580636/>
9. Sculley JA, Musick H, Krishnan JA. Telehealth in chronic obstructive pulmonary disease: before, during, and after the coronavirus disease 2019 pandemic. *Curr Opin Pulm Med*. 2022;28(2):93-98. doi:10.1097/MCP.0000000000000851 [DOI](#)
10. Janjua S, Carter D, Threapleton CJ, Prigmore S, Disler RT. Telehealth interventions: remote monitoring and consultations for people with chronic obstructive pulmonary disease (COPD). *Cochrane Database Syst Rev*. 2021;2021(7):CD013196. doi:10.1002/14651858.CD013196.pub2 [DOI](#)
11. Sabahi A, Hosseini A, Emami H, Almasi S. Telemedicine Services in Chronic Obstructive Pulmonary Disease: A Systematic Review of Patients' Adherence. *Tanaffos*. 2021;20(3):209-220.
12. Donner CF, ZuWallack R, Nici L. The Role of Telemedicine in Extending and Enhancing Medical Management of the Patient with Chronic Obstructive Pulmonary Disease. *Medicina (Kaunas)*. 2021;57(7):726. doi:10.3390/medicina57070726 [DOI](#)

13. Alghamdi SM. Content, Mechanism, and Outcome of Effective Telehealth Solutions for Management of Chronic Obstructive Pulmonary Diseases: A Narrative Review. *Healthcare (Basel)*. 2023;11(24):3164. doi:10.3390/healthcare11243164 [DOI](#)
14. Koh JH, Chong LCY, Koh GCH, Tyagi S. Telemedical Interventions for Chronic Obstructive Pulmonary Disease Management: Umbrella Review. *J Med Internet Res*. 2023;25:e33185. doi:10.2196/33185 [DOI](#)
15. Santana MJ, Manalili K, Jolley RJ, Zelinsky S, Quan H, Lu M. How to practice person-centred care: A conceptual framework. *Health Expect*. 2018;21(2):429-440. doi:10.1111/hex.12640 [DOI](#)
16. Edgman-Levitan S, Schoenbaum SC. Patient-centered care: achieving higher quality by designing care through the patient's eyes. *Isr J Health Policy Res*. 2021;10:21. doi:10.1186/s13584-021-00459-9 [DOI](#)
17. Shawwa L. The Use of Telemedicine in Medical Education and Patient Care. *Cureus*. 15(4):e37766. doi:10.7759/cureus.37766 [DOI](#)
18. Dinesen B, Nonnecke B, Lindeman D, et al. Personalized Telehealth in the Future: A Global Research Agenda. *J Med Internet Res*. 2016;18(3):e53. doi:10.2196/jmir.5257 [DOI](#)
19. Battineni G, Sagaro GG, Chintalapudi N, Amenta F. The Benefits of Telemedicine in Personalized Prevention of Cardiovascular Diseases (CVD): A Systematic Review. *J Pers Med*. 2021;11(7):658. doi:10.3390/jpm11070658 [DOI](#)
20. Bhaskar S, Bradley S, Chattu VK, et al. Telemedicine as the New Outpatient Clinic Gone Digital: Position Paper From the Pandemic Health System Resilience PROGRAM (REPROGRAM) International Consortium (Part 2). *Frontiers in Public Health*. 2020;8. doi:10.3389/fpubh.2020.00410 [DOI](#)
21. Zhang L, Maitinuer A, Lian Z, et al. Home based pulmonary tele-rehabilitation under telemedicine system for COPD: a cohort study. *BMC Pulm Med*. 2022;22:284. doi:10.1186/s12890-022-02077-w [DOI](#)
22. Bryant MS, Bandi VD, Nguyen CK, Lan C, Henson HK, Sharafkhaneh A. Telehealth Pulmonary Rehabilitation for Patients With Severe Chronic Obstructive Pulmonary Disease. *Fed Pract*. 2019;36(9):430-435.
23. Tański W, Stapkiewicz A, Szalonka A, Głuszczyk-Ferenc B, Tomasiewicz B, Jankowska-Polańska B. The Framework of The Pilot Project for Testing A Telemedicine Model in The Field of Chronic Diseases – Health Challenges and Justification of The Project Implementation. *Pol Merkur Lek*. 2024;51(5):674-680. doi:10.36740/Merkur202306115 [DOI](#)

ORCID AND CONTRIBUTIONSHIP

Wojciech Tański: 0000-0002-2198-8789 [A](#) [B](#) [D](#) [F](#)
 Andrzej Teplicki: 0009-0008-9242-2759 [A](#) [B](#) [D](#) [F](#)
 Anna Stapkiewicz: 0009-0001-2361-414X [A](#) [B](#) [C](#) [D](#) [F](#)
 Adrianna Szalonka: 0000-0002-0329-0926 [A](#) [B](#) [C](#) [E](#) [F](#)
 Izabela Kulas: 0009-0005-6923-2293 [E](#) [F](#)
 Beata Jankowska-Polańska: 0000-0003-1120-3535 [A](#) [B](#) [E](#) [F](#)

FUNDING SOURCE

The paper was funded by the statutory sources of the 4th Military Clinical Hospital in Wrocław.

ACKNOWLEDGMENTS

The publication was prepared within the framework of the project "Implementation and testing of pilot telemedicine solutions for the >>Chronic Diseases<< model in Wrocław and Lower Silesia province in 2022-2023" (No. 2/NMF/2172/00/127/2023/23) funded by the Norwegian Funds, operated by the Ministry of Health in cooperation with the Norwegian Directorate for Health. We would like to express our sincere gratitude to the dedicated and hardworking team that contributed to the successful implementation of the telemedicine project in the field of pulmonology. This endeavor would not have been possible without the collective efforts, expertise, and commitment of each team member. Special thanks to the project leaders, coordinators, administrators, technicians, and medical staff who demonstrated exceptional leadership skills, strategic vision, and effective communication throughout the entire process. We would like to thank the patients who participated in the pilot program for their willingness to embrace telemedicine solutions and for providing valuable feedback, contributing to the ongoing improvement of healthcare delivery.

CONFLICT OF INTEREST

The Authors declare no conflict of interest

CORRESPONDING AUTHOR

Adrianna Szalonka

Clinical Research Support Centre,
4th Military Clinical Hospital in Wroclaw

Wroclaw, Poland

e-mail: aszalonka@4wsk.pl

A – Work concept and design, **B** – Data collection and analysis, **C** – Responsibility for statistical analysis, **D** – Writing the article, **E** – Critical review, **F** – Final approval of the article

RECEIVED: 10.05.2024

ACCEPTED: 27.08.2024



Graphical modeling of additive color mixing. Perception of objects with different color shades for different observers

Ignat Ignatov¹, Teodora P. Popova², Alexander I. Ignatov¹, Ivan Angushev³

¹SCIENTIFIC RESEARCH CENTER OF MEDICAL BIOPHYSICS (SRCMB), SOFIA, BULGARIA

²UNIVERSITY OF FORESTRY, SOFIA, BULGARIA

³MEDICAL UNIVERSITY OF SOFIA, SOFIA, BULGARIA

ABSTRACT

Aim: To research subjective perceptions in additive color mixing.

Materials and Methods: 79 individuals were surveyed, and they determined the colors they perceived in two photographs. The results of color mixing were determined using statistical analysis, graphical modeling, and Python program figures.

Results: A new color is obtained by additive mixing monochromatic colors. Interestingly, different individuals perceive observed images in different ways. Mixing neighboring colors on the spectrum and those in different produces various visual effects. Distinction was found in the physical mixing of beams with different colors. Visual perception in the presence of two is subjective and is determined by the viewer's greater to one of the colors. Due to additive color mixing, additional parts of objects may appear golden or orange when there is a yellow color in a picture with blue tones. When the background is violet, the sensitivity of the blue cones decreases.

Conclusions: An experiment involving the observation of color photographs established that individuals who perceive orange-violet snow do not perceive the blue color in the dress. The analysis revealed that yellow light activates the green and red cones. In contrast, blue light activates the blue cones in the retina, highlighting the importance of cone activation of color perception. The contrast between yellow and blue can create a visual effect where parts of objects appear more pronounced or have more intense color, demonstrating the brain's processing of contrasting colors. The experiment also indicated a reduction in blue cone sensitivity with a violet background, illustrating chromatic adaptation. Different individuals may perceive colors differently based on background and lighting conditions, underscoring the subjectivity of visual perception. Finally, there is a debate over the dress's color perception. These findings suggest that individuals working on media products can enhance image quality by considering additive color blending and background effects.

KEY WORDS: graphical modeling, colors, shades, additive mixing, optical effects

Wiad Lek. 2024;77(9):1818-1824. doi: 10.36740/WLek/185414 DOI

INTRODUCTION

It is considered that human visual perception is the result of continuous evolution in animals. Color vision in animals is significant as it allows them to respond to visual signals in various situations. Animals use vision to find food and shelter, choose mates, and more [1,2]. The retina contains two morphologically distinct types of photoreceptors: rods and cones. Rods are responsible for vision in low light conditions, while cones function in higher light conditions. The highest concentration of cones is in the central area of the retina, where images of observed objects are formed, and it decreases significantly towards the periphery [3]. When light enters the eye, it stimulates the photoreceptors composed of photosensitive cells. Biochemical changes occur, leading to the generation of signals transmitted by various post-synaptic neurons in the retina. The information is then conveyed to bipolar and ganglion cells, whose axons

form the optic nerve. The signal then travels through the optic nerve to the visual cortex, where visual perception is formed [3]. The visual spectrum ranges from 380 to 750 nm, with the following color ranges – violet (380–450 nm) (70 nm), blue (450–485 nm) (35 nm), cyan (485–500 nm) (15 nm), green (500–565 nm) (65 nm), yellow (565–590) (25 nm), orange (590–625 nm) (35 nm), and red (625–740 nm) (125 nm) [4]. Normal color perception is a function of the nervous system, resulting from the transmission of information to the visual cortex. The development and improvement of color vision are poorly understood but likely depend on the training of cone photoreceptor pathways. In humans, the ability to distinguish colors is mediated by specific mechanisms in the retina and the brain. The perception of all colors can be achieved through additive or subtractive mixing of the three primary colors [5].

Additive color mixing is an exciting phenomenon.

It involves creating a different color by mixing two or more visible light sources of different colors. This phenomenon is responsible for modern color television, where screen colors are generated by sources of the three primary colors – red, green, and blue. Multicolored images are produced from these colors. The additive combination of red and green produces yellow. Respectively, the combination of green and blue results in cyan, and the combination of red and blue results in magenta.

Subtractive colors are used in paints and color filters [6]. The color reflected from a painted surface or fabric depends on amounts of three subtractive primary colors: cyan, magenta, and yellow. Additive mixing can be achieved technically in various ways. For example, this is done on computer monitors and television screens by adding lights from three primary sources of different colors. The same result is achieved when light from different sources is projected onto a screen rapidly, with the mixing occurring due to the persistence of vision. In color printing, dots of different colors are printed closely on paper, making them indistinguishable individually, and due to the limited resolving power of the eye, a specific color is perceived. This approach is also applied to color television [7].

Designers in interior and exterior design increasingly use these and other possibilities, as well as the results of mixing subtractive and additive colors.

Controlled colored light sources are used, and the options for possible color effects are expanding. Color compositions combine subtractive and additive elements, which design solutions relying less on purely subtractive color on surfaces.

Using the same technology, there are already projects for programmable colored lighting with customer-controlled colors in commercial establishments, children's play areas, spa rooms, hotel rooms, etc. [2].

Determining colors in the complex also depends on an individual's reaction to the physical, physiological, and psychological aspects of color. However, color differences can be objectively measured using additive color systems under specific conditions: the observer, viewing angle, light source, and the observed field's extent. The International Commission on Illumination (CIE), established in 1931, regulates definitions and standards for measuring colors and color differences. The primaries it defines are not real but imaginary, used to determine all other colors. The quantities of each primary color in a given color are used to determine its hue and saturation using special coefficients and equations [6].

AIM

This study aims to research subjective perceptions of additive color mixing.

MATERIALS AND METHODS

COLOR PHOTOGRAPHS

The experiments were conducted using two color photographs. The first photograph (taken by one of the co-authors (Alexander I. Ignatov) depicts a winter sunset over Vitosha Mountain, Bulgaria. The second photograph displays a dress with two colors – blue and black (Fig. 1).

EXPERIMENTS

A survey was administered to 79 individuals of varying ages, who determined the colors they perceived in the two presented photographs. Graphical modeling is applied to determine the result of additive color mixing.

The statistical processing of the results was performed using the classic Student-Fisher t-test.

RESULTS

Table 1 presents the results from the experiments on additive color mixing. An interesting finding in these studies is that different observers perceive the colors of both photographs differently.

The first group comprised 45 people who observed the dress's blue-black colors. The second group is with 34 people who observe the dress with unreal colors. The number of the participants is 79. Statistical analysis of the data using Student's t-test revealed a strong positive linear correlation at $p < 0.05$, with $r = -0.85$, indicating a significant relationship between the observers' surprise at the actual color of the dress.

ASSESSMENT OF SURPRISE BY GROUPS

The research was performed with 79 individuals, and from them, 27 women and 52 men.

Women (20) and men (18) see the real colors of the dress. Both groups show a relatively wide range of surprise ratings, with medians around 4-5. This suggests significant variation in how surprised participants in these groups are.

Men (7) who see the real colors in the dress. The ratings are more concentrated, with medians around 4-5.

Groups that see unreal colors of the dress (men and women (41)). These groups present higher medians



Fig. 1. Photographs used in the study of additive color mixing: left - sunset over Vitosha Mountain, Bulgaria; right - a dress with two accurate colors – blue and black [9].

of surprise rating (around 8-10), suggesting that they were significantly more surprised by the unreal colors of the dress. These groups also show greater variation in ratings, possibly due to different color sensitivities.

Groups that see the dress's unreal colors have higher surprise ratings than those that see the real colors. Most groups have significant variation, possibly due to differences in individual color perception and interpretation. These results show that color perception is subjective and can vary significantly depending on individual differences and the context in which the colors are seen.

The experiment's results unequivocally demonstrate that visual perception in the presence of two colors is subjective and can be influenced by the observer's greater sensitivity to one of the colors [6].

When a yellow hue is present against a backdrop of blue, the yellow light activates the green and red light-sensitive cones in the retina, while the blue light activates the green and blue-sensitive cones. The contracting colors may create a visual effect where parts of objects appear enhanced. As a result, additional parts of objects may appear enhanced. As a result, additional parts of objects may appear to have a more intense or vibrant color due to the contrast between yellow and blue.

Experiments have shown that using a violet background can affect the perception of blue cones, a phenomenon explained in various studies. Consequently, individuals who perceive snow in orange-violet or pink-violet may not see the blue color in the dress.

This image sparked an internet debate over whether

the dress is blue, black, white, or gold. However, the dress photograph was taken under specific conditions and is visible only on the screen, not in reality.

Therefore, the dispute over its actual colors cannot be conclusively resolved. Nevertheless, this is an example of the illusions that can be created through screens [8-11].

When an object's lighting changes in brightness or color, chromatic adaptation occurs, and the appearance of colored objects changes slightly as if the receptor mechanism's amplifications adapt to the surrounding light [3].

The phenomenon of simultaneous contrast, in which a surface changes its color depending on the background it is presented against, has been extensively studied.

When two colors are compared, they lose more or less of their shared color. For example, greenish-yellow appears more green on a yellow background and more yellow on a green background. The colors induced by the background are not precisely complementary, indicating the involvement of perceptual mechanisms beyond the receptors. Contrast situations are very complex, and the involved mechanisms are poorly understood. Unlike contrast, where the color and its surroundings are compared, this pertains to assimilation [3].

One type of cone is sensitive to short wavelengths near the blue end of the visible spectrum (S cones), while another type is sensitive to medium wavelengths, most responsive to green light (M cones).

Table 1. This results from observing snow at sunset and wearing a dress with multicolored stripes

Gender, Number	Snow at sunset	Dress	Assessment of surprise from the actual color of the dress
real colors of the dress			
women (20)	blue-red	blue-black	5, 6, 5, 4, 6, 5, 4, 3, 5, 4, 4, 3, 3, 5, 4, 3, 3, 4, 5, 5
men (18)	blue-red	blue-black	4, 6, 3, 7, 4, 3, 5, 4, 5, 5, 4, 4, 3, 3, 6, 4, 3, 5
men (7)	pink-red	blue-black	5, 4, 4, 4, 5, 3, 6
unreal colors of the dress			
men (8)	blue-orange	blue-gold	8, 7, 9, 9, 8, 5, 7, 8
men (5)	pink	blue-white	9, 9, 6, 9, 7
men (8)	orange-violet	yellow- white	10, 9, 10, 8, 7, 9, 9, 8
women (7)	orange-violet	golden-white	9, 9, 8, 10, 8, 10, 9
men (6)	orange	golden-white	10, 9, 9, 8, 8, 9

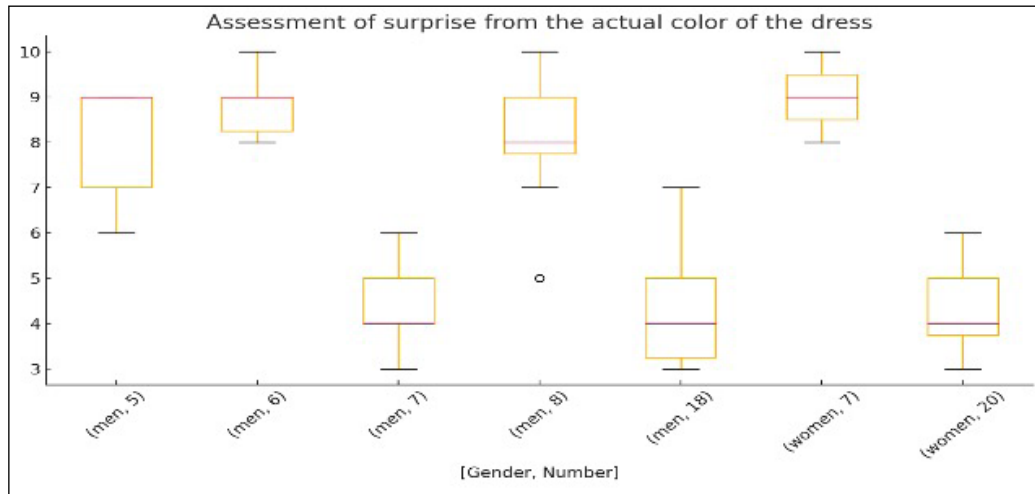


Fig. 2. Assessment of surprise from the actual color of a dress.

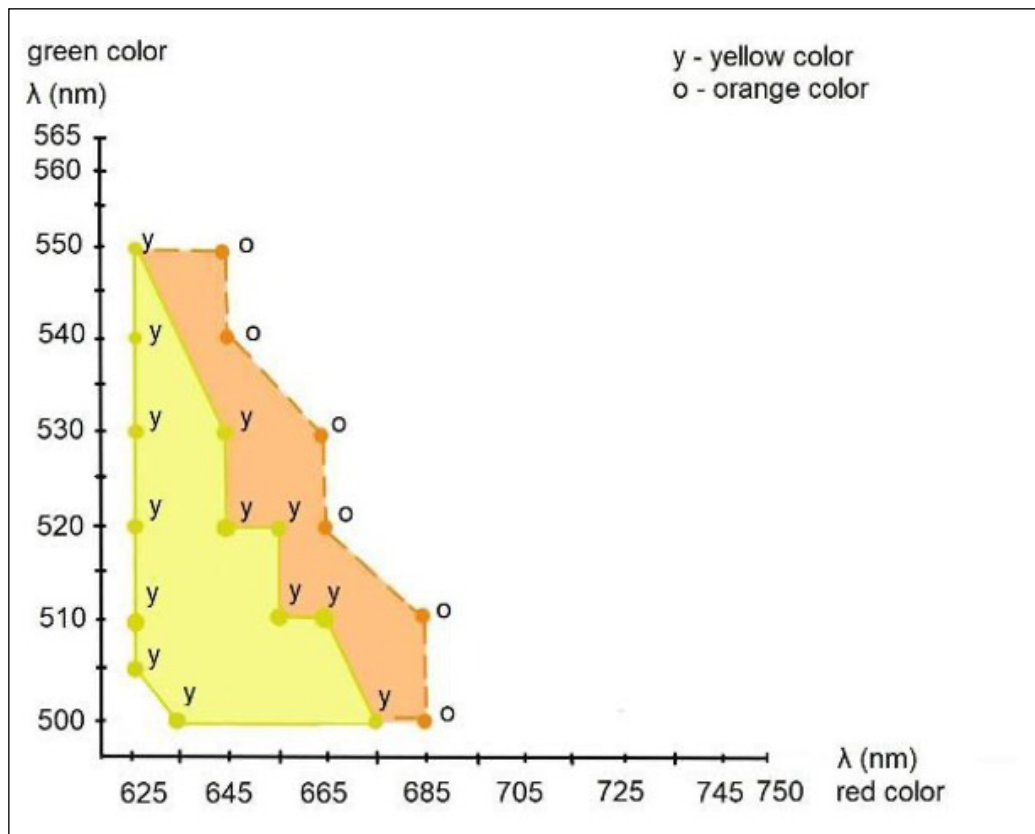


Fig. 3. Graphical modeling of additive mixing of green and red colors [13].

Humans are trichromats, as they have an additional type of cone, the L cone, which is sensitive to long wavelengths, falling in the red end of the visible spectrum [5]. The human retina has three types of cone cells – S, M, and L cells, each having different sensitivities to different parts of the visible spectrum. Since the sensitivity curves of cone cells overlap, monochromatic light cannot stimulate only one type of cone cell exclusively. The other types of cone cells react to a lesser degree.

Additive color mixing occurs when light of different wavelengths stimulates the cones, creating color axes between red-green, blue-red, and blue-green.

The additive mixing of red and green colors produces yellow and, under special conditions, orange. If the red light is significantly more intense than the green light, the brain may perceive the additive color as orange. The additive mixing of a red-green pair affects L and M cones.

The additive mixing of red and blue colors gives a magenta color, affecting the L and S cones. The results are perceived as mixed colors, a cyan color, affecting the M and S cones. The results are perceived as mixed colors within the visual spectrum range [8].

The vision analyzer forms images based on differences in light reflection from observed objects. The brightness of the background is differentiated from the central signal, emphasizing the object and achieving high sensitivity to light-dark contrast. Since the cone photoreceptors in the retina are sensitive to different wavelengths of light, there is a contrast in reflected light and the separation of the color spectrum.

There are cases of blue cone monochromacy caused by deletion mutations, which result in the lack of expression of the normal protein encoded by the OPN1LW and OPN1MW genes. As a result, the red and green M cones lose their sensitivity. Color vision defects can result from genetic anomalies and eye diseases, such as glaucoma and cataracts. Defects in color vision are also connected with anomalies and impairments of the retina optic nerves and from some diseases like diabetes [5,12].

DISCUSSION

One of the co-authors, Ignat Ignatov, proposes a method for graphical modeling in which the physical blending of green and red colors can be visualized, resulting in combined colors that are yellow or orange [13]. This is illustrated in Fig. 3.

When the visual analyzer is exposed to green and red colors, the M and L cones in the retina are activated. The brain perceives the average color as yellow or orange, serving as an average solution [14].

The spectral sensitivity of green is higher than that of red, around $\lambda=555$ nm.

Let's consider two observers. One observes a monochromatic yellow color. The other perceives yellow as a result of additive mixing between red and green. Both observers cannot distinguish who sees a monochromatic yellow color and who perceives a mixture of red and green.

Blue-sensitive cones are maximally stimulated by blue and violet light, while green-sensitive cones are maximally stimulated by yellow and green light. The red and yellow range most stimulate red-sensitive cones. The photo pigments in cones absorb photons with different wavelengths. Various methods can be used to add primary colors to achieve color mixing. In each method, photons with different wavelengths enter the eye from the same part of the visual field. They integrate into photoreceptors located in the outer segments of the cone cells. Individual molecules of photo pigments [15] absorb photons with different wavelengths.

Adding primary colors to achieve additive color mixing can occur through four primary methods. Still, in each of them, photons with different wavelengths enter the eye from the same part of the visual field. Their integration occurs in the photoreceptors located in the outer segments of the cone cells. Like a given photoreceptor, individual molecules of photo pigments [15] absorb photons with different wavelengths. On the other hand, in subtractive color mixing, the spectral light distributions are modified outside the eye through absorbing dyes.

Color vision is vital in human interactions with the surrounding environment, including professional and household activities, driving, etc. The loss of functional color vision leads to difficulties and disruptions in these activities and worsens the quality of life, including job performance. Diseases affecting the cone-rich macula, such as age-related macular degeneration, can cause early color distinguishing loss. Ocular hypertension and glaucoma can impair the optic nerve function and, thus, cause color vision defects. Retinal tears and detachments, diabetic retinopathy, and disorders affecting the optic nerve can also lead to color vision loss. Many drugs, as well as environmental factors such as exposure to ultraviolet rays, chemicals, and more, hurt this aspect [5].

In subtractive color mixing, the spectral light distribution is modified outside the eye through absorbing dyes. Dyes or pigments are mixed, not light. For example, in some color photography processes, layers of non-dispersing, selective filters are used. Combining the subtractive primary colors magenta and yellow pro-

duces red. The transmittance function of the resulting red is simply the product of the wavelengths on the transmittance function of the input colors. Black is obtained from all three subtractive primary colors (cyan, magenta, and yellow) are used, as very little light can pass through such a combination. If the filters are replaced with dyes in an ideally non-dispersing solution, the transmittance functions of the primary colors can be quantitatively altered depending on their concentrations, and a wide range of colors can be obtained. Dichromatic filters, like those used in color television cameras, do not absorb but reflect the component of light that is not transmitted, so the two components complement each other in color. The result is similar to applying pigments to the surface. Predicting color matches, including pigment mixture in a scattering medium, is not easy [15].

The most commonly used method for diagnosing color vision defects is “pseudochromatic” plate tests. However, they often fail to distinguish between different types of dyschromatopsia. Tests requiring patients to sort different discs based on color progression are more sensitive in detecting anomalies in color vision. Additional tests for color matching, which can be conducted and evaluated by a computer, as well as electrophysiological, genetic tests, and examination of retinal morphology, are applied in diagnosing and characterizing color vision defects [5]. The conditions

and experiments presented offer insights for professionals working in media products to improve image quality conditions based on additional color mixing and background.

CONCLUSIONS

An experiment involving the observation of color photographs established that individuals who perceive orange-violet snow do not perceive the blue color in the dress. The analysis revealed that yellow light activates the red and green cones. In contrast, blue light activates the blue cones in the retina, highlighting the importance of cone activation in color perception.

The contrast between blue and blue can create a visual effect where parts of objects appear more pronounced or have more intense color, demonstrating the brain’s processing of contrasting colors. The experiment also indicated a reduction in blue cone sensitivity with a violet background, illustrating chromatic adaptation. Different individuals may perceive color differently based on background and lighting conditions, underscoring the subjectivity of visual perception. Finally, the debate over the dress’s color emphasizes the role of specific lighting conditions in color perception. These findings suggest that individuals working on media products can enhance image quality by considering additive color blending and background effects.

REFERENCES

1. Yokoyama S, Radlwimmer FB. The Five-Sites Rule and Evolution of Red and Green Color Vision. *Mol Biol Evol.* 1998;5:560–567. doi: 10.1093/oxfordjournals.molbev.a025956. [DOI](#)
2. Osorio D, Vorobyev M. A review of the evolution of animal colour vision and vision communications signals. *Vision Res.* 2008;48(20):2042-2051. doi:10.1016/j.visres.2008.06.018. [DOI](#)
3. Viénot F, Le Rohellec J. Colorimetry and physiology – the LMS specification. *Digital color. Acquisition, perception, coding and rendering.* HAL open science. 2013, p.1-29.
4. Sliney DH. What is light? The visible spectrum and beyond. *Eye.* 2016;30(2):222–229. doi: 10.1038/eye.2015.252. [DOI](#)
5. Pasmarter N, Munakomi S. *Physiology, Color Perception.* StatPearls. Treasure Island (FL): StatPearls Publishing. 2023.
6. Patel B, Kanade P. Sustainable dyeing and printing with natural colors vis-à-vis preparation of hygienic viscose rayon fabric. *SM&T.* 2019;22:e00116. doi:10.1016/j.susmat.2019.e00116. [DOI](#)
7. Reda K, Szafir DA. Rainbows Revisited: Modeling Effective Colormap Design for Graphical Inference. *IEEE Trans Vis Comput Graph.* 2021;27(2):1032-1042. doi: 10.1109/TVCG.2020.3030439. [DOI](#)
8. Lander H. The presence of illusion: Magic and virtual reality. Dissertation submitted in partial fulfillment of the requirements for the degree of Master of Fine Art. Glasgow School of Art, University of Glasgow. 2015, pp.1- 34.
9. Ignatov I. Rhodopsin and bacteriorhodopsin. Electromagnetic conception for the eyesight in additive mixing and emotional perception of colors. *Journal of Health, Medicine and Nursing.* 2018;46:196-210.
10. Eisner A, MacLead DIA. Blue-sensitive cones do not contribute to luminance. *J. Opt. Soc. Am.* 1980;70(1):121-123. doi: 10.1364/josa.70.000121. [DOI](#)
11. Ignatov I, Vanlyan K. Electromagnetic conception of color vision in additive mixing of colors. Application in photography. *Art and psychology. J. Physiol. Med. Biophys.* 2020;64:9-13. doi: 10.7176/JMPB/64-02. [DOI](#)
12. Wang C, Hosono K, Kachi S et al. Novel OPN1LW/OPN1MW deletion mutations in 2 Japanese families with blue cone monochromacy. *Hum Genome Var.* 2016;3:16011. doi: 10.1038/hgv.2016.11. [DOI](#)

13. Ignatov I, Popova TP. Graphical modeling of additive color mixing. Analyses of electromagnetic effects as colors of the vision analyzer. *Ukr. J. Phys.* 2024;29(2):11-17.
14. Gao D, Barrionuevo P. The importance of intrinsically photosensitive retinal ganglion cells and implications for lighting design. *Journal of Solid State Lighting*. 2015. doi:10.1186/s40539-015-0030-0. [DOI](#)
15. Boynton RM.. *Color Science*, Editor: Robert A. Meyers. *Encyclopedia of Physical Science and Technology* (3rd ed), Academic Press. 2003, pp.289-313.

CONFLICT OF INTEREST

The Authors declare no conflict of interest

CORRESPONDING AUTHOR

Ignat Ignatov

Scientific Research Center of Medical Biophysics (SRCMB)

32 N. Kopernik srt., Sofia 1111, Bulgaria

e-mail: mbioph@abv.bg

ORCID AND CONTRIBUTIONSHIP

Ignat Ignatov: 0000-0002-4761-2982 [A](#) [C](#) [D](#) [E](#) [F](#)

Teodora P. Popova: 0000-0003-4330-7996 [D](#) [E](#) [F](#)

Alexander I. Ignatov: 0000-0001-6578-2523 [B](#)

Ivan Angushev: 0000-0002-2933-8051 [B](#)

[A](#) – Work concept and design, [B](#) – Data collection and analysis, [C](#) – Responsibility for statistical analysis, [D](#) – Writing the article, [E](#) – Critical review, [F](#) – Final approval of the article

RECEIVED: 14.01.2024

ACCEPTED: 27.02.2024

